Conflict Resolution in Autonomous Operations Area airspace

Vom Fachbereich Maschinenbau
an der Technischen Universität Darmstadt
zur
Erlangung des Grades eines Doktor-Ingenieurs (Dr.-Ing.)
genehmigte

Dissertation

vorgelegt von

Dipl.-Inform. Nima Barraci

aus Hagen

Berichterstatter:	Prof. Dr.-Ing. Uwe Klingauf
Mitberichterstatter:	Prof. Dr.-Ing. Manfred Boltze
Tag der Einreichung:	19. Oktober 2009
Tag der mündlichen Prüfung:	14. Dezember 2009

D17

Dedicated to my grandfather,
Dr.-Ing. Hossein Sina

After a time, you may find that having is not so pleasing a thing, after all, as wanting. It is not logical, but it is often true.

Mr. Spock

Kurzfassung

Das Flugsicherungs- und Flugverkehrsmanagementsystem steht vor einem Paradigmenwechsel. Flugzeuge werden zukünftig im so genannten *Autonomous Operations Area* Luftraum selbst für die Überwachung und Einhaltung der minimalen Separation verantwortlich sein. Von dieser Verlagerung der Verantwortlichkeit von der Flugsicherung an die Flugdeckbesatzung wird sich sowohl eine bessere und flexiblere Luftraumnutzung, als auch eine effizientere Flugdurchführung versprochen.

Um in diesem Luftraum operieren zu können, müssen Flugzeuge mit technischen Systemen ausgestattet werden, die eine Erkennung und Lösung von Luftverkehrskonflikten ermöglichen. Ein solches System hat zur Aufgabe, Konflikte mit anderen Luftraumteilnehmern zu erkennen und eine alternative, konfliktfreie Trajektorie zu berechnen. Dabei werden an die Trajektorie neben der Konfliktfreiheit meist noch die Fliegbarkeit sowie die Berücksichtigung von Optimierungsparametern als Anforderungen gestellt. Zu diesen zählen vor allem die Minimierung des notwendigen Kraftstoffes bzw. der notwendigen Zeit für das Resolutionsmanöver.

Die vorliegende Arbeit beschäftigt sich mit einem solchen System. Der Fokus liegt dabei auf der Lösung von Verkehrskonflikten unter gleichzeitiger Gewährleistung der Fliegbarkeit sowie der Integration eines Kostenindexes. Der Kostenindex, welcher heutzutage vom *Flight Management System* zur Bahnoptimierung verwendet wird, gibt das vom Flugzeugbetreiber angegebene Verhältnis von kraftstoffbezogenen zu zeitbezogenen Kosten an. Dieser Parameter wird im Rahmen dieser Arbeit in einen Konfliktlösungsalgorithmus auf Grundlage von künstlichen Kraftfeldern integriert. Die Fliegbarkeit der resultierenden Trajektorie wiederum wird durch Nutzung eines flugmechanischen Modells adressiert und bewertet.

Der in dieser Arbeit entwickelte Algorithmus wird in Schnellzeitsimulationen mit variierendem Kostenindex bewertet. Ziel der Auswertungen ist es die Konfliktfreiheit und Fliegbarkeit der resultierenden Trajektorie, sowie die Berücksichtigung des Kostenindex zu überprüfen. Dazu werden die alternativen Trajektorien mit der originalen, konfliktbehafteten Trajektorie des Flugzeuges und die Entfernungen am Punkt der geringsten Annäherung verglichen. Die laterale, vertikale und temporale Abweichung der alternativen Trajektorie zur originalen Trajektorie werden als Maß für die kraftstoffbezogenen, respektive zeitbezogenen Kosten verwendet und gegenüber gestellt.

Die Simulationsergebnisse zeigen, dass die Fliegbarkeit der Trajektorie durch die Integration des flugmechanischen Modells gewährleistet werden konnte. Während jedoch der provozierte Zusammenstoß der Flugzeuge durch den Konfliktlösungsalgorithmus auch in den betrachteten Grenzfällen verhindert werden konnte, wurde die minimal notwendige Separation nicht in jedem Fall hergestellt. Auch hat sich die Integration des Kostenindex als praktikabel gezeigt, wobei jedoch noch Verbesserungspotential vor allem in Bezug auf die Geschwindigkeitsresolution identifiziert werden konnte.

Abstract

A paradigm shift is at hand with the planned redesign of the *Air Traffic Management* and *Air Traffic Control* systems. The concept for the future air traffic system foresees that aircraft will monitor and maintain separation to each other by themselves in *Autonomous Operations Area* airspace. With this shift of responsibility for separation assurance from Air Traffic Control to the flight deck crews a more flexible and better airspace usage is expected. Furthermore, through the more flexible airspace usage, a gain in flight efficiency is also anticipated.

In order to operate in this airspace area, aircraft are required to be equipped with a system enabling them to detect and resolve air traffic conflicts. Upon detection of a conflict with another aircraft, the system is expected to compute an alternative trajectory which guides the aircraft around the conflict and back to its original trajectory. The alternative trajectory needs to adhere to several requirements, such as being clear of conflicts and being flyable. Further requirements that are often stated are to minimise the additional fuel and time required for the resolution.

This thesis is concerned with such a *Conflict Detection & Resolution* system. Primary focus lies on the resolution of air traffic conflicts while guaranteeing flyability and respecting the *Cost Index*. The *Cost Index* is nowadays used by the *Flight Management System* to optimise the flight profile in respect to the operators prioritisation of fuel-related to time-related costs. This paramter is included into the *Conflict Resolution* process which is based on *Artificial Force Fields*. Flyability of the trajectory is intended to be guaranteed through integration of a flight mechanics model.

The algorithm devised in this work is validated in fast time simulations with varying *Cost Index*. Objects of study are the distance at the *Closest Point of Approach*, the integration of the *Cost Index* and the flyability of the resulting trajectory. The first two objects of this study will be validated through comparison of the original and updated trajectory. The new trajectory is considered conflict free if the distance at the *Closest Point of Approach* is sufficiently large. The lateral, vertical and temporal differences between the two trajectories are used as measures for time- and fuel-related costs. Flyability of the resulting trajectory is validated by confirming adherence to the flight envelope and the constraints given by the flight mechanics model used.

The evaluation of the algorithm showed that by integration of a flight mechanics model flyability of the resulting trajectory could be assured. Regarding resolution of the conflicts, the algorithm could compute a trajectory which prevented the initially set up *Mid-Air Collision* between the aircraft. Though, the minimum required separation could not be achieved in all cases. The approach of integrating the *Cost Index* into the resolution process showed to be feasible, whereas especially regarding the speed resolution further enhancements have been found to be necessary.

Acknowledgements

This thesis was prepared and written during my time as research associate at the Institute of Flight Systems and Automatic Control. I would like to thank Prof. Dr.-Ing. Uwe Klingauf – head of the Institute and supervisor of this thesis – for having made this preparation possible, for the discussions, his scientific advise and his trust in my work. I would also like to thank Prof. Dr.-Ing. Manfred Boltze, second reviewer of this thesis. A special thank goes to him and to the members of the examination committee for accomplishment of the doctoral examination under the special circumstances of that day.

A great thank is also due to the members of the former research group *Cockpit* and the research groups *Simulation & ATM* and *System Engineering and Navigation*, but especially to Dipl.-Ing. Mark Azzam, Dipl.-Inform. Siegfried Bauer, Dipl.-Wirtsch.-Ing. Andreas Greulach, Dipl.-Ing. Jochen Schaab, Dipl.-Ing. Frank Schmidt-Brücken and Dipl.-Ing. Heike Meinert for their time to discuss my ideas. Those discussions were a valuable input and significantly supported the conclusion of this thesis. For her thorough review of my thesis I would like to underline my gratitude to Heike.

The support of the administrative staff at the Institute, especially during the last months of the thesis, may not remain unmentioned. For their guidance through the administrative jungle and for their support I owe my thanks to Erika Purpus and Angela Scholtis.

Without the contributions of my students Raad Bahmani, Michael Rösch and Volker Roth this work in its present form would not have been possible. To them I would like to express my gratitude and acknowledgement.

Finally I would also like to thank Captain Mark Hartmann for inspiring me to follow the research topic of airborne conflict resolution. For their support during my studies and during the preparation of this thesis my warmest thanks are due to my mother Sussan Sina, my grandfather Hossein Sina and my partner Heike Meinert.

Contents

List of Symbols

The following lists summarise the symbols of the variables used throughout this work.

Latin letters

acr	Aircraft
d	Distance
d_{CPA}	Distance between ownship and intruder at CPA
D	Drag
h	Altitude
H	Lateral area
L	Lift
m	Aircraft mass
p	Position
p_{CPA}	Position of the CPA ($\in \mathscr{P}$)
ROC	Rate of climb/descent
t_{CPA}	Time to Closest Point of Approach (CPA)
ts	Trajectory segment
T	Thrust
Ti	Temporal area
V	Vertical area
x	Coordinate
y	Coordinate
z	Coordinate
Z	Zone around an aircraft

Sets, Subsets and Elements

$\mathscr{A}$	Set of aircraft
$\mathscr{P}$	Set of aircraft positions
$\mathscr{T}$	Set of trajectory points
$\mathscr{T}_{acr_n} \subseteq \mathscr{T}$	Trajectory Change Points of Aircraft acr_n

Greek letters

γ	Flight Path Angle
ϵ	Elevation Bearing
θ	Pitch
$\lambda^\diamond$	Latitude
μ	Aerodynamic bank
ν	Thrust specific fuel consumption
ξ	Arbitrary angle
ρ	Roll
σ	Bearing
ϕ	Bank
$\phi^\diamond$	Longitude

χ	Track
ψ	Heading
Ψ	Yaw

Indices

C	Fixed Costs (independent of time)
F	Fuel-related costs per flight minute
g	geodetic coordinate system
o	Ownship
i	Intruder
T	Time-related costs per flight minute

List of Acronyms

ACAS	Airborne Collision Avoidance System
ACM	Airborne Conflict Management
ADS	Automatic Dependant Surveillance
ADS-A	Automatic Dependant Surveillance - Addressed
ADS-B	Automatic Dependant Surveillance - Broadcast
ADS-C	Automatic Dependant Surveillance - Contract
AFDS	Auto Flight Director System
AFM	Autonomous Flight Management
AIP	Aeronautical Information Publication
AMAN	Arrival Manager
ANSP	Air Navigation Service Provider
AOA	Autonomous Operations Area
ASAS	Airborne Separation Assistance System
ATC	Air Traffic Control
ATCO	Air Traffic Control Officer
ATM	Air Traffic Management
ATFM	Air Traffic Flow Management
ATS	Air Traffic Service
BADA	Base of Aircraft Data
BDT	Business Development Trajectory
CAS	Calibrated Airspeed
CAZ	Collision Avoidance Zone
CI	Cost Index
CD	Conflict Detection
CD&R	Conflict Detection & Resolution
CDM	Collaborative Decision Making
CR	Conflict Resolution
CDTI	Cockpit Display of Traffic Information
CNS	Communications, Navigations, Surveillance
COTS	Commercial of the shelf
CPA	Closest Point of Approach
DMOD	Distance Modification
DR	Dead Reckoning
ECAC	European Civil Aviation Conference
ESRA	EUROCONTROL Statistical Reference Area
ETA	Estimated Time of Arrival
ETO	Estimated Time Over
EUROCONTROL	European Organisation for the Safety of Air Navigation
FAA	Federal Aviation Administration
FANS	Future Air Navigation System
FBW	Fly by wire
FIR	Flight Information Region
FIS	Flight Information Service
FL	Flight Level
FMS	Flight Management System
FSM	Finite State Machine
FPA	Flight Path Angle
FSR	Institute of Flight Systems and Automatic Control - Flugsysteme und Regelungstechnik

GPS	Global Positioning System
GPWS	Ground Proximity Warning System
GS	Ground Speed
HMI	Human Machine Interface
IATA	International Air Transport Association
ICAO	International Civil Aviation Organisation
IFBP	Inflight Broadcast Procedure
IFR	Instrument Flight Rules
ISA	International Standard Atmosphere
ISO	International Organization for Standardization
JPDO	Joint Planning and Development Office
LRC	Long Range Cruise
LNAV	Lateral Navigation
MAC	Mid-Air Collision
MCDU	Multipurpose Control Display Unit
MRC	Maximum Range Cruise
NAS	National Airspace System
NASA	National Aeronautics and Space Administration
NAT	North Atlantic
ND	Navigation Display
NDB	Non-Directional Beacon
NextGen	Next Generation Air Transportation System
NMAC	Near Mid-Air Collision (MAC)
NUP2+	North European ADS-B Network Update Programme, Phase II+
OEP	Operational Evolution Plan
OPF	Operations Performance File
OTS	Organised Track System
PAZ	Protected Airspace Zone
PC	Personal Computer
PIC	Pilot In Command
PT	Predicted Trajectory
RA	Resolution Advisory
RADAR	Radio Detection and Ranging
RBT	Reference Business Trajectory
RCAF	Runway Collision Avoidance Function
RITA	Research and Innovative Technology Administration
RNAV	Area Navigation
RNP	Required Navigational Performance
ROCD	Rate of climb/descent
RTA	Required Time of Arrival
RTCA	Radio Technical Commission for Aeronautics
RTO	Required Time Over
RVSM	Reduced Vertical Separation Minima
SAR	Specific Air Range
SBT	Shared Business Development Trajectory
SES	Single European Sky
SESAR	Single European Sky Air Traffic Management (ATM) Research
SL	Sensitivity Level
STO	Scheduled Time Over
SV	State Vector
SVS	Synthetic Vision System
TA	Traffic Advisory

TAS	True Airspeed
TBO	Trajectory Based Operations
TC	Trajectory Change
TCAS	Traffic Collision Avoidance System
TCP	Trajectory Change Point
TIS-B	Traffic Information Service - Broadcast
TLS	Target Level of Safety
TMA	Terminal Manoeuvring Area
TMR	Trajectory Management Requirement
TRL	Technology Readiness Level
TTG	Time to go
TUD	Technische Universität Darmstadt
UAV	Unmanned Aerial Vehicle
UML	Unified Modeling Language
UTC	Universal Time Coordinated
VNAV	Vertical Navigation
VOR	Very High Frequency Omnidirectional Radio Range
WATRS	West Atlantic Track System
XTE	Cross Track Error

1 Introduction

Heavier-than-air flying machines are impossible.

Lord Kelvin, 1892

WORLD-WIDE air traffic is expected to grow significantly within the next years. Alone for the *EUROCONTROL Statistical Reference Area* (ESRA) which covers major parts of the European airspace (cf. [MW04, Appendix B] for details) a growth factor between 1.6 (under the assumption of continuing regionalization and weak economies; Scenario D in Figure 1.1) to 2.1 (under the assumption of increasing globalization and strong economies; Scenario A in Figure 1.1) by the year 2025 compared to 2003 is anticipated. Figure 1.1 from [MW04] illustrates this prognosis for four scenarios with different assumptions regarding the economic situation[1]. Other estimations anticipate a growth by the factor of three by the year 2020 compared to today for world-wide air traffic [FLY05]. To cope with this growth changes to the current Air Traffic Management operational concept and to the way air traffic is organised are required.

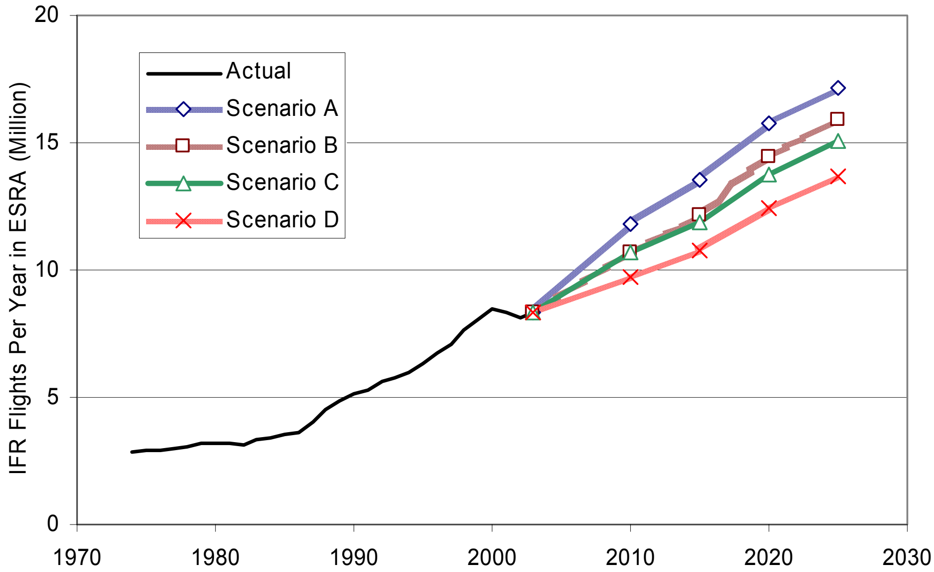

Figure 1.1: IFR flights in ESRA (from [MW04])

International air traffic is organised in accordance to regulations and recommendations setup by the *International Civil Aviation Organisation* (ICAO). The regulations, described in the 18 annexes to the *Chicago Convention* [ICA06], are required to be implemented by the member states into federal law. Annex 2 [ICA90] and Annex 11 [ICA01] are concerned with the *Rules of the Air* and *Air Traffic Services (ATSs)*.
Air Traffic Services (ATSs) are comprised of three services [ICA01], namely

[1] Assumptions for Scenario B are moderate economic growth without significant changes from the status quo and current trends; for Scenario C strong economic growth with strong government regulation on economic issues has been assumed. For further details refer to [MW04, Section 1.3].

1. *Air Traffic Control* (ATC) service '[...] to prevent collisions between aircraft.' (also on the manoeuvring area and between obstructions) and to '[...] expedite and maintain an orderly flow of air traffic.'

2. *Flight Information Service* (FIS) to '[...] provide advice and information useful for the safe and efficient conduct of flights.'

3. *Alerting service* to '[...] notify appropriate organisations regarding aircraft in need of search and rescue aid, and assist such organisations as required. [...]'

Air Traffic Control (ATC) is responsible for the orderly flow of air traffic. In order to allow Air Traffic Control with its control centres at different locations to fulfil this duty the airspace is subdivided into different Flight Information Regions (FIRs) (distinguished between upper and lower regions) which are further partitioned into sectors, each with a maximum capacity and within the responsibility of one or more Air Traffic Control Officers (ATCOs). Aircraft traverse these sectors on predefined routes and are separated vertical, lateral and longitudinal from each other. Upon reaching sector boundaries or boundaries of the FIR they are passed over from ATCO to ATCO or from center to center. Factors influencing the maximum capacity are *inter alia* the number of Air Traffic Control Officers responsible for the airspace, the design and structure of the airspace and the current meteorological situation [Men04].

1.1 Motivation for a redesign of the Air Traffic Management system

The limited capacity on the ground has to cope with growing air traffic. The European and U.S. airspace are good examples for this development. Together they are with a share of 65% in worldwide air traffic the worlds busiest airspace areas [Gmf] and capacity problems have been experienced in the past in both areas. The lessons learned from the traffic situations in these areas were driving factors to the redesign of the Air Traffic Management system.

1.1.1 European Airspace

In the summer of 1999 about 21% of all flights in the European Civil Aviation Conference (ECAC) area[2] (see Figure 1.2) were delayed [EUR00]. With 79,5%, ATC Capacity accounted most to those delays followed by *Weather* with 6,7%.
As a consequence of this '[...] disastrous situation in the summer of 1999 [...]' [EC99, Introduction, Paragraph 7] the European Commission initiated the SES project to identify solutions in order to prevent a renewal of this situation in the future.

Contributing Factors
The Commission identified in its communiqué that three factors were responsible for the delays in 1999, namely delays caused by

- *Operators* due to operational and logistic reasons – approximately 25%.
- *Airports* due to saturation of infrastructure – approximately 25%.
- *Airspace* due to saturation – approximately 50%.

[2] ECAC member states 1999 [Eca]: Albania, Armenia, Austria, Belgium, Bulgaria, Croatia, Cyprus, Czech Republic, Denmark, Estonia, Finland, France, Germany, Greece, Hungary, Iceland, Ireland, Italy, Latvia, Lithuania, Luxembourg, Malta, Moldova, Monaco, Netherlands, Norway, Poland, Portugal, Romania, Slovakia, Slovenia, Spain, Sweden, Switzerland, The former Yugoslav Republic of Macedonia, Turkey and the United Kingdom

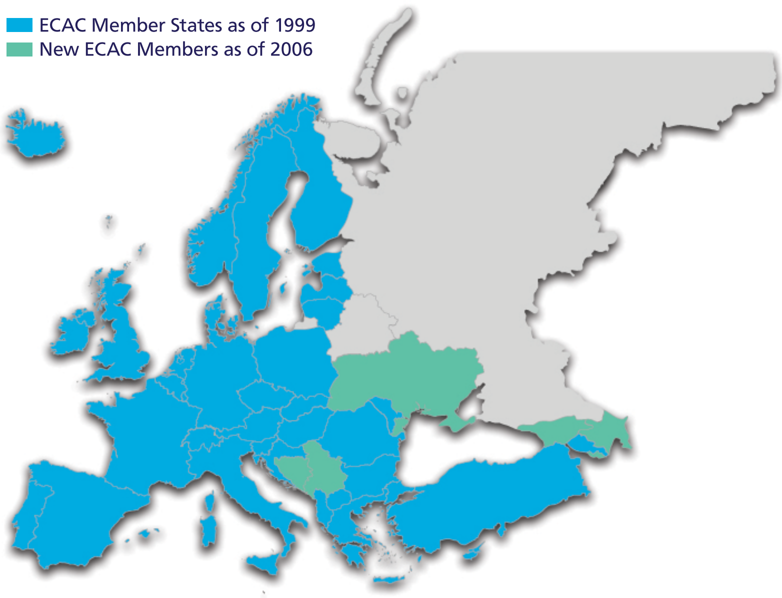

Figure 1.2: European Civil Aviation Conference (ECAC) member states (as listed in [Eca])

Annex I of this communiqué details the situation of air traffic delays and congestions in the European ATM System as of 1999. Key deficiencies identified were that

- the European ATM System was not measured and could therefore only '[...] hardly be managed effectively [...]',
- the safety data at European level was neither consistent nor always available *and*
- ATM was responsible for half of all delays in 1998.

Due to the lack of consistent information, no conclusion regarding the cost effectiveness of the ATM system could be made. Even though the Air Traffic Flow Management (ATFM) delay decreased in 2006 to 11.6% and ATC capacity only accounted with 38.7% to all delays [EUR07][3], ATC capacity still was the cause for 60% of all en-route delays.

Conclusions
The Commission identified that '[...] the management of Europe's skies rest on antiquated methods and principles.' [EC99] and concluded that a reorganisation would be necessary in order to be able to cope with growing air traffic. Key requirements as of [EC99] were

- the need of a collective management of airspace,
- the subdivision of sectors and routes regardless of frontiers *and*
- the division of airspace between civil and military must take account of the new geopolitical realities and form part of a consistent and efficient framework.

One technical mean to respond to the rise in air traffic identified was to increase the airspace capacity. The airspace capacity is limited by '[...] the methods used to manage air traffic [...]' and '[...] by the limits on the number of aircraft an air traffic controller is able to control [...]' [EC99, Annex II, Part II, Paragraph 19]. The authors conclude that

[3] New ECAC member states compared to 1999: Azerbaijan, Bosnia and Herzegovina, Georgia, Serbia and Ukraine

> 'Increasing airspace capacity means therefore either changing the whole concept and give pilots appropriate tools to be able to avoid mid-air collisions on their own; or increase the number of aircraft an air traffic controller can handle by providing him/her with appropriate facilitating tools; or a combination of both.' [EC99, Annex II, Part II, Paragraph 19]

Single European Sky - High Level Group Report
Following the communiqué from the European Commission, a high-level group was set up with the task to formulate recommendations for the future European Airspace System. The report pointed out that the European Airspace should be able to facilitate new concepts such as *free routing* and should be treated as a *Single European Sky* [Com00].

1.1.2 U.S. National Airspace System

In 1999 about 20% of all U.S. domestic flights by carriers with at least 1% of domestic scheduled-service passenger revenue were delayed[4] (about 5.3 million flight operations, see Section D.1). In the same year about 7.3 million flight operations in the ECAC area were analysed; about 21% of those flights were delayed as well.

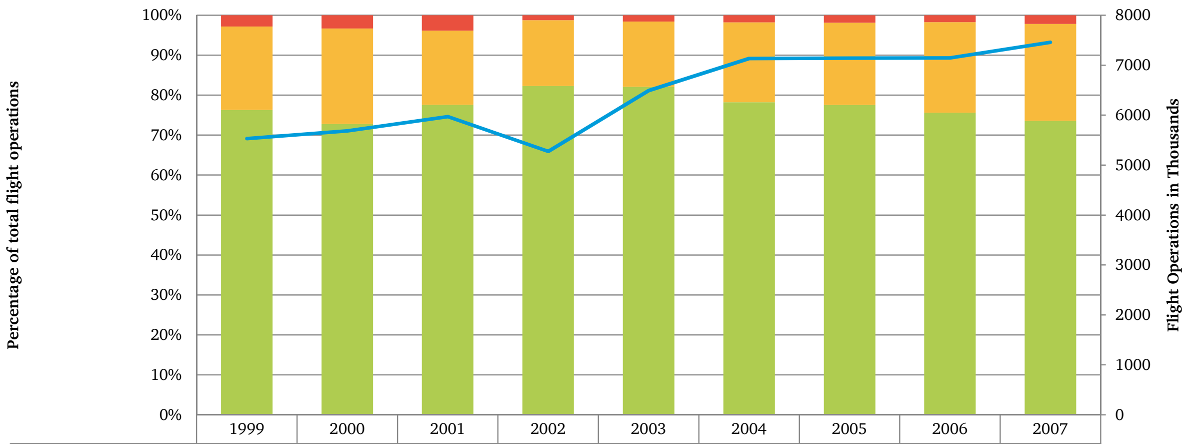

	1999	2000	2001	2002	2003	2004	2005	2006	2007
Cancelled (%)	2,79%	3,30%	3,87%	1,24%	1,56%	1,79%	1,87%	1,71%	2,16%
Delayed (%)	20,85%	23,86%	18,51%	16,47%	16,30%	19,94%	20,53%	22,62%	24,20%
Ontime (%)	76,11%	72,59%	77,40%	82,14%	81,96%	78,08%	77,40%	75,45%	73,42%
Flight Ops (in 1000)	5527,884	5683,047	5967,78	5271,359	6488,54	7129,27	7140,595	7141,922	7455,458

Figure 1.3: U.S. Flight Delays Statistics for domestic carriers with at least 1% of domestic scheduled-service passenger revenue (data from [Rit])

The percentage of delayed flights from 1999 to 2007 was with approximately 16% in 2003 at its lowest value, whereas about one quarter of all flights were delayed in 2007. This coincides with the gain in flight operations which also reached their highest value in 2007 (see Figure 1.3).
Since 2003, the Research and Innovative Technology Administration (RITA) statistics also include the actual cause for delays. It can be noted that even though the share of traffic delays accounted to the National Airspace System (NAS) decreased from approximately 40% in 2003[5] to about 30% in 2007 (see Figure 1.4) it is still together with late arriving aircraft the most prevalent delay cause (see Subsection D.1.2). Also in 2003, the Federal Aviation Administration (FAA) initiated a study focusing on the future capacity needs in the NAS. The U.S. National Airspace System includes all players in the airspace system such as *Air Traffic Management (ATM)*, *Air Traffic Control (ATC)* and *airport* authorities which is also reflected through the Next Generation Air Transportation System (NextGen) concept which covers

4 An aircraft is delayed if it arrives/departs at least 15 minutes delayed at/from the gate
5 Data for 2003 only covers the months July to December

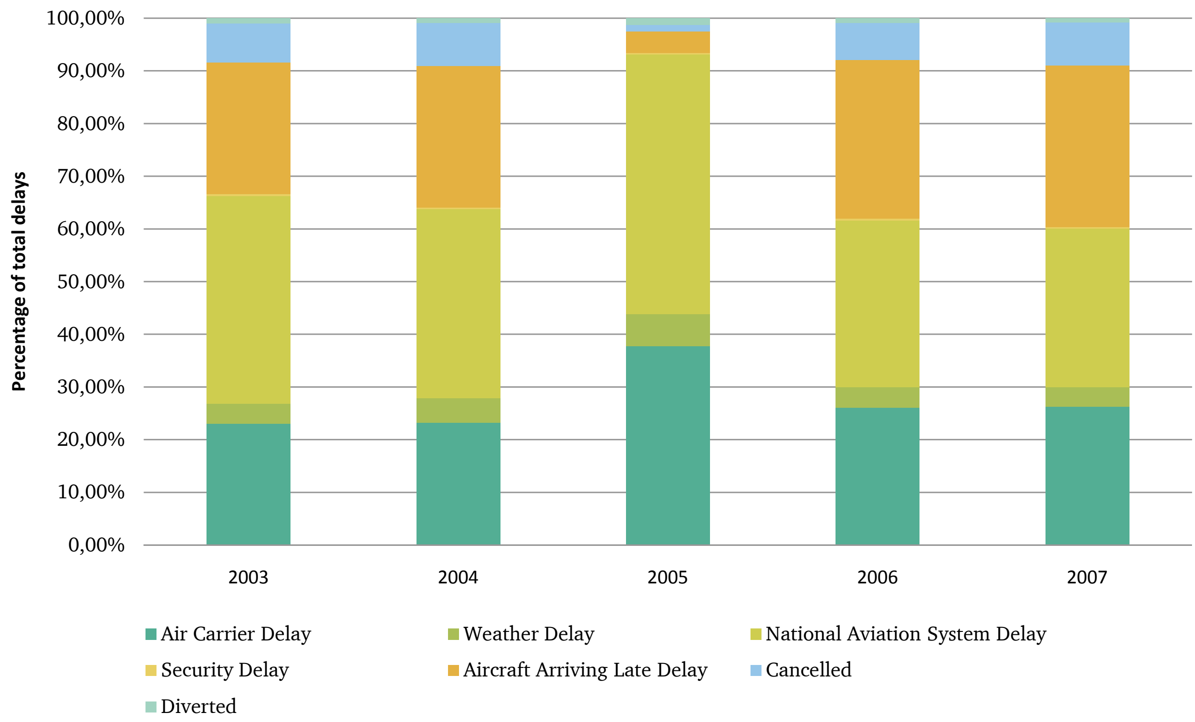

Figure 1.4: Cause for delays of U.S. carriers with at least 1% of domestic scheduled-service passenger revenue (data from [Rit])

– in contrast to Single European Sky (SES) – the whole journey from arriving at the departure airport to leaving the airport at the destination (*curb-to-curb*). This study identified that '[...] additional demands placed upon the NAS will strain the system´s capacity.' [Fac].

Contributing Factors

The study identified, based on Operational Evolution Plans (OEPs) for the 35 busiest airports in the U.S.[6], that the NAS is not capable to meet future capacity needs. The OEPs cover four core problem areas, namely

1. airport weather conditions,
2. en route severe weather,
3. en route congestion *and*
4. arrival/departure rate.

Similar to Europe, the highest delay rates in the U.S. NAS are during the summer months June to August. During these months the summer travel seasons collides with adverse and unpredictable weather conditions [LPY01].

Conclusions

In response to this prognosis the *Vision 100 - Century of Aviation Reauthorization Act* law [Nexb] was enacted in 2003. With this law, the Joint Planning and Development Office (JPDO)[7] was tasked to bring NextGen (formerly referred to as *Next Generation Air Transportation System* – NGATS) on-line by 2025.

6 As of [Fac] the 31 large hubs plus Memphis International Airport, Cleveland Hopkins International Airport, Ronald Reagan Washington National Airport and Portland International Airport

7 The JPDO is comprised of six government agencies, the U.S. Department of Transportation, the U.S. Department of Defense, the Federal Aviation Administration (FAA), the U.S. Department of Homeland Security, the Department of Commerce, the National Aeronautics and Space Administration (NASA) and the Office of Science & Technology Policy.

1.2 Description of the novel Air Traffic Management system

The International Civil Aviation Organisation (ICAO) *Global Air Traffic Management Operational Concept* [ICA05b] defines the framework for the ATM system operational concept. The concept foresees *inter alia* for *traffic synchronisation* the key conceptual change that '[...] four-dimensional (4-D) trajectory control [...]' [ICA05b, 2.1.5 a)] will be applied. The trajectories will be negotiated with the goal to be conflict-free. Regarding *airspace user operations* the concept anticipates '[...] individual aircraft performance, flight conditions, and available ATM ressources [...]' [ICA05b, 2.1.6 d)] to allow for dynamically-optimised 4-D trajectory planning. In the domain of *conflict management* the concept identifies a three-layered approach (see Figure 1.5(a)).

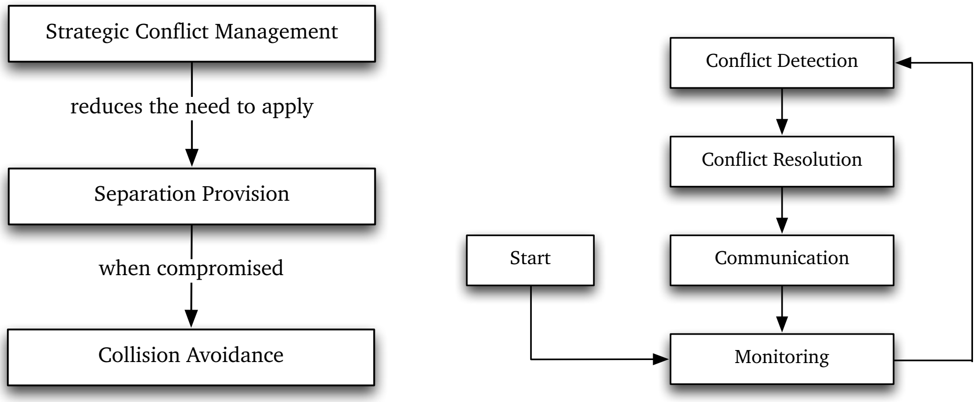

(a) Three Layer Conflict Management Approach

(b) Separation Provision process

Figure 1.5: Conflict management & separation provision as of [ICA05b]

Strategic Conflict Management

ICAO uses the term *strategic* in this context as '[...] in advance to tactical [...]'[8]. Strategic Conflict Management is considered to be achieved through airspace organisation and management and covers the earliest planning stage up to shortly before departure. Though, especially for long-haul flights, strategic conflict management may also be applied after departure, depending on the best mean to resolve a conflict. Strategic conflict management is comprised of

1. airspace organisation and management,
2. demand and capacity balancing *and*
3. traffic synchronisation.

Separation Provision

Separation Provision is the second layer of conflict management and shall guarantee that aircraft at least respect the applicable minimum separation. According to [ICA05b] separation provision may be seen as an iterative process (Figure 1.5(b)) in which upon conflict detection a resolution is identified and communicated to the conflicting parties. Then, the execution of the resolution is monitored and – in case applicable minimum separation will be undershot – further resolution manoeuvres will be identified.
Ensuring safe separation is the responsibility of the *seperator*. ICAO defines the separator as '[...] the agent responsible for separation provision [...]' which can, depending on the separation mode, also be delegated to an aircraft. Several situations are defined:

[8] [Bar+06] summarises definitions for the terms *strategic* and *tactical*. Further information may be found in Section A.3

Self-separation:	The airspace user is responsible for separation in respect to one or more hazards.
Distributed:	Different predetermined separators are defined for different hazards.
Co-operative:	Role of separation is delegated temporarily until a termination condition sets in.

Hazards to which aircraft need to be separated from are as of [ICA05b]:

- while airborne
  - other aircraft
  - terrain
  - atmospheric constraints (weather, wake turbulence)
  - incompatible airspace activities
- and while on ground
  - surface vehicles
  - other obstructions while on the apron and manoeuvring area

Common to all situations is that for each hazard a separator needs to be responsible for separation provision.

Collision Avoidance
Collision Avoidance systems come into action when both layers, *Strategic Conflict Management* and *Separation Provision* have failed. Collision Avoidance systems will not be used for determination of the Target Level of Safety (TLS) of the ATM system. But, although independent of, they need to be compatible with the applicable separation mode.

1.3 Shift of responsibilities

The future Air Traffic Management concept includes a shift of responsibilities for certain operation areas from Air Traffic Control to the flight deck crews. In the current ATM system, the Pilot In Command (PIC) is '[...] responsible for the operation of the aircraft in accordance with the rules of the air [...]' [ICA90]. The task of ensuring the applicable separation between aircraft is within the responsibilities of ATC. Under special circumstances this task can already be delegated from ATC to the flight deck crew (e.g. visual acquisition of the preceding aircraft during approach). Though, except for special airspace areas such as the IFBP region over African airspace (cf. Section B.2, [Iata]), this is not common practice for the en-route phase of flight. Even for airspace areas such as the North Atlantic (NAT) airspace where a lack of ground infrastructure hinders ATC to control the air traffic via RADAR, procedural means are applied for separation assurance and ATC is still responsible for this task [ICA05a].
With the future ATM system, the delegation of separation provision and assurance will become standard operation for designated airspace areas which may only be used by appropriately equipped aircraft. In the concepts of operations for the *Single European Sky* (SES) and *Next Generation Air Transportation System* (NextGen), this shift is an integral part of the change from clearance-based to Trajectory Based Operations.

Single European Sky ATM Research
The Single European Sky ATM Research (SESAR) programme – co-funded by the European Commission and EUROCONTROL – is concerned with the implementation of the aims set up by SES. At the core of the *Single European Sky* Concept of Operations [Ses] lies the *Trajectory Management*. In SESAR several *Trajectory States* are defined, namely:

BDT	Business Development Trajectory
SBT	Shared Business Development Trajectory

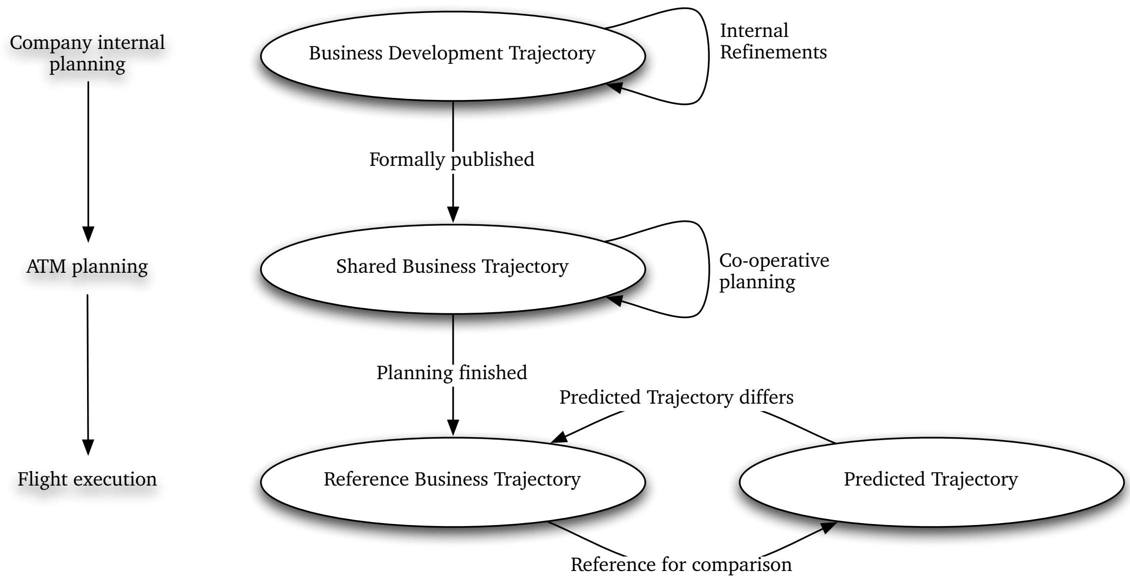

Figure 1.6: SESAR - Trajectory Management concept as of [Ses]

RBT Reference Business Trajectory
PT Predicted Trajectory

In SESAR additionally *Other Trajectories* may exist which are considered to be interim formats used internally by systems working with the trajectories, e.g. aircraft systems.
Figure 1.6 outlines the trajectory life-cycle as described in the Concept of Operations. The trajectory may exist from initial planning to the actual execution in different phases. While being under development and internal to the user's organisation, the trajectory may be changed, updated or completely discarded and is referred to as *Business Development Trajectory* (BDT). In order to begin the collaborative planning process, the user's organisation may introduce the Business Development Trajectory (BDT) into the ATM environment. At this stage the trajectory is referred to as *Shared Business Development Trajectory* (SBT). During the planning process the trajectory may undergo certain refinements which then lead to the *Reference Business Trajectory* (RBT). For the flight execution the Reference Business Trajectory (RBT) is the reference. Upon deviation – intended or unintended – from the RBT, the *Predicted Trajectory* (PT) is calculated with the aim to return the aircraft to its Reference Business Trajectory.
This concept introduces the *4D Trajectory*, which is in SESAR defined as

> *'A set of consecutive segments linking waypoints and/or points computed by FMS (airborne) or by TP (ground) to build a vertical profile and the lateral transitions; each point defined by a longitude, a latitude, a level and a time.' [Ses]*

Next Generation Air Transportation System

Similar to SESAR, the Next Generation Air Transportation System (NextGen) Concept of Operations [Nexa] also considers the implementation of airspace regions in which aircraft may operate autonomously, i.e. in which aircraft are responsible for the provision of separation (Self-Separation Operations). Independent of the mode – Air Navigation Service Provider (ANSP)-managed or self-separated – the key operational change in NextGen is the transition from clearance-based to Trajectory Based Operations (TBO). TBO requires the introduction of technologies allowing to predict and communicate the future aircraft trajectory. In 2006, NASA summarised that the technologies for trajectory prediction were only used in a few specialised areas (namely time-based arrival metering, en-route conflict detection) and in Flight Management Systems [SBL06].

Compatibility between SESAR and NextGen
Even though the nomenclature and scopes of SESAR and NextGen differ in certain aspects, their concepts are in principle compatible [UM08]. Without loss of generality the terms Business Development Trajectory (BDT), Shared Business Development Trajectory (SBT), Reference Business Trajectory (RBT) and Predicted Trajectory (PT) will be used to reference SESAR's trajectory life-cycle.

1.4 Motivation and goals of this thesis

Compared to the history of civil aviation the concept of self-separation which emerged in the mid 1990s is quite young. A good overview on the development of the Air Traffic Management system and the birth of the *free flight* concept is given by Ruiz. As of [Rui02] the *International Civil Aviation Organisation* created in 1989 a Special Committee for coordination and monitoring of the development of the *Future Air Navigation System* (FANS). In 1993 the work of this committee was concluded with the FANS concept which is also known as the CNS/ATM (Communications, Navigations, Surveillance/Air Traffic Management) system.
This gave birth to the idea of *free flight*[9]. Following this, both the *Federal Aviation Administration* (FAA) and the *European Organisation for the Safety of Air Navigation* (EUROCONTROL) initiated projects aiming at implementation of the Future Air Navigation System (FANS). In 1995 the *Radio Technical Commission for Aeronautics* (RTCA) proposed based on the FANS concept an incremental approach from the current ATC to an ATM system enabling free flight [Tas95] (cf. Figure 1.7). Notably, even though some steps have been achieved like introduction of Reduced Vertical Separation Minima (RVSM) in oceanic airspace or the design of Area Navigation (RNAV) procedurs [Nav], self-separation is not even in low-density airspace current operational practice for IFR flights. Reason for this might be that the

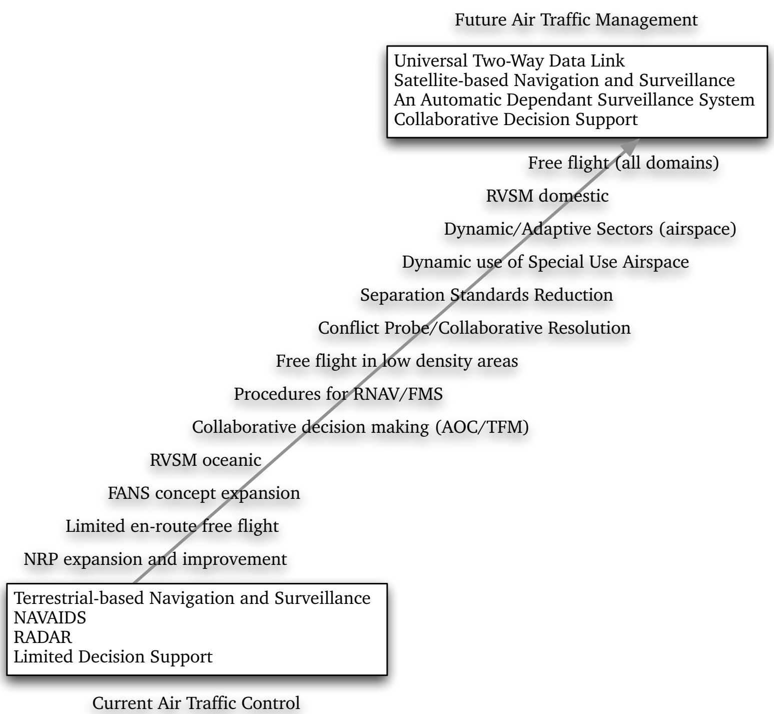

Figure 1.7: Approach to the future ATM system (after [Tas95])

9 This concept is also frequently referred to as *Airborne Separation Assurance* or *autonomous operations*.

subject of self-separation is still a matter of research and numerous systems up to the Human Machine Interface are concerned.
In a first step towards the future ATM system, the FAA initiated *Free Flight Phase 1* in 1998. On the other side of the Atlantic ocean EUROCONTROL included the free flight concept in 1999 in its *European Air Traffic Management System Operational Concept Document (OCD)* (reference to [Eur] in [Rui02]).

1.4.1 Airborne Conflict Detection & Resolution

Central to the future Air Traffic Management operational concept is the delegation of the task of separation provision from Air Traffic Control to the flight deck crews. In order to be able to fulfil this new task, aircraft are required to implement means for Airborne Conflict Management [SC 00b] which is comprised of

- Conflict Detection,
- Conflict Prevention *and*
- Conflict Resolution [SC 00b].

A high degree of automation is required to enable Airborne Conflict Management. On-board systems will need to be able to identify violation of separation minima in a *strategic*, i.e. long-term timeframe (cf. Section A.3 for an overview on terminology regarding time frames). Resolutions for these conflicts need to be computed in order to offer the flight deck crew an alternative routing. In case coordination with other traffic participants is required, those updated trajectories need to be communicated, shared and validated. This has to be achieved independent of ground infrastructure.
One of the goals of this thesis is to describe a system allowing for Airborne Conflict Management and to embed it into the complete ATM system as outlined in the concepts of operations [Ses; Nexa]. System dependencies and interactions will be described therefore.

1.4.2 Guaranteeing flyability

Common to all approaches to airborne Conflict Resolution is the requirement that the resulting trajectory needs to be actually flyable by the aircraft. This may be guaranteed by

- allowing only manoeuvres up to a certain complexity (e.g. *Dubins curves* [Too+07]),
- limiting the resolution to one dimension (e.g. restricted to vertical manoeuvres as in TCAS version II [Tca]),
- allowing only basic manoeuvres which need to be executed manually (e.g. GPWS *Pull up* command [SC 76]) *or*
- by constraining the path search algorithm (e.g. by adding non-linar constraints [Rag+04]).

It is obvious that this requirement is necessary to be met by the Conflict Resolution algorithm since otherwise such a system would not be operationally acceptable. Therefore it is one of the goals of this work to design a Conflict Resolution (CR) system which guarantees the flyability of the resulting trajectory by design.

1.4.3 Integration of Cost Index

Aircraft operators today use the Flight Management System Cost Index [Fms] to achieve minimum trip costs. The Cost Index denotes the ratio between time and fuel-related costs which differ depending on the operator's business model [Sch08]. While one of the benefits expected with the introduction of *Autonomous Operations Area* airspace is that airspace users will be able to fly on their preferred routes and flight levels and thus to achieve a more economic flight in respect to their business model, the Conflict Resolution required for operating in this airspace should not disregard the operator's goal. Different approaches to Conflict Resolution under consideration of constraints exist. Kuchar and Yang identified in their survey on Conflict Detection & Resolution systems the class of *Optimised Conflict Resolution* [KY97; KY00]. Caveat to many optimised Conflict Resolution approaches is the calculation time required to retrieve an *optimal* solution. Algorithms based on heuristic approaches try to mitigate this issue through limiting their search space a priori (e.g. [Too+07]). Though, this may lead to a resulting trajectory which generation process might not be easily traceable by the flight deck crews.

This work surveys how the Cost Index can be integrated into the Conflict Resolution process to allow for prioritisation of the manoeuvres.

1.5 Structure of this thesis

This thesis is organised in eight chapters and is concluded by seven appendices.

The present chapter introduced the challenges in the evolvement of air traffic and the necessities for changing the current Air Traffic Management concept. The goals of this thesis, to integrate the Cost Index into the Conflict Resolution process and to compute a flyable trajectory have been described and a rationale for this was given.

An overview on the fundamentals of Autonomous Operations Area airspace and the systems required to operate in this airspace area is given in Chapter 2. The current state of research will be visited in this chapter in respect to the issues identified in Chapter 1. Furthermore, some general definitions will be given which are required for the subsequent chapters. Chapter 3 and Chapter 4 present the concept for a Conflict Detection and Conflict Resolution system. The emphasis of this thesis lies on the Conflict Resolution system which will be extended to allow for integration of a prioritisation criteria regarding fuel- and time-costs. Therefore, Chapter 4 will detail the Conflict Resolution algorithm devised in this work to achieve the aforementioned goals. Chapter 5 describes the realisation of the concept, gives an overview on the class architecture and the evaluation workflow to be applied. The evaluation environment and the variables to be compared are summarised in the setup and scenario descriptions in Chapter 6. In Chapter 7, the evaluation and the results are described. This thesis is concluded with a summary and outlook in Chapter 8.

Further information can be found in the appendices. Some further definitions are summarised in Appendix A. Information regarding separation minima in the airspace areas used for evaluations in this work are given in Appendix B. Tables and figures detailing the evaluation runs are presented in Appendix C. The system devised in this thesis uses information which is part of the ADS-B dataset. This information is used by Conflict Detection and Conflict Resolution. The Conflict Detection algorithm is based on the TCAS system. Information on ADS-B and TCAS are summarised in Appendix E. Appendix D and Appendix F summarise further information on the data sources used in this work and the BADA parameters used for performance calculations. Further details on the algorithms devised in this work may be found in Appendix G.

2 Fundamentals and current state of research

> I think nuclear-powered aeroplanes are the answer beyond 2050.
>
> Ian Poll, Professor of Aerospace Engineering at Cranfield University, 2008.

Opposed to the early years of commercial aviation, today's aircraft are equipped with technologies such as Traffic Collision Avoidance System (TCAS) or Automatic Dependant Surveillance - Broadcast (ADS-B) which allow them to detect other aircraft which may pose a threat due to infringement of ownship's protection zone[1]. In order to allow aircraft to operate autonomously in certain, dedicated airspace areas as it is foreseen within the ICAO Global ATM concept and both the SESAR and the NextGen concepts of operation, it is necessary to enable them to not only detect but also to resolve a conflict, thus to allow them to fulfil the delegated task of separation assurance.
This chapter is concerned with fundamentals on Autonomous Operations Area airspace and the current state of research. Section 2.1 gives information on the context of Autonomous Operations Area airspace and introduces a common terminology. The current operational practice in the *Cruise* phase and the means to optimise the flight are summarised in Section 2.2. Section 2.3 is dedicated to a distinction between Conflict Detection & Resolution approaches. The current state of research with focus on Conflict Resolution is presented with a choice of concepts from literature in Section 2.4. A high-level concept for the Conflict Detection & Resolution system devised in this work is derived in Section 2.5. Finally, Section 2.6 concludes this chapter with a summary on the findings.

2.1 Introduction

Flights which require a flight plan to be filed before conduction should not get in conflict with other traffic or terrain during perfect day operations. Safety margins are set up in such a way that aircraft, when flying on the same or intersecting routes, will not infringe other aircraft's protection zones. In the context of SESAR, the Reference Business Trajectory (RBT) has been introduced which represents the aircraft's planned 4D trajectory [Ses] (cf. paragraph 1.3). A number of events, such as separation provision, diversion or failure to comply with the Reference Business Trajectory, may require an update of it. In such a case the aircraft systems are to calculate a Predicted Trajectory (PT) which either guides the aircraft back to its Reference Business Trajectory or which is valid until the RBT can be rejoined (cf. Figure 2.1). Once a PT which rejoins the initial RBT has been successfully calculated, this trajectory becomes the new RBT.

2.1.1 The 4D trajectory

The *4D trajectory* has become the primary mean of representation of the aircraft's flight path in modern Flight Management Systems [How90] and in the context of SESAR and NextGen. Other than in a flight plan, the 4D trajectory does not necessarily include *Waypoints* but *Trajectory Change Points*, which are points where a new heading, a new speed or flight level are commanded. A more detailed description

[1] The first Mid-Air Collision of commercial airliners took place on the 7th of April 1922 between a French and a British biplane [Nyt]

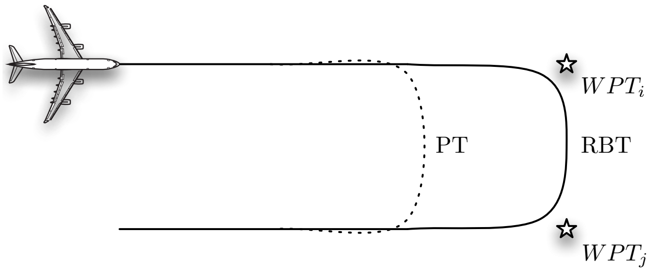

Figure 2.1: Reference Business Trajectory and Predicted Trajectory

for Trajectory Change Points from [SC 02] defines them as points '[...] where an anticipated change in the aircraft's velocity vector will cause an intended change in trajectory [...]'.
Commencing from a definition for the *position of an aircraft* in the following a formal description for Trajectory Change Points is derived for further reference in this work.

Definition 2.1 (Aircraft Position). *The position of an aircraft* acr_n *is a 3-Tupel* $p \in \mathscr{P}, p = \{(x, y, z) | x, y, z \in \mathbb{R}\}$. x *and* y *describe the lateral and longitudinal position of the aircraft, whereas the elevation is described by* z.

For two positions p_1 and p_2 as of Definition 2.1 the distances are defined as

$$\text{horizontal distance}: \quad p_1 -_h p_2 = r \cdot 2 \cdot \operatorname{atan2}\left(\sqrt{a}, \sqrt{1-a}\right) \tag{2.1}$$

$$\text{with} \quad a = \sin\left(\frac{x_2 - x_1}{2}\right)^2 + \cos(x_1) \cdot \cos(x_2) \cdot \sin\left(\frac{y_2 - y_1}{2}\right)^2 \tag{2.2}$$

$$\text{vertical distance}: \quad p_1 -_v p_2 = z_1 - z_2 \tag{2.3}$$

Equation 2.1 and Equation 2.2 are the *Haversine* formula for calculation of great circle distances between two points on an ellipsoid [The06]. In Equation 2.1, r denotes the radius of the ellipsoid; in Equation 2.2, x_1, x_2 and y_1, y_2 are given in radians. Further information on distance calculation may be found in [Map]. Vertical distance (Equation 2.3) is the difference between z_1 and z_2 in meters.
In order to be able to describe a four dimensional trajectory, it is necessary to specify the position of an aircraft with a time t. The time t can be compared to *Universal Time Coordinated* (UTC) which should be synchronous on all aircraft within ±1 minute [Ari, Section 4.3.1.7].

Definition 2.2 (Trajectory Point). *A Trajectory Point* $tp_n \in \mathscr{T}, n \in \mathbb{N}$ *is a Tupel* $tp = \{(p, t) | p \in \mathscr{P}, t \in \mathbb{N}\}$, *where* p *is an aircraft position as of Definition 2.1 and* t *a discrete point in time. The relations* $<_t$, $=_t$ *and* $>_t$ *for two trajectory points are defined by their time attributes.*

Definition 2.2 allows to set up an order on the trajectory points. For two trajectory points $tp_n = (p_n, t_n)$ and $tp_m = (p_m, t_m)$ the following holds true:

$$tp_n <_t tp_m \Leftrightarrow t_n < t_m$$
$$tp_n =_t tp_m \Leftrightarrow t_n = t_m$$
$$tp_n >_t tp_m \Leftrightarrow t_n > t_m$$

Definition 2.3 (Trajectory Change Point). *A trajectory point is a Trajectory Change Point if for two TPs* $tp_n = (p_n, t_n), tp_m = (p_m, t_m)$ *with* $t_n < t_m$ *at least one of the following constraints hold true:*

- $[\psi_{c,n}] \neq [\psi_{c,m}]$
- $[h_{c,n}] \neq [h_{c,m}]$

- $[V_{TAS,c,n}] \neq [V_{TAS,c,m}]$.

Here ψ_c*,* h_c *and* $V_{TAS,c}$ *refer to the* commanded *variables.*

Definition 2.4 (Minimal TCP set)**.** *A set of Trajectory Change Points* $\mathcal{T}_{TCP}$ *is said to be minimal, if removal of one TCP* $tp_n \in \mathcal{T}_{TCP}$*, would cause this point not being passed within the boundaries given through the requirements regarding lateral (Required Navigational Performance,* $\Delta\lambda^{\diamond}_{max}$*), vertical (*$\Delta h_{max}$*) or temporal (Estimated Time Over,* Δt_{max}*) adherence to the planned trajectory.*

In SESAR the Trajectory Management Requirements are introduced to set limitations regarding adherence to the 4D trajectory which may vary depending on the airspace type and look-ahead time [Ses]. Finally, Definition 2.5 introduces a *trajectory segment* which is a connection between two Trajectory Change Points.

Definition 2.5 (Trajectory Segment)**.** *A trajectory segment of* acr_i *is a tupel* $\mathrm{ts} = (tp_n, tp_m), tp_n, tp_m \in \mathcal{T}_{acr_i}, tp_n <_t tp_m$ *and* $\nexists tp_x \in \mathcal{T}_{acr_i}$ *for which* $tp_n <_t tp_x <_t tp_m$*.*

As of Definition 2.5 a trajectory segment is a connection between two in time ordered Trajectory Change Points between which no other Trajectory Change Point exists.
The benefit of the availability of 4D Trajectory data has been inter-alia evaluated in the European Research project North European ADS-B Network Update Programme, Phase II+ (NUP2+)[Con05]. The approach followed in NUP2+ included downlinking Flight Management System (FMS) Estimated Time of Arrival (ETA) data to the destinations airport Arrival Manager (AMAN).

2.1.2 Flight phases and aircraft specification

A flight is subdivided into different phases. Depending on the context in which a flight is described, several (partially) overlapping definitions exist which may be defined according to the workload [Bar+06] or to the configuration of the aircraft, respectively the aircraft performance [Nui04b; Sch08]. In general, most definitions concur regarding the *Cruise* phase which is also referred to as *en-route* phase. This work is concerned with this phase which is usually bounded by the *Top of Climb* (T/C or TOC) and *Top of Descent* (T/D or TOD) [A34a; A34b] as illustrated in Figure 2.2.

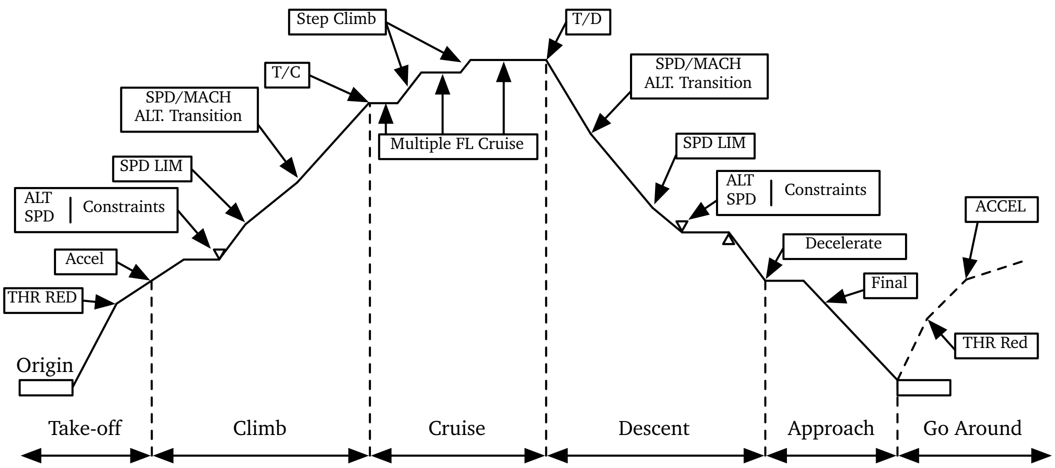

Figure 2.2: Flight plan - Vertical definition (after [A34b])

The Cruise phase

Depending on the aircraft type, different minima and maxima speeds and altitudes exist. The Base of Aircraft Data by EUROCONTROL provides for several aircraft parameters in respect to the flight phase

[Nui04b]. As of BADA, the minimum speed for jet aircraft in cruise configuration at an altitude larger than 15.000ft ($= 4572m$) is calculated via

$$V_{min} = \max(1.3 \cdot V_{stall}, M_b) \text{ [Nui04b].} \tag{2.4}$$

While M_b is a function of the lift coefficient, an initial buffet onset lift coefficient, actual pressure, the current Mach number, the wing reference area and the aircraft weight, V_{stall} (among other parameters) is provided for each modeled aircraft in the Base of Aircraft Data (BADA) aircraft performance operational file. For the scope of this work it is assumed that an aircraft is moving at least at $V_{min} = 1.3 \cdot V_{stall}$.
The parameters given in the BADA *Operations Performance File* for each aircraft are also used to calculate the maximum operating speed V_{MO} in knots, the maximum operational Mach number M_{MO} and the maximum operational height h_{MO}.
Without limiting the scope of this work, in the following two *Long Range* aircraft will be used. The *Airbus A340-300* and *Boeing 747-400* have been chosen since both aircraft had in their categories the highest traffic share in European airspace in 2004 [She04] (cf. Table 2.1). For both aircraft, Table 2.2

Table 2.1: Traffic shares, wake and range classes for selected aircraft [She04]

Aircraft Type	Wake Class	Range	Share Traffic
A340-300	Heavy	Long	0,8876%
747-400	Heavy	Long	1,6642%

summarises the minimum and maximum speeds as given through Equation 2.4 and the BADA Operations Performance File (OPF).

Table 2.2: Minimum and maximum speeds for selected aircraft [Bad]

Aircraft Type	V_{min} [kts]	V_{MO} [kts]	M_{MO} [Mach]	h_{min} [ft]	h_{max} [ft]
A340-300	184,6	330	0,86	10000	41000
747-400	237,9	365	0,92	10000	45000

Simplifying definitions
For the scope of this work several simplifications are made in respect to environmental conditions.
It is assumed that still-air condition is given, i.e. neither head-, tail- nor crosswind components add or subtract from the ground speed. Thus, during level flight the True Airspeed equals the Ground Speed:

$$V_{TAS} = V_{GS} \tag{2.5}$$

Furthermore, the aerodynamic force lies in the plane of symmetry of the aircraft, resulting in an equality of heading and track:

$$\psi = \chi \tag{2.6}$$

Regarding transmission of information between aircraft no latencies are considered. The positional accuracy is as well ideal.

2.1.3 Description of a conflict

Before an algorithm can detect a conflict, the conflict needs to be properly defined. An aircraft that causes a conflict or is about to cause a conflict is considered as a *threat* to ownship. In the context of Airborne Collision Avoidance Systems (ACASs), ICAO introduces the term *threat* as any intruder which deserves

> *special attention either because of its close proximity to own aircraft or because successive range and altitude measurements indicate that it could be on a collision or near-collision course with own aircraft [ICA02, pp. 4-2].*

whereas the *intruder* is defined as

> *An SSR*[2] *transponder-equipped aircraft within the surveillance range of ACAS for which ACAS has an established track [ICA02, pp. 4-2].*

To allow for definition and implementation of the Conflict Detection & Resolution (CD&R) system, these definitions need to be formalised. In the following, ownship (i.e. the aircraft detecting a conflict and calculating a resolution) is designated as acr_o and intruder as acr_i. An additional index will distinguish multiple intruders where necessary.

Definition 2.6 (Conflict). *An aircraft* acr_o *is in* conflict *to another aircraft (or object)* acr_i *if its current applicable protection zone* Z *(cf. Definition 3.1) is infringed, thus if* $p_i \in Z$*.*

This definition can be applied to any kind of object and also be extended to zones, e.g. bad weather areas Z_W where a conflict would be defined as the non empty intersection between Z_W and Z. For the scope of this work only conflicts between aircraft will be considered.

2.2 Current operational practice during Cruise

During the *Cruise* phase, flight deck crews of modern airliners usually use the *Flight Management System* (FMS) for navigation and control of the aircraft. The FMS is a tool intended to support the flight deck crew to achieve an efficient and economic flight and calculates therefore a three- or four-dimensional trajectory for a given flight plan [BW01; How90]. These calculations may also take environmental conditions such as wind into consideration [Ari; A34a]. The Flight Management System acts as an interface between the flight deck crew, the navigation system and the flight control system [Bro01].
The Flight Management System is on the outer control loop of aircraft flight control, flight guidance and flight management architecture as illustrated in Figure 2.3 for a Fly by wire (FBW) aircraft. It is concerned with the actual *flight mission* and has as primary mean for interaction the Multipurpose Control Display Unit (MCDU). The FMS interfaces the Auto Flight Director System (AFDS) as described in the following. Based on the flight plan and aircraft specific parameters, the FMS's flight guidance function computes a vertical (VNAV) and lateral profile (LNAV). The Lateral Navigation (LNAV) function at least requires information on

1. current aircraft position *and*
2. active route

to compute the lateral profile. It compares the current horizontal position of the aircraft to the flight plan derived required position. In case of deviations larger than the Required Navigational Performance,

[2] Secondary Surveillance Radar

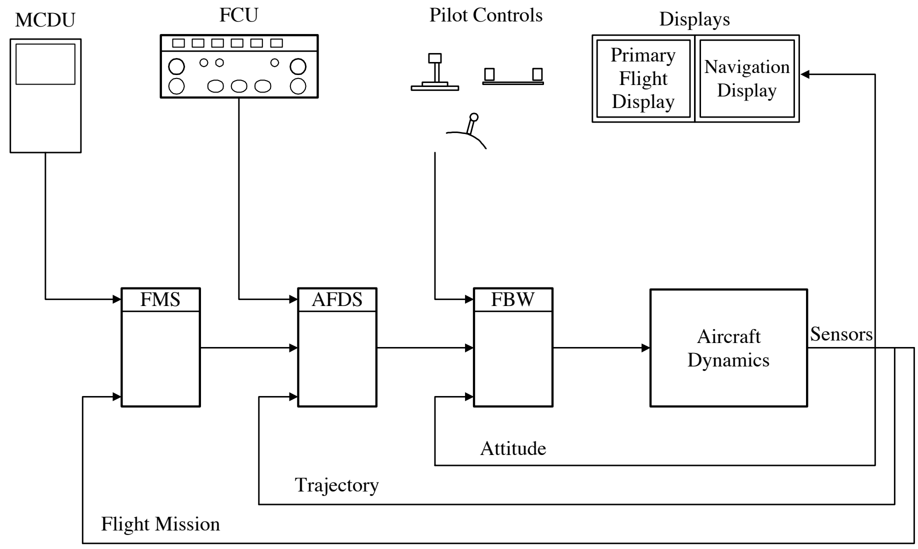

Figure 2.3: Schematic of control loops of flight controls, dynamics and management (from [MS08])

the FMS commands the necessary control signals to the AFDS to guide the aircraft back to the required flight path [BW01][3].
Other than the LNAV function, the Vertical Navigation (VNAV) function also takes the Cost Index into account for its computations. The VNAV function requires for its computation at least information on

1. aircraft gross weight,
2. Cost Index *and*
3. cruise altitude.

The VNAV function controls pitch θ and thrust T within the flight plan given boundaries [BW01]. Both functions also take constraints from Air Traffic Control into account which may be uploaded automatically via data-link or entered by the flight deck crew via the Multipurpose Control Display Unit (MCDU). Figure 2.4 illustrates the architecture of a generic FMS as described in [Ari].

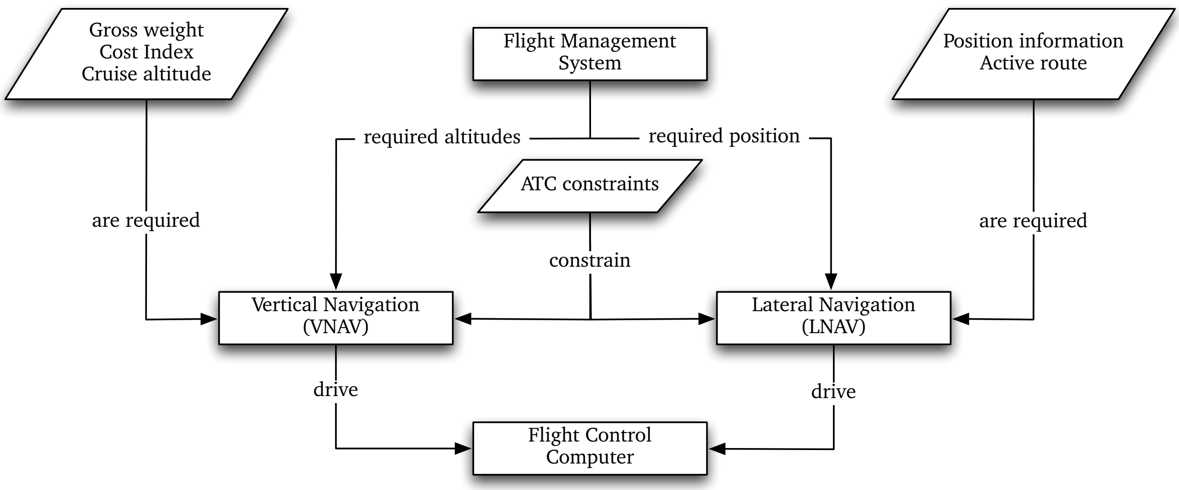

Figure 2.4: Architecture of a FMS as of [Ari]

3 The LNAV guidance function controls roll ρ [How90].

Optimisation of the flight plan

The operational costs of an airline can be subdivided into direct and indirect operational costs. Among the indirect costs, items are summarised such as *Station & Ground* costs or *Passenger Service* costs. The *direct operating costs* include as major cost item *fuel* costs [Bad06]. Due to rising fuel prizes – the cost for one gallon jet fuel grew from about 60¢ in 1990 to 195¢ in 2006 [U.S] (Figure 2.5) which is a raise by more than 200%. – the direct operating costs have become dominant. Especially due to the importance

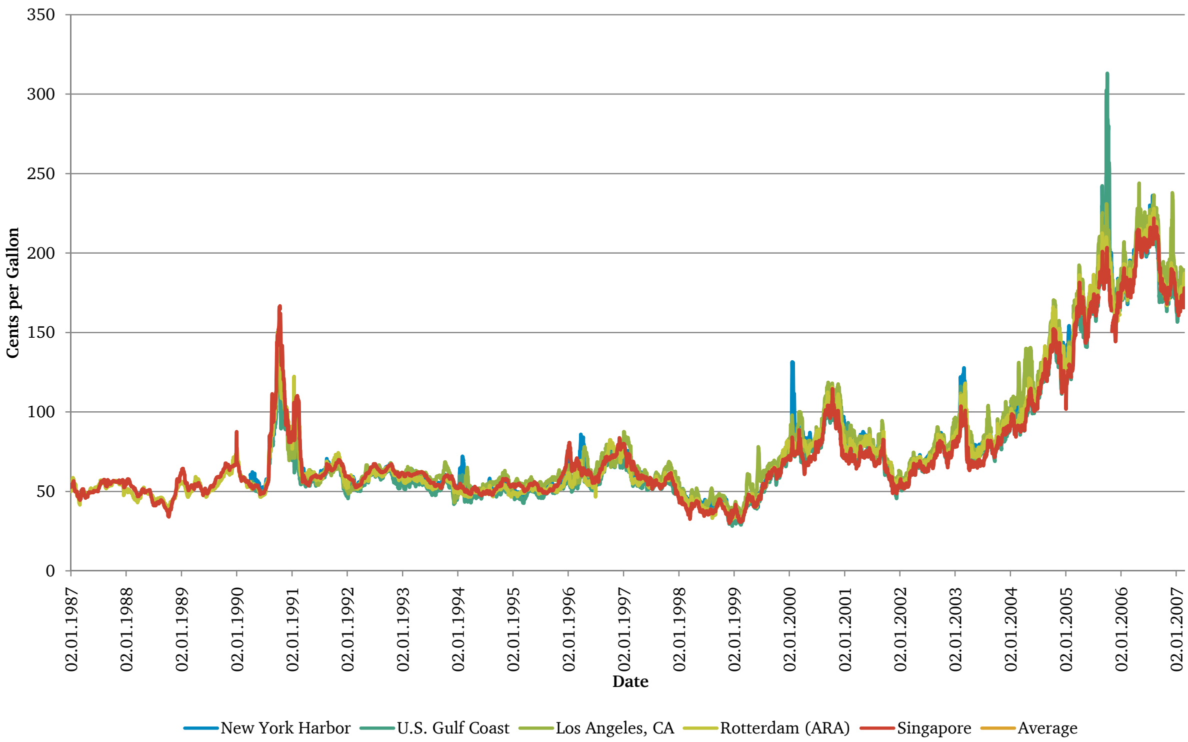

Figure 2.5: Jet Fuel Prices (data from [U.S])

of fuel costs, the optimisation of these costs in respect to the operators cost structure and policy has gained importance. One of the tools available to the operator to *optimise* the fuel consumption is the Flight Management System *Cost Index* (CI). In current Flight Management Systems it impacts during the *Cruise* phase the climb strategy, i.e. the number and positions of step climbs and by this the vertical profile, and ECON MACH and ECON SPEED [A34a; Fms]. Figure 2.6 illustrates the ECON MACH number which is the vertex of the *Direct operating costs* curve. With the CI, the operator can set the ratio between *time costs* $C_T[\frac{€}{min}]$ and *fuel costs* $C_F[\frac{€}{kg}]$ which is scaled depending to the manufacturer to the respective minimum and maximum values [Fms] to his preference. The effect of the CI to the total costs of a trip are given in Equation 2.7 and Equation 2.8.

$$C = C_F \cdot \Delta F + C_T \cdot \Delta T + C_C \tag{2.7}$$

$$CI = \frac{C_T}{C_F} \tag{2.8}$$

with

C_C	fixed costs - independent of time [€]
ΔF	trip fuel [kg]
ΔT	trip time [min].

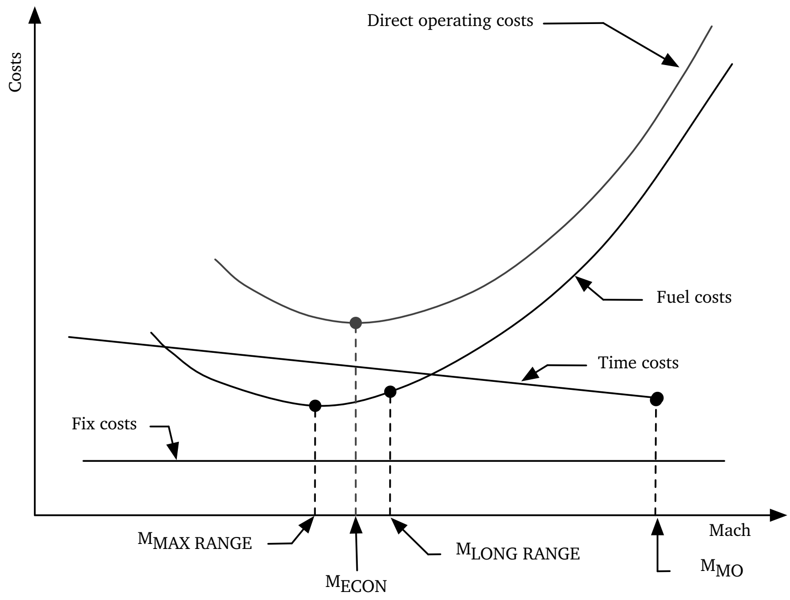

Figure 2.6: ECON Mach depending on actual costs (after [Sch08])

Depending on the manufacturer of the FMS, the CI varies from 0 to 99 (Smith FMS) or from 0 to 999 (Sperry/Honeywell) [Fms]. Taking the Airbus A340 with a Honeywell FMS as reference, the CI setting is as follows:

CI = 0	minimum fuel consumption ⇒ maximum range
CI = 999	minimum time
CI = LRC	Long Range Cruise

Beside ECON SPEED/ECON MACH, two further operationally important settings independent of the Cost Index setting are *Long Range Cruise* (LRC) and *Maximum Range Cruise* (MRC) which are both defined in respect to the aircraft's *Specific Air Range* (SAR) (cf. Figure 2.6). The SAR describes the distance an aircraft can fly with a given amount of fuel. Usually it is given in $\frac{m}{kg}$ or $\frac{nm}{lb}$. The SAR is a function of True Airspeed (TAS) V_{TAS}, altitude h, aircraft mass m and depends on the current aircraft configuration. LRC specifies a Mach setting where the aircraft's Specific Air Range is approximately 1% below its maximum at a significant gain in trip time [Kli07], while MRC specifies a Mach setting where the aircraft's Specific Air Range is maximal.

Current application of flight path optimisation

The Cost Index influences the numbers and positions of step climbs during the cruise phase and, if speed is set to FMS *managed* and either ECON MACH or ECON SPEED are selected, also the aircraft's speed.

The possibility to operate the aircraft according to the FMS computed *optimised* trajectory is limited by airspace constraints. Step climbs which are required to follow the optimal altitude need to be requested and approved by ATC. Variable speeds such as ECON SPEED/MACH which *inter alia* depend on the current altitude, wind and aircraft weight are not always feasible as in the North Atlantic Organised Track System airspace where the Mach number technique (i.e. a constant Mach number is requested from ATC and maintained upon entering this airspace area, cf. Section B.1) is used for assuring safe separation. With this, the impact of the Cost Index on the actual flight profile is severely constrained.

2.3 Distinction between Conflict Detection & Resolution systems

Current operational procedure for most airspace areas is, that Air Traffic Control is responsible for detection of violation of separation minima and assignment of proper resolution manoeuvres[4]. Beside this, passenger aircraft with more than 30 seats are required to carry an *Airborne Collision Avoidance System* (ACAS) as a *safety net* function. This system comes into action as a last ressort when the minimum separation has been or is about to be violated in the imminent future. The time frame of such a system is usually a few minutes at most.

As outlined in Section 1.3, autonomous Conflict Detection & Resolution is still a matter of research. Numerous approaches exist which differ in their goals, the models they use and the manoeuvres they allow for resolution. Kuchar and Yang conducted a frequently referenced survey on Conflict Detection & Resolution approaches (see e.g. [KF02; GM02; AG06; EE99; Ges+02]), in which they categorised 62 approaches regarding the basic functional requirements of a Conflict Detection & Resolution system into different phases as illustrated in Figure 2.7 [KY97; KY00].

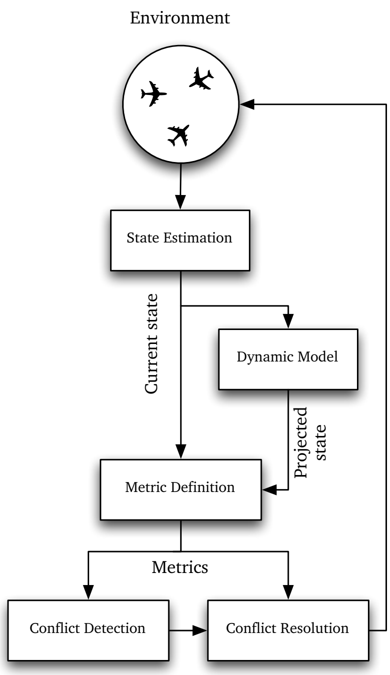

Figure 2.7: Conflict Detection & Resolution (after [KY97])

The steps outlined by Kuchar and Yang detail the separation provision process as of [ICA05b] (see also Section 1.2) further. Based on position and intent information of other aircraft, their current and projected states are used to calculate metrics such as the distance at the Closest Point of Approach. These information are passed to Conflict Detection and Conflict Resolution. The latter calculates a resolution if necessary. The projection of the current state into the future requires a (dynamic) model. Kuchar and Yang partitioned in this survey the approaches in respect to this model (Figure 2.8(a)) and to the Conflict Detection & Resolution approach (Figure 2.8(b)).

4 One exception is the Inflight Broadcast Procedure (IFBP) area where this task is already delegated to the flight deck crews [Bau+06]. Further information on this area may be found in Section B.2

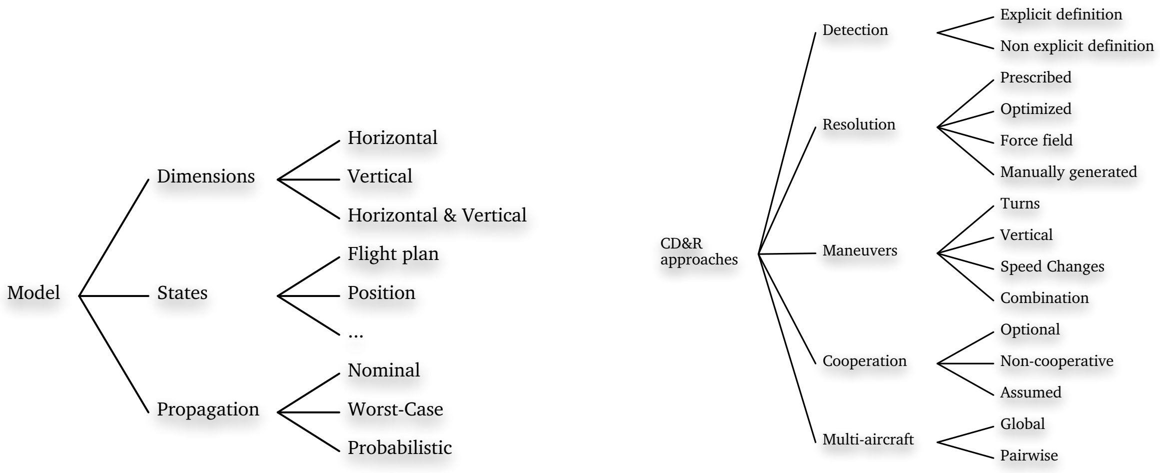

(a) Modelling approaches (b) Conflict Detection & Resolution process

Figure 2.8: Partitioning of ACM approaches as of [KY97]

2.3.1 Modelling approaches

Kuchar and Yang distinguish the modelling approaches of the CD&R algorithms surveyed by the *dimensions* they cover, the *state variables* and the *propagation model* they use [KY97].

Dimension
The *dimension* relates to the planes the model involves, i.e. the horizontal plane, the vertical plane or both planes. Depending on the threat the Conflict Detection & Resolution system addresses, limitation to one plane might be favourable (due e.g. to complexity) or even necessary. The Ground Proximity Warning System for example is such a CD&R system which is limited to the vertical plane.

State
Another discriminating information are the *state* variables used by the algorithm to derive the current and future state of aircraft. This may include information on current position and speed vector, the flight plan, the closing speed or similar states.

Propagation
Regarding the propagation model, three different approaches were identified by Kuchar and Yang. Using *nominal propagation*, the current states of the aircraft are projected into the future without consideration of any uncertainties. On the opposite, with *worst case* propagation, certain aircraft states are set to extreme values and are then projected into the future. Similar to worst case propagation, *probabilistic propagation* assumes for certain state values deviations which are extended by a probability value. With both propagation models, *probabilistic* and *worst case*, the area in which the aircraft could be grows with the propagation time. It is important to note, that the more precise the knowledge about the trajectories is, the better are conflict detection and resolution [WE98].

2.3.2 Conflict Detection & Resolution approaches

Regarding the Conflict Detection & Resolution approaches, Kuchar and Yang introduced as discriminating parameters the requirement of an explicit *detection* of the conflict, the *resolution* techniques, the allowed *manoeuvres*, the aspect of *cooperation* and the approach towards the solution of *multi-aircraft* conflicts.

Conflict Detection approach

In respect to *Conflict Detection*, Kuchar and Yang distinguish between *explicit* and *non explicit* detection. While in the first case, the model explicitly defines when a conflict has been detected and hence a resolution is necessary (e.g. based on the distance at the Closest Point of Approach), this is not the case with *non explicit* models. Here, no explicit threshold and no clear distinction between *conflict* and *non-conflict* exist.

Conflict Resolution approach

The Conflict Resolution approach is distinguished in four classes. Conflict Resolution based on *prescribed resolution manoeuvres* requires a set of input conditions (e.g. current altitude, Flight Path Angle and configuration) and manoeuvres (e.g. *Pull-up*) or actions. Based on the set of input conditions, the algorithm decides which manoeuvre to select for resolution. Conflict Resolution systems like the Ground Proximity Warning System [SC 76] and the Runway Collision Avoidance Function [SZZM07] are based on prescribed resolution manoeuvres. *Optimisation approaches* either calculate based on a pre-defined cost function or choose from a pre-calculated set of Conflict Resolution manoeuvres. Kuchar and Yang name '[...] game theory, genetic algorithms, expert systems, or fuzzy control [...]' [KY00] as underlying techniques for optimisation approaches. With the Traffic Collision Avoidance System (TCAS) they also give an example for a system based on an optimisation approach. TCAS selects from a pre-computed set of resolution manoeuvres '[...] the least-aggressive manoeuvre that still provides adequate protection.' [KY00]. Conflict Resolution based on *artificial force* or *potential fields* models[5] '[...] treat each aircraft as a charged particle and use modified electrostatic equations to generate resolution maneuvers.' [KY00]. According to a further comparison of Conflict Detection & Resolution approaches by Chaloulos et al., artificial/potential field methods are not popular in aircraft CD&R due to the inability to '[...] ensure bounded inputs that are feasible with respect to the aircraft performance.' [Cha+07]. Finally, *manually generated* Conflict Resolution approaches depend on an external, non automatic source (e.g. flight deck crew, Air Traffic Control Officer) to propose a new trajectory resolving the conflict. In case the proposed trajectory does not resolve the conflict, the system asks for a new proposal.

Allowed manoeuvres

A Conflict Resolution system may limit itself to certain resolution manoeuvres. For example the Traffic Collision Avoidance System (Version II) only allows for vertical resolution manoeuvres. The principle manoeuvre types are *horizontal* (referred to as *turns* in [KY97; KY00]), *vertical*, *speed* manoeuvres or a *combination* thereof.

Cooperation

Cooperation relates to the acceptance '[...] of some form of cooperative solution between aircraft.' [KY97]. The three distinctions made are *non-cooperative* where no cooperation is assumed, *cooperative* where aircraft coordinate their actions (referred to as *Assumed* by Kuchar and Yang) or *optional*. Chaloulos et al. detail the distinction *non-cooperative* manoeuvres further by assuming that '[...] each aircraft solves the situation without a coordination with the conflicting aircraft [...]' [Cha+07], which requires that all aircraft that are part of the conflict have also detected it. They point out that problems arising from non-coordinated CR manoeuvres – like aircraft generating new conflicting trajectories – may be mitigated through *implict* coordination which is based on compatible algorithms or through the application of certain rules.

Multi-aircraft

Regarding resolution of multi-aircraft conflicts, a distinction is made between the *global* approach with which all aircraft conflicts are resolved simultaneously and the *pairwise* approach. With the latter approach the conflicts are resolved sequentially.

[5] This approach to Conflict Resolution originates in the field of robotics [III00; Zeg98].

2.3.3 Implementation of Conflict Resolution approaches

Regarding the implementation of the Conflict Resolution algorithm also different approaches have been identified. Anderson and Goodchild distinguish in their survey on candidate functional logic processes and algorithms for safe separation technologies [AG06] between *adjoined* and *embedded* forms of the Conflict Resolution implementation which depends on the formulation of the Conflict Resolution process.

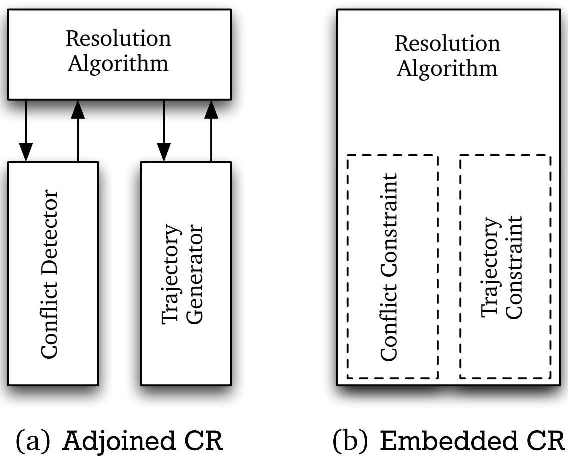

Figure 2.9: Distinction between Conflict Resolution (CR) forms (from [AG06, Figure 9])

Anderson and Goodchild describe therefore the CR process by three principal generic components, the *resolution algorithm*, the *conflict detector* and the *trajectory generator*. The *resolution algorithm* determines the control values to achieve a conflict-free trajectory while respecting constraints provided by the *conflict detector* and the *trajectory generator*. The *conflict detector* computes the constraints by testing against a conflict metric with pre-defined thresholds (i.e. separation minima). The *trajectory generator* constraints the resolution by providing it with only feasible trajectories, i.e. trajectories which respect certain flight mechanical constraints.

Adjoined Conflict Resolution
In this approach the resolution algorithm, the conflict detector and the trajectory generator are separate and exchangeable[6] processes (cf. Figure 2.9(a)). Anderson and Goodchild state, that this modularity constitutes the advantage of the approach while a formal safety verification may be difficult.

Embedded Conflict Resolution
The *conflict detector* and *trajectory generator* are defined implicitly in the CR process. Constraints given through the conflict(s) and flyability requirements and the trajectory are integrated into the CR process (cf. Figure 2.9(b)). Lack of transparency through the integration of conflict and trajectory contraints in the CR algorithm is according to Anderson and Goodchild the main disadvantage.

2.4 Selected works from current research

The Autonomous Operations Area (AOA) concept requires enhancements and new technologies in numerous areas such as *digital data exchange*, *Collaborative Decision Making tools* and novell *Human Machine Interfaces* for visualization of conflicts and illustration of alternative trajectories. This section is

[6] if the same interface is used

concerned with works in the area of *Conflict Resolution* algorithms which are at the core of any Airborne Conflict Management system, reflecting the fundamentals as well as the current progress made in this field in respect to the aeronautics domain. In the following, selected algorithms from the four classes identified by Kuchar and Yang will be presented, described and discussed in respect to the technique applied for *airborne Conflict Detection & Resolution*, how they *guarantee flyability of the resulting trajectory* and how it is achieved that the resolution respects certain *optimisation* parameters.

2.4.1 Prescribed resolution manoeuvres

A Conflict Resolution system based on *prescribed resolution manoeuvres* selects from a set of *a priori* available resolutions the most adequate. Two *safety-net* systems – one already operational and one currently under research – that implement the resolution in this way are the *Ground Proximity Warning System* (GPWS) [SC 76] and the *Runway Collision Avoidance Function* (RCAF) [SZZM07]. Another algorithm – which explicitly deals with resolution manoeuvres for the en-route phase in the context of free flight – has been devised for estimation of the impact of CR manoeuvres [BSC96].
The Ground Proximity Warning System (GPWS) and the Runway Collision Avoidance Function (RCAF) use information from on-board sensors to derive the current situation of the aircraft. The GPWS is directed towards resolution of terrain conflicts and implements a number of warnings which are activated when the aircraft is not properly configured while closing on terrain (e.g. landing gear not extended). The RCAF is intended to advice the flight deck crew on other traffic on the runway while being either configured for take-off or during approach. Both systems provide beside warnings also resolution advisories. Other than GPWS and RCAF the algorithm by Bilimoria, Sridhar, and Chatterji [BSC96] deals with the resolution of traffic conflicts while en-route. It derives the necessary changes to speed, altitude or heading from the geometry of the conflict. The choice what kind of manoeuvre is required (speed, altitude or heading change) is not dealt with by the algorithm. Consequently, combinations of manoeuvres are not possible as well.

Flyability of the resulting manoeuvre
Both *safety-net* systems leave the execution of the Conflict Resolution manoeuvre to the flight deck crews. The principle commands for resolution of a conflict are *Pull-up* (GPWS) and *Abort Take-off* or *Go-Around* (RCAF). The RCAF uses a model of the aircraft and information on current attitude and speed to decide whether the implementation of the resolution manoeuvre is feasible, e.g. whether the own aircraft can be brought to a stop before colliding with the intruder on the runway. The free-flight algorithm presented in [BSC96] does not constraint the resolution but the analysis of the effect of Conflict Resolutions using this algorithm assumes certain acceleration, bank and Flight Path Angle (FPA) maxima.

Optimisation
The Conflict Resolution algorithms of both systems do not take any optimisation criterion or a preference into account for their resolution. Especially the latter would also not be practicable for *safety-net* systems since GPWS and RCAF issue basic commands requiring the flight deck crew to either stop the aircraft (RCAF) or to gain altitude (RCAF and GPWS). Selection of the manoeuvre type is done by the user with Bilimoria, Sridhar, and Chatterji's algorithm. Beside this, no preferences are taken into account.

Application to Airborne Conflict Management
Algorithms based on prescribed resolution manoeuvres are feasible or – because no time-consuming computation for the resolution is required – may even be necessary for resolution of short term conflicts. Conflict Resolution algorithms which resolve conflicts in a *strategic* time-frame are not constrained by rigorous computation time limitations, which explains why in Kuchar and Yang's surveys only one out of five Conflict Resolution algorithms which use prescribed resolution manoeuvres is not concerned with

terrain, runway or approach conflict alerting [KY97; KY00]. The algorithm presented in [BSC96] was devised to estimate the effect of Conflict Resolution manoeuvres on free flight. Due to its focus on this analysis and its limitation to either lateral, vertical or speed resolutions, using this algorithm in an Airborne Conflict Management system would not be feasible.

2.4.2 Optimised resolution

Conflict Resolution algorithms which base on an *optimised resolution* implement a cost function which needs to be minimised. This cost function may include several parameters such as the fuel-flow or the distance to other aircraft. Optimised Conflict Resolution approaches are also already operational such as with the *Traffic Collision Avoidance System* (TCAS). Other algorithms, especially when they implement a heuristic approach to Conflict Resolution, are still under research.
An example for a Conflict Resolution algorithm using *rule based* optimisation is the resolution part of the TCAS system. Upon detection of a conflict, the TCAS systems of both aircraft coordinate their resolutions [Tca]. When the decision has been made whether to climb or descend, the TCAS algorithm selects from a set of potential climb and descend manoeuvres the least aggressive which still provides adequate protection [KY97].
Tooren et al. developed an algorithm for sense and avoid applications for Unmanned Aerial Vehicles (UAVs) based on search trees [Too+07]. For a given start and end point, the search tree algorithm calculates an alternative connection between the two points under the constraint of avoiding entry into an obstacle zone (cf. Figure 2.10). For each search node in the tree, a number of short trajectory segments

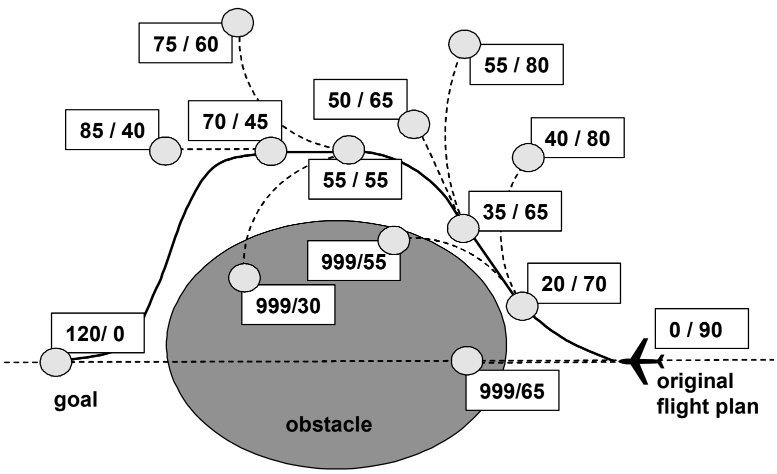

Figure 2.10: CD&R search tree illustration (from [Too+07])

are computed by a manoeuvre space generator. Also for UAV applications, Rathbun et al. present a path search algorithm to avoid moving into conflict areas based on genetic algorithms [Rat+02]. The *genetic* or *evolutionary algorithm* generates a *population* of alternative trajectories consisting of linear and curved path segments (limited to the horizontal plane) which are to connect a start point and an end point. With an initial set of possible paths, the current population is *mutated*, i.e. recombined to produce offsprings. The algorithm uses beside the standard evolutionary algorithm functions *mutate and propagate* and *crossover* [Kin94] also the functions *go to goal* and *mutate and match* as mutation mechanisms. The *go to goal* function uses a point-to-point join function to connect a segment near to the end with the goal location while *mutate and match* randomly calculates an alternative route for an existing segment and replaces it. The offsprings are evaluated and subsequently a selection will be used to create new offsprings. The selection is based on the evaluation, while – to avoid reaching a local minimum or maximum – also a certain percentage of not promising candidates usually is selected [Kin94]. If a minimum has been reached, the alternative path (trajectory) is returned. Figure 2.11 illustrates this process.

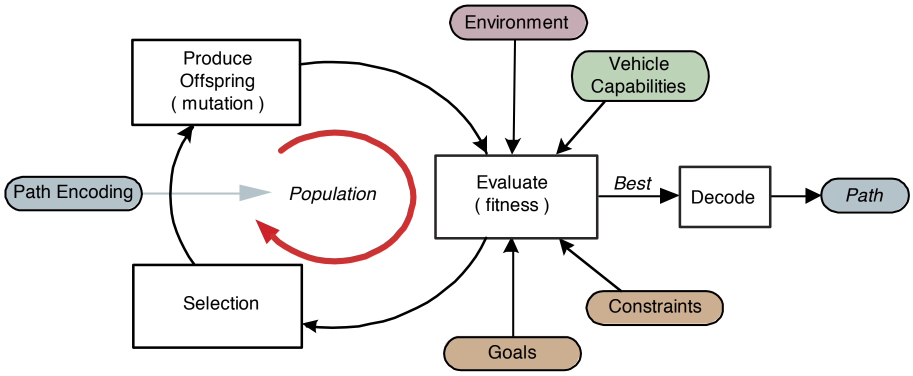

Figure 2.11: Path generation using Evolutionary search (from [Rat+02])

Flyability of the resolution manoeuvre

With rule-based optimisation algorithms such as TCAS, flyability is assured through pre-defined manoeuvres. Depending on input parameters such as the current FPA for example, the selection of the manoeuvre needs to guarantee flyability. Similar, the path search algorithm uses path segments wich are computed by a manoeuvre space generator. With this approach a set of possible manoeuvres is computed which take the current state of the vehicle into account. Tooren et al. used this approach for Conflict Resolution of an UAV. The set returned by the manoeuvre space generator was comprised of linear segments and curved segments but could also contain '[...] complicated elements like (3D) Dubins sets.' [Too+07]. Finally, with *genetic algorithms*, a third approach is possible. Here, the possible resolution manoeuvres do not necessarily need to be respected during generation of the path but during selection of the *fittest* path. To facilitate this, vehicle capabilities are also parameters to the fitness function used for selection of the next populations members. Rathbun et al. extended this by also integrating motion constraints into the mutation mechanism which recombines paths.

Optimisation

The TCAS algorithm implements optimisation by selecting from a pre-computed set of manoeuvres and comparing them against some criteria. This approach is only limited by the number of manoeuvres to choose from and the number of criteria to compare against. With search tree algorithms, the optimisation parameters are used to reduce the number of branches that need to be traversed in order to derive the *optimal* path. Therefore, the optimisation function attributes each node in the search tree with the *current costs* (costs accumulated from the start point to the current point) and the *estimated costs* to the end point. For the latter a heuristic estimation function is used. The optimisation criteria are encoded in the cost function. With this approach, promising nodes are expanded and followed first, which enhances overall performance of the algorithm. The opposite approach is followed with optimisation based on genetic algorithms. With this approach, a population of different resolutions is computed from which the algorithm selects the most promising ones (and also some inferior ones to prevent reaching of local minima). Beside the flyability concerned parameters as described above, also parameters such as *distance between end of path and goal*, *probability of obstacle clearness* and *fuel costs* were weighted through a gain and integrated into the cost function by Rathbun et al. Figure 2.11 illustrates this search algorithm.

Application to Airborne Conflict Management
With TCAS one algorithm based on an optimisation approach is already operational in use. Though, application of this approach may not be feasible for a system which covers the vertical and horizontal dimension and allows a combination of resolution manoeuvres. The amount of possible resolutions would be significantly larger. Other than the TCAS optimisation approach, an approach based on search trees as presented by Tooren et al. could be extended to the long-term domain. Disadvantage of this, as well as of optimisation approaches based on genetic algorithms, is, that usually the end point is also needed to be known. The path search algorithm used by Tooren et al. only effectively reduces the search space if the return point to the original flight path is known. For genetic algorithms this constraint is valid as well, but may be mitigated by introducing not the distance to the destination but e.g. the Cross Track Error, the vertical distance and the temporal distance to the Reference Business Trajectory into the cost function. For all algorithms based on optimisation approaches it is important to note, that with the number of resolution manoeuvres that may be commanded the complexity of the problem grows and thus also the computation time required.

2.4.3 Force Field resolution

One approach originating from the field of robotics (see e.g. [KK91]) to Conflict Resolution is modelling aircraft as charged particles. This approach, which is *inter alia* referred to as *Artificial Force Field*, *Force Field* or *Potential Field* computes a resolution based on the attractive and repulsive forces acting on the aircraft. Conflict Resolution systems based on *Force Fields* have been among the first algorithms surveyed in the context of *Free Flight* and are currently also investigated for their use in UAV sense-and-avoid systems (see e.g. [PKG08]). By human-in-the-loop and fast time simulations, Hoekstra was able to show in 2001 the feasibility of this approach [Hoe01]. He used an implementation based on the algorithm by Eby and E. Kelly III [EE99] which computed for each conflict a vertical and lateral resolution from which the pilot could choose from in the human-in-the-loop evaluations. During these evaluations, the algorithm's outputs were advisories regarding *ground speed*, *track*, *vertical speed* and *altitude*.
Figure 2.12 illustrates the basic concept of drawing and repulsive forces used in this model. Aircraft are charged similar and act as repulsive forces against each other while the destination is charged opposite to the aircraft and acts as a drawing force. The algorithm has been modified for airborne application and computes horizontal and vertical resolution manoeuvres. If multiple conflicts exist, the avoidance vectors, calculated using the *modified potential field* model, are combined by summing up the horizontal components and taking the maximum and minimum altitudes for the vertical components.

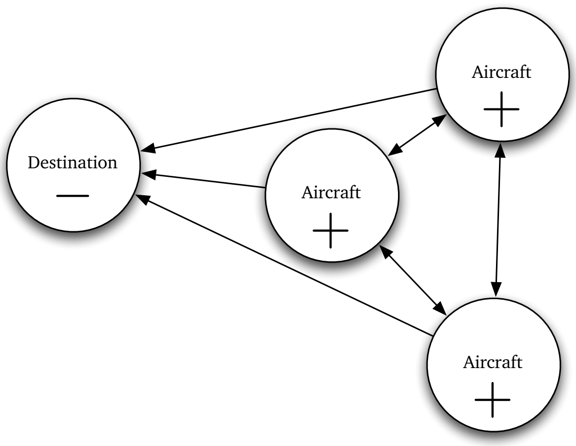

Figure 2.12: Illustration of charged particle Conflict Resolution (after [EE99])

Flyability of the resolution manoeuvre
The Conflict Resolution algorithm used by Hoekstra is initiated with ownship's current speed vector. The flyability is guaranteed through adaption of the resulting speed vector to the aircraft's velocity and acceleration limitations. Other algorithms rely on the gradually growing force[7] to ensure flyability of the manoeuvre [EE99; DZ97].

Optimisation
During Hoekstra's human-in-the-loop evaluations, the pilot was to choose between two resolution types, a vertical and a horizontal resolution. Due to the cylindric geometry of the protection volume around ownship, both types could be used to solve the problem and the operators preference could be included by this into the Conflict Resolution process. Duong and Zeghal followed a similar approach in which an human operator could modify the alternative trajectory according to his preference [DZ97].

Application to Airborne Conflict Management
The application of *Force Field* Conflict Resolution algorithms in low-density and medium-density airspace has been shown in simulations [DZ97; III00] and human-in-the-loop evaluations [Hoe01]. They have '[...] proven extremely robust [...]' [III00] and can also be used for modelling of avoidance areas [DZ97]. Kuchar and Yang have identified a few issues that need to be addressed when applying a *Force Field* approach. With a *Force Field* approach, sharp discontinuities in the commanded resolution manoeuvre due to the forces acting on the aircraft could occur which might lead to a physically not feasible solution. Furthermore, *Force Field* algorithms might require the aircraft to move for a long period of time in response to the forces acting on it. This could result in a complex resolution [KY00].

2.4.4 Manually generated resolution manoeuvres

Manually generated resolution manoeuvres rely on an human operator to generate a potential resolution [KY00]. Usually, this resolution is checked back by the Conflict Detection system and if the new trajectory is conflict free it is accepted. Kuchar and Yang state as advantage of this approach that information which may not be available to the Conflict Detection & Resolution system can be taken into account by the user (such as knowledge on bad weather areas). Manually generated resolutions also have no limitation regarding the number or combination of manoeuvres. The algorithmic interesting part of a Conflict Detection & Resolution system based on manually generated resolution manoeuvres is the Conflict Detection part. The works summarised by Kuchar and Yang are all primarily concerned with this component. Most algorithms use intent data communicated via Automatic Dependant Surveillance - Broadcast or a similar 4D trajectory representation to detect conflicts between ownship and other traffic (e.g. [DZ97; IE97]).

Flyability of the resolution manoeuvre
Guaranteeing flyability of the resolution manoeuvre is the responsibility of the human operator. A feasibility check may be done afterwards to assure flyability of the new trajectory or the choice on alternative waypoints may be limited a priori. For both approaches, knowledge about the aircraft performance are required.

Optimisation
With manually generated resolutions the optimisation in respect to arbitrary criteria is within the human operator's discretion.

[7] The force acting on the aircraft is defined in respect to the distance between ownship and intruder.

Application to Airborne Conflict Management

In low density traffic situations, Conflict Resolution algorithms relying on manually generated resolution manoeuvres may be feasible. The time span of several minutes before conflict might be sufficient to analyse the traffic situation and to derive appropriate steps. Though, in high density traffic environments this might not be practicable. The complexity of the traffic situation may be too high for a resolution to be easily derived. One approach to mitigate this is to present the flight deck crew with a Conflict Resolution option in their secondary flight plan and to compute a new one if the option has been declined [Bir+07]. The secondary flight plan can be displayed on the Navigation Display to visualise the resolution and support the decision making process of the flight deck crew.

2.5 Concept for a CD&R system required for AOA operation

Aim of introducing Autonomous Operations Area airspace is a better utilization of the airspace and the possibility for the users to choose trajectories conforming to their preferences. In case of a conflict, the Conflict Resolution system shall calculate a resolution which brings the aircraft back to its Reference Business Trajectory. The FMS Cost Index is nowadays used for weighting time-related against fuel-related costs and already impacts the aircraft's vertical profile and speeds. This already available tool should be used to prioritise the choice of the Conflict Resolution manoeuvre. These requirements lead to the decisions on the *model* and *Conflict Detection & Resolution approach* which are described in the following.

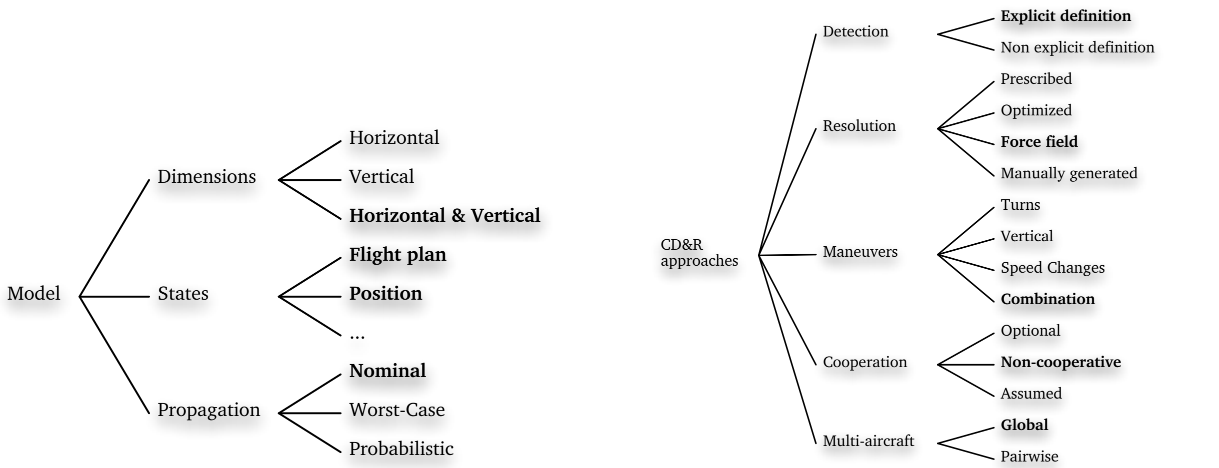

(a) Modelling approaches (b) Conflict Detection & Resolution process

Figure 2.13: Selected approach (in bold) for ACM system conceived in this work

2.5.1 Model

A Conflict Detection & Resolution system for operation in Autonomous Operations Area airspace needs to detect and resolve conflicts with other traffic. Due to the flexibility of the airspace usage, a limitation of the model on one dimension is not feasible as vertical as well as lateral separation is required. Therefore the model used in this work needs to cover the *horizontal and vertical dimension*.

To retrieve the current position of ownship and intruder, the *position* state information is required as well. For projecting the positions into the future in order to detect conflicts, the *flight plan* which contains all Trajectory Change Points is used as information source. Information only about the current position and

the velocity vector would not be sufficient since the Conflict Detection & Resolution system needs to cover the whole flight within AOA airspace which might contain multiple speed vector changes.
With a time-frame of a few minutes up to several hours for the Conflict Detection & Resolution system, any other propagation method than *nominal* would result either in high computation times or false alerts. Therefore, the algorithms devised in this work use a nominal propagation model. Figure 2.13(a) summarises the choices on the model made.

2.5.2 Conflict Detection & Resolution approach

In the following, the choices regarding the Conflict Detection & Resolution approach chosen within this work are explained regarding *Conflict Detection method*, *Conflict Resolution method*, the allowed *resolution manoeuvres* and consideration of *cooperation* and *multi-aircraft conflicts*. The decisions made are based on the goals and scope of this thesis as outlined in Section 1.4. Figure 2.13(b) summarises these choices which are highlighted in bold.

Conflict Detection method
With the resolution of a conflict being one of the goals of a Conflict Detection & Resolution system, it is found necessary to have an *explicit definition* of conflicts for their detection. This also allows a greater flexibility in implementation of the CD&R system, since the Conflict Detection (CD) and CR components can be implemented independent of each other.

Conflict Resolution method
The choice of the resolution method depends on the requirements towards the Conflict Resolution system and the applicable constraints. As outlined in Section 1.4, the Conflict Resolution system shall calculate conflict-free trajectories upon detection of a conflict in a strategic time-frame. The Conflict Resolution process shall also incorporate a prioritisation regarding fuel- and time-costs of the resolution manoeuvre and guarantee flyability. Additionally, the application of such a system to the aeronautic domain imposes the additional constraint, that the computed resolution needs to be reproducible, i.e. for two identical conflict scenarios the resolutions computed need to be identical as well.
Prescribed resolution manoeuvres (cf. Subsection 2.4.1) are considered not feasible for strategic Conflict Resolution under the given constraints as the number of manoeuvres required to adhere to the prioritisation given through the Cost Index are likely to exceed the scope of applicability of this class of resolution algorithms. Furthermore, the major advantage of these algorithms lies in the area of short-term or safety-net functions as they have to provide a resolution advisory within a very limited time-frame. For long-term Conflict Detection & Resolution, constraints regarding e.g. computation time, which apply to short-term systems, are not of concern. Optimised Conflict Resolution algorithms may take advantage of the strategic time-frame in which the resolution has to be computed. Nevertheless, if the optimisation criteria is more complex or if several criteria need to be respected, significant computation time might be required to generate a resolution (cf. Subsection 2.4.2). In these cases often heuristic approaches are used to compute a valid result in a limited time, which violates the requirement of reproducibility of the resolution. While this requirement does not need to be adhered to when generating a resolution manually – in this case the human operator is responsible for the resolution – the task of resolving conflicts may become to complex to be addressed manually. Under consideration of the rise of aircraft movements, the further reduction of separation minima and the rising complexity in trajectory planning, Conflict Resolutions which are generated manually (cf. Subsection 2.4.4) may not be feasible. Especially when introducing additional requirements such as consideration of the Cost Index, computational aids are expected to be required. Algorithms based on Force Fields assure reproducibility since they do not include any heuristics and apply a physical model for computing the resolution. Caveat of algorithms of this class is, that they may compute not feasible manoeuvres as outlined in Subsection 2.4.3. Since

it is expected that these issues can be addressed by a proper extension of the Force Field algorithm, an algorithm of this class will be used for the Conflict Resolution system devised in this thesis.

Resolution Manoeuvres

Especially the combination of all three manoeuvre types is necessary for Conflict Resolution which has to respect the operators preferences given through the Cost Index, since each manoeuvre type impacts the flight differently. A turn under constant speed and altitude will change the distance to be travelled and thus the flight time. On the other hand, a climb at constant ground speed will result in a change in fuel consumption. Since these degrees of freedom in manoeuvre choice are also expected to be necessary for a proper integration of the Cost Index, the CR algorithm needs to support any *combination* of turn, vertical and speed manoeuvres.

Cooperation

With the focus of this work on integrating the Cost Index into the Conflict Resolution process, cooperation aspects during the CR are not concerned. Therefore, a *non-cooperative* Conflict Resolution algorithm is devised, even though cooperation is found to be a necessary feature when designing a CD&R system for use in AOA airspace.

Multi-aircraft conflicts

Finally, multi-aircraft conflicts are addressed simultaneously, i.e. *global*. This has the advantage, that in a situation where multiple aircraft are involved in a conflict, the resolutions computed for one aircraft do not need to be revised in case they cause further conflicts. A pairwise solution would have this disadvantage, since each Conflict Resolution only focusses on one intruder.

2.5.3 Implementation of Conflict Resolution approach

The decision on the model and the Conflict Detection & Resolution approach impacts the implementation of the Conflict Detection & Resolution system. Especially the CR, which needs to allow for integration of the Cost Index, and the architecture of the system, which needs to integrate itself into the current system design, are of interest.

Conflict Resolution type

Following an approach to CR based on *Force fields*, a Conflict Resolution of the *embedded* form allows for better formulation of the CR process. With this formulation, the trajectory generator and conflict detector are both part of the Conflict Resolution algorithm. The expected benefit with this choice is, that the Conflict Resolution algorithm does not need to rely on external components to ensure flyability of the resulting trajectory.

Architecture

The current system design as described in Section 2.2 puts the Flight Management System in charge with all mission relevant tasks. In modern aircraft it already has interfaces to the weather radar and data-link systems [How90; MS08; MS03]. The Conflict Detection system needs to access information on current state and intent of ownship and other traffic. Furthermore, the Conflict Resolution system needs to update the current flight plan with an alternative one resolving the conflicts. Consequently, the FMS is the system to extend to enable Airborne Conflict Management. Figure 2.14 illustrates the framework of the Conflict Detection & Resolution system devised in the scope of this work. The FMS provides the CD function with the calculated Trajectory Change Points (TCPs) for ownship in respect to the flight plan and selection by the flight deck crew. Conflict Detection uses these TCPs and those from other aircraft

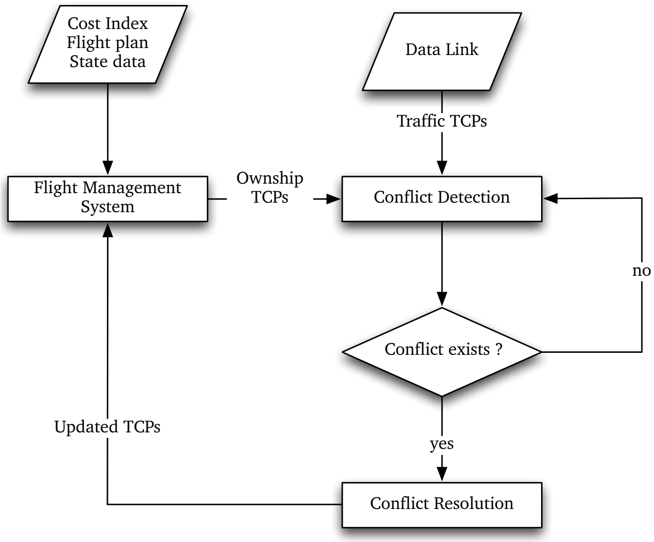

Figure 2.14: Flowchart of Conflict Detection & Resolution (CD&R) process

transmitted via ADS-B to identify infringements of ownship's protection zone. In case a conflict exists, the CR function determines a resolution and communicates it to the Flight Management System.

2.5.4 Guaranteeing flyability

One requirement to the Conflict Resolution algorithm is to guarantee the flyability of the resulting trajectory. Approaches to guarantee flyability include a trajectory generator component [Too+07], constraining of the resolution depending on equations of motion [Rag+04] or eliminating not flyable trajectories [Rat+02]. Depending on the complexity of the manoeuvres allowed, each solution may require significant computation time, especially when a trajectory generator component is required to compute alternatives. The requirement to guarantee flyability is addressed in this work by integrating a flight mechanics model of the aircraft into the Conflict Resolution process. The interface to this model shall provide similar features as the autopilot of an FBW aircraft, i.e. heading control, altitude control and speed control (see also Figure 2.3). With the Conflict Resolution algorithm commanding new control values to resolve the conflict and the model executing these commands, it is expected that the flight mechanical constraints for the aircraft are respected.

2.5.5 Integration of Cost Index

The Cost Index weights fuel-related against time-related costs and thus prioritises certain manoeuvres. The approach to integration of the Cost Index into the CR is to assign in a first step to each manoeuvre type the costs that it causes. Subsequently, the Cost Index will be used to prioritise the manoeuvres according to the costs they are expected to cause.

2.5.6 Goals & Hypotheses

With autonomous operations, the applicability of the Cost Index is expected to be less constrained since in AOA airspace aircraft are expected to follow their preferred trajectory. Though, in AOA airspace flight deck crews are required to fulfil the delegated task of separation provision.

The high level goals of this thesis are derived from this situation and are to develop and evaluate a Conflict Resolution algorithm which resolves air traffic conflicts, ensures flyability of the resulting trajectory and integrate the FMS's Cost Index. This leads to the following requirements that shall be met by the Conflict Resolution algorithm:

1. The resulting trajectory is flyable.
2. The resulting trajectory is conflict free.

Furthermore, the following hypotheses regarding the integration of the Cost Index into the Conflict Resolution process are to be validated in this thesis:

1. A smaller Cost Index will have a lesser impact on fuel-related than on time-related costs.
2. A larger Cost Index will have a larger impact on fuel-related than on time-related costs.

2.6 Summary

With the introduction of Autonomous Operations Area airspace major operational changes are upcoming. The new privileges and possibilities in this airspace area require novel systems enabling Airborne Conflict Management. This chapter has devised a system for Airborne Conflict Management with focus on the Conflict Resolution component. Different implementations to both, the *model* for Conflict Detection & Resolution and the Conflict Detection & Resolution approach, were summarised from current research. Based on this summary, a decision for a Conflict Detection & Resolution system based on *Artificial Force Fields* has been made. For detection of conflicts, an algorithm based on the distance at the Closest Point of Approach has been chosen. Furthermore, the integration of a Conflict Detection & Resolution system into the current aircraft control loops has been described. The Flight Management System has been identified therefore as the adequate system to be extended or interfaced.

3 Conception of a Conflict Detection system

An algorithm must be seen to be believed, and the best way to learn what an algorithm does is to try it.

Donald E. Knuth, *The Art of Computer Programming*

BEFORE a conflict can be resolved it has to be detected. Irrespective of the technique used to detect a conflict, certain parameters such as the Closest Point of Approach (p_{CPA}) and the distance between ownship and intruder at CPA (d_{CPA}) need to be calculated. If the distance at the Closest Point of Approach is less than a certain separation (vertical or horizontal) minima, a conflict has occurred (cf. Definition 2.6). The present chapter is concerned with the Conflict Detection component of the system devised in this work. Section 3.1 introduces to Conflict Detection by describing the requirements to the system and the Conflict Detection process. Following the definition of a conflict as of Subsection 2.1.3, Section 3.2 covers the subject of Protected Airspace Zones which violation is considered a conflict. Section 3.3 is concerned with the concept for the Conflict Detection algorithm, its implementation and applicability as a *strategic* Conflict Detection algorithm. Finally, this chapter concludes with a summary in Section 3.4.

3.1 Introduction

The Conflict Detection (CD) process is comprised of different steps, of which each might add a certain error, e.g. depending on the maturity of the onboard equipment, the accuracy of ownship position estimation may vary. The CD process as depicted in Figure 3.1 starts with an estimation of the current state based on traffic and ownship information. These states are hence projected into the future (*Trajectory Prediction*, cf. Section 2.3) to identify potential conflicts (*Distance Calculation*). Depending on the conflict detection timeframe, the system must adhere to different requirements.

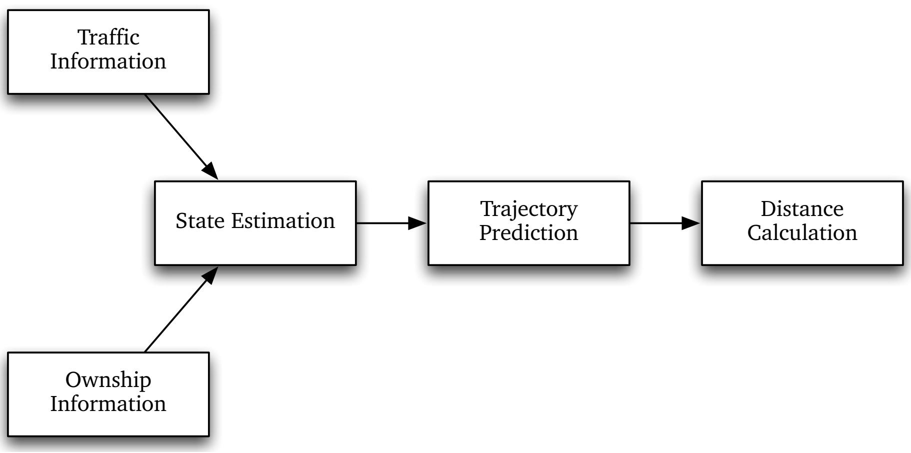

Figure 3.1: Conflict Detection process derived from [AG06]

Requirements to Conflict Detection
The Conflict Detection system shall allow operation within AOA airspace. Thus, *strategic* or *long-term* (cf. Section A.3) Conflict Detection is required. The CD system needs to ensure that

1. all conflicts between the current position and the next TCP are detected if ownship is in AOA airspace *and*
2. all conflicts for (subsequent) trajectory segments which touch AOA airspace are detected.

As outlined in Subsection 2.5.2, the Conflict Detection algorithm shall support an explicit definition for conflicts.
Traffic and Ownship Information: While ownship state information required by Conflict Detection can be retrieved from on-board systems such as the Flight Management System, information on other traffic needs to be accessed from other sources. The *Cockpit Display of Traffic Information* for example may access for the depiction of traffic information sources like ADS-B, TIS-B or TCAS [SC 00a]. TCAS and ADS-B use data retrieved via the Mode-S Transponder (cf. Section E.1 and Section E.2).
The minimum information set required for an aircraft (including ownship) acr_i contains

1. an unique identifier,
2. the current position p_{acr_i} *and*
3. a (minimum) set of TCPs $tcp \in \mathcal{T}_{acr_i}$ (cf. Definition 2.4).

The unique identifier and position information are included in the State Vector Report, while the TCP information are included in the Trajectory Change Report[1].
State Estimation: State estimation refers to the estimation of the current traffic situation [AG06]. The CD system uses the traffic and ownship information as described above for its estimation.
Trajectory Prediction: The trajectory projection is achieved by applying a *nominal propagation* model to each trajectory segment ts. Irrespective of the CD algorithm used, the Trajectory Prediction subsystem should only project trajectories for segments which are overlapping in time. To allow prediction using nominal propagation, the speed vector $\vec{v}$ is needed to be known. The speed vector can be derived for a trajectory segement $ts = (tcp_i, tcp_j)$ as

$$\begin{aligned} \vec{v}_k &= \left(\frac{s}{\Delta t}, 0, \frac{\Delta h}{\Delta t}\right)^T \text{ with} \\ \Delta t &= tcp_j -_t tcp_i, \\ s &= tcp_j -_h tcp_i \text{ and} \\ \Delta h &= tcp_j -_v tcp_i. \end{aligned} \tag{3.1}$$

With the speed vector transformed to the geodetic coordinate system, the start position (either tcp_i or p_{acr_i}) and the destination tcp_j the next positions can be calculated[2].
Conflict Detection: A conflict occurs when the minimum allowed distance is violated (cf. Definition 2.6). Depending on the airspace, different minimum distances with respect to the bearing σ between ownship and other traffic may exist. Current separation minima for aircraft using the North Atlantic Organised Track System are an example for such a case. When Mach number technique is applied, the minimum longitudinal separation is between 5 and 10 minutes, while the lateral separation is at least 50.5 NM [Nor05a]. The vertical separation minima is either 1000ft or 2000ft depending on the flight level. Appendix B summarises the applicable separation minima for the IFBP airspace area over Africa and within

[1] as of the definition of ADS-B dataset, cf. Section E.2
[2] Algorithm G.1 (Appendix G) describes the necessary calculation in detail.

the NAT Organised Track System (OTS). The minimum longitudinal, lateral and vertical distances constitute a protection volume or Protected Airspace Zone around the aircraft (Figure 3.2). Definition 3.1 introduces a definition for an arbitrary zone around a position depending on certain state information (at least position information).

Definition 3.1 (Zone)**.** *A zone* $z_i \in \mathscr{Z}$ *is a set of points* $z_i = \{(x, y, z) | (x, y, z) \in f(\vec{s})\}$ *where* f *is an arbitrary function defining the dimensions of the protection zone and* $\vec{s}$ *is a vector of state information.*

Common zone definitions around aircraft are cubic zones [Vie97] and cylindrical zones [Hoe01; Ges+02; Tca; Bau+06]. The dimensions of these zones may depend on current air- and vertical speed [Tca; Ges+02] or relative speed between ownship and intruder [BK08]. Section 3.2 compares different implementations of zones (around aircraft) as of Definition 3.1.

3.2 Protected Airspace Zones around aircraft

The zone definitions around aircraft take the applicable minimum separation (Appendix B summarises separation minima for a selected number of airspaces) into account. The protection zone around an aircraft is defined with respect to aircraft's own position. Other, equivalent approaches, define the protection zone only around intruders and vary their sizes. For example Geser et al. introduce a static protection zone around intruders, which is twice as large as the current applicable ownship's protection zone [Ges+02]. The protection zone P is defined as

$$P = \{(x, y, z) | x^2 + y^2 < D^2 \text{ and } |z| < H\} \text{ [Ges+02].}$$

Here, the z-axis points upward, D and H denote the diameter and height of the protection zone. A conflict occurs if $p_o \in P$.

Types of zones

[SC 00b] introduces two zones, the Protected Airspace Zone (PAZ) and the Collision Avoidance Zone (CAZ). The PAZ is defined as a '[...] variably sized zone based on legal separation requirements [...]' while the CAZ is a '[...] safety zone based on aircraft size with appropriate buffers [...]' [SC 00b]. Figure 3.2 illustrates this concept.

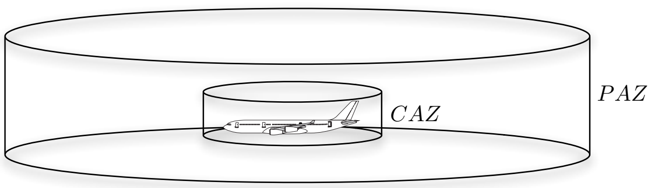

Figure 3.2: Conflict Zones after [SC 00b]

The dimensions of the zones do not necessarily need to be static distance values. TCAS for example provides Resolution Advisories (RA) and Traffic Advisories (TA) depending on the time to the Closest Point of Approach (CPA) between ownship and traffic[3] [Tca]. Reason for this is to enable information of the flight deck crew through caution or warning alerts. In the following, different protection zones around ownship are described. A distinction between *static zone definitions*, i.e. zone definitions not taking aircraft state information into account, and *state dependant zone definitions* is made.

[3] Only TCAS II. Refer to Section E.1 for further details.

Requirements to zone implementation
The PAZ needs to correspond to legal separation requirements [SC 00b]. Furthermore, its dimensions need to be expressed either as a fixed distance or a fixed time [ICA96]. Distances or times may vary depending on the airspace, the type of traffic and the means of separation provision.
Therefore, the zones used for Conflict Detection need to

1. allow different longitudinal, lateral and vertical separation minima,
2. allow the definition on separation minima depending on time or distance *and*
3. allow the alteration of zone definitions.

Especially for zones with variable dimensions it is necessary to express the current *intrusion* as a relation between minimum allowed distance and current distance between ownship and intruder. Therefore the zone implementation shall also allow to derive an intrusion $i_{v/h}$ denoting the vertical and respectively horizontal proximity in respect to the minimum distance for arbitrary zones.

3.2.1 Static Zone Definition

In the following static zones are described, i.e. zones where current aircraft state information and information about the intruder have no impact on the dimensions of the protection zone.

Spheric Zone
A spheric zone Z_s around the current position $p_o = (x_o, y_o, z_o)$ with the uniform propagation d_{min} (minimum distance) is defined as

$$Z_s = \{(x, y, z) | (x - x_o)^2 + (y - y_o)^2 + (z - z_o)^2 \leq d_{min}^2\}. \tag{3.2}$$

Major advantage of this zone definition is its straight-forward implementation. A sphere as described by Equation 3.2 is symmetrical with respect to the spheres origin (p_o). Therefore no rotational (or other, in respect to computation time expensive) operations need to be applied during the simulation.

Cylindric Zone
A cylindric zone Z_c around the current position $p_o = (x_o, y_o, z_o)$ with the propagation d_h (minimum horizontal distance) and d_v (minimum vertical distance) is defined as

$$Z_c = \{(x, y, z) || z_o - z| \leq d_v \wedge (x - x_o)^2 + (y - y_o)^2 \leq d_h^2\}. \tag{3.3}$$

One system that uses a cylindrical protection zone around ownship is the Traffic Collision Avoidance System [Tca]. The vertical dimension of the protection zone depends on ownships altitude [4]. The cylindric zone as defined in Equation 3.3 can be extended to allow for different upward and downward vertical propagations.

[4] Section E.1 gives an overview on TCAS implementations.

Cylindric Zone with elliptic base

A cylindric zone Z_{ce} with an elliptic base around the current position $p_o = (x_o, y_o, z_o)$ with the propagation d_{lat} (minimum lateral distance), d_{lon} (minimum longitudinal distance) and d_v (minimum vertical distance) is defined as

$$Z_{ce} = Z_c \cup \left\{ (x, y, z) | (x - x_o) \geq 0 \wedge |y - y_o| \leq d_{lat} \wedge (x - x_o) \geq \sqrt{\left(1 - \frac{(y - y_o)^2}{d_{lat}^2}\right) \cdot d_{lon}^2} \right\}. \quad (3.4)$$

Figure 3.3 illustrates a cylindric zone as described by Equation 3.4. This zone definition allows integration of protection zones with different longitudinal and lateral minima. Furthermore, this definition can be extended to allow for a zone propagation depending on state information (see Subsection 3.2.2). The application of this zone requires a rotation depending on aircraft heading.

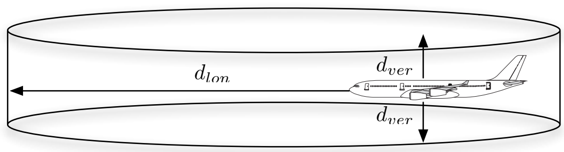

(a) Side View

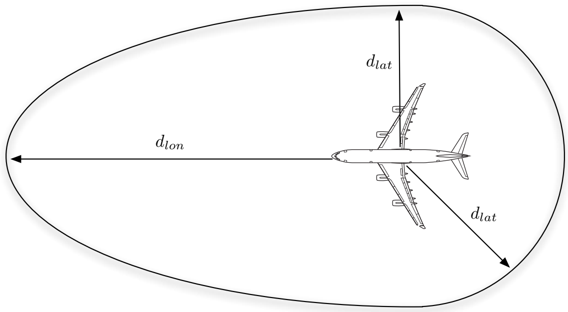

(b) Top View

Figure 3.3: Cylindric Zone with elliptic base

3.2.2 State Dependant Zone Definition

By taking state information into account, the Protected Airspace Zone geometry can be defined more flexible, e.g. if a longitudinal separation of 10 minutes is required, the Protected Airspace Zone may extend in the longitudinal dimension up to the distance which can be travelled at current speed within that time. Regarding state dependance it can be distinguished between ownship and intruder states.

Ownship Speed Zone

Current Conflict Detection algorithms such as the TCAS algorithm take ownship Rate of climb/descent (ROCD) into account (cf. Section E.1). With the assumption of ownship lying in the centre of a cartesian coordinate system with the axis of the coordinate system aligned to the aircraft's body fixed axis system, the current climb and sink rate as well as the aircraft's heading are already implicitly taken into account. Neither ROCD nor the heading impact the geometry of the PAZ.
Since longitudinal separation may be given as a fixed distance or in clock minutes [ICA01; ICA07b], Conflict Detection also needs to take ownship's current speed into account. This can be achieved by a further extension of the PAZ zone definition. If the current applicable minimum separation is given in clock minutes t, the actual longitudinal distance is calculated as $d_{lon} = \vec{v}_{gs,o} \cdot t$.

Relative Speed Zone

Beside ownship state information it may be beneficial to take intruder state information for definition of the PAZ into account. [BK08] compared Conflict Resolution manoeuvres based on two static (i.e. Z_c

and Z_{ce}) and two state dependant zone definitions. While the first state dependant zone took ownship speed into account (as described above), the second PAZ definition took the relative speed into account. For two aircraft flying towards each other on the same track the look-ahead distance was extended. This *Relative Speed Zone* achieved the best minimum distance between ownship and intruder during a Conflict Resolution manoeuvre. This zone definition required as additional state information the intruder's speed vector $\vec{v}_{gs,i}$.

Modified Relative Zone

One caveat of the relative speed zone as introduced in [BK08] is the frequent switch of Conflict Resolution activation and deactivation. This could be put to ownship's heading changes at large distances which moved the intruder out of the Protected Airspace Zone. When ownship tried to recapture the flight plan, the Protected Airspace Zone shifted along with the heading and the intruder again caused a conflict. Furthermore, for conflicts where the intruder approached ownship from the side the Conflict Resolution manoeuvres had to be executed at bank angles larger than 25° which is considered as the maximum for long-term, strategic manoeuvres. To prevent this behaviour, the relative speed zone has been updated not to take the intruder's speed but the bearing to the intruder into account (cf. Figure 3.4(a)). If the difference between bearing to the intruder and ownwships heading $\Delta\sigma = |\sigma - \psi|$ is within 45°, ownship's PAZ is not aligned to its heading but the bearing (cf. Figure 3.4(b)).

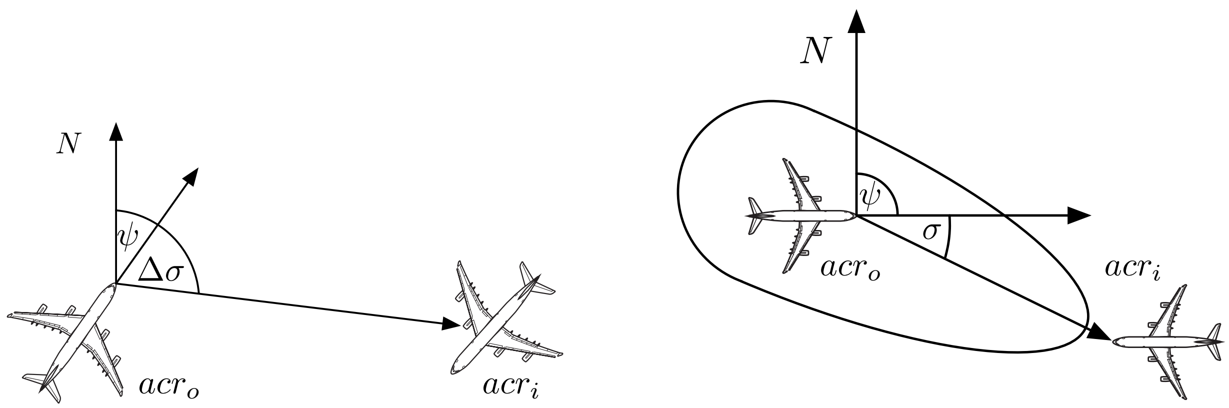

(a) Delta Bearing $\Delta\sigma$ (b) PAZ aligned by bearing

Figure 3.4: Protected Airspace Zone alignment by bearing to intruder

PAZ and CAZ distinction

With the integration of state information into the zone definition a distinction between the *Collision Avoidance Zone* and the *Protected Airspace Zone* for the Conflict Detection & Resolution system devised in this work can be made. The CAZ which shall not be infringed is given by the cylindric zone Z_C with $d_h = d_{lat}$ (cf. Equation 3.2). The PAZ is enclosing the Collision Avoidance Zone and takes further state information into account, allowing integration of further separation requirements.

3.2.3 Protected Airspace Zone Intrusion

Depending on the geometry of the Protected Airspace Zone, different minimum distances apply (e.g. for Z_{ce} the lateral minimum distance is larger than the longitudinal). By relating the current distance of the intruder to the maximum allowed distance, lateral and vertical intrusion can be compared between different zone implementations. Lateral i_h and vertical intrusion i_v are defined similarly:

$$i_{v/h}(d_{v/h,cur}, d_{v/h,min}) = \begin{cases} 0 & , d_{v/h,cur} > d_{v/h,min} \\ 1 - \frac{d_{v/h,cur}}{d_{v/h,min}} & , d_{v/h,cur} < d_{v/h,min} \\ 1 & , \text{ else} \end{cases} \tag{3.5}$$

$$\text{with: } d_{v,cur} = |p_o -_v p_i|$$
$$d_{h,cur} = p_o -_h p_i$$

With $f_Z : \mathbb{R}^3 \longrightarrow \mathbb{R}^3$ a function defining a zone, the minimum allowed horizontal distance depending on the bearing σ between p_o and p_i is defined as follows:

$$d_{h,min} = \max(H) \tag{3.6}$$

$$H = \left\{ d | d = \sqrt{x^2 + y^2}, (x, y, z) \in f_Z \land (x, y) \in f_\sigma \right\} \tag{3.7}$$

$$f_\sigma = \begin{cases} \{(x,0) | x \in \mathbb{R}^+\} & , \sigma = 0° \lor \sigma = 360° \\ \{(x,0) | x \in \mathbb{R}^-\} & , \sigma = 180° \\ \{(0,y) | y \in \mathbb{R}^+\} & , \sigma = 90° \\ \{(0,y) | y \in \mathbb{R}^-\} & , \sigma = 270° \\ \{(x,y) | y = \frac{\sin\sigma}{\cos\sigma} \cdot x \land x, y > 0\} & , \sigma > 0° \land \sigma < 90° \\ \{(x,y) | y = \frac{\sin\sigma}{\cos\sigma} \cdot x \land x > 0, y < 0\} & , \sigma < 360° \land \sigma > 270° \\ \{(x,y) | y = \frac{\sin\sigma}{\cos\sigma} \cdot x \land x, y < 0\} & , \sigma < 270° \land \sigma > 180° \\ \{(x,y) | y = \frac{\sin\sigma}{\cos\sigma} \cdot x \land x < 0, y > 0\} & , \sigma < 180° \land \sigma > 90° \end{cases} \tag{3.8}$$

The maximum allowed distance calculates to $d_{h,min} = \sqrt{x_{P_i}^2 + y_{P_i}^2}$. The definition as of Equation 3.6 and Equation 3.7 allow the description of $d_{h,min}$ for arbitrary functions f_Z. The vertical distance depending on the elevation bearing ϵ is defined similar to $d_{h,min}$. Section A.4 details the intrusion calculation further.

3.3 The Conflict Detection algorithm

One requirement to the Conflict Detection algorithm is, that it needs to support the explicit definition of a conflict. Therefore, a metric and a threshold are required. Since separation minima relate to the distances between two aircraft, the choice of the distance at the *Closest Point of Approach* (CPA) as metric for Conflict Detection has been frequently made [Vin+97; IE97; CM04; GM02][5]. The distance at the CPA can subsequently be used to calculate, wether the intruder lies in the Protected Airspace Zone of ownship or not.
With this approach, the following information are necessary to be computed for each ownship trajectory segment (see Definition 2.5) by the Conflict Detection algorithm:

d_{CPA} Distance between ownship and conflicting traffic at CPA,

p_{CPA} Position of the CPA *and*

t_{CPA} Time to CPA.

[5] Other approaches based on probability also exist, while here also the estimated distance between ownship and intruder is used as a metric for Conflict Detection [YK97; Vie97].

Distance at the CPA

The *distance at the CPA* is the slope distance between acr_o and acr_i. The slope distance is calculated by calculating the horizontal (d_h) and vertical (d_v) distances between acr_o and acr_i as

$$d_{CPA} = \sqrt{d_v^2 + d_h^2}. \tag{3.9}$$

The error can be expressed as a function of the protection zone and is negligible due to the vicinity of ownship and traffic. In order to be able to estimate the distance at the Closest Point of Approach, the projection of ownship and intruder states into the future is necessary. With Equation 3.1 this can be calculated for each trajectory segment when the time to the Closest Point of Approach is known.

Time to CPA

For two aircraft acr_o, acr_i with speeds $\vec{v}_{o,g}, \vec{v}_{i,g}$ the *Time to CPA* is calculated as

$$t_{CPA} = \left| \frac{p_o - p_i}{\left\| \vec{v}_{o,g} - \vec{v}_{i,g} \right\|} \right|. \tag{3.10}$$

This calculation is also used by the Conflict Detection component of the TCAS algorithm, where the time to CPA is compared against a threshold τ. For further details on the *simple τ criterion* (Equation 3.10) refer to [Vie97, Section 2.2.1].

With the time to CPA and the current position known, the position of ownship and intruder can be calculated.

Position of the CPA

The *position of the CPA* is calculated by projecting the positions of ownship and intruder by t_{CPA} seconds into the future. As outlined in Subsection 2.5.1 a nominal propagation model is used for this. The projection as described in Section G.1 ensures conformance to RNP class 0.1 (185.2m, cf. Section A.2) and follows great circle paths.

3.3.1 Implementation

The Conflict Detection algorithm is executed once for every ownship trajectory segment $ts = (tcp_{o,j}, tcp_{o,n})$ with a set of intruder Trajectory Change Points. For each ownship trajectory segment the first step of the Conflict Detection algorithm as illustrated in Figure 3.5 is to compute the set of all in time overlapping possible intruder trajectory segments. If the set is non-empty, the computation of Closest Point of Approach information commences with the first intruder trajectory segment as described in Section 3.3. The implementation of the algorithm ensures that, for non equal start times $tcp_{o,j} \neq_t tcp_{i,k}$ either ownship or intruder is initialised with the correct position. The Conflict Detection uses the distance at the Closest Point of Approach and the geometry of the Protected Airspace Zone around the aircraft to decide whether a conflict occurred – in which case the CPA information is added to the return set – or not. In both cases, the current intruder trajectory segment is removed from the set to proceed further.

Further details on the implementation of the TCAS algorithm may be found in Section G.3.

3.3.2 Application of the TCAS logic to strategic Conflict Detection

The Traffic Collision Avoidance System is by design a short-term or safety-net CD&R system. The metric used by the Conflict Detection component of the TCAS is based on the time to the Closest Point of Approach. This time information is required for the strategic Conflict Detection algorithm to allow

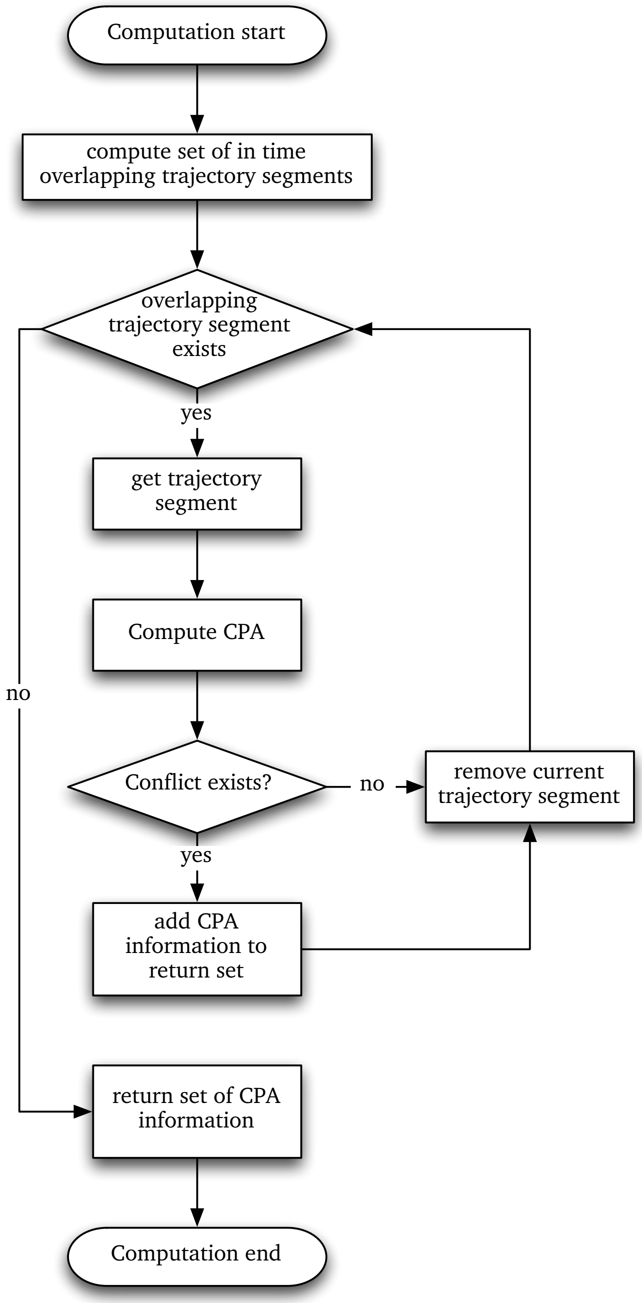

Figure 3.5: Flow diagram of Conflict Detection algorithm

projection of ownship and intruder positions into the future. The CD TCAS algorithm used for strategic or long-term Conflict Detection as presented here also derives the time to CPA by dividing the current distance through the closing speed (cf. Equation 3.10). Other than the TCAS algorithm, the *strategic* TCAS algorithm does not compare against a time threshold τ to trigger an alert. Due to the conceptual shift from a short term – *safety net* – CD system to a strategic one, a time threshold is not needed to prevent nuisance alerts. Similarly, a modification like Distance Modification (DMOD) is not required since the algorithm calculates the distance at CPA irrespective of the time to CPA. Though, due to the linear propagation used between Trajectory Change Points, inaccuracies might occur when moving from one trajectory segment to the next.

Inaccuracy in circular path segments

The Conflict Detection algorithm as described above uses linear propagation to calculate the next position for aircraft and intruder. In circular path segments this results in a lateral difference between prediction and actual trajectory including introduction and execution of the circular path and subsequent return to the next trajectory segment (cf. Figure 3.6).

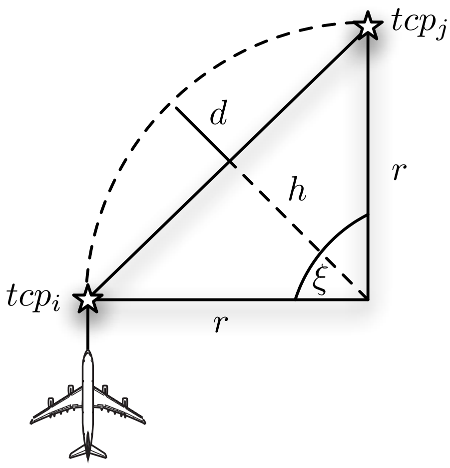

Figure 3.6: Maximum distance error in circular path segment

The maximum distance error with respect to a circular path segment flown with radius r and angle ξ calculates to

$$
\begin{aligned}
d &= r - h \text{ with} \\
h &= \begin{cases} r & ,\text{if } \xi = 180^\circ \\ r \cdot \sin(90^\circ - \frac{1}{2}\xi) & ,\text{else} \end{cases} \\
d &= \begin{cases} r & ,\text{if } \xi = 180^\circ \\ r \cdot (1 - \sin(90^\circ - \frac{1}{2}\xi)) & ,\text{else} \end{cases} .
\end{aligned}
\tag{3.11}
$$

The difference d (Equation 3.11) is minimal $d_{min} = 0$ for a path segment with angle $\xi = 0^\circ$ (which is a straight segment). The maximum error is achieved when flying a full circle, i.e. $\xi = 180^\circ$. In this case the error calculates to $d_{max} = r$. For a controlled turn under RNP class 1 requirements above FL 200 the positional error for an 180° turn is $41.7km$ [Pan, Section 7, Chapter 1]. A compensation of the positional error can be achieved by introduction of pseudo-TCPs every $185.2m$ during a turn. By this, Conflict Detection using the strategic TCAS algorithm in circular path segments can be mapped to straight segments.

Conclusion

By relying exclusively on Trajectory Change Point and the aircraft's current state information, which are necessary to be transmitted by any aircraft travelling in AOA airspace, the requirement that conflicts (on straight segments) within this airspace area are detected, is fulfilled. To achieve this, the ADS-B State Vector and Trajectory Change reports (cf. Subsection E.2.1) as outlined in Section 3.1 can be used. Since the position calculation algorithm used for projecting positions into the future employs great circle navigation within an accuracy of RNP class 0.1, Conflict Detection on straight segments is enabled. For circular path segments Conflict Detection with this algorithm can only be assured when the positional error can be compensated (cf. Subsection 3.3.2). Fulfilment of the second requirement to the Conflict Detection algorithm, that all trajectory segments but the current which lie in AOA airspace are checked for conflicts as well, depends on the number of TCPs transmitted in an ADS-B Trajectory Change report and the transmission ranges. ADS-B classes *A3 - Extended* and *A3+ - Extended* requires the transmission of $n+1$ Trajectory Change Points (cf. Subsection E.2.2). The look-ahead distance and thus the time-frame for Conflict Detection depends on the number of TCPs transmitted and the minimum radio range (for *A3+* minimum 120 NM). This requirement can only be met with the assumption, that all TCP information are available to all airspace users.

3.4 Summary

A Conflict Resolution algorithm requires certain input data such as the position of the CPA between ownship and intruder p_{CPA}, the time to Closest Point of Approach t_{CPA} and the distance at CPA d_{CPA} between ownship and intruder. If the distance is below a certain threshold, a conflict is said to have occurred. This chapter has introduced Conflict Detection systems required for operation in Autonomous Operations Area airspace. Necessary outputs of a Conflict Detection system to facilitate Conflict Resolution have been presented as well as an approach to generalise and compare the implementation of Protected Airspace Zones. For Conflict Detection, an implementation using the distance at the Closest Point of Approach has been presented. To compute the distance, the algorithm computes the time to the Closest Point of Approach and hence projects the current position into the future. This implementation calculates for at least two different sets of Trajectory Change Points (ownship and one intruder) the output values required for Conflict Resolution.

Further refinements

Conflict Detection depends on the accuracy of Trajectory Change Point information. The implementation of the Conflict Detection algorithm as presented in this work in Subsection 3.3.2 uses Trajectory Change Point information and zone definitions for Conflict Detection. If the predicted Trajectory Change Points used for Conflict Detection do not correspond to the actual Trajectory Change Points, conflicts might occur which have not been detected. Several external factors such as wind effects may cause such a discrepancy. By taking additional information such as wind and temperature forecasts into account for trajectory prediction, the accuracy of the Flight Management System's predicted TCPs may be enhanced [CSB96].

4 Conception of a Conflict Resolution system

There are two critical points in every aerial flight-its beginning and its end.

Alexander Graham Bell, 1906.

After detection of a conflict one or more Closest Point of Approach (CPA) exist for which the minimum applicable separation is undershot. In such cases, ownship has to deviate from its Reference Business Trajectory to resolve the conflict. This Conflict Resolution may require a number of heading changes, altitude changes, speed changes or a combination thereof. The different manoeuvres can be associated to different costs. In case several possible resolution manoeuvres exist, the operator may choose one which minimises his additional costs in respect to his optimisation goal.
In Section 2.2 the FMS Cost Index (CI) which is used to optimise the lateral flight plan and the speeds has been introduced. This chapter is concerned with the Conflict Resolution algorithm and the integration of the Cost Index into the resolution process. Section 4.1 introduces the requirements to the Conflict Resolution system and the measures for deviation from the Reference Business Trajectory. Section 4.2 describes the resolution manoeuvres considered legal. Finally, Section 4.3 presents an implementation based on *Artificial Force Fields*. This implementation is used for simulation and evaluation to be discussed in subsequent chapters. This chapter concludes with a summary in Section 4.4.

4.1 Introduction

Conflict Resolution is called upon violation of ownship's Protected Airspace Zone by another aircraft and receives information on the Closest Point of Approach[1] from Conflict Detection. The *Conflict Resolution Model* computes, based on these information and the optimisation goal given through the *Cost Index*, an alternative trajectory. The required output of the Conflict Resolution system is a set of Trajectory Change Points which are derived from the trajectory generated by the *Conflict Resolution Model*.

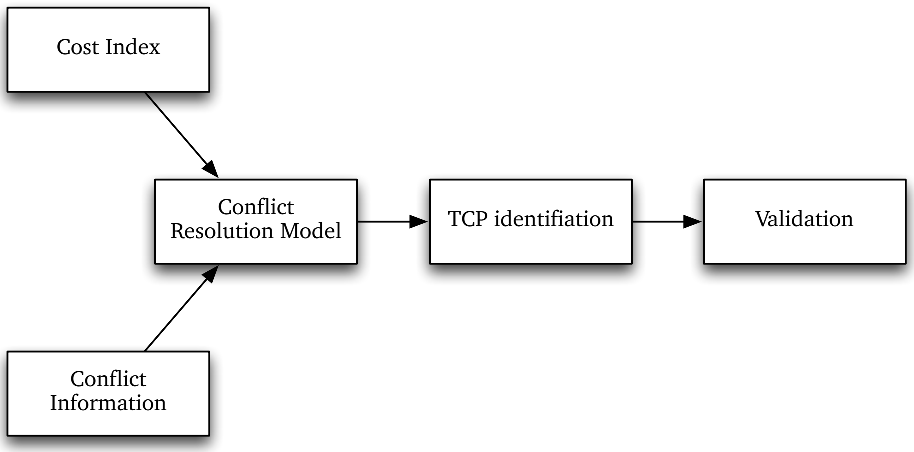

Figure 4.1: Conflict Resolution process applied in this work

[1] inter alia position of, distance at and time to/distance to the CPA

The CR process as illustrated in Figure 4.1 begins with application of a *Conflict Resolution Model* which is initiated with information on the conflict and the prioritisation criteria given through the Cost Index. The conflict information include beside CPA information also the trajectory segments of ownship and intruder where the conflict occurred. The *TCP identification* converts the output of the Conflict Resolution Model into a set of TCPs which are subsequently validated against the requirements to the CR algorithm.

Requirements to CR

The aim of Conflict Resolution is to calculate a conflict free trajectory for ownship. The conflict free trajectory is described as an ordered set of Trajectory Change Points $\mathcal{T}_{CR} = \{tcp_s, tcp_{s+1}, ...tcp_e | tcp_i <_t tcp_{i+1}\}$ where tcp_s and tcp_e denote the first (start) and last (end) point of the CR manoeuvre. By definition $tcp_s, tcp_n \in \mathcal{T}_o$ holds true. The CR system needs to ensure that

1. the minimum separation between ownship and other traffic for each ownship trajectory segment $ts_o = (tcp_i, tcp_j)$ is respected,
2. the deviation from the RBT takes the Cost Index into account *and*
3. the new trajectory is flyable, i.e. the flight envelope is respected.

Minimum separation: The first requirement states that the trajectory computed by Conflict Resolution has to be conflict free. Subsection 3.2.3 introduced the lateral and vertical intrusion, i_h and i_v. Since the new trajectory for ownship computed by the Conflict Resolution algorithm needs to be conflict free, ownship's Collision Avoidance Zone shall not be infringed, thus for all intrusion tuples at time t $i^{(t)} = (i_h, i_v)$ between the starting and ending Trajectory Change Points tcp_s and tcp_e the following shall hold true:

$$\forall i \forall t \in [t_s ... t_e], i = (0, 0). \tag{4.1}$$

Deviation from RBT: It is assumed, that the Reference Business Trajectory is the optimal 4D trajectory considering constraints and requirements from all concerned parties (cf. paragraph 1.3). Three kinds of deviations or a combination therefore from the Reference Business Trajectory may be necessary to resolve a conflict:

- a lateral deviation,
- a vertical deviation *or*
- a deviation from the Estimated Time Over.

The conflict free trajectory should take the operators flight plan optimisation goal into account which is expressed by the FMS Cost Index [Fms]. While in Section 4.2 the possible manoeuvres and the associated costs are discussed, at this stage it can already be appreciated that each of the deviations should be minimal [Rui02].

Flyability of trajectory: The resulting trajectory shall be flyable and respect the aircraft's flight envelope. For maximum and minimum speeds and altitudes the BADA specifications [Nui04b] for the cruise phase shall be applied as described in Subsection 2.1.2. Therefore, depending on the aircraft model used, the *speed* and *altitude* envelopes introduced in Table 2.2 shall be respected

$$h_{min} \le h_c \le h_{max} \tag{4.2}$$

$$V_{min} \le V_c \le V_{max}. \tag{4.3}$$

Here, h_c and V_c denote the commanded altitude and speed, respectively.
Furthermore, the limitations given through the BADA model as described in Appendix F need to be respected during Conflict Resolution.

4.2 Description of possible resolution manoeuvres

For avoiding a conflict the aircraft may either change its heading to achieve a lateral deviation, change its altitude to achieve a vertical deviation, change its speed to achieve a temporal deviation from its RBT or a combination of them. Each change to the RBT is considered as a TCP as of Definition 2.3 and requires an update of the aircraft's Predicted Trajectory.

Manoeuvre phases

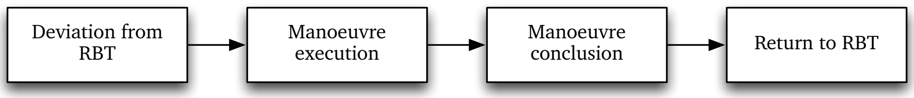

Figure 4.2: Manoeuvre phases

A conflict resolution manoeuvre consists of four manoeuvre phases as illustrated in Figure 4.2.
Deviation from Reference Business Trajectory: The Conflict Resolution manoeuvre starts with a *deviation from the Reference Business Trajectory*. The threshold when a lateral, vertical or temporal offset is actually considered a deviation may vary depending on the airspace type. In SESAR this is referred to as the Trajectory Management Requirement or TMR. While Section A.1 gives more details on Trajectory Management Requirements, here it is assumed that the Conflict Resolution manoeuvre begins with a lateral deviation greater than $\Delta\lambda^{\diamond}_{max}$, a vertical deviation greater than Δh_{max}, a deviation from Scheduled Time Over (STO) by more than Δt_{max} or a combination thereof.
Manoeuvre execution: With ownship's deviation from the RBT the *manoeuvre execution* begins. During this phase the Conflict Resolution algorithm computes an alternative trajectory – the Predicted Trajectory – to maintain safe separation between ownship and other traffic. The alternative trajectory may consist of an arbitrary number of Trajectory Change Points and has to respect the aircraft's flight and speed envelope.
Manoeuvre conclusion: Once the conflict has been resolved, i.e. ownship's Protected Airspace Zone is not infringed, the manoeuvre is concluded and the aircraft is guided back to its Reference Business Trajectory. If the Reference Business Trajectory cannot be rejoined up to the current trajectory segments target Trajectory Change Point, the Predicted Trajectory has to rejoin the Reference Business Trajectory on the subsequent trajectory segment.
Return to Reference Business Trajectory: With the *return to the Reference Business Trajectory* the Conflict Resolution manoeuvre is concluded.

4.2.1 Change of heading

A change of heading constitutes a deviation from the Reference Business Trajectory to the left or to the right. Figure 4.3 illustrates a deviation from ownship's RBT to the right by ψ'. The separation from and rejoin to the RBT constitute each a non-reducible TCP (tcp_s, tcp_e) as of Definition 2.4. Along the new path segment several additional TCPs may exist. The manoeuvre is executed maintaining a constant altitude h and a constant ground speed V_{GS}.

Consequence of a heading change

A heading change results in a change of the travelled distance between tcp_s and tcp_e compared to the original Reference Business Trajectory. The PT's distance between tcp_s and tcp_e is denoted as s', the RBT's as s in Figure 4.3.

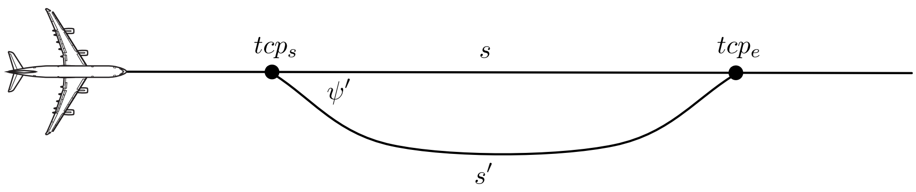

Figure 4.3: Lateral Conflict Resolution manoeuvre

Theorem 4.1 (Impact of a heading change)**.** *Under zero wind condition during level flight and at constant speed, a heading change impacts the distance to be travelled. The impact on the Specific Air Range is neglectable.*

Proof. A lateral Conflict Resolution manoeuvre is comprised of

- heading changes to deviate from the RBT,
- maintain of lateral deviation *and*
- heading changes to return to RBT.

During a Conflict Resolution manoeuvre several lateral deviations may occur. The lateral deviation is achieved with a heading change which necessitates a curved segment. The radius and the angle of the curved segment depend on the heading difference ψ'. The length of such a curved segment is always less than the comparable horizontal length [Kli07]. Additionally, with a lateral deviation and subsequent rejoin of the RBT in respect to position, a longitudinal offset between the current and the planned position exists [Rui02] and thus additional distance has to be travelled. For the curved segment necessary to achieve a change of heading the thrust required to maintain the current speed and altitude is higher than during level flight. The lift L in respect to aerodynamic bank angle μ calculates to

$$L = \frac{mg}{\cos\mu} \quad \text{after [Kli07, Equation 5.5]} \tag{4.4}$$

Under still-air conditions and during level flight, Equation 4.4 can be formulated in respect to bank ϕas

$$L = \frac{mg}{\cos\phi}. \tag{4.5}$$

The maximum bank angle for civil aircraft $\phi_{max,civ(OTHER)}$ for flight phases other than take-off, landing and holding is according to BADA 45° [Nui04b]. With Equation 4.5, the maximum multiple of lift calculates to $L_{m,max} = \sqrt{2}$ at an bank angle of 45°, respectively −45°. The bank angle for strategic manoeuvres is expected to stay within the boundaries of $[-25°, 25°]$ [Bar+06]. At this angle the multiple of lift calculates to $L_{m,\pm 25°} = 1.1034$. □

Measure for the impact of a heading change

As measure for the impact of a heading change, the area H enclosed by the Predicted Trajectory and the original Reference Business Trajectory between tcp_s and tcp_e is introduced. The horizontal area H is defined as

$$H = \int\int_{\mathscr{A}} f_{RBT} \cup f_{PT} d\sigma. \tag{4.6}$$

with f_{RBT} and f_{PT} interpolations of the RBT's and PT's points and $\mathscr{A}$ the area of integration given through tcp_s and tcp_e. With the changed distance to be travelled at the same ground speed it is assumed, that this manoeuvre mainly impacts the flight time and thus the Estimated Time Over at subsequent TCPs and the Estimated Time of Arrival at destination.

4.2.2 Change of altitude

Similarly to the heading change manoeuvre, the change of altitude manoeuvre is a deviation from ownship's RBT in the vertical plane. Figure 4.4 illustrates a vertical deviation from aircraft's RBT by a change of its pitch by θ'. The separation from and rejoin to the RBT both constitute a non-reducible TCP as of Definition 2.4. Again, along the new path segment several additional TCPs may exist. The manoeuvre is executed maintaining a constant heading ψ and a constant ground speed V_{GS}.

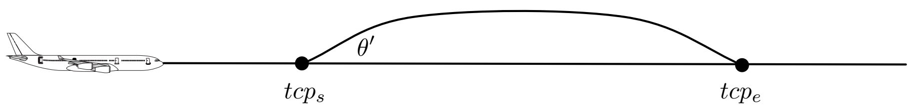

Figure 4.4: Vertical Conflict Resolution manoeuvre

Consequence of an altitude change
The aircraft's vertical profile differs from the Reference Business Trajectory if a change of altitude is commanded. While assuming a constant ground speed and without change of the ground track it is considered that the altitude change impacts fuel consumption.

Theorem 4.2 (Impact of altitude change)**.** *An altitude change at constant heading and constant ground speed impacts the fuel consumption.*

Proof. A change of altitude is comprised of

1. climb/descend to new altitude,
2. maintain of new altitude *and*
3. descend/climb to RBT altitude.

During a Conflict Resolution manoeuvre several altitude changes may occur. The thrust specific fuel consumption ν is a function of True Airspeed and calculates to

$$\nu = C_{f1} \cdot (1 + \frac{V_{TAS}}{C_{f2}}) \text{ [Nui04b].} \tag{4.7}$$

In Equation 4.7 C_{f1} and C_{f2} denote aircraft type specific parameters [2]. Cruise fuel flow f_{cr} calculates to

$$f_{cr} = \nu \cdot T \cdot C_{fcr} \text{ [Nui04b].} \tag{4.8}$$

In Equation 4.7 C_{fcr} is the cruise fuel flow correction factor which varies depending on the aircraft type. With True Airspeed being a function of current air pressure and dynamic pressure – thus depending on altitude – cruise fuel flow also varies with altitude. During climb and descent phases at constant ground speed the required thrust T and thus the fuel consumption varies as well. □

[2] Details on these parameters and constraints regarding the fuel consumption calculation as of BADA may be found in Appendix F.

Measure for impact of an altitude change
The vertical area enclosed by the original RBT's and actual PT's vertical profile is used as the measure for impact.

$$V = \int_{tcp_s}^{tcp_e} f_{RBT}\, dt - \int_{tcp_s}^{tcp_e} f_{PT}\, dt. \tag{4.9}$$

Unlike Equation 4.6, in Equation 4.9 f_{RBT} and f_{PT} are interpolations of the vertical profile.

4.2.3 Change of speed

A change of speed between two TCPs $tcp_{o,n}$ and $tcp_{o,n+1}$ causes a longitudinal deviation from the aircaft's Reference Business Trajectory. The initialisation of a speed change, i.e. the event when a new speed is commanded, constitues a non-reducible Trajectory Change Point. The Reference Business Trajectory is rejoined, when the Estimated Time Over at the target Trajectory Change Point is at most Δt_{max} seconds. Again, as soon as the RBT is rejoined, a further non-reducible Trajectory Change Point marks the end of the resolution process. If the Reference Business Trajectory cannot be rejoined in respect to time until reaching $tcp_{o,n+1}$, the delay needs to be further reduced on the next trajectory segment.

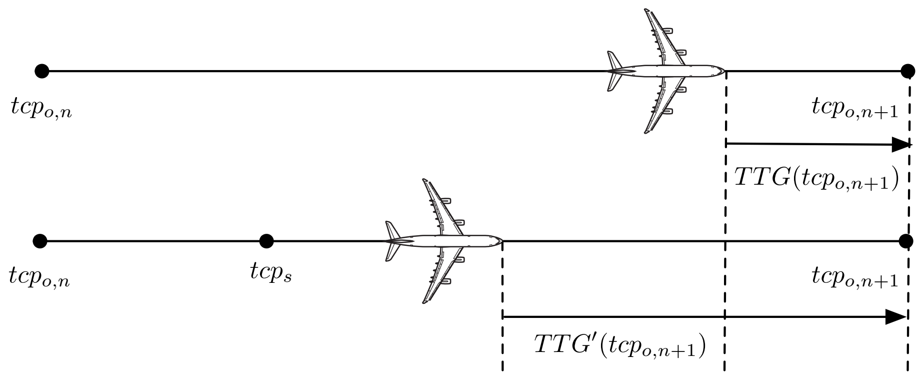

Figure 4.5: Speed Conflict Resolution manoeuvre

Figure 4.5 compares a resolution manoeuvre (lower aircraft) between the Trajectory Change Points $tcp_{o,n}$ and $tcp_{o,n+1}$ to the uninterrupted Reference Business Trajectory (upper aircraft). At TCP tcp_s the resolution starts with reducing ownships speed which results in a change of the Time to go (TTG) to the destination Trajectory Change Point $tcp_{0,n+1}$ (denoted as $TTG'(tcp_{o,n+1})$ in Figure 4.5). The Reference Business Trajectory is rejoined when the difference between $TTG'(tcp_o, n+1)$ and $TTG(tcp_o, n+1)$ is equal or less than Δt_{max}.

Consequence of change of speed
With heading ψ and ground speed V_{GS} constant, the change of speed causes a longitudinal deviation from the aircraft's Reference Business Trajectory. This can be expressed as a delayed or early arrival at the target point.

Theorem 4.3 (Impact of speed change)**.** *A speed change at constant heading and constant altitude impacts the fuel consumption.*

Proof. A change of speed is comprised of the phases

1. Acceleration / Deceleration to new speed,

2. Maintaining new speed,
3. Acceleration / Deceleration to reach RBT timeframe *and*
4. Acceleration / Deceleration to RBT speed.

Irrespective of the phase (acceleration, deceleration or maintaining of new speed), the thrust specific fuel consumption increases (decreases) with increasing (decreasing) True Airspeed (cf. Equation 4.7). The cruise fuel flow varies with thrust (cf. Equation 4.8). □

Measure for cost of a speed change
The cost of a speed change is quantified as the trend of delay between the Estimated Time Over and the Scheduled Time Over at the destination Trajectory Change Point $\Delta t = |t_{ETO} - t_{STO}|$ over flight time:

$$Ti = \int_{tcp_s}^{tcp_e} |t_{ETO} - t_{STO}| \, dt \tag{4.10}$$

4.3 Conflict Resolution system following an artificial force field concept

Upon detection of an infringement of ownship's Protected Airspace Zone, Conflict Resolution is initiated. As described in Section 2.5, the implementation of Conflict Resolution in this work is based on Artificial Force Fields [Hoe01; III00; Zeg98; DZ97]. The basic principle behind (Artificial) Force Field Conflict Resolution is to attribute all elements like the destination airport, the next waypoint and similar elements with a drawing force, and all hazardous elements like other traffic with a repulsive force.

Fulfilment of requirement
The Artificial Force Field Conflict Resolution has been chosen to fulfill the requirement regarding conflict clearness of the resulting trajectory (Violation of CAZ and PAZ, Section 4.1). The requirement is fulfilled if Equation 4.1 holds true for the resulting trajectory.

4.3.1 Definition of Forces

For the implementation used in this work, a similar approach as described in [DZ97] has been implemented. Two kinds of forces are used for the Artificial Force Field Approach. *Repulsive Forces* $\vec{F}_{rep}$ are caused by hazardous objects or environmental conditions while *Attractive Forces* $\vec{F}_{att}$ are directed towards the next planned Trajectory Change Point.
The *Resulting Force* $\vec{F}_{res}$ is the sum of the attractive and repulsive forces.

$$\vec{F}_{res} = k_a \cdot \vec{F}_{att} - k_r \cdot \vec{F}_{rep} \tag{4.11}$$

All forces can – if necessary – be weighted by a gain (in Equation 4.11 k_a and k_r).

Repulsive Force
All traffic violating ownship's Protected Airspace Zone are attributed with a repulsive force. The direction of the force $\vec{F}_i$ depends on the relative position of the traffic while its length is derived from the intrusion (cf. Equation 3.5). Thus, the force $\vec{F}_{rep}$ is defined as the sum of all repulsive forces acting on ownship:

$$\vec{F}_{rep} = \sum_{i=0}^{n} \vec{F}_i \tag{4.12}$$

In Equation 4.12 n denotes the number of all traffic items violating ownship's PAZ.The Force $\vec{F}_i$ is defined as

$$\vec{F}_i = \max(i_v, i_h) \cdot \mathbf{T}_D(\psi_r)\mathbf{T}_E(\epsilon_r)(1,0,0)^T \qquad (4.13)$$
$$\psi_r = \sigma_i - \psi_o$$

In the following the horizontal and vertical component of the repulsive vector, as well as the length of the repulsive vector will be detailed. A description of the rotational matrices $\mathbf{T}_E$ and $\mathbf{T}_D$ can be found in Section A.5.

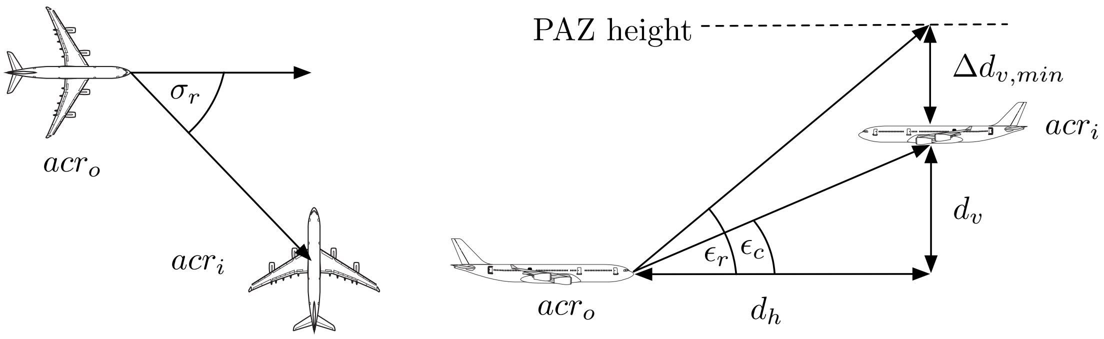

(a) Horizontal Component (b) Vertical Component

Figure 4.6: Repulsive Force

Horizontal component: The horizontal component of the vector is calculated using the relative bearing between ownship and intruder (cf. Figure 4.6(a)).
Vertical component: The vertical component of the vector is calculated by comparing the current elevation bearing ϵ_c to the required elevation bearing ϵ_r at the current horizontal distance (cf. Figure 4.6(b)).
Length: The length of the repulsive vector is given through the intrusion of ownship's Protected Airspace Zone (cf. Equation 3.5).

Attractive Force

The aim of Conflict Resolution is to resolve a conflict and guide ownship back to its Reference Business Trajectory. Therefore, the next Trajectory Change Point tcp_j before the conflict occurred, acts as an attractive force to ownship. The attractive force is defined as

$$\vec{F}_{att} = k_{tcp_j} \cdot \mathbf{T}_D(\sigma_{tcp,j})\mathbf{T}_E(\epsilon_{tcp,j})(1,0,0)^T \qquad (4.14)$$

In Equation 4.14, $\sigma_{tcp,j}$ and $\epsilon_{tcp,j}$ refer to the bearing, respectively elevation bearing, to the RBT's Trajectory Change Point tcp_j.
The length of the attractive force depends on the distance between ownship and the next TCP at time t_i. For an ordered set of TCP with $tcp_h <_t tcp_i <_t tcp_j <_t tcp_k$ and $tcp_i \leq t_i <_t tcp_j$ (cf. Figure 4.7) three zones are defined around the target Trajectory Change Point tcp_j, the

- delay zone between d_t^- and $tcp_j -_t tcp_h$,
- on-time zone between d_t^+ and d_t^- *and*
- early zone between 0 and d_t^+.

The definition of the zone boundaries depends on the the Trajectory Management Requirement regarding Estimated Time Over and Scheduled Time Over Δt_{max}, the initially planned time between the last TCP and the next TCP t_{tcp_i,tcp_j}, ownship's current distance to the target Trajectory Change Point d_c and the time since the last TCP $t_c = p_{acr_o} -_t tcp_i$.

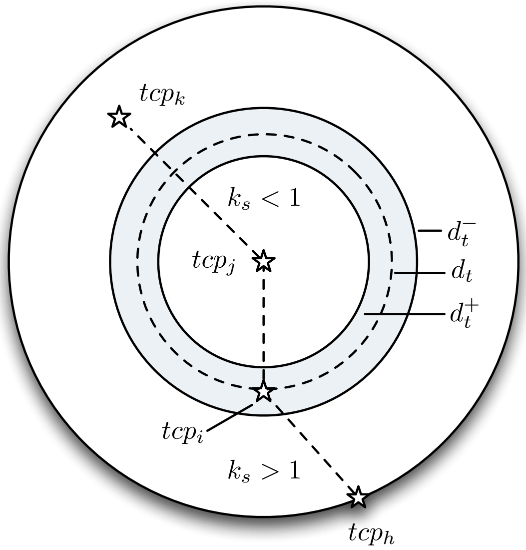

Figure 4.7: Attractive Force Gain depending on distance

Nominal Zone: The nominal zone is bounded by d_t^- and d_t^+. If ownship's current distance to the target Trajectory Change Point is between these boundaries, no gain is added to the attractive force. If the aircraft continues to stay within these boundaries, the deviation between the Scheduled Time Over and Estimated Time Over is within the Trajectory Management Requirement for the time Δt_{max}. The distance threshold calculates to

$$d_t = \frac{tcp_i - tcp_j}{tcp_j -_t tcp_i} \cdot t_c. \tag{4.15}$$

$$\tag{4.16}$$

Delay Zone: The delay zone is bounded by d_t^- and the Trajectory Change Point preceding the last TCP. If ownship is in this zone, the gain of the attractive force is increased. The distance threshold calculates to

$$d_t^- = \frac{tcp_i - tcp_j}{tcp_j -_t tcp_i} \cdot (t_c + \Delta t_{max}). \tag{4.17}$$

Early Zone: This zone is bounded by 0 and d_t^+. If ownship is about to arrive too early at the target Trajectory Change Point, the gain of the attractive force is reduced. The distance threshold calculates to

$$d_t^+ = \frac{tcp_i - tcp_j}{tcp_j -_t tcp_i} \cdot (t_c - \Delta t_{max}). \tag{4.18}$$

The gain calculates to

$$k_{tcp_j} = \begin{cases} k_{tcp_j,*} & \text{, if } t_c + \Delta t_{max} > tcp_j -_t tcp_i \\ k_{tcp_j,+} & \text{, else} \end{cases} \tag{4.19}$$

with

$$k_{tcp_j,*} = \begin{cases} d_c/d_t^- & \text{, if } d_t^+ \leq d_c \leq d_t^- \\ d_c/d_t^+ & \text{, if } d_c < d_t^+ \\ d_c/d_t & \text{, if } d_c > d_t^- \end{cases}$$

and

$$k_{tcp_j,+} = 2 + \frac{d_c}{tcp_i - tcp_j}.$$

The gain k_{tcp_j} in Equation 4.19 calculates as the ratio of the current distance compared to the early, nominal or delayed distance unless the time already travelled plus the maximum delay time $t_c + \Delta t_{max}$ is already larger than the initially planned time to go between tcp_j and tcp_i. In this case the gain calculates depending on the ratio between the current distance to the distance between the two Trajectory Change Points.

Result

The resulting force $\vec{F}_{res} = (x, y, z)^T$ is the output of the Artificial Force Field Conflict Resolution algorithm. The x-z component of the force is translated into the commanded heading while the z-component in combination with the Protected Airspace Zone height at the position of the intruder d_h is translated into the commanded altitude. The speed is derived from the length of the resulting vector.
The heading required calculates to

$$\psi_f = \tan(y, x), \tag{4.20}$$

the (Force Field) altitude calculates to

$$h_f = h + d_h \cdot z \tag{4.21}$$

and the (Force Field) speed calculates to

$$V_{TAS,f} = ||\vec{F}_{res}|| \cdot V_{TAS}. \tag{4.22}$$

The command values for altitude (Equation 4.21) and speed (Equation 4.22) are bounded by the speed and altitude envelope values depending on the aircraft type (cf. Table 2.2).

4.3.2 Integration of the Flight Management System Cost Index

The command values derived from the resulting force $\vec{F}_{res}$ do not respect the operators optimisation goal formulated through the Cost Index. For integration of the Cost Index, the command values need to be compared to the current aircraft speed, altitude and heading. Given the impact of lateral (cf. Theorem 4.1), vertical (cf. Theorem 4.2) and speed manoeuvres (cf. Theorem 4.3), the following dependencies are formulated:

- a Cost Index between 0 and 499 increases the preference for a lateral manoeuvre *and*
- a Cost Index between 499 and 999 increases the preference for a vertical and for a speed manoeuvre.

Fulfilment of requirement
The operators flight plan optimisation goal is taken into account by integration of the Cost Index into the Conflict Resolution. This relates to the requirement regarding *cost efficiency* of the resulting trajectory (cf. Section 4.1).

4.3.2.1 Gains on commanded values

The FMS Cost Index is integrated into the Conflict Resolution process by adding gains to the command values. In the following, gains for heading k_h, altitude k_a and speed k_s commands are used.

Change of heading
The larger the Cost Index, the less preferable is a heading change since it primarily impacts the distance to be travelled. At constant speed and altitude, this results in an extension of flight time. Therefore, the CI dependant gain k_h impacts the commanded heading as follows:

$$\psi_c = \sigma + k_h \cdot \Delta\psi \quad (4.23)$$
$$\text{with } \Delta\psi = \text{dif}(\sigma, \psi_f).$$

Figure 4.8 illustrates $\Delta\psi$ and ψ_f. The difference between two angles calculates to

$$\text{dif}(\psi_1, \psi_2) = \begin{cases} \psi_1 - \psi_2 & \text{, if } \psi_1 - \psi_2 > 180° \\ -(\psi_2 - \psi_1) & \text{, else.} \end{cases}$$

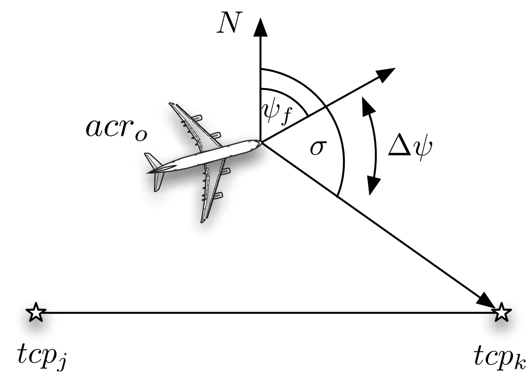

Figure 4.8: Illustration of $\Delta\psi$

Change of altitude
With a smaller Cost Index the preference for fuel saving manoeuvres becomes larger. Since an altitude change primarily affects the fuel consumption (cf. Theorem 4.2), the gain k_a impacts the commanded altitude as follows:

$$h_c = h + k_a \cdot (z \cdot Z_v). \quad (4.24)$$

In Equation 4.24, z and Z_v refer to the vertical component of the resulting force and the vertical width of the Protected Airspace Zone, respectively.

Change of speed
Similar to an altitude change, a change of speed impacts the fuel consumption (cf. Theorem 4.3). Therefore the gain k_s impacts the commanded speed as follows:

$$V_{TAS,c} = V_{TAS}(k_s \cdot (||\vec{F}_{res}|| - 1) + 1). \tag{4.25}$$

4.3.2.2 Estimation of gains

The Conflict Resolution necessitates a change of either heading, altitude or speed or a combination of them. The gains k_h, k_a and k_s (for heading, altitude and speed) are used to reduce the deviation from the Reference Business Trajectory under consideration of the Cost Index.

Boundaries
It is necessary to define boundaries for the gains. The maximum value for all gains shall be 1, i.e. the values for heading, altitude and speed derived from $\vec{F}_{res}$ are commanded without changes. The lower limit is a gain of 0, i.e. the respective commanded value is ignored.
Furthermore, the following requirements shall be met:

$$k_h = k_s = k_a \Rightarrow k_h, k_s, k_a \neq 0 \tag{4.26}$$
$$k_h = k_s = k_a \Rightarrow k_h, k_s, k_a \neq 1 \tag{4.27}$$

Equation 4.26 guarantees that at least one resolution manoeuvre is commanded. Equation 4.27 forbids that all gains are equally set to 1 which corresponds to a Conflict Resolution manoeuvre where the Cost Index is not considered at all in the resolution process[3].

Heading gain k_h
The shortest path between the current position of the aircraft and the target Trajectory Change Point can be traversed by following the bearing σ. Therefore, any commanded heading different from the bearing σ to the target Trajectory Change Point results in a longer distance to be travelled (cf. Figure 4.8). Thus, at an Cost Index setting of CI = 999, i.e. time-related costs are predominant, the bearing shall be followed ($k_h = 0$). The longer distance to be traversed and the curved segments necessary to achieve a heading change lead to a higher fuel consumption on the trajectory segment. Though, with the Specific Air Range not (considerably) affected (cf. Theorem 4.1), the new commanded heading shall be followed when fuel-costs are predominant, i.e. with an Cost Index setting of CI = 0. The heading gain k_h calculates to

$$f_{k_h}(CI) \quad = 1 - \frac{CI}{999} \tag{4.28}$$

Altitude gain k_a
A change of altitude with speed and heading constant results in a change of fuel consumption (cf. Theorem 4.2). With time-related costs predominant, a change of altitude would lead to a change in fuel consumption and thus Specific Air Range while the distance to be travelled and the time required would not be affected. Therefore, at an Cost Index setting of CI = 999 a change of altitude shall be at maximum while at CI = 0 a vertical force shall be disregarded.
The altitude gain k_a calculates to

$$f_{k_a}(CI) \quad = \frac{CI}{999}. \tag{4.29}$$

[3] This setting is used for the return to Reference Business Trajectory upon deviation when no repulsive forces act on ownship and for selection of a Protected Airspace Zone implementation.

Speed gain k_s
Similarly to an altitude manoeuvre, a speed manoeuvre primarily impacts fuel consumption (cf. Theorem 4.3). If time-related costs are dominant compared to fuel-related costs, i.e. with a CI larger than 499, it is necessary to conform more to the required speed change. Therefore, with a CI of 999 the speed change gain shall be maximum. With a Cost Index setting smaller than 499 the gain on the commanded speed shall be reduced and be minimal at a CI setting of 0.
The altitude gain k_s calculates to

$$f_{k_s}(CI) = \frac{CI}{999}. \tag{4.30}$$

Gains during manoeuvre phases
It is likely that the Conflict Resolution manoeuvre and thus also the repulsive forces acting on ownship end before the ownship has returned to its Reference Business Trajectory. Therefore, during the fourth manoeuvre phase – the return to the Reference Business Trajectory – the force of the target Trajectory Change Point still acts on ownship. While for the temporal and vertical deviation the force of the target Trajectory Change Point can be applied as described in Subsection 4.3.2.1 (Equation 4.24 and Equation 4.25) this is not the case for the lateral deviation. Regarding the lateral deviation, ownship is not expected to follow the bearing to the Trajectory Change Point but to rejoin the track between the RBT's Trajectory Change Points where the conflict occurred. This is achieved through reduction of the Cross Track Error by using the flight plan recapture method of the underlying aircraft library (cf. Subsection 4.3.3 and Subsection 5.2.3).

Summary
Table 4.1 summarises the gains for for the different manoeuvre phases (cf. Section 4.2) and the Cost Index settings of 0, 499 and 999 respectively.

Table 4.1: Gains per manoeuvre phase for selected Cost Index settings

Manoeuvre Phase	Cost Index	k_h	k_a	k_s
1-3	0	1	0	0
	499	≈ 0.5	≈ 0.5	≈ 0.5
	999	0	1	1
4	irrespective	n/a	1	1

4.3.3 Integration of flight dynamics model

One requirement to the Conflict Resolution generated trajectory is the requirement of flyability. This means, that the trajectory generated needs to respect the aircraft's flight envelope and flight dynamics. This implementation of an *Artificial Force Field* Conflict Resolution algorithm adresses this requirement through integration of a flight dynamics model. This aircraft model is based on EUROCONTROL's Base of Aircraft Data as described in [Nui04b]. As part of an *event-based traffic simulation*, Roth encapsulated the BADA aircraft model in a library, allowing *inter alia* to automatically execute a flight-plan and – when necessary – to override the command values $C = (\psi_c, h_c, V_{TAS,c})$ for heading, altitude and speed [Rot07]. Subsection 5.2.3 details the implementation of and interface to the aircraft model.

4.3.4 The Artificial Force Field Conflict Resolution algorithm

The algorithm devised in this work uses a fast time simulation of ownship's and intruder's movements to compute the resolution. Figure 4.9 illustrates the Conflict Resolution process. Starting with an initialization of ownship and intruder positions, the algorithm computes aircraft movement at a simulation step size of $t = 1s$. If ownship's Protected Airspace Zone is infringed by an intruder, the repulsive force de-

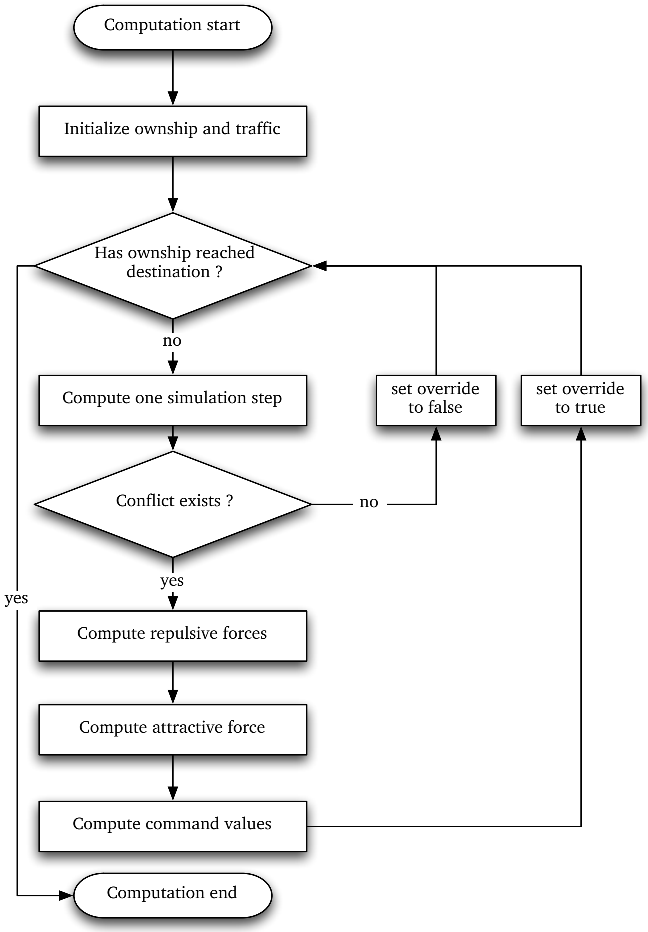

Figure 4.9: Flow diagram of Artificial Force Field Conflict Resolution algorithm

pending on the bearing and the vertical and lateral intrusions is computed as outlined in Subsection 3.2.3 and Section 4.3. Subsequently, the attractive force of the Reference Business Trajectory is computed and the required command values are derived. By overriding the automatic flight plan following function of the underlying flight dynamics model, the computed heading, speed and altitude are commanded. In case ownship's Protected Airspace Zone is not infringed, the automatic flight plan following function follows and, if necessary, recaptures the flight plan.
Details on the implementation of the flight dynamics model will follow in Subsection 5.2.3. Further details on the implementation of the Artificial Force Field Conflict Resolution algorithm may be found in Section G.4.

4.4 Summary

A Conflict Resolution system is an essential component for aircraft operating in Autonomous Operations Area airspace. This chapter has introduced to an implementation for a Conflict Resolution algorithm based on *Artificial Force Fields*.

With information on the conflict and a preference on the resolution's impact on the costs given through the Cost Index, the Conflict Resolution algorithm calculates an alternative trajectory for ownship.

To allow for integration of the Cost Index, the different manoeuvres that can be commanded – i.e. a heading, altitude or speed change – have been associated to time-related and fuel-related costs. With this association, manoeuvre preferences were derived from the Cost Index. A small Cost Index causes a preference for heading changes to resolve conflicts while with a large Cost Index speed or vertical manoeuvres are more likely.

To allow comparison of Conflict Resolution manoeuvres with different Cost Index settings, several parameters have been introduced. Safety related evaluation will be achieved by comparing the number and degree of infringements of ownship's Protected Airspace Zone. To compare the costs of the resolutions, three metrics have been introduced in this chapter. Impact of heading changes are measured by the horizontal area enclosed by the original and alternative trajectories. Similarly, altitude changes are measured by the vertical area enclosed by the original and alternative trajectories. Finally, with the trend of the delay in respect to the flight time, a measure for costs caused by speed changes has been introduced.

One requirement to the Conflict Resolution generated trajectory is the flyability, i.e. the *flight envelope* has to be respected. To guarantee that the computed trajectory is flyable, the *Force Field* algorithm has been extended to include an aircraft model based on EUROCONTROL's Base of Aircraft Data. The target heading, speed and altitude are commanded to this aircraft model. The execution of the flight plan and – when given – other commands are handled by the aircraft model implementation.

5 Realisation of the CD&R system concept

> When this one feature [balance and steering] has been worked out, the age of flying machines will have arrived, for all other difficulties are of minor importance.
>
> From *The Papers of Eilbur and Orville Wright*, Vol. 1, McGraw-Hill, New York, 1953

The Conflict Detection & Resolution system and its algorithms conceived in this work have been implemented in C++ to evaluate them in fast time simulations. This chapter gives an overview on this implementation and the simulation environment. Section 5.1 introduces to the realisation of the concept while Section 5.2 explains the class architecture and the modular concept of the Conflict Detection & Resolution system. Section 5.3 describes the steps taken for an evaluation run while Section 5.4 concentrates on the evaluation environment and describes the setup used for the simulations. Finally, Section 5.5 summarises this chapter.

5.1 Introduction

Chapter 3 and Chapter 4 have detailed the concept for the Conflict Detection and Conflict Resolution components of the system devised in this work. The aim of the implementation was to provide the Conflict Detection and Conflict Resolution functionality via interfaces which are independent of the implementation, thus allowing the exchange of the functional logic. The basic approach is illustrated in Figure 5.1. The Conflict Detection & Resolution system is initiated with the flightplans of ownship

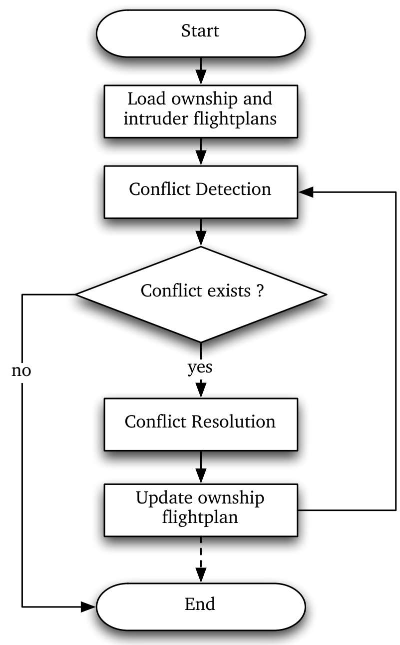

Figure 5.1: Flowchart of Conflict Detection & Resolution process

and intruder. The Conflict Detection requires at least these information to perform its computations.

Upon detection of a conflict, the Conflict Resolution module is initiated with – again – the flightplans of ownship and intruder and a set of conflict information. The set includes references to the Trajectory Change Points between which conflicts have been detected and information on the conflict as specified in Chapter 3, i.e. time to, distance at and position of all CPA. After a resolution has been computed, normal operation would be to feed it back into the Conflict Detection system to verify that it is conflict free and if not, to compute a new alternative resolution. For evaluation in scope of this work, the resulting trajectory is not re-iterated if it is not conflict-free but also returned for further comparison (cf. Section 5.3).

5.2 Class Architecture

The CD&R system conceived in this work has been implemented as an object-oriented architecture in C++, allowing the exchange of certain functions such as the Conflict Detection algorithm (cf. Chapter 3). This approach allows to evaluate different algorithms by implementing new classes and integrating them into the architecture.
The data structures common which have to be used by all classes are defined in the abstract classes

- ConflictDetectionResolutionModule,
- ConflictDetectionModule and
- ConflictResolutionModule.

Conflict Detection and Conflict Resolution implementations are chosen by instantiating classes derived from ConflictDetectionModule and ConflictResolutionModule, respectively. The common exchange format of trajectory information is the 4D Trajectory. The 4D Trajectory has been encapsulated in the Trajectory class. Figure 5.2 illustrates the Conflict Detection & Resolution classes and the dependencies to the *navigation* and *aircraft* classes.

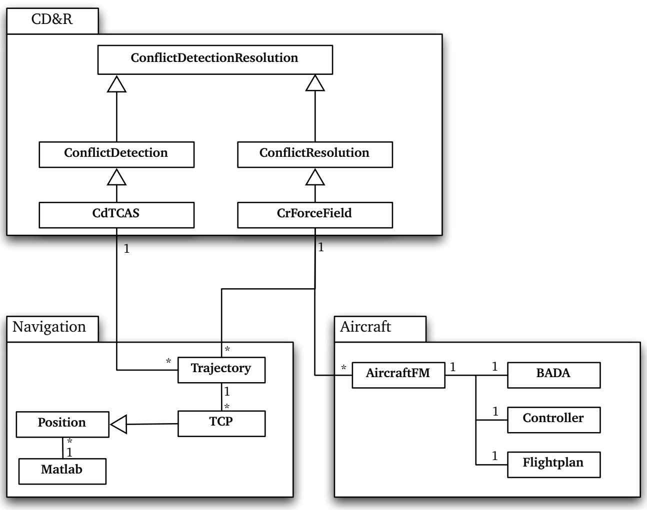

Figure 5.2: Conflict Detection & Resolution (CD&R) system UML diagram

5.2.1 Conflict Detection & Resolution classes

The Conflict Detection & Resolution system conceived in this work operates on Trajectory Change Points. The classes ConflictDetectionModule and ConflictResolutionModule[1] implement administrative func-

[1] In Figure 5.2 referred to as ConflictDetection and ConflictResolution

tions (such as to reset the CR module) and require each derived class to implement functions required for Conflict Detection and Conflict Resolution.

ConflictDetection

This class implements all functions required by Conflict Detection modules derived from it. The class exports the function GETCONFLICTS which calls the respective implementation of the Conflict Detection algorithm from the derived classes.

ConflictResolution

The CONFLICTRESOLUTION class holds similarly to CONFLICTDETECTION all common Conflict Resolution functions such as logging. It furthermore implements a Finite State Machine guaranteeing that Conflict Resolution can only be called if inputs such as ownship and intruder trajectories have already been provided. The class furthermore also allows to provide the CR algorithm with zones that are required to avoid when calculating a resolution[2].

CdTCAS

The CDTCAS class holds the implementation of the *strategic* TCAS algorithm as described in Chapter 3. The class returns a list of CPA information for each trajectory segment of ownship. Furthermore, based on the separation minima provided to the class as a ZONE object, the CD algorithm attributes each CPA as a conflict if required.

CrForceField

The CRFORCEFIELD class holds the implementation of the Artificial Force Field Conflict Resolution algorithm as described in Chapter 4. The CRFORCEFIELD class implements the virtual function COMPUTERESOLUTION of CONFLICTDETECTION to compute the resolution manoeuvre. This function requires as one input parameter an object of type COSTINDEX. The COSTINDEX class implements the Cost Index as described in Subsection 4.3.2. The Artificial Force Field algorithm devised in this work necessitates a flight dynamics model of the aircraft, therefore the CRFORCEFIELD class instantiates for each aircraft an AIRCRAFTFM object (cf. Subsection 5.2.3).

5.2.2 Navigation classes

All navigation related classes not requiring a model of aircraft dynamics are summarised in the NAVIGATION library. Beside other classes within the library, the most important namely TRAJECTORY, TRAJECTORYCHANGEPOINT, POSITION and the MATLAB interface MATLABNAV are briefly described.

Trajectory

The TRAJECTORY class holds for an aircraft an ordered set of Trajectory Change Points. On this set operations can be executed such as the calculation of future positions, return of (in time) overlapping TCPs between two trajectories or calculation of deviation from the Reference Business Trajectory on a trajectory segment.

Trajectory Change Point

The TRAJECTORYCHANGEPOINT class implements a Trajectory Change Point as of Definition 2.3. Furthermore, the class also implements Trajectory Management Requirements which are valid from the current TCP to the subsequent and the TCP dataset as defined for a Trajectory Change Report [SC 02]. Details on Trajectory Management Requirements may be found in Section A.1.

[2] The current implementation of the Conflict Resolution algorithm does not take these zones into account.

Position
The Position class implements a position as of Definition 2.1. All distance and comparison related functions as well as functions to calculate future positions given a (geodetic) speed vector, time and azimuth are implemented in this class.

MatlabInterface
Certain navigational calculations are implemented through an interface to Matlab. The functions to calculate

- distances (getDistanceGreatCircle and getDistanceRhumbLine),
- bearings (getAzimuthGreatCircle and getAzimuthRhumbLine) *and*
- future positions (getNextPositionGreatCircle and getNextPositionRhumbLine)

use the Matlab interface to call the Mapping Toolbox [Map] functions *azimuth.m*, *distance.m*, *track1.m*, *track2.m*, *reckon.m* and *distdim.m*. The Matlab interface is implemented as a *singleton* class [Eck99], guaranteeing that at most one instance is created during program execution.

5.2.3 Aircraft Classes

The *Trajectory* class does not implement a flight dynamics model but uses linear propagation to calculate future positions (cf. Subsection 5.2.2) between points. For Conflict Detection on straight segments this is sufficient, but for a simulation of aircraft movement as required by the Artificial Force Field Conflict Resolution algorithm aircraft dynamics need to be modelled as well. The Aircraft classes implement an aircraft dynamics model based on the Base of Aircraft Data [Nui04b]. The implementation is based on Roth's implementation for an event-based traffic simulation for TUD's fixed-based research flight simulator and flight simulation environment [Rot07]. Changes made to these classes are summarised in Subsection 5.2.4.

AircraftFM
The AircraftFM represents an aircraft object which can be initialised with BADA supported aircraft types [Nui04a]. The aircraft is set up with a flight plan consisting of 4D position information and ETOs for the waypoints. The waypoints can either be setup as *fly-by* or *fly-over* waypoints. The AircraftFM simulates aircraft dynamics at a step size of $1s$. Roth's implementation simulate the flight within aircraft specific boundaries (flight and speed envelope) and the BADA constraints, e.g. the maximum absolute bank and the maximum roll rate. Under normal operation the aircraft accomplishes the flight with a precision of RNP 0.1 [Rot07]. The library exports functions allowing to override the accomplishment of the flight plan by commanding new heading, altitude or speed. In case heading, altitude and speed are not overridden, AircraftFM automatically recaptures the original flight plan. Figure 5.3 illustrates the simulation process.

Controller
The Controller classes generate control values for the *Lateral*, *Vertical* and *Velocity* controller. The created values are processed in the AircraftFM class, taking the limitations given by the BADA aircraft model into account. Further information on the implementation may be found in [Rot07].

BADA
The BADA classes hold the implementation of all flight performance related calculations. The implementation by Roth follows the BADA model as described in [Nui04b]. The BADA classes load aircraft specific parameters retrieved from BADA Operations Performance Files to *inter alia* calculate flight and speed envelope and maximum Rate of climb/descent.

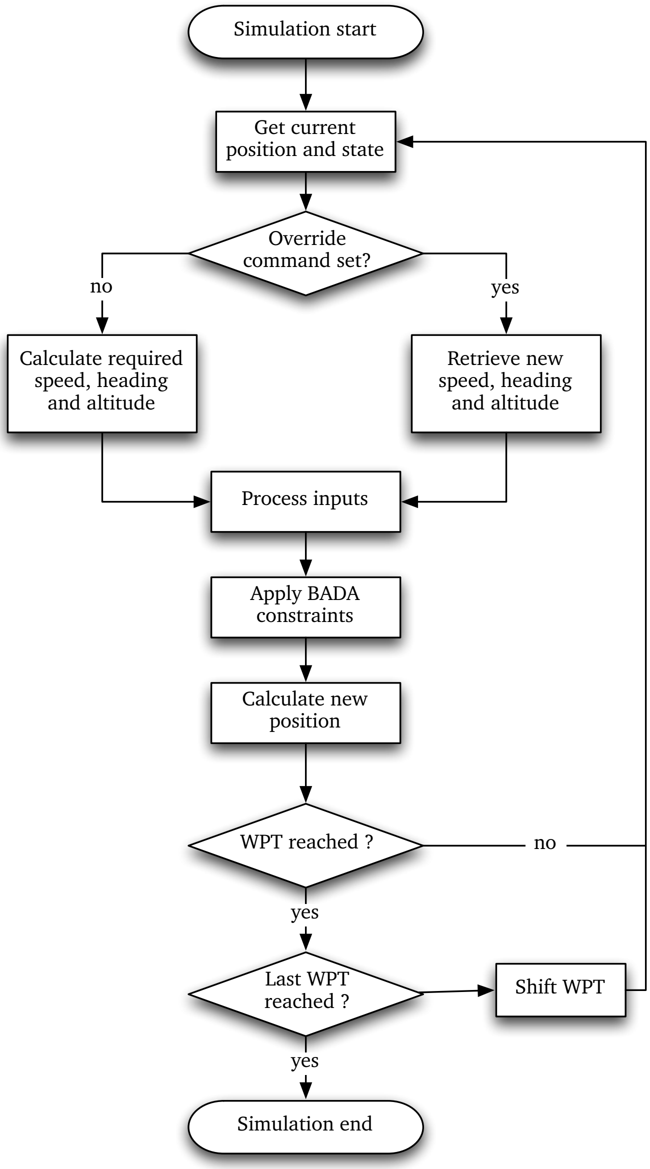

Figure 5.3: AIRCRAFTFM simulation overview

Flightplan

The FLIGHTPLAN classes represent the aircraft's flightplan by a list of waypoints. Each waypoint consists of

- Position $(\lambda^{\diamond}, \phi^{\diamond}, h)$,
- Estimated Time Over *and*
- waypoint type (*fly-by* or *fly-over*).

For the scope of this work, a Trajectory Change Point is translated into the waypoint structure by attributing the waypoint as a *fly-over* waypoint. This guarantees that the waypoint is approached within at least 185.2m (RNP 0.1).

5.2.4 Changes made to Aircraft Library

This subsection summarises the changes made to *Control Value Generator* from the aircraft library implemented in the event-based traffic simulation application [Rot07].

Control Value Generator
The implementation of the control value generator as of [Rot07] was laid out for slow speed conditions as during landing or initial climb. Altitude changes during cruise at high speeds ($> 200\frac{m}{s}$) resulted in significant overshooting.
In order to allow for short term altitude changes in the cruise phase as required by Conflict Resolution algorithms, the control value generator for vertical control was updated. The control value γ_c is a function of

- current altitude h,
- demand altitude h_d,
- rate of climb/descent ROC and
- true air speed V_{TAS}.

The control value generator function f_{γ_c} is defined as:

$$f_{\gamma_c} = \text{sgn}(\Delta h) \cdot \begin{cases} \min(\gamma_{max}, \text{atan}(\frac{\Delta h}{V_{TAS}})) & \text{if } t_{lo} > t_{h_d} \wedge \text{sgn}(\gamma) = \text{sgn}(\Delta h) \\ 0.001 \cdot \min(100, \Delta h - t_{lo} \cdot \text{ROC}) & \text{else} \end{cases} \tag{5.1}$$

$$\Delta h = h_d - h$$
$$t_{lo} = \frac{\text{ROC}}{a_{z,max}} \tag{5.2}$$
$$t_{h_d} = \frac{\Delta h}{\text{ROC}}$$

For evaluation of the value generator an Airbus A340-300 has been simulated. The aircraft weight was set to $210000kg$ (aircraft nominal weight as of BADA). The aircraft was commanded to climb from FL240 (7315.2) to FL410 ($12496.8m$) and after maintaining the new altitude for $60s$ back to FL240.
The maximum normal acceleration $a_{z,max}$ (Equation 5.2) is defined as $a_{z,max} = 5\frac{ft}{s^2} \approx 1.524\frac{m}{s^2}$ [Nui04b]. Figure 5.4(a) illustrates the step response for an altitude change by $5181.6m$ at constant Mach $M = 0.81$. The climb from $7315.2m$ to $12496.8m$ is achieved within $571s$, corresponding to an average ROCD of $9\frac{m}{s}$ or $1771\frac{ft}{min}$. With the TAS required for maintaining a constant Mach number decreasing until reaching the tropopause at $11000m$, the climb rate benefits from the available power (cf. [SM02]). The descent to $7315.2m$ is achieved in $535s$, corresponding to an average ROCD of $-9.6\frac{m}{s}$ or $1889\frac{ft}{min}$. The maximum ROCD during climb was $17.56\frac{m}{s}$ and $-22.67\frac{m}{s}$ during descent. With $1.53\frac{m}{s^2}$ the maximum acceleration overshot the $a_{z,max}$ constraint slightly. Figure 5.4(b) illustrates the ROCD and acceleration.

5.3 Evaluation Sequence

Figure 5.5 illustrates the sequence of steps implemented to evaluate the conceived Conflict Detection & Resolution system. The evaluation sequence is subdivided into the *Conflict Detection*, *Conflict Resolution*, creation of *Reference Trajectory* and the *Validation* parts.

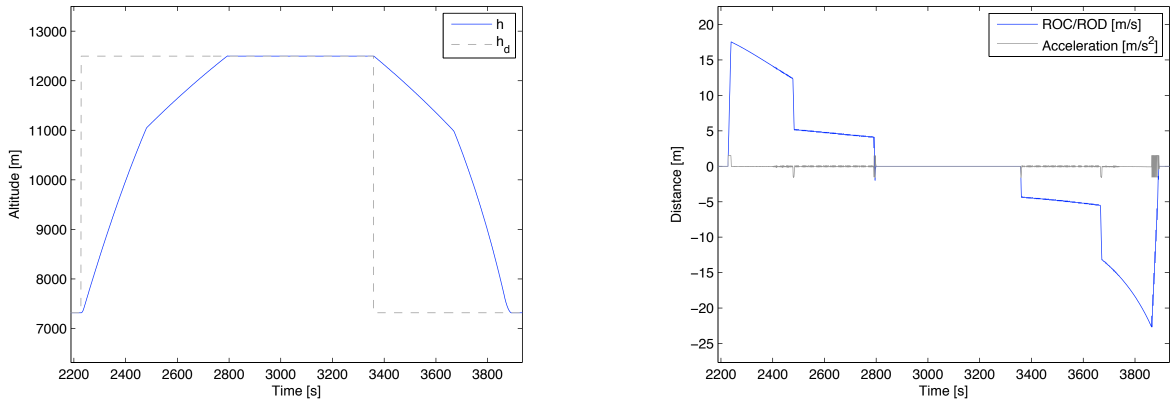

(a) Step response (b) ROCD and acceleration

Figure 5.4: Behaviour of simulated aircraft during change of altitude

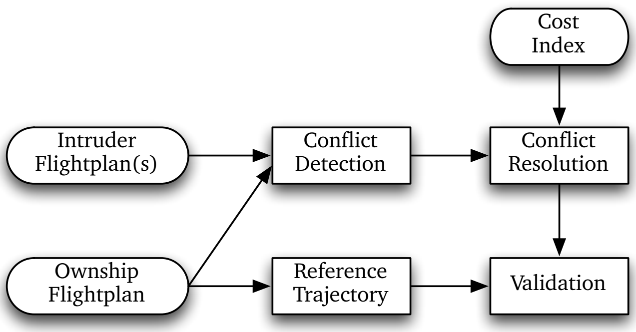

Figure 5.5: Program Sequence used for evaluation

Conflict Detection

With ownship and intruder flighplans (given as trajectories) as input, the Conflict Detection using the CdTCAS implementation is executed. The result, a list of CPAs is subsequently passed on to the Conflict Resolution module along with the original list of TCPs and markers between which TCPs the conflict(s) occurred.

Reference Trajectory

An uninterrupted (i.e. without conflict) flight of ownship following the original flight plan is simulated and logged for later comparison against the new route. For simulation of the route an instance of the AircraftFM class is created with the Trajectory Change Points translated to *fly-over* waypoints.

Conflict Resolution

Using the Artificial Force Field algorithm as implemented in CrForceField, the Conflict Resolution module computes a set of alternate TCPs between the two TCPs where the conflict occurred. The output of the module is an ordered set of Trajectory Change Points.

Validation

The new trajectory is validated by running a Conflict Detection on the original intruders and updated ownship route. For this Conflict Detection the strategic TCAS algorithm (CdTCAS) is used again. Irrespective of the result of this second Conflict Detection the new trajectory is also compared against the original trajectory.

5.4 Evaluation Environment

For evaluation of the Conflict Resolution the outputs of each of the evaluation steps are written to log files. These log files are later evaluated using MATLAB scripts. This section summarises the outputs logged and the evaluation process.

Evaluation process

Each scenario is processed with a Cost Index setting within the boundaries of 0 and 999, whereas it is incremented by 100 during each simulation step (except for the first step where it is incremented by 99). Additionally, a Conflict Resolution manoeuvre is calculated without any gains on lateral, vertical or speed manoeuvres, i.e. without an Cost Index setting.

Outputs

The common exchange format between the modules are trajectories comprised of a set of Trajectory Change Points. These TCPs need to be translated into a representation of the actual flown route for evaluation. As outlined in Subsection 5.2.3, the AIRCRAFT classes are used to generate such a representation of the trajectory. Figure 5.6 illustrates the sequence applied for the generation of the *alternate* and *reference trajectories*. Those steps of the evaluation sequence which use AIRCRAFTFM class for simulation of aircraft movement[3] produce a log file with the aircraft positions at an intervall of 1*s*. These log files are used for later comparison of the aircraft trajectories, i.e. the evaluation of the lateral, vertical and temporal deviation from the Reference Business Trajectory. Furthermore, the status of the Conflict Resolution (active/inactive) and the distances (vertical, horizontal and slant distance) between ownship and all intruders are logged as well. Table 5.1 summarises the variables recorded which are used for later evaluation, while Table D.2 (Section D.2) lists further variables recorded (for validation of the changes made to the AIRCRAFT classes). Depending on the number of intruders (Table 5.1, row 8) the logs entries regarding distance and status of the resolution (Table 5.1, rows 9-12) are repeated.

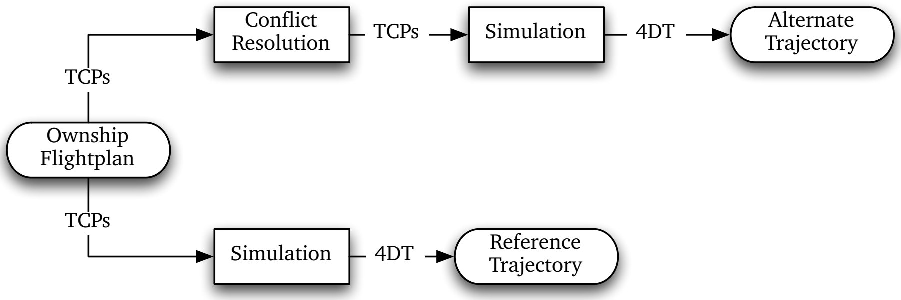

Figure 5.6: Sequence for generation of trajectories

5.5 Summary

The evaluation of the integration of the Cost Index into the Conflict Resolution process is achieved through fast time simulations of selected scenarios. This chapter has introduced to the realisation of the Conflict Detection & Resolution concept devised in this work. The implementation of the CD&R concept has been described. This implementation can be extended to support other CR (and also CD) algorithms by implementing new derivatives from the respective super classes. This concept is eased through the introduction of a common exchange format, the trajectory which is comprised of an ordered set of Trajectory Change Points. Flight dynamics are simulated by accessing the AIRCRAFT classes implemented

[3] i.e. *Conflict Resolution* and creation of *Reference Trajectory*.

Table 5.1: List of recorded variables (used for evaluation)

Variable	Conflict Resolution	Alternate Trajectory	Reference Trajectory
Timestamp	✓	✓	✓
Index	✓	✓	✓
$\lambda^{\diamond}, \phi^{\diamond}, h$	✓	✓	✓
ψ, V_{TAS}	✓	✓	✓
XTE	✓	–	–
ΔETO	✓	–	–
$\psi_C, h_c, V_{TAS,c}$	✓	–	–
No. Intruder	✓	–	–
Distance	✓	–	–
d_h	✓	–	–
d_v	✓	–	–
Resolution	✓	–	–

as part of an event-based traffic simulation. Changes to the *Control Value Generator* have been made to reduce the overshooting of the aircraft when commanding new altitude during the cruise phase (at speeds $\geq 200\frac{m}{s}$). Furthermore, with the utilisation of an interface to the MATLAB environment, functions operating on the earth ellipsoid could be externalised. This allowed to access MATLAB scripts which have been thoroughly reviewed and tested for implementing navigation functions. Finally, the evaluation sequence has been described, with the comparison of aircraft trajectories plotted at an interval of $1s$ being the logs used for later evaluation using MATLAB scripts.

6 Evaluation strategy

> In many situations, the performance of an algorithm of interest cannot be estimated analytically (Those who can, do. Those who cannot, simulate).
>
> Yaakov Bar-Shalom and Xiao-Rong Li, *Estimation and Tracking: Principles, Techniques and Software*

THE preceding chapters described the operational concept of the future Air Traffic Management system and presented a concept and an implementation for a Conflict Detection & Resolution system necessary for operating in Autonomous Operations Area airspace. Several requirements were identified which are needed to be met by the system. This chapter is concerned with the means used to validate adherence to those requirements and the integration of the Cost Index. Section 6.1 introduces to the evaluation strategy used in this work and derives the principle scenarios from the hypotheses. A detailed description of the scenarios is given in Section 6.2. The evaluation variables and measurements are described in Section 6.4. Section 6.5 concludes this chapter with a summary on the findings.

6.1 Introduction

The aim of the Conflict Detection & Resolution system devised in this work is to detect air traffic conflicts and to resolve them under consideration of the Cost Index while ensuring flyability of the resulting trajectory. For the detection of air traffic conflicts an algorithm has been presented in Chapter 3 which uses an explicit definition of conflicts and is based on the distance at the Closest Point of Approach. The resolution algorithm, based on *Artificial Force Fields*, has been described in Chapter 4. The algorithm presented there is expected to ensure flyability by integration of a flight mechanics model and to respect the selected Cost Index setting.

Following the realisation of the concept devised (Chapter 5), means for evaluation are necessary to be identified. Different strategies can be used depending on the aim of the evaluation and the maturity of the application. Evaluation strategies for Conflict Detection & Resolution systems include *analytic evaluations* (e.g. [GM02; Ges+02; BSC96]), evaluations with the help of *(fast-time) simulations* (e.g. [DAC96; EE99; Rat+02; Vie97; Too+07]) and *human factors assessments* (e.g. [Hoe01; Kri+03; DZ97])[1]. Regarding assessment of the maturity of an application, which is also needed to be known in order to identify an evaluation strategy, the *Technology Readiness Level* (TRL) concept [Man95; Dep05] has become a *de-facto* standard. This concept has been introduced by NASA and was later further developed and adapted to different technology domains[2]. The TRL scale usually consists of nine levels with *TRL1* being the lowest level and *TRL9* being the most advanced level of development (cf. Figure 6.1). The first TRLs are concerned with the basic principles and the system concept. The stages up to the development and evaluation of a prototype are concerned with analytical and experimental evaluation of critical functions and component validation in laboratory, respectively relevant, environments. The later stages cover evaluation of prototypes in high-fidelity and field environments.

The *analytical* evaluation of the performance of algorithms is usually used during the first stages of research and development but also in combination with assessments through simulation. This approach

[1] Duong and Zeghal [DZ97] integrated a prototype into a network of cockpit simulators for concept demonstration.
[2] Further information on the TRL concept are summarised in Section A.7

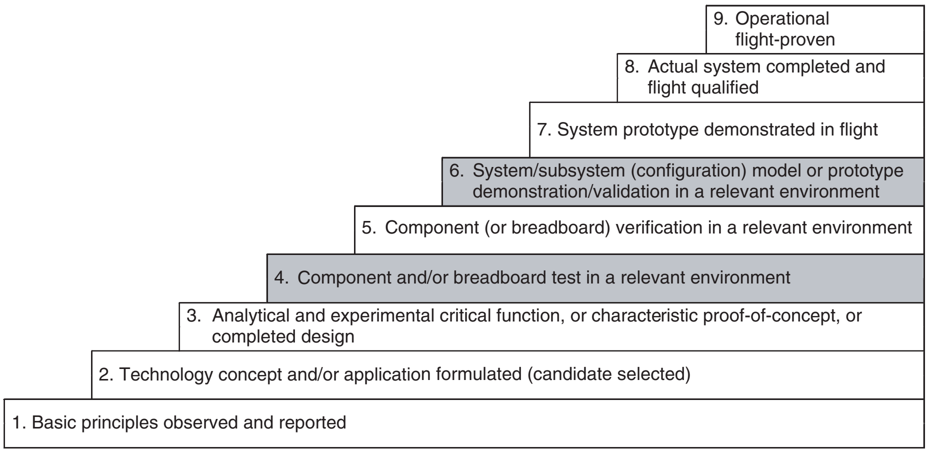

Figure 6.1: Technology Readiness Level from [Com02]

is used to give a formal proof that certain requirements are met by the conceived system and usually requires a consistent mathematical description of the problem. This evaluation technique is facilitated by resolution algorithms which use a (parameterised) set of possible resolutions, such as turns with different radii. Geser et al. for example could give a mathematical proof for their *geometric* Conflict Resolution algorithm [Ges+02] where they allowed different combinations of line and circle segments. The proof was focused on the construction of the resolution and the adherence to the requirements to keep a minimum separation from the intruder and to meet a given Required Time of Arrival (RTA). The flyability related constraints were considered to be dealt with by an external module.
Evaluations using *(fast-time) simulations* are mainly concerned with one component of a complex system and are usually used to verify analytical or theoretical assessments or to give a proof-of-concept. They are also used as an alternative to the analytical evaluation if the complexity of the system hinders a sound mathematical assessment. Evaluations using (fast-time) simulations usually cover *corner cases* or *worst case scenarios*. This evaluation technique was *inter alia* used by Eby and E. Kelly III to show that potential field algorithms are a robust solution to the problem of Conflict Detection & Resolution [EE99]. They used a variety of scenarios reaching from two to eight aircraft conflicts. Fast-time simulations can also be used to prepare human-factors assessments (see e.g. [Hoe01]) or to identify interesting scenarios for further evaluation.
Human factors assessments with *human-in-the-loop* evaluations are used when interaction and pilot usability are surveyed or if pilot input is required. Advantage of this evaluation technique is, that operational concerns stated by the pilots can be surveyed and if necessary considered in the further development of the system. Human factors evaluations are often concerned with novel display systems (see e.g. [Sin08; Bau10]) or with evaluation of novel procedures in respect to pilot workload (see e.g. [Wip05]). This type of evaluation is usually applied at later maturity levels of an application, ideally also in preparation for field trials and evaluations in an operational environment (cf. e.g. [Wip+03; Sin+06]). The *human-in-the-loop* assessments by Hoekstra followed an offline fast-time traffic simulation of the conceived CD&R system and were aimed at estimation of workload, crew situational awareness, pilot acceptance and evaluation of the CDTI in respect to cluttering [Hoe01, Chapter 10]. Similarly, the evaluations by Krishnamurthy et al. were aimed at evaluating the ability of pilots to meet constraints and solve conflict situations in the proximity of hazards, investigate pilot use of airborne Conflict Resolution systems and study pilot interactions in an over-constrained conflict situation [Kri+03].

Evaluation approach applied
With the focus of this thesis on the evaluation of the impact of the Cost Index on the resolution process and the assurance of flyability of the resulting trajectory, simulations with different scenarios have been

chosen as evaluation strategy. This strategy allows variation of the Cost Index during the scenarios and ensures repeatability. The fast-time simulations can be used to verify the expected impact of the gains on the CR process as described in Subsection 4.3.2.1. Furthermore, by the design of Mid-Air Collisions which require evasive manoeuvres for resolution, the assurance of flyability can be evaluated. The selected evaluation approach is also in line with the maturity of the application which already advanced the conceptual stages but does not yet qualify for large scale evaluations such as *human-in-the-loop* assessments.

6.1.1 Evaluation of adherence to requirements

Two requirements have been formulated which are needed to be met by the Conflict Detection & Resolution system devised in this work (cf. Subsection 2.5.6).

The first requirement is, that flyability of the resulting trajectory is guaranteed by the design of the algorithm, i.e. no flyability check is required to be performed after computation of the resolution manoeuvre. Constraining factors are acceleration limits, maximum bank and roll rate, maximum pitch and maximum Rate of climb/descent (ROCD). Furthermore, the flight envelope needs to be adhered to as well, i.e. maximum and minimum speeds and altitude. In order to validate this requirement, it is therefore necessary to design a scenario in such a way, that the maxima and minima (for speed and altitude) will be met.

The second requirement is, that the Conflict Resolution needs to ensure that a conflict-free trajectory is calculated. A trajectory is considered conflict-free if the distance between ownship and intruder is larger than the Collision Avoidance Zone. The Protected Airspace Zone, which takes ownship state information into account and which is at least as large as the Collision Avoidance Zone, will be infringed due to the design of the algorithm. A repulsive force acts on ownship if and only if the intruder is already within the Protected Airspace Zone volume. Here, the degree of infringement is of interest which is expressed by the *intrusion* (cf. Subsection 3.2.3).

It is expected that an evasive resolution manoeuvre will be required when an intruder approaches ownship from the side and ownship implements a Protected Airspace Zone aligned to its heading as illustrated in Figure 6.2. By this, the Protected Airspace Zone is infringed at its smallest propagation and ownship will react later compared to a conflict where the intruder approaches from ahead. A distance of

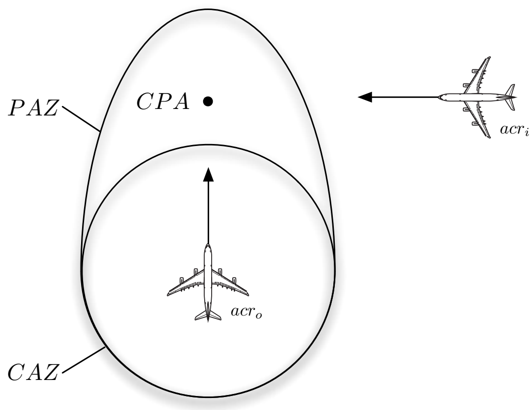

Figure 6.2: Intruder approaching from the side

$d_{CPA} = 0m$ at the Closest Point of Approach can be considered as a highly unlikely worst-case scenario. Such a Mid-Air Collision will also require of ownship a maximum deviation from the Reference Business Trajectory, which eases the evaluation of the impact of the Cost Index integration.

6.1.2 Evaluation of hypotheses

Goal of this thesis is to show and validate the integration of the Cost Index into the Conflict Resolution process. The hypothesis is, that the Conflict Resolution algorithm can be devised in such a way, that a small Cost Index setting will have a lesser impact on fuel-related than on time-related costs. Opposed to that, a large Cost Index setting shall have a larger impact on fuel-related than on time-related costs.
To assess the impact of the Cost Index on the resolution process, a conflict needs to be equally resolvable by either the sole application of a lateral, vertical or speed manoeuvre. With this, the effect of the prioritisation on the selected manoeuvre can be surveyed.
Furthermore, another interesting scenario would be to survey the impact of the Cost Index setting on a resolution, where one degree of freedom less can be used for resolving the conflict. The two *remaining* possible resolution manoeuvres should have an opposite dependency on the Cost Index, so that at least one manoeuvre can be used for resolving the conflict.

6.2 Scenario Description

For evaluation of the Conflict Detection & Resolution system and the Cost Index integration, three scenarios have been designed. Each of the scenarios contains a traffic conflict which one aircraft (*ownship*) tries to resolve using the *Artificial Force Field* Conflict Resolution algorithm as described in Chapter 4.
Two of the scenarios, i.e. *Scenario I* (Subsection 6.2.1) and *Scenario III* (Subsection 6.2.3), are located within the Inflight Broadcast Procedure area over Africa. The second scenario, *Scenario II* (Subsection 6.2.2), is located over the North Atlantic Organised Track System.
In the following, for each scenario a description will be given on

- the flight plans,
- the Closest Point of Approach,
- the Protected Airspace Zone geometry *and*
- the evaluation goal.

Furthermore, the reference Conflict Resolution trajectory – i.e. the Conflict Resolution trajectory not considering the Cost Index – will be presented. Therefore Conflict Resolution trajectories based on different Protected Airspace Zone implementations (cf. Section 3.2) will be compared. The zone implementation achieving the smaller distance at the Closest Point of Approach while maintaining safe separation will be used for the Cost Index integration evaluation runs.

Trajectory Management Requirement
For all scenarios, the Trajectory Management Requirement regarding adherence to the Reference Business Trajectory is set to:

$$\Delta\lambda^{\diamond}_{max} = 185.2m \qquad \text{(lateral compliance to trajectory)}$$
$$\Delta h_{max} = 185.2m \qquad \text{(vertical compliance to trajectory)}$$
$$\Delta t_{max} = 20s \qquad \text{(compliance to Scheduled Time Over)}$$

The requirement for lateral adherence to the planned trajectory $\Delta\lambda^{\diamond}_{max}$ is derived from the Required Navigational Performance (RNP) for Terminal Manoeuvring Areas [ICA99] (RNP class 0.1, cf. Section A.2). The same maximum error has been chosen for the vertical deviation allowed Δh_{max}. The requirement regarding compliance to the Scheduled Time Over Δt_{max} is taken from an example for tight Trajectory Management Requirement (TMR) parameters [Ses].

6.2.1 Scenario I – IFBP region

Scenario I is aimed at the evaluation of the Conflict Resolution manoeuvre in respect to the Cost Index set. Therefore a conflict between two aircraft is set up where acr_o detects a conflict and computes a resolution with a CI ranging from 0 to 999. The intruder aircraft is supposed to intercept ownship's trajectory from the side as illustrated in Figure 6.3. Ownship and intruder are both simulated using an aircraft model of an *Airbus A340-300*.

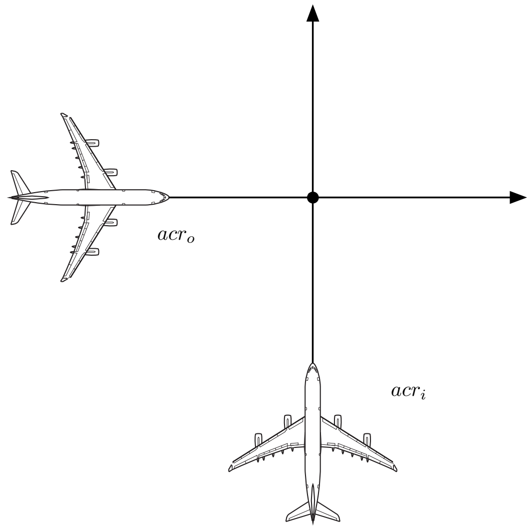

Figure 6.3: Illustration of Scenario I conflict situation

Flightplan

Table 6.1 and Table 6.2 summarise the flight plans of acr_o and acr_i. The conflict is set up to occur over waypoint *FL* where both aircraft are supposed to arrive at the same Required Time Over (RTO) and the same flight level ($10058m =$ FL330).

Table 6.1: acr_o Flightplan - Scenario I

Waypoint	Latitude ($\lambda°$) [deg]	Longitude ($\phi°$) [deg]	Altitude [m]	RTO [hh:mi:ss]
AMDIR	19.056667	14.785278	10058	04:00:00
BURAT	16.946667	14.864444	10058	04:16:00
DETEL	14.651111	14.948333	10058	04:34:00
FL	12.141694	15.038306	10058	04:57:00
RINIP	8.917500	15.345833	10058	05:27:00
UMOSA	8.000000	15.432222	10058	05:34:00

Table 6.2: acr_i Flightplan - Scenario I

Waypoint	Latitude ($\lambda°$) [deg]	Longitude ($\phi°$) [deg]	Altitude [m]	RTO [hh:mi:ss]
ERESA	11.639167	19.779167	10058	03:58:00
DENAT	11.882778	17.575833	10058	04:34:00
FL	12.141694	15.038306	10058	04:57:00
KORUT	13.340833	10.633333	10058	05:35:00

Scenario Goal
The Cost Index is the test variable in Scenario I. Initially, the conflict can be resolved by either applying

- a change of heading (to the left or to the right of ownship's track),
- a change of speed (deceleration and subsequent acceleration or vice versa) or
- a change of altitude (descent followed by climb or vice versa).

Through variation of the Cost Index the allowed resolution manoeuvres are prioritised and if necessary combined.
Furthermore, the conflict point is over waypoint *FL* which makes a compensation of any delays introduced through the Conflict Resolution manoeuvre on this trajectory segment unlikely. It is expected, that Conflict Resolution manoeuvres with a high Cost Index setting will have less delay at the waypoint *FL* than those with a lower setting.

Protected Airspace Zone geometry
The dimensions of the Protected Airspace Zone are:

d_{lon}	10 min
d_{lat}	$2407.6m$
d_{ver}	$304.8m$

A longitudinal separation of 10 minutes for aircraft on crossing tracks (cf. Section B.2) is considered applicable. Lateral dimension of the Protected Airspace Zone correspond to the TCAS protection volume parameter for Traffic Adivsories between FL200-FL420 (cf. Section E.1). PAZ height is given by the Reduced Vertical Separation Minima of 1000ft ($\approx 304.8m$).

Closest Point of Approach
The Conflict Detection algorithm identifies the point at $(\lambda^\diamond, \phi^\diamond, h) = (12.1417°, 15.0383°, 10058.0m)$ as Closest Point of Approach. Table 6.3 summarises the CPA information. With intruder at the same position, vertical and lateral distances at CPA are $0m$.

Table 6.3: Scenario I - Closest Point of Approach

	Latitude ($\lambda^\diamond$) [deg]	Longitude ($\phi^\diamond$) [deg]	Altitude [m]	ψ
CPA	12.1417	15.0383	10058	174.61
Intruder	12.1417	15.0383	10058	286.07

Protected Airspace Zone implementation
With longitudinal separation given in *minutes*, the Protected Airspace Zone implementation is required to include at least ownship state information. Three PAZ implementations allow this (cf. Subsection 3.2.2). For comparison, the *Ownship Speed Zone* Z_S and *Modified Relative Zone* Z_R have been chosen. While the first implementation only includes ownship speed into the Protected Airspace Zone layout, the modification to Relative Speed Zone also takes the bearing to the intruder into account.
Table 6.4 summarises the results of CR simulations with the Artificial Force Field algorithm using the *Ownship Speed Zone* and *Modified Relative Zone* implementations. The first part of the table summarises the *safety* related parameters while the second part is concerned with the *cost* related parameters. Parameters regarding the *trajectory* are summarised in the last part of Table 6.4.
Horizontal, vertical and temporal deviation for the *Modified Relative Zone* Z_R implementation are larger than for the *Ownship Speed Zone* Z_S implementation due to the distance between ownship and intruder when ownship's Protected Airspace Zone is infringed for the first time. The *Ownship Speed Zone* zone

Table 6.4: Scenario I - Comparison of CR Zone implementations

	Ownship Speed Zone Z_S	Modified Relative Zone Z_R
Distance at CPA $[m]$	1192.60	7996.90
Horizontal Distance at CPA $[m]$	1192.46	7995.98
Vertical Distance at CPA $[m]$	-18.52	-121.26
#PAZ intrusions	1	29
Maximum intrusion tuple	(0.504710, 1.000000)	(0.906286, 1.000000)
Duration of PAZ intrusions [s]	14	298
Conflict solved	ϟ	✓
H $[km^2]$	2.80	233.36
V $[km^2]$	12.54	38.62
Ti $[s^2]$	888.81	2639119.16
minimum com. Speed $[\frac{m}{s}]$	189.44	160.84
maximum com. Speed $[\frac{m}{s}]$	245.31	201.90
minimum act. Speed $[\frac{m}{s}]$	198.84	160.84
maximum act. Speed $[\frac{m}{s}]$	205.88	202.32
minimum com. Altitude $[m]$	10137.00	10059.50
maximum com. Altitude $[m]$	10209.60	10180.00
minimum act. Altitude $[m]$	10058.00	10058.20
maximum act. Altitude $[m]$	10093.20	10179.70

implementation is violated for the first time at a distance of $2327.63m$ and the intrusion lasts for 14 seconds. With the PAZ aligned along ownship's heading, an intruder approaching sideways violates the PAZ at its smaller lateral propagation. During the 14 seconds of intrusion the speed is commanded within the boundaries of $189.44\frac{m}{s}$ and $245.31\frac{m}{s}$ while the minimum and maximum speeds achieved are $198.84\frac{m}{s}$ and $205.88\frac{m}{s}$, respectively.
The *Modified Relative Zone* zone implementation, which longitudinal propagation is aligned to ownship's bearing to the intruder, is infringed at $122891.00m$. The intrusion lasts for 298 seconds, allowing ownship to achieve minimum and maximum speeds of $160.84\frac{m}{s}$ and $202.32\frac{m}{s}$.
Figure 6.4(a) and Figure 6.4(b) illustrate the Estimated Time Over deviations over flight time, illustrating the earlier deviation from Reference Business Trajectory of the aircraft using the *Modified Relative Zone* zone implementation. The grey shaded area indicates where Conflict Resolution is active[3].
Zone implementation for CI evaluations: The minimum distance during Conflict Resolution using the Ownship Speed Zone implementation Z_S is with 1192.46 below the minimum lateral distance required. The longitudinal propagation is at least as large as the lateral (cf. Equation 3.4), thus minimum separation is still violated. Therefore, for evaluations of the Cost Index integration into the resolution for Scenario I the *Modified Relative Zone* implementation is used.

6.2.2 Scenario II – NAT airspace

Scenario II investigates a conflict in North Atlantic airspace. A conflict between two aircraft intercepting each other on the same track is set up as illustrated in Figure 6.5. Aim of this scenario is to evaluate possible Conflict Resolution manoeuvres in respect to their deviation from RBT. The *Boeing 747-400* serves as aircraft model for both ownship and intruder.

[3] The peeks in ΔETO are due to a waypoint shift.

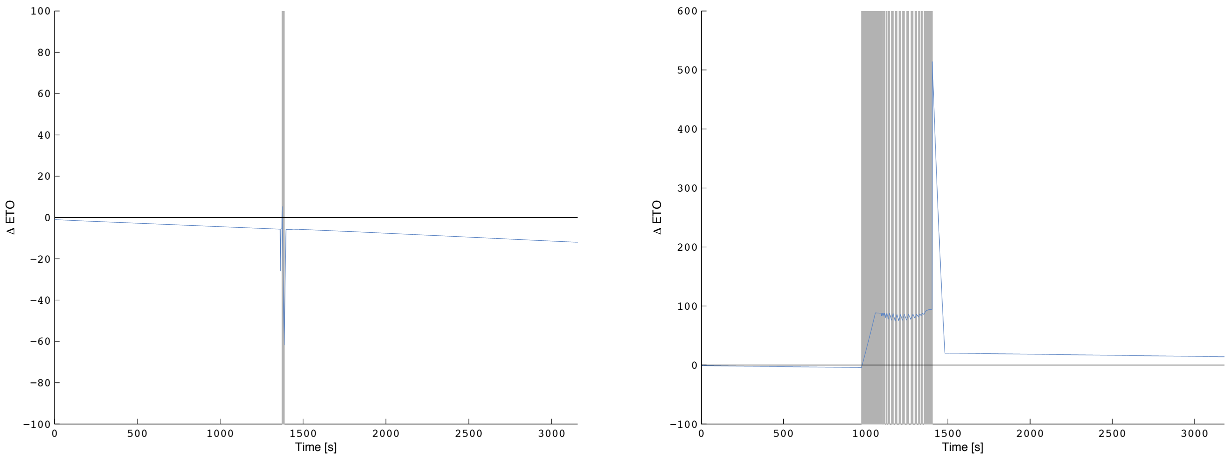

(a) Ownship Speed Zone Z_S (b) Modified Relative Zone Z_R

Figure 6.4: Development of ETO error during Conflict Resolution

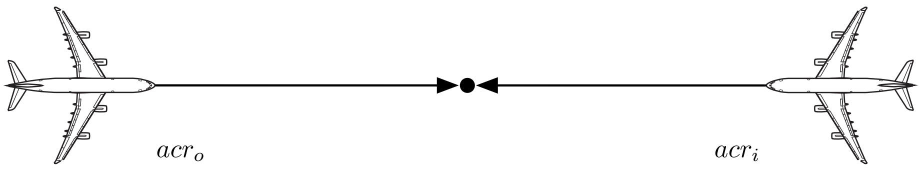

Figure 6.5: Illustration of Scenario II conflict situation

Flightplan

Table 6.5 and Table 6.6 summarise the flight plans for ownship and intruder. Both aircraft are supposed to have a conflict between waypoints 54N030W and 53N040W.

Table 6.5: acr_o Flightplan - Scenario II

Waypoint	Latitude ($\lambda^\diamond$) [deg]	Longitude ($\phi^\diamond$) [deg]	Altitude [m]	RTO [hh:mi:ss]
54N020W	54.000000	−020.000000	11277	02:18:00
54N030W	54.000000	−030.000000	11277	03:02:00
53N040W	53.000000	−040.000000	11277	03:49:00
52N050W	52.000000	−050.000000	11277	04:37:00

Table 6.6: acr_i Flightplan - Scenario II

Waypoint	Latitude ($\lambda^\diamond$) [deg]	Longitude ($\phi^\diamond$) [deg]	Altitude [m]	RTO [hh:mi:ss]
52N050W	52.000000	−050.000000	11277	02:18:00
53N040W	53.000000	−040.000000	11277	03:02:00
54N030W	54.000000	−030.000000	11277	03:49:00
54N020W	54.000000	−020.000000	11277	04:37:00

Scenario Goal

Other than in *Scenario I*, the conflict can only be solved with a Conflict Resolution consisting of at least vertical or lateral manoevures. Both aircraft are heading directly towards each other, therefore a sole change of speed may not solve the conflict. The Cost Index is varied to change preference of lateral and vertical manoeuvres.

Protected Airspace Zone geometry
The dimensions of the Protected Airspace Zone are:

d_{lon}	15 min
d_{lat}	2407.6m
d_{ver}	304.8m

For this scenario the longitudinal separation of 15 minutes conforms with the minimum separation for two turbojet aircraft on the same track (cf. Section B.1). Lateral separation corresponds to the TCAS Traffic Advisory threshold between FL200 and FL420. The height of the Protected Airspace Zone is given through the implementation of Reduced Vertical Separation Minima over NAT Organised Track System between FL290 and FL410 (cf. Table B.3).

Closest Point of Approach
The Closest Point of Approach calculates to $(\lambda^{\diamond}, \phi^{\diamond}, h) = (53.604300°, -35.060100°, 11277.00m)$ with a horizontal distance of $124.5m$ and a vertical distance of $0m$. Table 6.7 summarises the CPA information.

Table 6.7: Scenario II - Closest Point of Approach

	Latitude ($\lambda^{\diamond}$) [deg]	Longitude ($\phi^{\diamond}$) [deg]	Altitude [m]	ψ
CPA	53.6043	−35.0601	11277	260.41
Intruder	53.6045	−35.0582	11277	80.42

Protected Airspace Zone implementation
As for Scenario I, a Protected Airspace Zone implementation which takes current state information into account is required since longitudinal separation is given in minutes. The two implementations compared in Table 6.8 are Ownship Speed Zone Z_S and Modified Relative Zone Z_R.
The distance at which Conflict Resolution is activated is $123453.00m$ using zone Z_S and $132438.00m$ using zone Z_R. Figure 6.6(a) and Figure 6.6(b) illustrate the development of the slant distance between ownship and intruder, while the grey shaded areas indicate an active Conflict Resolution and thus an infringement of ownship's Protected Airspace Zone.
A more detailed view on the development of the distance between ownship and intruder is depicted in Figure 6.7. With ownship's PAZ aligned to the bearing in the boundaries of $[-45°, 45°]$ (cf. Subsection 3.2.2), the conflict is resolved at a much larger distance (cf. Figure 6.7(a)) compared to the *Ownship Speed Zone* implementation as shown in Figure 6.7(b).
Zone implementation for CI evaluations: With a horizontal distance at CPA of $2228.27m$, the *Ownship Speed Zone* fails to compute a resolution maintaining minimum separation of at least $2407.6m$ by $179.33m$, corresponding to about 13%. The vertical distance at CPA is with $247.37m$ also too small compared to the required $304.8m$ (≈ 1000ft). Since the distance at CPA using the *Modified Relative Zone* implementation is more than seven times larger than the required minimum distance, both PAZ implementations will be used for evaluation of the Cost Index integration.

6.2.3 Scenario III – IFBP region

In the third evaluation scenario, a conflict between three aircraft is simulated. Scenario III is an extension of Scenario I over the Inflight Broadcast Procedure region. With a second intruder aircraft flying

Table 6.8: Scenario II - Comparison of CR Zone implementations

	Ownship Speed Zone Z_S	Modified Relative Zone Z_R
Distance at CPA $[m]$	2241.96	15455.50
Horizontal Distance at CPA $[m]$	2228.27	15454.60
Vertical Distance at CPA $[m]$	-247.37	-163.60
#PAZ intrusions	4	5
Maximum intrusion tuple	(0.960644, 1.000000)	(0.897297, 1.000000)
Duration of PAZ intrusions [s]	265	178
Conflict solved	ϟ	✓
H $[km^2]$	107.39	786.43
V $[km^2]$	70.28	40.86
Ti $[s^2]$	53940.62	43228.81
minimum com. Speed $[\frac{m}{s}]$	218.56	218.19
maximum com. Speed $[\frac{m}{s}]$	271.46	271.46
minimum act. Speed $[\frac{m}{s}]$	218.78	218.74
maximum act. Speed $[\frac{m}{s}]$	244.39	247.92
minimum com. Altitude $[m]$	11277.00	11277.00
maximum com. Altitude $[m]$	11529.40	11447.50
minimum act. Altitude $[m]$	11276.30	11275.90
maximum act. Altitude $[m]$	11528.20	11446.00

towards the waypoint *FL* (cf. Table 6.9), the three aircraft are intended to have a conflict as illustrated in Figure 6.8.

Flightplan

With a third aircraft to arrive at waypoint *FL* at 04:57:00 and at $10058m$, a conflict between three aircraft is created. The flightplans for ownship (acr_o) and the intruder aircraft from Scenario I (in this scenario $acr_{i,0}$) remain unchanged (cf. Table 6.2 and Table 6.1), Table 6.9 summarises the new intruder's flightplan.

Table 6.9: $acr_{i,1}$, Flightplan - Scenario I

Waypoint	Latitude (λ°) [deg]	Longitude (ϕ°) [deg]	Altitude [m]	RTO [hh:mi:ss]
RINIP	8.917500	15.345833	10058	04:17:00
FL	12.141694	15.038306	10058	04:57:00
DETEL	14.651111	14.948333	10058	05:22:00
BURAT	16.946667	14.864444	10058	05:38:00
AMDIR	19.056667	14.785278	10058	05:54:00

Scenario Goal

Goal of this scenario is to show how the *Artificial Force Field* Conflict Resolution algorithm resolves multiple conflicts. The possible resolution manoeuvres in this scenario are the same as in Scenario II. A change of speed, which would have solved the conflict in Scenario I, is not sufficient since intruder $acr_{i,0}$ is flying towards ownship on the same track and flight level.

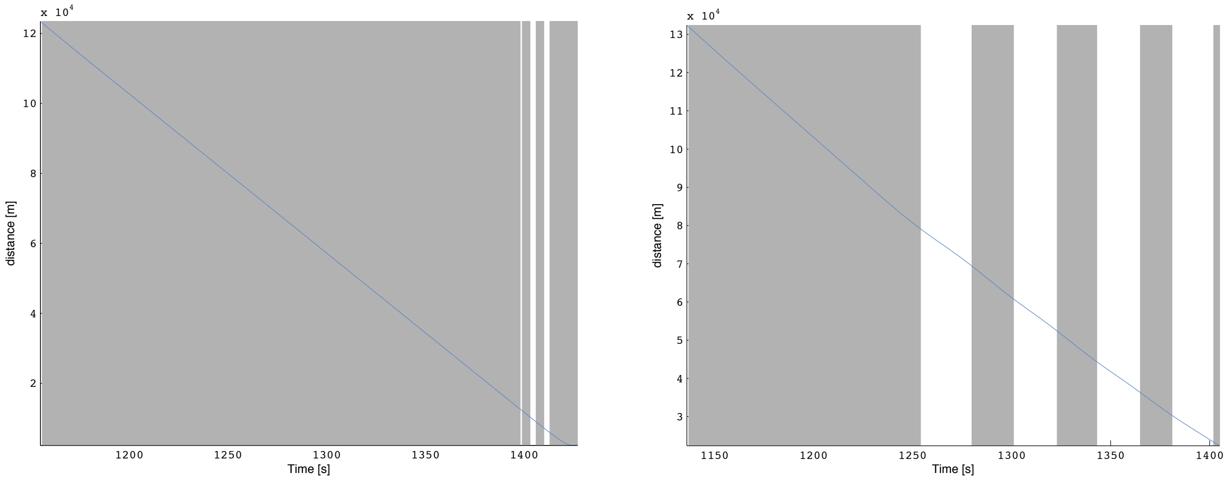

(a) Ownship Speed Zone Z_S (b) Modified Relative Zone Z_R

Figure 6.6: Development of slant distance from begin to end of Conflict Resolution

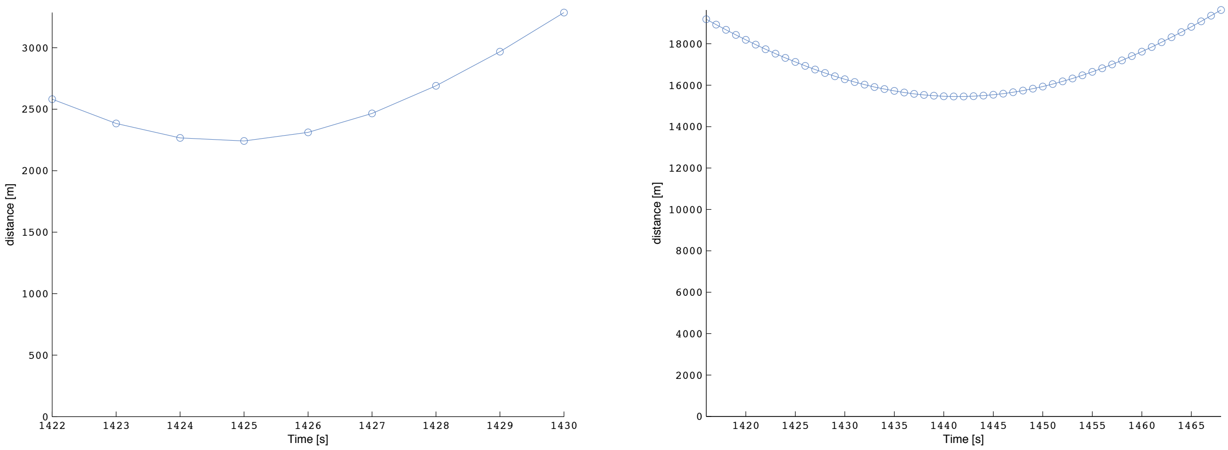

(a) Ownship Speed Zone Z_S (b) Modified Relative Zone Z_R

Figure 6.7: Development of slant distance during and after Conflict Resolution

Protected Airspace Zone geometry

The geometry of the Protected Airspace Zone for this scenario is equal to the Protected Airspace Zone geometry of Scenario I (cf. Subsection 6.2.1), i.e:

d_{lon}	10 min
d_{lat}	2407.6m
d_{ver}	304.8m

Protected Airspace Zone implementation

With longitudinal separation given in clock minutes, as for Scenario I and II the zone implementations Ownship Speed Zone and Modified Relative Zone are compared. Table 6.10 summarises the results from simulations with Cost Index integration disabled.

While with both Protected Airspace Zone implementations the conflict with the intruder coming from the side can be solved, the conflict with the intruder approaching on the same track can only be solved using the *Modified Relative Zone* implementation.

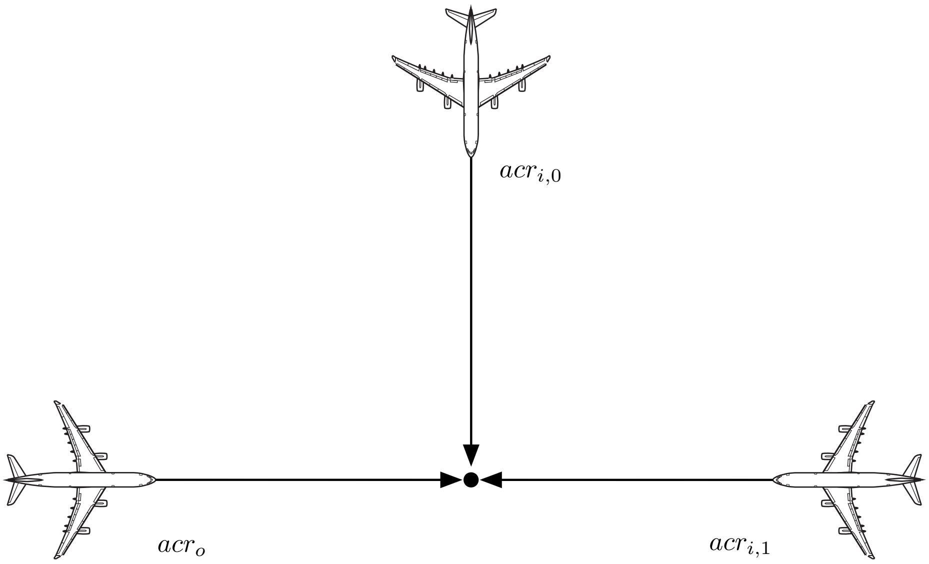

Figure 6.8: Illustration of Scenario III conflict situation

The distance at the Closest Point of Approach using the *Ownship Speed Zone* implementation is with $1565.68m$ too small. The vertical distance at the Closest Point of Approach is with $-264.83m$ not sufficient to meet the requirements for Reduced Vertical Separation Minima of 1000ft by $39.97m$.
The second intruder $acr_{i,1}$ is passed at a minimum distance of $2614.31m$ using zone implementation Z_S, respectively $5623.31m$ with zone implementation Z_R. No conflict is detected on the Conflict Resolution trajectory between ownship and $acr_{i,1}$.
Zone implementation for CI evaluations: For further evaluation the implementation using the *Modified Relative Zone* Z_R used. Both conflicts could be solved using this Protected Airspace Zone implementation.

6.3 Simulation Environment

As outlined in Chapter 5, the conceived Conflict Detection & Resolution system was implemented in C++ and laid out to allow for fast-time simulations. The fast time simulations were performed on a Commercial of the shelf Personal Computer with the following specifications:

CPU	Intel Pentium 4 3.80 GHz
Main Memory	3 GB
Operating System	Microsoft Windows XP

The fast time simulations were executed as batch jobs. Twelve simulations were run for each of the scenarios resulting in 36 simulations in total. Depending on the scenario setup one evaluation run (cf. Section 5.3) took about 10 minutes, covering between 45 to 60 minutes of flight per aircraft at an simulation step size of $t = 1s$.
The simulation was implemented in C++ and compiled against the *Microsoft Visual Studio 6.0* compiler.

6.4 Evaluation Variables & Measurements

The fundamental assumption of this work is that the aircraft's Reference Business Trajectory as outlined in the SES Concept of Operations [Ses] is regarding resource utilisation, stakeholders interests and

Table 6.10: Scenario III - Comparison of CR Zone implementations

	Ownship Speed Zone Z_S	Modified Relative Zone Z_R
	Closest Point of Approach - $acr_{i,0}$	
Distance at CPA $[m]$	1565.68	4980.28
Horizontal Distance at CPA $[m]$	1543.12	4973.87
Vertical Distance at CPA $[m]$	-264.83	-252.49
#PAZ intrusions	2	2
Maximum intrusion tuple	$(0.973698, 1.000000)$	$(0.951446, 1.000000)$
Duration of PAZ intrusions [s]	243	306
Conflict solved	ϟ	✓
	Closest Point of Approach - $acr_{i,1}$	
Distance at CPA $[m]$	2614.31	5623.31
Horizontal Distance at CPA $[m]$	2602.08	5617.53
Vertical Distance at CPA $[m]$	-252.55	-254.76
#PAZ intrusions	1	42
Maximum intrusion tuple	$(0.974567, 0.232283)$	$(0.938411, 1.000000)$
Duration of PAZ intrusions [s]	35	298
Conflict solved	✓	✓
H $[km^2]$	193.45	439.35
V $[km^2]$	24.32	29.27
Ti $[s^2]$	17553.98	44261.95
minimum com. Speed $[\frac{m}{s}]$	160.56	160.93
maximum com. Speed $[\frac{m}{s}]$	256.42	256.36
minimum act. Speed $[\frac{m}{s}]$	161.28	160.94
maximum act. Speed $[\frac{m}{s}]$	202.80	208.61
minimum com. Altitude $[m]$	10061.60	10060.30
maximum com. Altitude $[m]$	10325.60	10318.50
minimum act. Altitude $[m]$	10056.20	10058.00
maximum act. Altitude $[m]$	10325.30	10318.50

constraints ideal. Any deviation from the RBT is considered to cause additional costs (e.g. additional flight time).

In Section 2.2, the Flight Management System has been introduced along with the Cost Index which is one mean to optimise the flight path in respect to a given optimisation criteria (low fuel consumption vs. extended range or minimum flight time). The same approach has been chosen for the CD&R system devised in this work. The resolution manoeuvre is to be chosen in such a way that the Cost Index is respected. Therefore, the principal test variable is the Cost Index which is varied in the boundaries from 0 to 999 as described in Section 2.2.

The evaluations are partitioned into *safety related*, *cost related* and *trajectory related* evaluations.

Safety related evaluations

The safety related evaluations are concerned with the violation of ownship's Protected Airspace Zone and Collision Avoidance Zone. Therefore, the following variables are of interest:

1. Number and duration of PAZ penetration(s),
2. Degree of infringement *and*
3. Distance, Position and Heading at Closest Point of Approach d_{CPA} .

Number and duration of PAZ penetration: The number and duration of Protected Airspace Zone penetrations are used to conclude how often Conflict Resolution had to deviate the aircraft from its orignal flight plan. Due to different zone implementations, a penetration of the Protected Airspace Zone does not necessarily constitute a conflict. To confirm that the PAZ violation actually constitutes a conflict, information on the CPA are required.
Degree of infringement: The Conflict Resolution algorithm as devised in this work can only calculate a resolution manoeuvre if the Protected Airspace Zone has been infringed. The gains on the possible resolution manoeuvres may delay a resolution. Therefore, the degree of infringement expressed as *vertical* and *lateral intrusion* (cf. Subsection 3.2.3) are recorded and compared.
Distance, Position and Heading at CPA: Due to the different longitudinal and lateral separation minima information not only on the distance between ownship and intruder and the position of the intruder at the Closest Point of Approach is required, but also on the heading of ownship.

Cost related evaluations
Section 4.2 described how the possible resolution manoeuvres are expected to impact either fuel consumption or flight time. The three measures introduced are

1. lateral deviation from RBT – H,
2. vertical deviation from RBT – V *and*
3. temporal deviation from RBT – Ti.

Lateral deviation from RBT: The vertical deviation from Reference Business Trajectory measured as H (cf. Equation 4.6) is used for comparing the impact on flight time.
Vertical and temporal deviation from RBT: The vertical deviation from Reference Business Trajectory measured as V, respectively temporal deviation Ti (cf. Equation 4.9 and Equation 4.10) are used for comparing the impact on fuel consumption.

Trajectory related evaluations
The variables summarised under *trajectory related evaluations* allow to compare the resulting trajectories regarding flyability and adherence to the flight envelope.
Minimum and maximum speeds: The speed commands are required to stay within the aircraft's speed envelope. Even if the Estimated Time Over at the target Trajectory Change Point cannot be met within the constraints given through the Trajectory Management Requirements, speeds outside the aircraft's envelope shall not be commanded. Furthermore, logs of the aircraft's actual speed are used to confirm flyability of the trajectory.
Minimum and maximum altitude: As for minimum and maximum speeds, the aircraft is required to stay within the altitude envelope. Logs reflecting the altitude of the simulated aircraft are used to confirm flyability of the trajectory regarding the vertical profile.
Further records: Further variables such as the bank ϕ and bank rate $\dot{\phi}$ are recorded as well to draw conclusions regarding the flyability.

6.5 Summary

The Conflict Resolution algorithm devised in this work is evaluated against *Safety*, *Cost* and *Trajectory* related constraints. This chapter has presented which variables are used for each of these categories to conclude the impact of Autonomous Flight Management and the Conflict Resolution algorithm on aircraft safety, resolution costs and trajectory flyability. The integration of the Cost Index into the Artificial Force Field Conflict Resolution algorithm will be evaluated through fast time simulations of three scenarios. The first scenario is devised in such a way that heading changes, speed changes and altitude changes will all solve the conflict. This scenario will allow to draw conclusions regarding the impact of the Cost Index integration on the costs of the deviation from the Reference Business Trajectory. A scenario where solution space is limited is dealt with in Scenario II. Here, the conflict of two aircraft which are on collision course can only be resolved through heading or altitude changes. The scenario is used to evaluate how the Conflict Resolution algorithm will resolve the conflict with one degree of freedom less and the Cost Index to prioritise the remaining two possibilities. Finally, with the third scenario a conflict between three aircraft is simulated. This scenario is used to show how a global resolution is computed and how the Cost Index setting impacts the overall costs of the Conflict Resolution.

7 Evaluation

> If you want to go up, pull back on the yoke. If you want to go down, pull back a little more. If you want to go down real fast and spin around and around and around, just keep pulling back.
>
> Aviation proverb

WITH a preselection regarding the Protected Airspace Zone implementations made, this chapter is concerned with the evaluation of Cost Index integration into the Conflict Resolution process. Three scenarios, two in the Inflight Broadcast Procedure area over Africa and one in the North Atlantic Organised Track System, have been set up to evaluate the integration of the Cost Index.
Section 7.1 introduces the evaluations by giving a short overview on the expectations for the three scenarios. Each scenario is subsequently detailed further in Sections 7.2, 7.3 and 7.4 where the results are presented and conclusions are discussed. Section 7.5 closes this chapter with a summary.

7.1 Introduction

The Cost Index is integrated into the Conflict Resolution process by introducing gains on the command values heading, altitude and speed (cf. Subsection 4.3.2.1 and Subsection 4.3.2.2). The gains have been defined in such a way that for a high Cost Index setting – i.e. time costs are predominant – speed and altitude changes are preferred. Similarly, for a low Cost Index setting the commanded heading will more likely match the required heading computed by the *Artificial Force Field* Conflict Resolution algorithm.
In the preceding chapter, simulations with Cost Index integration deactivated have been discussed with the aim to identify the appropriate Protected Airspace Zone (PAZ) implementation which has been chosen depending on the distance at the Closest Point of Approach. In Scenario I, using the *Modified Relative Zone* implementation has solved the conflict over the Inflight Broadcast Procedure area and maintained safe separation to the intruder and is therefore used for the evaluations described in Section 7.2. Both zone implementations will be used for evaluation in scope of Scenario II since the minimum allowed distance was only slightly undershot using the *Ownship Speed Zone* while the *Modified Relative Zone* implementation could solve the conflict. This scenario will be discussed in Section 7.3. Section 7.4 is concerned with Scenario III and the three aircraft conflict over African airspace. In this scenario, the *Modified Relative Zone* implementation is used as it could resolve the conflict with both intruders. Table 7.1 summarises the scenarios and the zone implementations used for evaluation.

Table 7.1: Cost Index evaluations

	Ownship Speed Zone Z_S	Modified Relative Zone Z_R
Scenario I		✓
Scenario II	✓	✓
Scenario III		✓

Requirements
For all scenarios the following two requirements need to be fulfilled for different Cost Index settings:

R_α The requirements regarding flyability are met.

R_β The updated trajectory is conflict free.

Remark
In the following, only lateral intrusion will be considered in the evaluations. Due to scenario design, aircraft are all flying on the same flight level when approaching each other, the maximum vertical intrusion is always equal to one. Furthermore, for the illustration of heading development over simulation time, *polar plots* are used. These plots illustrate the heading in a fashion similar to the compass rose (North-up) while the simulation time is depicted on the radials[1].

7.2 Scenario I – IFBP region

Scenario I – as described in Subsection 6.2.1 – allows by its construction any combination of resolutions. The Cost Index will be varied to evaluate the impact on manoeuvre costs. The variation of the Cost Index is made to validate the following hypotheses:

H_1 A larger Cost Index will result in a smaller lateral deviation.

H_2 A larger Cost Index will result in a larger vertical deviation.

H_3 A larger Cost Index will result in a smaller temporal deviation.

Scenario specific constraints
The *Airbus A340-400* has been used as aircraft model for simulation in Scenario I. The conflict occurs at an altitude of $10058.00m$. The minimum and maximum speeds at this altitude calculate to:

$$V_{min} = 160.04\frac{m}{s} \tag{7.1}$$
$$V_{max} = 257.32\frac{m}{s} \tag{7.2}$$

V_{min} and V_{max} shall not be under-, respectively overshot during Conflict Resolution. Further details may be found in Appendix F.

7.2.1 Results

For the Cost Index evaluation runs of Scenario I the *Modified Relative Zone* implementation was used. With this zone implementation, the Conflict Resolution was initiated comparable early at a distance of $122891.00m$ due to the alignment of the Protected Airspace Zone along the bearing to the intruder (cf. Subsection 6.2.1). This allowed ownship to deviate from its Reference Business Trajectory at a larger distance to the Closest Point of Approach. Figure 7.1 illustrates three resolutions with different Cost Index settings (in blue) up to the point in time when the original trajectory (in white) meets the intruder (illustrated in red) at the conflict point. All alternative trajectories illustrated in Figure 7.1 resolve the conflict through speed changes and lateral, respectively vertical deviation from the Reference Business Trajectory. The RBT is later rejoined before passing the conflict point. In the following the *Safety*, *Cost* and *Flyability* related measures of this scenario are summarised.

[1] A further description of these plots can be found in Section A.6.

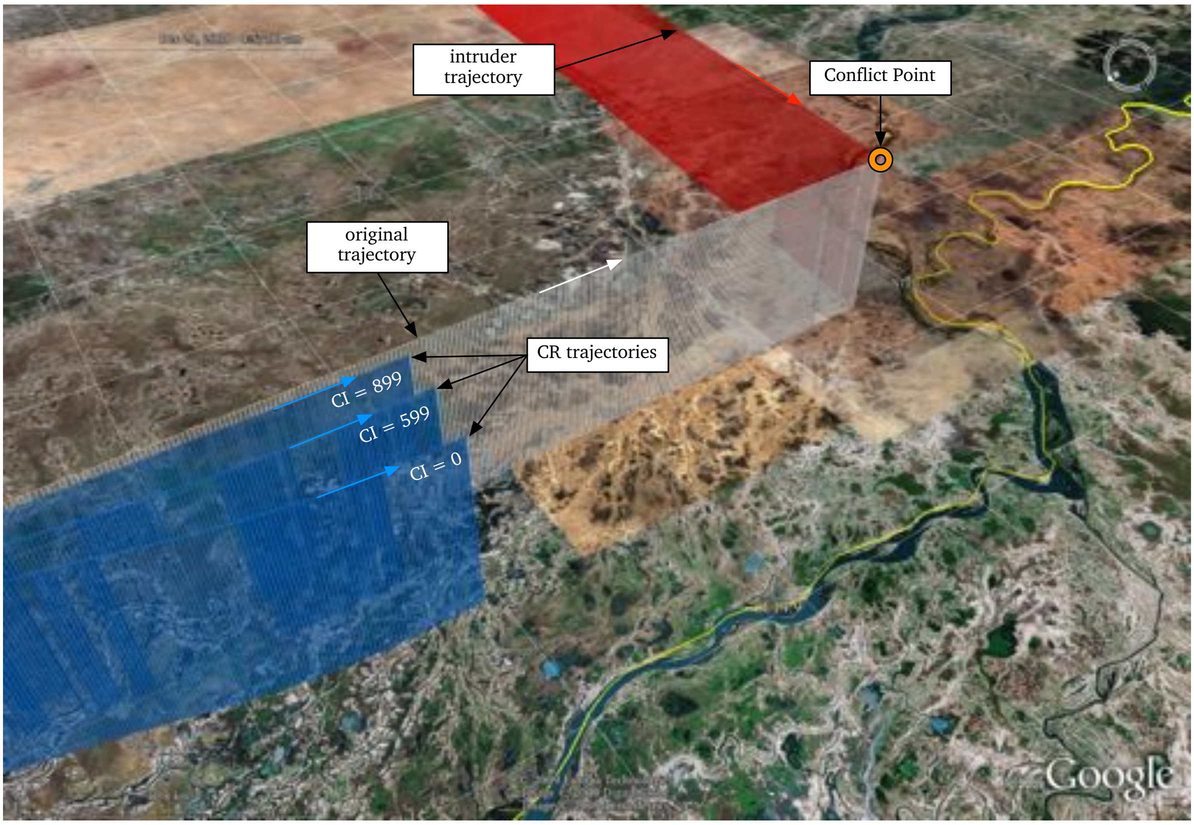

Figure 7.1: S1 - Illustration of Conflict Resolution manoeuvre (Google Earth)

Safety

The conflict at $(\lambda^\circ, \phi^\circ, h) = (12.1417^\circ, 15.0383^\circ, 10058.0m)$ could be solved with all Cost Index settings except for CI $= 0$. The duration of the PAZ infringement for CI $= 0$ was $206s$, while it varied for other settings between $301s$ to $441s$. Over all simulation runs, the degree of PAZ infringement varied only slightly in the boundaries of 0.906829 to 0.915686.

With the conflict not being resolved at CI $= 0$, the smallest distance at the Closest Point of Approach with $1150.45m$ and no vertical separation was also achieved at this setting. The next smaller slant distance of $7711.08m$ (horizontal distance of $7710.52m$ and vertical distance of $-92.71m$) was achieved at a Cost Index setting of 199.

Figure 7.2 illustrates the development of the slant distance for Cost Index settings 0, 99, 599 and 999. These runs are also detailed in Table 7.2 while further results on safety related measures are summarised in Table C.1 (Subsection C.1.2).

Table 7.2: S1 - Safety related measures for CI $\in \{0, 99, 599, 999\}$

	Distance at CPA			Intrusion		
Cost Index	Slant $[m]$	Horizontal $[m]$	Vertical $[m]$	#	maximum	duration $[s]$
0	1150.45	1150.45	0.00	31	0.912646	206
99	7806.29	7806.04	−62.12	16	0.908216	301
599	7517.15	7516.19	−120.23	25	0.914339	337
999	8904.76	8904.02	−114.36	1	0.911502	441

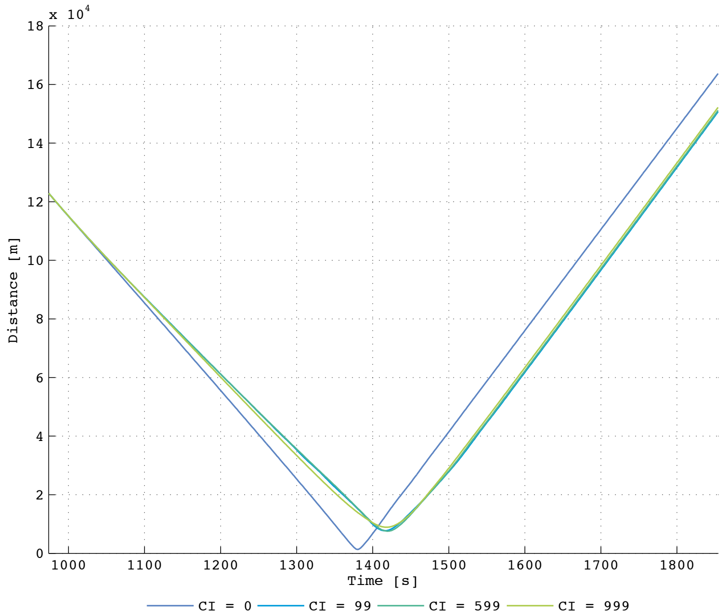

Figure 7.2: S1 - Development of slant distance between ownship and intruder

Cost

The horizontal area enclosed by the Reference Business Trajectory and the updated trajectory was – for CI settings with which the conflict could be solved – between $218.24km^2$ (CI = 99) and $9.74km^2$ (CI = 999). The vertical area grows from $18.77km^2$ (CI = 99) to $44km^2$ (CI = 999). At a CI setting of 0, the enclosed horizontal and vertical areas compute to $98.81km^2$ and $0km^2$. The temporal area enclosed reduces from $45694.01s^2$ (CI = 99) to $34808.14s^2$ (CI = 999) with exception of $0s^2$ and $42735.43s^2$ at a CI of 0 and 599, respectively. In the latter case the temporal zone grows by $130.87s^2$ compared to CI = 499. The results of the aforementioned CI runs are summarised in Table 7.3 while all results can be found in Table C.2 (Subsection C.1.2). Figure 7.3 illustrates the development of heading, altitude and difference to the Estimated Time Over at the target Trajectory Change Point of the validation run.

Table 7.3: S1 - Cost related measures for CI $\in \{0, 99, 499, 599, 999\}$

Cost Index	$H[km^2]$	$V[km^2]$	$Ti[s^2]$
0	98.81	0.00	0.00
99	218.24	18.77	45694.01
499	197.88	41.92	42604.56
599	192.59	43.03	42735.43
999	9.74	44.33	34808.14

Flyability

The evaluations regarding flyability of the trajectory are based on recordings of the aircraft's speed, altitude, the eulerian angles[2] and the derivatives thereof. The maximum bank angle of 35° has been achieved in the evaluation runs CI = 99 and CI = 199 with a maximum roll rate of $3\frac{°}{s}$. The pitch achieved varied in the boundaries of 0° and 0.67°. The results from these CI runs are summarised in Table 7.4. Further results may be found in Subsection C.1.2, Table C.3.

2 Only bank and pitch are considered.

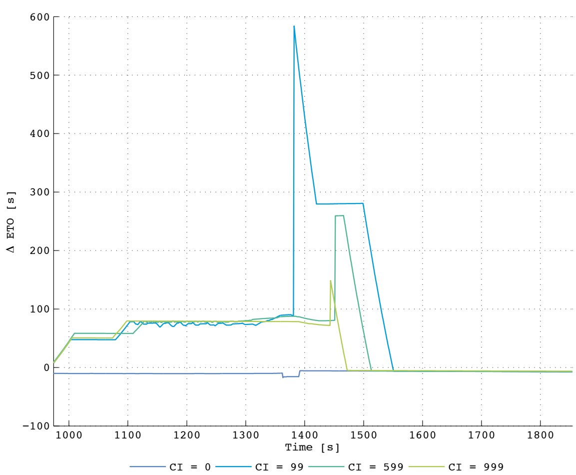

(a) ΔETO

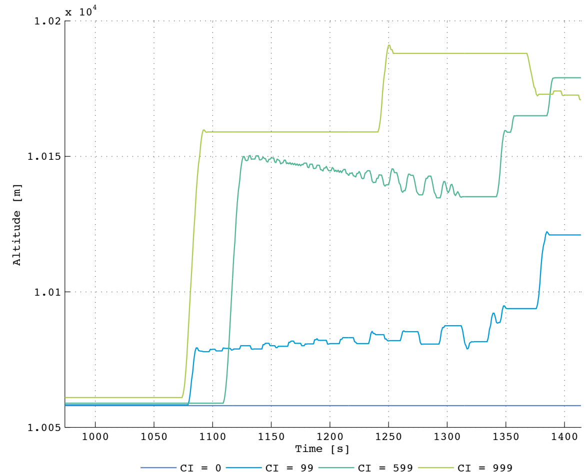

(b) Altitude

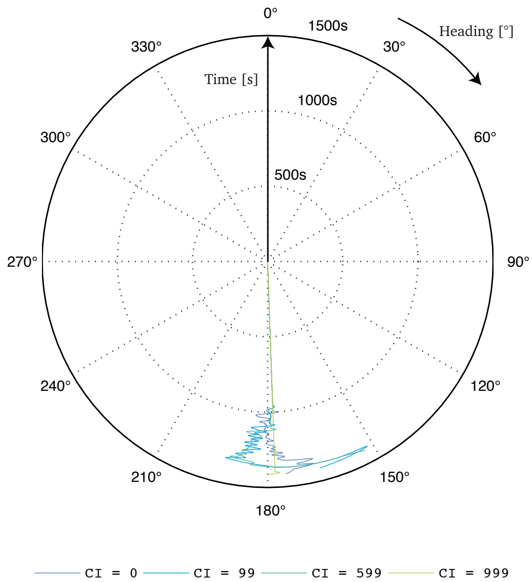

(c) Heading

Figure 7.3: S1 - Development of heading, altitude and ΔETO for CI $\in \{0, 99, 599, 999\}$

Table 7.4: S1 - Maximum bank, pitch and first degree derivatives for for CI $\in \{0, 99, 599, 999\}$

Cost Index	$\phi[°]$	$\dot{\phi}[\frac{°}{s}]$	$\theta[°]$	$\dot{\theta}[\frac{°}{s}]$
0	20.95	3.00	0.00	0.00
99	35.00	3.00	0.34	0.05
599	19.88	3.00	0.67	0.54
999	0.03	0.01	0.43	0.43

The minimum commanded speeds are within the boundaries of $160.21\frac{m}{s}$ (CI $=99$) and $160.84\frac{m}{s}$ (CI $=999$). The maximum commanded speeds are within the boundaries of $207.24\frac{m}{s}$ (CI $=999$) and $245.35\frac{m}{s}$ (CI $=0$). Commanded and achieved altitudes are within the boundaries of $[10058.00m, 10188.00m]$ and $[10055.40m, 10188.00m]$, respectively. Table 7.5 summarises the speeds and altitudes achieved for Cost Index settings of 0, 99, 599 and 999. Further results are summarised in Table C.4 (Subsection C.1.2).

Table 7.5: S1 - Commanded and achieved speeds and altitudes for CI $\in \{0, 99, 599, 999\}$

	com. speed $[\frac{m}{s}]$		act. speed $[\frac{m}{s}]$		com. altitude $[m]$		act. altitude $[m]$	
Cost Index	min	max	min	max	min	max	min	max
0	200.05	245.35	200.05	204.15	10058.00	10058.00	10058.00	10058.00
99	160.21	245.27	160.21	208.47	10058.10	10121.20	10057.40	10121.20
599	160.64	245.07	160.64	208.07	10058.90	10179.10	10057.90	10179.10
999	160.84	240.38	160.84	207.10	10059.50	10188.00	10056.00	10188.00

7.2.2 Discussion

The general requirements as described in Section 7.1 and the scenario specific hypotheses H_1, H_2 and H_3 (cf. Section 7.2) are discussed in the following.

General requirements
One caveat of Conflict Resolution based on Artificial Force Fields is the possibility of requiring not flyable trajectories to resolve the conflict. Through integration of an aircraft model based on EUROCONTROL's Base of Aircraft Data, it was intended to guarantee flyability while re-establishing the required safe separation to other aircraft. For Scenario I, the conflict between two aircraft could be solved except for the evaluation run with a Cost Index setting of 0.
Flyability: The speed and altitude envelope of the aircraft model are respected by the Conflict Resolution algorithm. The speeds commanded and achieved are within the limitations valid at the altitude (cf. Equation 7.1 and Equation 7.2). The altitudes are also below the maximum altitude of 12496.80m ($\approx$ 41000ft). The maximum bank achieved during Conflict Resolution of 35° is still within the BADA boundaries, but by 20° too high to attribute the manoeuvre as *strategic* [Bar+06] (cf. Appendix A). Maximum pitch remains below 0.7°. Turn rate and pitch rate are with a maximum of $3\frac{\circ}{s}$ and $0.54\frac{\circ}{s}$ also within the boundaries setup through BADA constraints (cf. Section F.5). Therefore, requirement R_α is met.
Separation: The distance achieved at the Closest Point of Approach is – except for $CI = 0$ – sufficient and no conflicts are detected with the updated trajectory used for ownship. With a Cost Index setting of 0, a distance of 1150.45m has been achieved at the Closest Point of Approach which violates the Collision Avoidance Zone around ownship.
The reason for the failure to solve the conflict lies within the construction of the Protected Airspace Zone around ownship and the resolution manoeuvre applied. As expected, the Conflict Resolution did not use speed or altitude changes for resolving the conflict but tries to solve the conflict with the intruder approaching from the side with heading changes. At the beginning of the simulation this caused the intruder to move out of the $[-45°, 45°]$ arc in which ownship's Protected Airspace Zone is aligned along the bearing to the intruder (cf. Subsection 3.2.2 – Modified Relative Zone).
Figure 7.4(a) illustrates the development of the intrusion of ownship's Protected Airspace Zone as of Equation 3.5 for the CI evaluations 0, 99, 599 and 999 while Figure 7.4(b) shows the heading during computation of the *Artificial Force Field* Conflict Resolution algorithm. As soon as the intruder moved out of ownship's PAZ, the original flight plan was recaptured. This caused that the overall lateral deviation from the Reference Business Trajectory is minor and that ownship passed the intruder at a small distance. Even though the collision of the two aircraft at the waypoint *FL* could be prevented, the separation is not sufficient and thus the conflict was not resolved.
Requirement R_β is not met due to Protected Airspace Zone geometry.

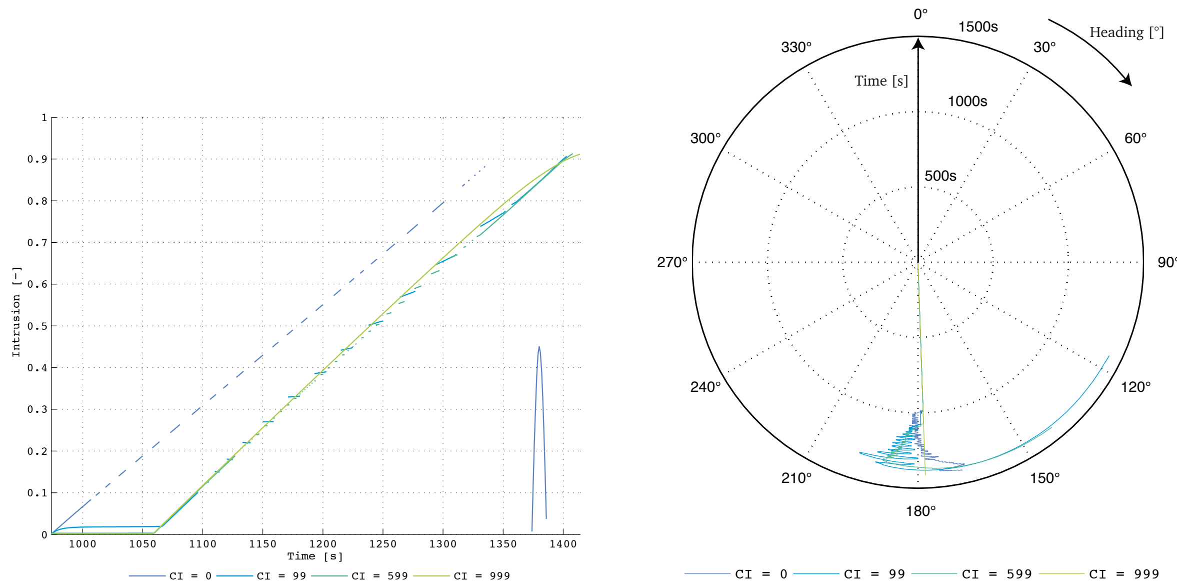

(a) Degree of lateral intrusion of ownship PAZ (b) Heading

Figure 7.4: S1 - Lateral Intrusion and heading during CR for CI $\in \{0, 99, 599, 999\}$

Scenario specific hypotheses

Scenario I was aimed at the evaluation of the impact of Cost Index variation on the measures for fuel related and time related costs. These costs have been mapped to the lateral, vertical and temporal areas H, V and Ti.

Lateral deviation: Similar to the fulfilment of requirement R_β regarding minimum separation, the lateral deviation between the Reference Business Trajectory and the updated trajectory developed as expected (cf. Table 7.3) except for CI $= 0$. The maximum lateral deviation of $218.24 km^2$ was achieved with a Cost Index setting of 99 while it was minimal at CI $= 999$. The deviation at the latter Cost Index setting was caused by the required heading change on the transition from the trajectory segment *DETEL-FL* to *FL-RINIP* (cf. Table 6.1). Since the Conflict Resolution did not resolve the conflict as expected for CI $=0$, the Cost Index could not influence the resolution process as expected. As for other CIs the lateral deviation developed correctly, hypotheses H_1 can be considered as valid.

Vertical deviation: Regarding the development of the vertical area, the assumption was, that with heading changes disallowed (the gain for heading changes at an Cost Index of 999 is $k_h = 0$, cf. Equation 4.28 – Subsection 4.3.2.2) the vertical area would be maximal. This assumption was not completely fulfilled as the largest vertical deviation was achieved at CI $= 899$ with $44.96 km^2$ compared to $44.33 km^2$ at CI $= 999$. Figure 7.5(a) illustrates the development of altitude during the validation run while Figure 7.5(b) illustrates the intrusion of ownship's PAZ as of Equation 3.5 during computation of the *Artificial Force Field* Conflict Resolution algorithm. With a Cost Index of 899, ownship climbs again at $t = 1396s$ due to a higher intrusion of its Protected Airspace Zone, causing a higher vertical deviation compared to CI $= 999$. Thus, hypothesis H_2 is not fulfilled.

Temporal deviation: The overall trend for temporal deviation was, that it grew smaller from CI $= 99$ to CI $= 999$, the evaluation run CI $= 0$ not considered due to the aforementioned reason. Though, at a Cost Index setting of 599 the temporal deviation grew larger instead of smaller by $130.87 s^2$ compared to the previous run (CI $= 499$). As the waypoint shift contributes to the overall temporal deviation[3] an evaluation up to the waypoint shift shows, that at $t_s = 1352s$ the temporal deviation of CI $= 499$ is

[3] The peeks in ΔETO development illustrated in Figure 7.3(a) are due to the waypoint shift.

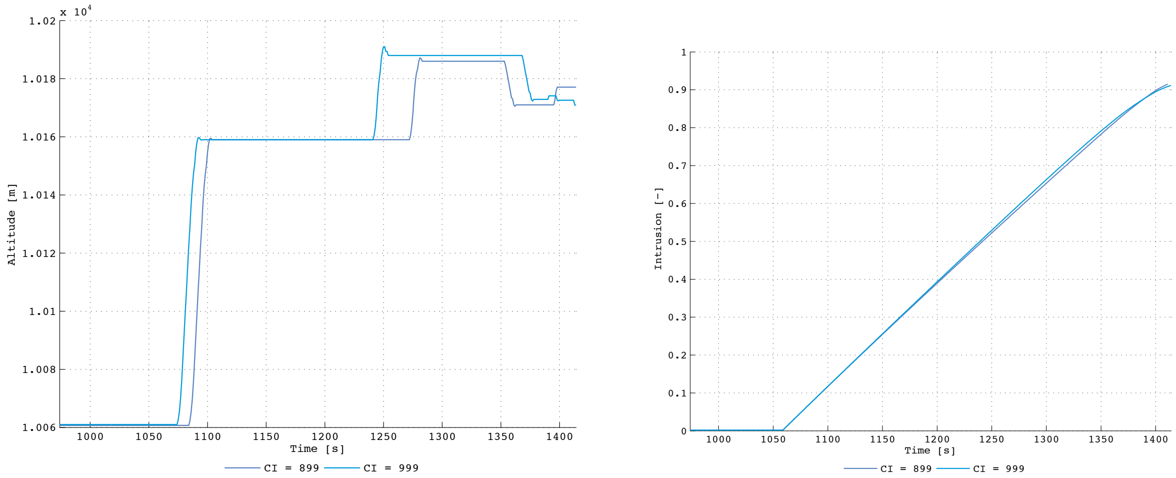

(a) Altitude during execution of new trajectory

(b) Lateral intrusion during Conflict Resolution

Figure 7.5: S1 - Altitude and intrusion for CI $\in \{899, 999\}$

$39057.67s^2$ while it computes to $38707.08s^2$ at CI $= 599$ ($t_s = 1353s$). Therefore, the temporal deviation developed as expected and hypotheses H_3 can be validated.

7.3 Scenario II – NAT airspace

In Scenario II another Mid-Air Collision needs to be resolved by the Conflict Resolution system. Other than in Scenario I, the conflict can not be resolved by sole application of speed changes since the intruder approaches ownship on the same track from ahead (cf. Subsection 6.2.2). Beside the adherence to requirements R_α and R_β, the following hypotheses are to be verified:

- H_4 A larger Cost Index will result in a smaller lateral deviation.
- H_5 A larger Cost Index will result in a larger vertical deviation.
- H_6 Cost Index variation for CI > 0 will have no effect on temporal deviation.

During simulation runs with deactivated Cost Index integration, the *Ownship Speed Zone* implementation failed to solve the conflict as the required lateral and vertical separation were undershot by $179.33m$ and $57.43m$. As this constitutes a violation of the minimum separation by only about 13%, respectively 17% and the Mid-Air Collision could be prevented, this zone implementation as well as the *Modified Relative Zone* implementation which solved the conflict are used for the evaluations in this section.

Scenario specific constraints

The *Boeing 747-400* has been used as aircraft model for simulation in Scenario II. The conflict is set up at an altitude of $11277m$. The minimum and maximum speeds at this altitude for the *747-400* calculate to

$$V_{min} = 218.12\frac{m}{s} \tag{7.3}$$

$$V_{max} = 271.47\frac{m}{s} \tag{7.4}$$

V_{min} and V_{max} may not be under- respectively overshot during Conflict Resolution.

7.3.1 Results

Both zone implementations – *Ownship Speed Zone* and *Modified Relative Zone* – have been evaluated regarding the Cost Index integration. The evaluation runs using the *Ownship Speed Zone* implementation are detailed in Subsection 7.3.1.1 while Subsection 7.3.1.2 covers the *Modified Relative Zone* implementation.

In Figure 7.6, three examples of alternative trajectories with varying Cost Index setting using the two different zone implementations (*Ownship Speed Zone* – Z_S depicted in blue and *Modified Relative Zone* – Z_S depicted in green) are illustrated up to the point in time, when the Closest Point of Approach is reached by the original trajectory (conflict point). With the intruder approaching from ahead, all alternative trajectories separate from the Reference Business Trajectory at a similar distance to the Closest Point of Approach. The difference between the two zone implementations becomes evident when comparing the (lateral) deviations from the Reference Business Trajectory with the illustrated Cost Index setting of 899.

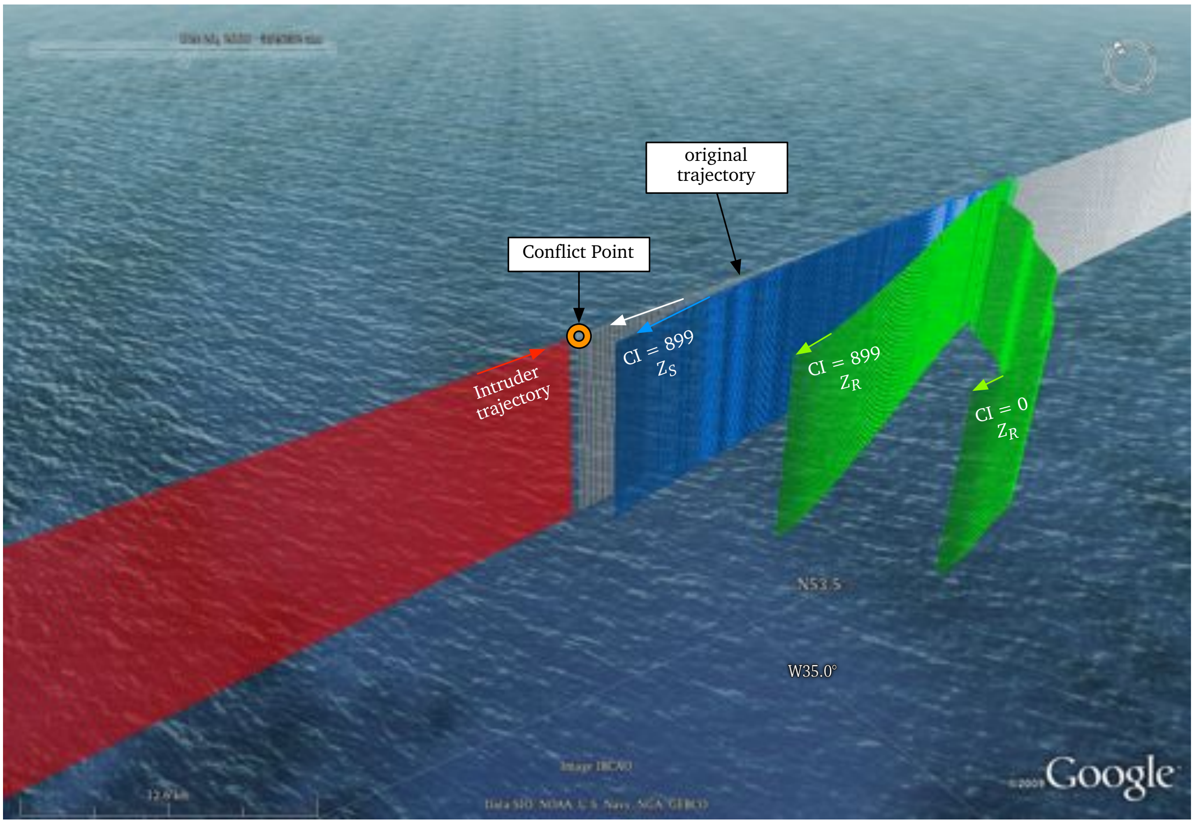

Figure 7.6: S2 - Illustration of Conflict Resolution manoeuvre (Google Earth)

7.3.1.1 Ownship Speed Zone

The evaluation runs using the *Ownship Speed Zone* implementation, which is aligned along the heading of ownship, are detailed in this subsection in respect to the *Safety*, *Cost* and *Flyability* related measures. In the following, the results of selected Cost Index runs are presented while all results are summarised in Subsection C.2.2.

Safety

With growing Cost Index, the horizontal distance at the Closest Point of Approach decreases from 2192.56m to 162.49m while the absolute vertical distance increases from 0m to 258.20m. Table 7.6

summarises the safety related measures of this scenario using Ownship Speed Zone implementation for minimum, maximum and average Cost Index setting. Further results may be found in Table C.5.

Table 7.6: S2 - Ownship Speed Zone implementation - Safety related measures for CI $\in \{0, 499, 999\}$

	Distance at CPA			Intrusion		
Cost Index	Slant $[m]$	Horizontal $[m]$	Vertical $[m]$	#	maximum	duration $[s]$
0	2192.56	2192.56	0.00	5	0.975698	250
499	2191.61	2181.34	−211.84	5	0.965931	264
999	305.07	162.49	−258.20	1	0.981931	276

The development of the slant distance between ownship and intruder for the aforementioned settings is illustrated in Figure 7.7. The slant distance is minimal at a CI of 999 with $305.07m$.

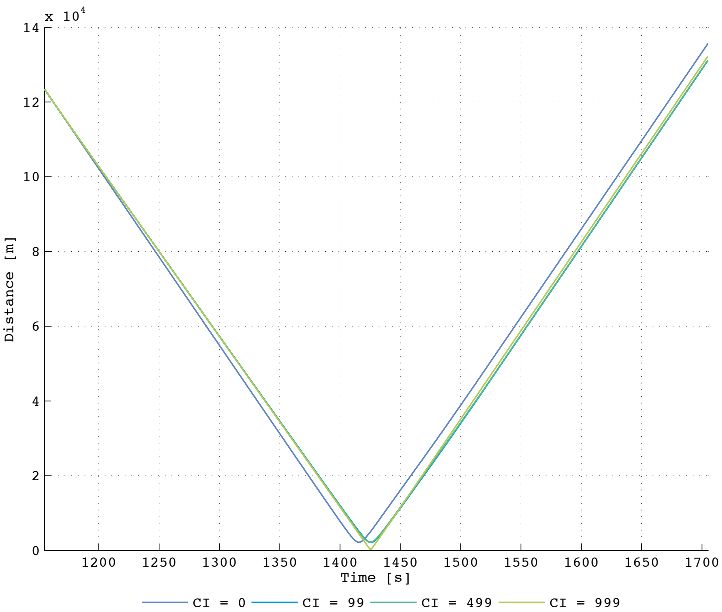

Figure 7.7: S2 - Ownship Speed Zone - Development of slant distance between ownship and intruder for CI $\in \{0, 99, 499, 999\}$

Cost

The horizontal deviation from the Reference Business Trajectory stays between $20.56km^2$ at CI $= 999$ and $97.88km^2$ at CI $= 499$. Over all CI runs no trend can be identified except for a major decrease from CI $=$699 with $85.59km^2$ to 799 with $53.37km^2$. The vertical deviation increases over all runs from $0km^2$ at CI $=$0 to $28.32km^2$ at CI $= 999$. Temporal deviation is minimal at a Cost Index setting of 0 with $0s^2$ while for other Cost Index settings the temporal deviation is between $64287.57s^2$ and $68240.26s^2$. The results for minimum, maximum and average Cost Index are summarised in Table 7.7. The measures from all Cost Index runs can be found in Table C.6.

Flyability

At a Cost Index setting of 499, the maximum bank angle of all CI runs was achieved with 31.31°. The maximum pitch was achieved with 0.83° at CI $= 999$. The maximum bank, pitch, roll rate and pitch rate for maximum, minimum and average CI settings are summarised in Table 7.8. The speeds commanded are within the boundaries of $[218.20\frac{m}{s}, 271.46\frac{m}{s}]$. The maximum commanded speed was not achieved with a maximum speed over all runs of $258.33\frac{m}{s}$. The achieved altitude remains within the boundaries

Table 7.7: S2 - Ownship Speed Zone implementation - Cost related measures for CI $\in \{0, 499, 999\}$

Cost Index	$H[km^2]$	$V[km^2]$	$Ti[s^2]$
0	92.40	0.00	0.00
499	97.88	15.06	65730.69
999	20.56	28.32	64595.47

Table 7.8: S2 - Ownship Speed Zone implementation - Flyability related measures for CI $\in \{0, 499, 999\}$ (1/2)

Cost Index	$\phi[°]$	$\dot{\phi}[\frac{°}{s}]$	$\theta[°]$	$\dot{\theta}[\frac{°}{s}]$
0	29.41	3.00	0.00	0.00
499	31.31	3.00	0.84	0.40
999	0.70	0.51	0.83	0.39

of $[11277.00m, 11545.90m]$. Table 7.9 summarises minimum and maximum values for commanded and achieved speeds and altitudes for minimum, maximum and average Cost Index settings as well as for CI $= 99$ where the minimum speed of all runs was commanded and achieved. Further measures are summarised in Table C.7 and Table C.8.

Table 7.9: S2 - Ownship Speed Zone - Flyability related measures for CI $\in \{0, 99, 499, 999\}$ (2/2)

	com. speed $[\frac{m}{s}]$		act. speed $[\frac{m}{s}]$		com. altitude $[m]$		act. altitude $[m]$	
Cost Index	min	max	min	max	min	max	min	max
0	237.63	237.63	237.63	237.63	11277.00	11277.00	11277.00	11277.00
99	218.20	271.46	218.21	258.33	11277.10	11389.00	11276.70	11387.90
499	218.38	271.46	218.48	258.27	11277.70	11497.00	11277.00	11495.70
999	218.56	271.46	218.78	257.31	11278.50	11545.90	11277.00	11545.90

7.3.1.2 Modified Relative Zone

This subsection is concerned with the Cost Index evaluation runs of Scenario II where the *Modified Relative Zone* implementation, which is aligned along the bearing to the intruder (cf. Subsection 3.2.2), has been used. The *Safety*, *Cost* and *Flyability* related results for selected CIs are presented here while all results may be found in Subsection C.2.3.

Safety

The maximum slant distance at the Closest Point of Approach was achieved at a Cost Index setting of 0 with $16591.10m$. The horizontal distance with this Cost Index setting is the largest over all CI runs while the vertical distance is with $0m$ also the smallest value achieved. Vice versa, at a Cost Index of 999 the largest absolute vertical distance and the smallest horizontal distance were achieved with $-259.25m$ and $38.29m$, respectively. The results for these two Cost Index runs, along with the average CI setting of 499 are summarised in Table 7.10. The development of the distance is also illustrated in Figure 7.8. The safety related measures of all evaluation runs are summarised in Table C.9.

Table 7.10: S2 - Modified Relative Zone - Safety related measures for CI $\in \{0, 499, 999\}$

Cost Index	Distance at CPA Slant $[m]$	Horizontal $[m]$	Vertical $[m]$	Intrusion #	maximum	duration $[s]$
0	16591.10	16591.10	0.00	5	0.886000	170
499	15321.80	15321.30	−121.34	5	0.896911	180
999	262.06	38.29	−259.25	1	0.999811	296

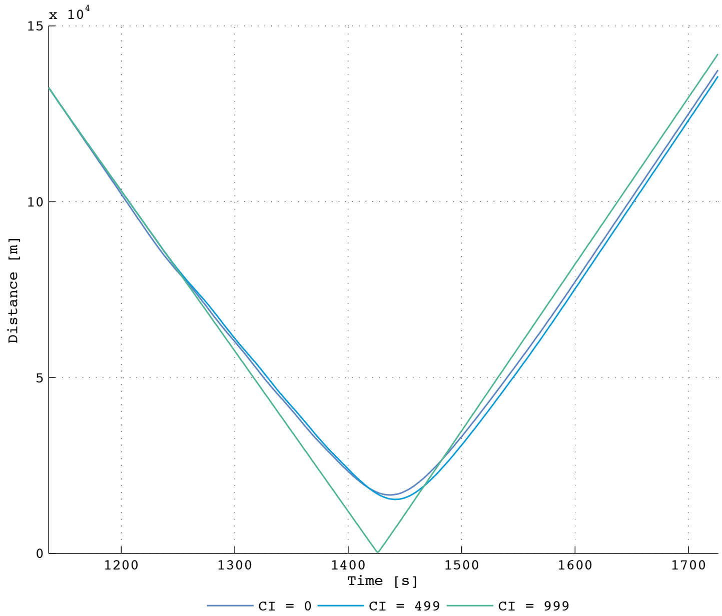

Figure 7.8: S2 - Modified Relative Zone - Development of slant distance between ownship and intruder for CI $\in \{0, 499, 999\}$

Cost

The lateral deviation from the Reference Business Trajectory decreased from $1084.05km^2$ at CI $= 0$ to $21.29km^2$ at CI $= 999$. Up to CI $= 799$ the lateral deviation remains between $1084.05km^2$ and $782.08km^2$ and shrinks by about 48% from CI $= 799$ to CI $= 899$. The vertical deviation grew with growing Cost Index from $0km^2$ to $48.68km^2$. Temporal deviation is minimal at a Cost Index setting of 0. Except for that setting, time related costs are within the boundaries of $55981.03s^2$ and $66634.25s^2$. The results from the aforementioned runs along with the average CI run are summarised in Table 7.11. Further results may be found in Subsection C.2.3.

Table 7.11: S2 - Modified Relative Zone - Cost related measures for CI $\in \{0, 499, 799, 899, 999\}$

Cost Index	$H[km^2]$	$V[km^2]$	$Ti[s^2]$
0	1084.05	0.00	30414.53
499	936.20	23.75	55981.03
799	782.08	35.07	63563.92
899	379.71	39.10	63812.32
999	21.29	48.68	66634.25

Flyability

With the *Modified Relative Zone*, the maximum allowed bank of 35° and the maximum allowed roll rate of $3\frac{\circ}{s}$ have been achieved for Cost Index runs 0 to 699. For the runs from CI = 799 onward the maximum bank during resolution reduced towards 2.19°. For CI = 999 the largest pitch and pitch rate over all simulation runs have been achieved with 2.19° and $0.83\frac{\circ}{s}$, respectively. These Cost Index settings, along with the average CI of 499 are summarised in Table 7.12. The development of the heading during these CI runs is also illustrated in Figure 7.9. Further results may be found in Table C.11.

Table 7.12: S2 - Modified Relative Zone implementation - Flyability related measures for CI $\in \{0, 499, 699, 799, 999\}$ (1/2)

Cost Index	$\phi\,[°]$	$\dot{\phi}\,[\frac{\circ}{s}]$	$\theta\,[°]$	$\dot{\theta}\,[\frac{\circ}{s}]$
0	35.00	3.00	0.00	0.00
499	35.00	3.00	0.33	0.31
699	35.00	3.00	0.32	0.28
799	31.52	3.00	0.27	0.27
999	2.19	2.03	0.83	0.39

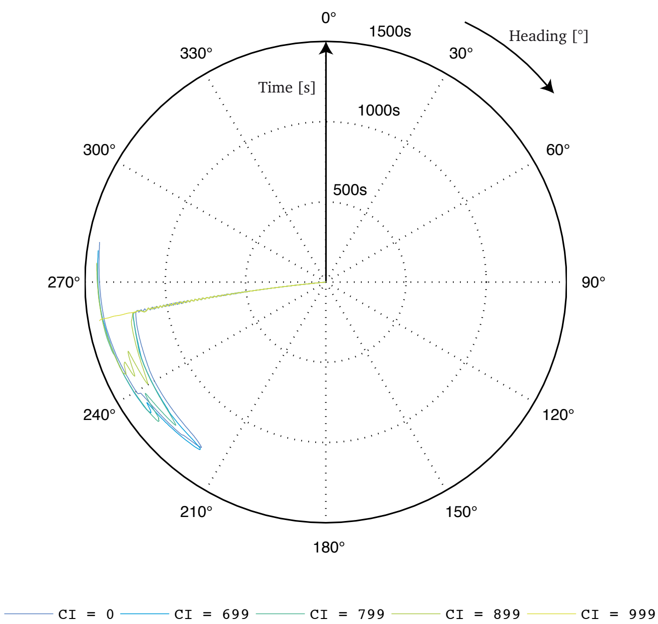

Figure 7.9: S2 - Modified Relative Zone - Development of heading for CI $\in \{0, 699, 799, 899, 999\}$

The speeds commanded are within the boundaries of $[218.17\frac{m}{s}, 271.46\frac{m}{s}]$. While the minimum commanded speed was nearly achieved with $218.19\frac{m}{s}$, the maximum speed reached was $263.54\frac{m}{s}$. The maximum commanded altitude – which was also achieved – did not exceed $11546.10m$. The minimum altitude remained at the initial altitude of $11277.00m$. Table 7.13 summarises the measures for the aforementioned Cost Index settings. All results are summarised in Section C.2, Table C.11 and Table C.12.

7.3.2 Discussion

The general requirements as described in Section 7.1 and the scenario specific hypotheses are discussed in the following for both, *Ownship Speed Zone* and *Modified Relative Zone* implementation.

Table 7.13: S2 - Modified Relative Zone implementation - Flyability related measures for CI $\in \{0, 99, 499, 999\}$ (2/2)

Cost Index	com. speed $[\frac{m}{s}]$		act. speed $[\frac{m}{s}]$		com. altitude $[m]$		act. altitude $[m]$	
	min	max	min	max	min	max	min	max
0	237.63	271.46	237.63	261.85	11277.00	11277.00	11277.00	11277.00
99	218.17	271.46	218.19	263.54	11277.10	11315.30	11277.00	11315.30
499	218.19	271.46	218.45	263.4	11277.70	11402.50	11276.80	11402.50
999	218.19	271.46	218.74	257.55	11278.40	11546.10	11277.00	11546.10

General requirements

With the *Boeing 747-400*, a different aircraft has been chosen for evaluation in scope of Scenario II. The conflict over oceanic airspace could only be resolved by a heading change, an altitude change or a combination thereof. A sole speed change would not have solved the conflict since both aircraft were approaching each other on the same track.

Flyability: Regarding the flyability of the trajectory, it can be noted that the underlying aircraft model has ensured in both scenarios that only a flyable trajectory was computed. The speeds and altitudes remained within applicable boundaries (cf. Equation 7.3, Equation 7.4 and Table 2.2). Furthermore, the BADA constraints regarding pitch rate and maximum bank could be met as well with a maximum pitch rate of $0.4\frac{\circ}{s}$ (using *Ownship Speed Zone* implementation, cf. Table C.7) and a maximum bank of 35° (using *Modified Relative Zone* implementation, cf. Table C.11). Therefore requirement R_α is met.

Separation: Using the *Ownship Speed Zone* as Protected Airspace Zone implementation for the simulations without Cost Index integration could not solve the conflict. This also holds true for the evaluation runs with Cost Index integrated into the resolution computation where the best separation was achieved with $2237.27m$ (CI $= 0$).

Using the *Modified Relative Zone* implementation, the conflict was solved for all runs except for CI $= 999$ where no lateral Conflict Resolution was allowed (cf. Figure 7.10). Here the vertical separation of $259.25m$ is not sufficient to consider the conflict as solved. With conflicts not being resolved, requirement R_β is not met.

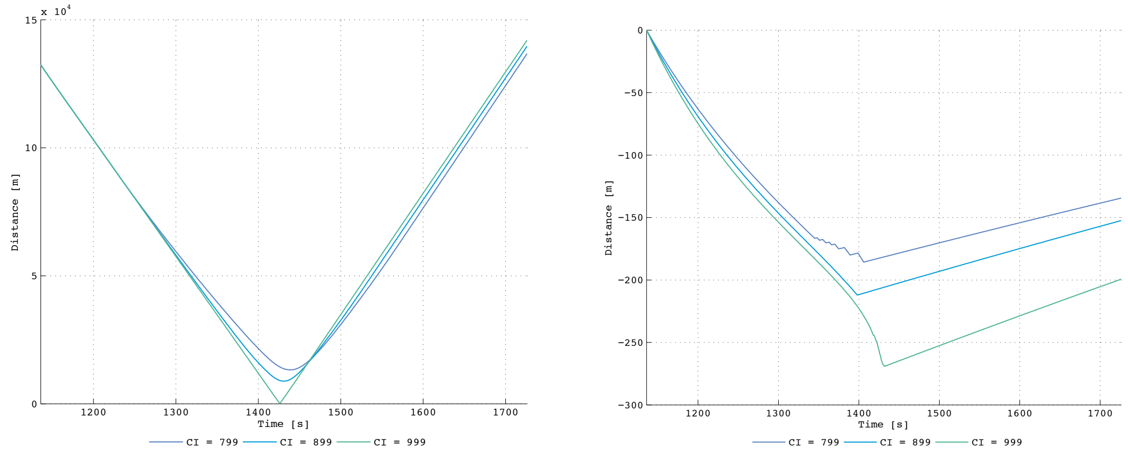

(a) Lateral distance (b) Vertical distance

Figure 7.10: S2 - Modified Relative Zone implementation - Vertical and Lateral distance for CI $\in \{799, 899, 999\}$

Scenario specific hypotheses

This scenario was aimed towards evaluation of the impact of Cost Index integration under the constraint, that one degree of freedom less can be used for resolving the conflict (i.e. speed resolution).

Lateral deviation: Using the *Ownship Speed Zone* implementation, lateral deviation was not reduced with a growing Cost Index as expected. Reason for this lies within the design of the scenario. With the intruder approaching on the same track from ahead, ownship was repelled into the direction where it came from, thus a 180° turn would have been necessary (cf. Figure 7.11(a)).

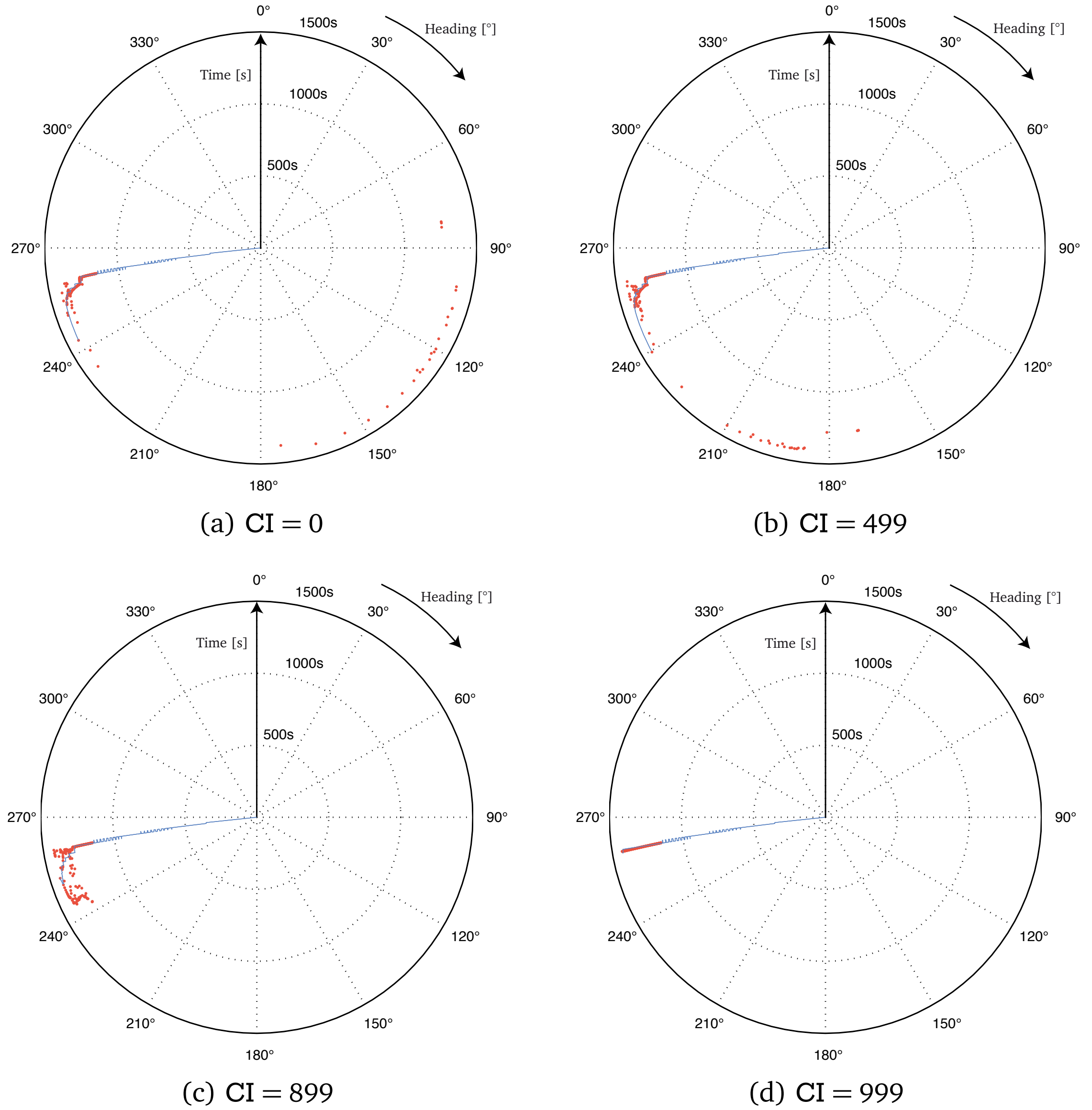

(a) CI = 0 (b) CI = 499

(c) CI = 899 (d) CI = 999

Figure 7.11: S2 - Ownship Speed Zone - Commanded (red) and actual heading (blue) during Conflict Resolution

With growing Cost Index the deviation required by the Conflict Resolution between the bearing to the target Trajectory Change Point and the heading derived from the force acting on ownship is reduced as of Equation 4.23. Since the target heading is commanded to the underlying aircraft model (cf. Subsection 5.2.3), it cannot immediately be achieved. This results in a similar lateral deviation for the majority of the Cost Index settings (Figure 7.11(b) and Figure 7.11(c) illustrate the actual and commanded headings for CI = 499 and CI = 899).

The evaluation runs using the *Modified Relative Zone* implementation lead to a similar result with lateral deviation starting to notably shrink at a Cost Index of 799. Due to the alignment of the Protected Airspace Zone along ownship's bearing to the intruder, the repulsive force could act for a longer uninterrupted time span which allowed more consistency regarding the commanded heading. Figure 7.12 illustrates the commanded and actual headings using the *Modified Relative Zone* implementation for Cost Index settings of 0, 499, 899 and 999. Due to the aforementioned discrepancies, hypotheses H_4 cannot be

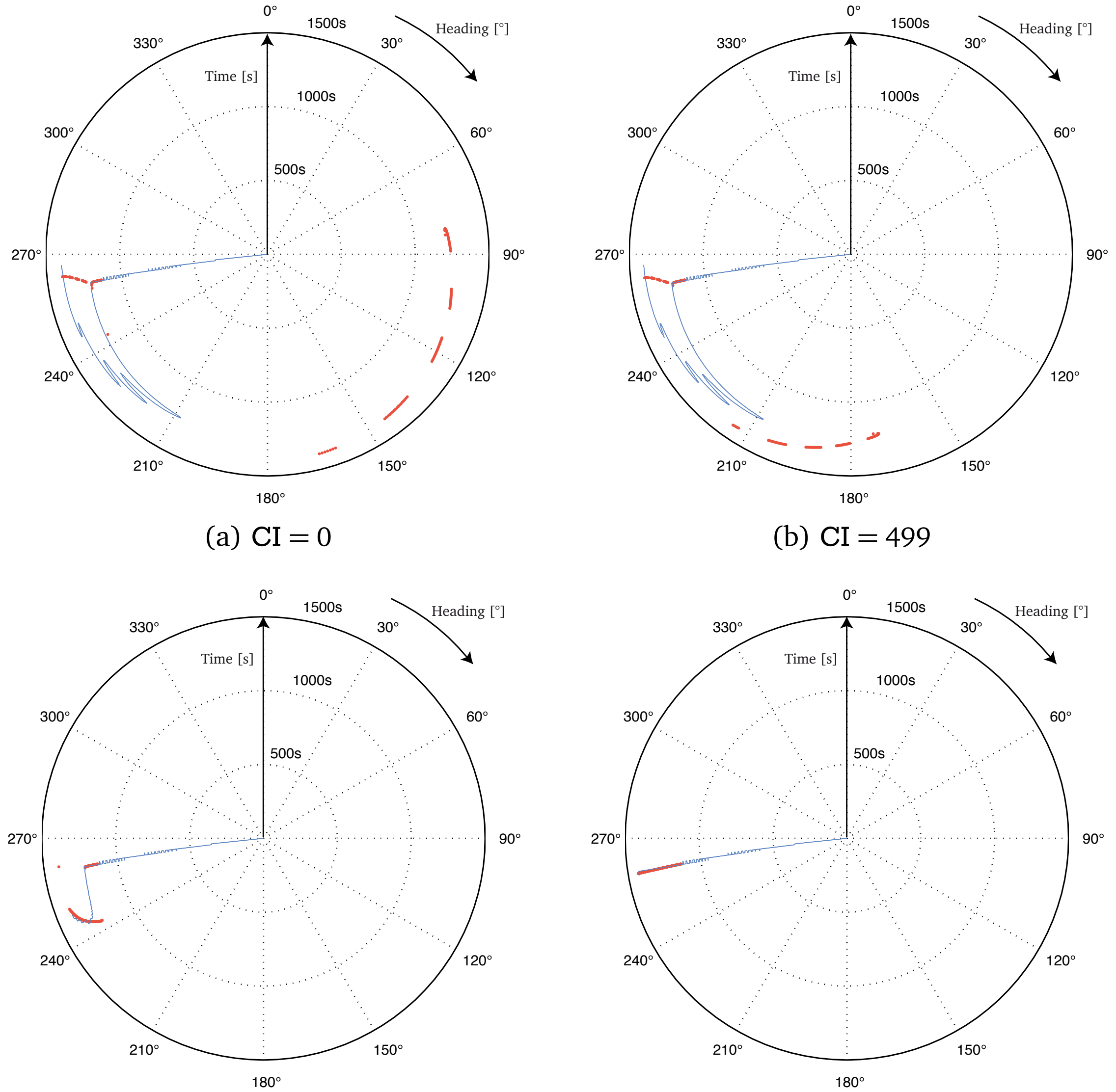

(a) CI = 0 (b) CI = 499

(c) CI = 899 (d) CI = 999

Figure 7.12: S2 - Modified Relative Zone - Commanded (red) and actual heading (blue) during Conflict Resolution

validated.

Vertical deviation: Vertical deviation from Reference Business Trajectory grew as expected with both Protected Airspace Zone implementations. The minimum deviation of $0km^2$ was achieved with a Cost Index setting of 0 due to vertical manoeuvres not being allowed. Maximum vertical deviation with $28.32km^2$ (Ownship Speed Zone) and $48.68km^2$ (Modified Relative Zone) were both achieved with a Cost Index setting of 999. Even with a Cost Index setting of 999 where a vertical manoeuvre is implemented without dampening, the required vertical separation could not be achieved. It is expected that with a longer look-ahead period the vertical deviation would grow until reaching the required vertical separation. Even though in this scenario the required separation could not be achieved, hypothesis H_5 can be validated since the vertical deviation grew as expected.

Temporal deviation: Regarding temporal deviation, only simulation runs with a Cost Index setting other than 0 differ significantly since with CI$=0$ no changes to the planned speed could be commanded. Using the *Ownship Speed Zone* implementation, the ETO difference remained below the Trajectory Management Requirement of $\Delta t_{max} = 20s$. With the *Modified Relative Zone* implementation, the lateral deviation achieved during Conflict Resolution was large, causing a delay of more than $20s$. For all other Cost

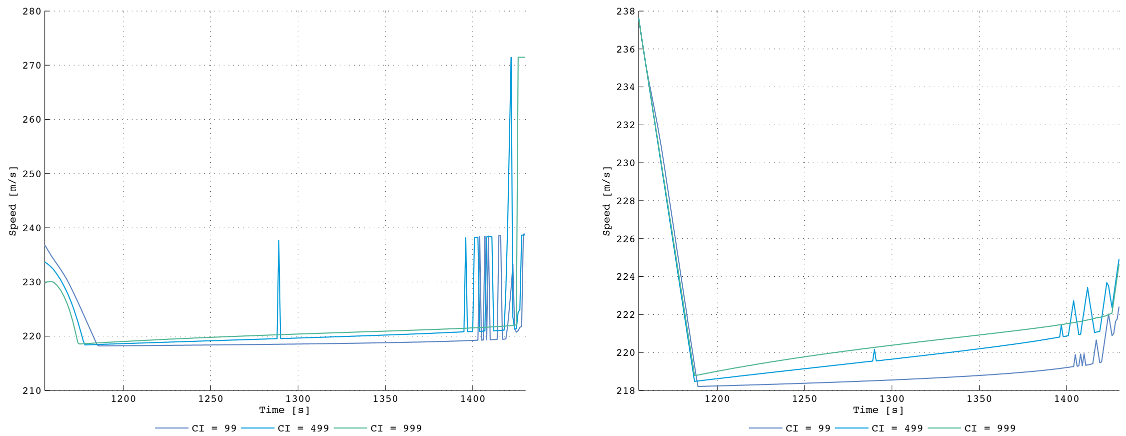

(a) Commanded speeds (b) Achieved speeds

Figure 7.13: S2 - Ownship Speed Zone implementation - Speeds during CR for CI $\in \{99, 499, 999\}$

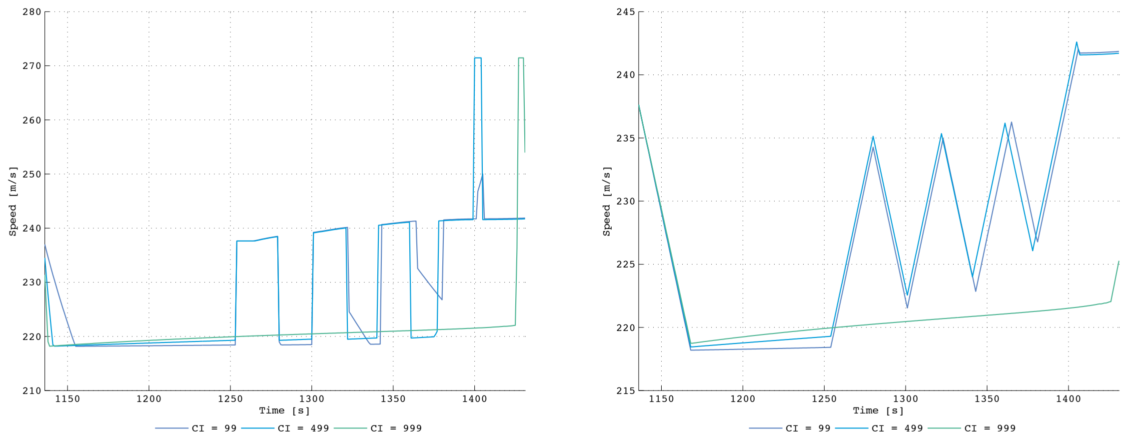

(a) Commanded speeds (b) Achieved speeds

Figure 7.14: S2 - Modified Relative Zone implementation - Speeds during CR for CI $\in \{99, 499, 999\}$

Index settings, the temporal deviations remained within the boundaries of $[64287.57s^2, 68240.26s^2]$ and $[55981.03s^2, 66634.25s^2]$ for *Ownship Speed Zone* and *Modified Relative Zone*. It was expected, that for all Cost Index settings larger than 0, the temporal deviation would be comparable, but nevertheless smaller for larger Cost Index settings. The reason why this expectation was not fulfilled lies within the time required to achieve the commanded speeds. Figure 7.13 and Figure 7.14 illustrate the commanded and achieved speeds for Cost Index settings 99, 499 and 999 for both Protected Airspace Zone implementations[4]. Notably, with a larger Cost Index, a smaller speed is commanded earlier than with a smaller Cost

[4] The peeks in commanded speed close to the end of the Conflict Resolution time span are caused by the aircraft trying to recapture the Reference Business Trajectory when its Protected Airspace Zone is not infringed (cf. Subsection 5.2.3).

Index (cf. Figure 7.13(a) and Figure 7.14(a)). All commanded speeds reach $218\frac{m}{s}$ at $t_{\text{CI}=99} = 1185s$, $t_{\text{CI}=499} = 1178s$ and $t_{\text{CI}=999} = 1174s$ (*Ownship Speed Zone*) and $t_{\text{CI}=99} = 1154s$, $t_{\text{CI}=499} = 1142s$ and $t_{\text{CI}=999} = 1140s$ (*Modified Relative Zone*). Conflict Resolution start time was $t_s = 1155s$ using the *Ownship Speed Zone* and $t_s = 1136s$ using the *Modified Relative Zone* implementation. With maximum longitudinal acceleration limited by BADA to $0.6096\frac{m}{s^2}$ (cf. Section F.5), the commanded speed could be met before being limited by the speed envelope. Therefore, during all simulations the aircraft decelerated at a comparable rate, neglecting effects of the Cost Index setting to the temporal deviation. Hypothesis H_6 is therefore not met since the Cost Index did not impact the temporal deviation as required.

7.4 Scenario III – IFBP region

In Scenario III, a Mid-Air Collision between three aircraft was set up within the Inflight Broadcast Procedure area over African airspace. In this scenario two aircraft approached ownship, one from the side as in Scenario I and one from ahead as in Scenario II (cf. Subsection 6.2.3). Beside adherence to the requirements R_α and R_β, the following hypotheses are to be verified:

H_7 A larger Cost Index will result in a smaller lateral deviation.

H_8 A larger Cost Index will result in a larger vertical deviation.

H_9 A larger Cost Index will result in a smaller temporal deviation.

Scenario specific constraints
The speed and altitude envelope are equal to Scenario I (cf. Subsection 7.2.2), i.e. the following constraints need to be met:

$$\begin{aligned} V_{min} &= 160.04\frac{m}{s} \\ V_{max} &= 257.32\frac{m}{s} \end{aligned}$$

V_{min} and V_{max} may not be under-, respectively overshot during Conflict Resolution.

7.4.1 Results

Scenario I has been extended by a third aircraft approaching the waypoint FL at the same Flight Level and time as ownship. The following paragraphs summarise the measures on *Safety*, *Costs* and *Flyability* for Scenario III, using the *Modified Relative Zone* implementation. Figure 7.15 illustrates the two conflicting aircraft (coming from the upper left corner and from above, both in red) and the resolutions calculated with different Cost Index settings for ownship (coming from the lower left corner) up to the point in time where the original trajectory depicted in white reaches the Closest Point of Approach (conflict point).

Safety
While the Mid-Air Collision at $(\lambda^\diamond, \phi^\diamond, h) = (12.1417°, 15.0383°, 10058.0m)$ could be mitigated with all Cost Index settings, the evaluations with Cost Index settings 299, 499, 599 and 999 failed to prevent an intrusion of ownship's Collision Avoidance Zone. With Cost Index settings 299, 499 and 599, the required minimum separation to $acr_{i,0}$, which approached ownship from the side, could not be achieved while the conflict with $acr_{i,1}$ could not be resolved at a setting of 999. The smallest distance over all CI runs between ownship and intruder $acr_{i,0}$ was reached with $894.92m$ at CI = 299 (vertical distance of $-273.41m$ and horizontal distance of $852.14m$). At CI = 999, ownship passed intruder $acr_{i,1}$ at a distance of $274.18m$ (vertical distance of $-274.11m$ and horizontal distance of 24.26). Figure 7.16 and

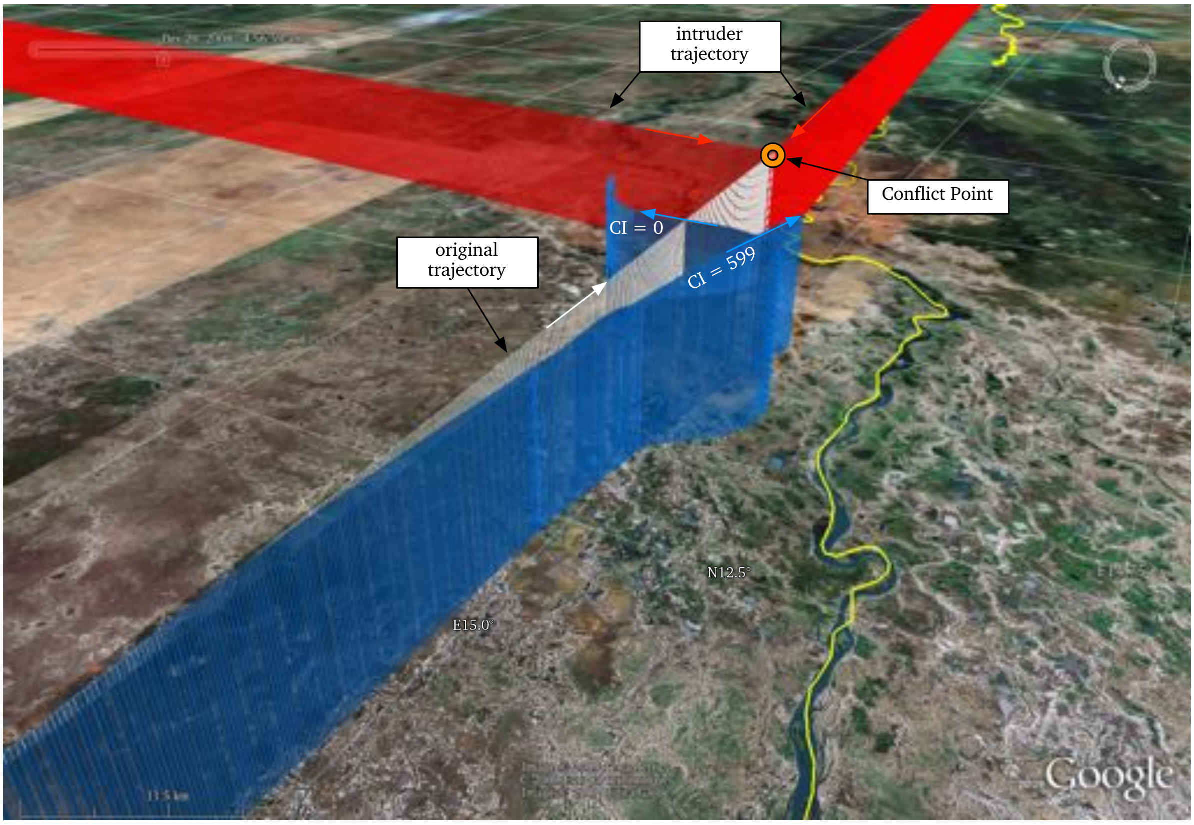

Figure 7.15: S3 - Illustration of Conflict Resolution manoeuvre (Google Earth)

Figure 7.17 illustrate the development of horizontal (Figure 7.16(a) and Figure 7.17(a)) and vertical (Figure 7.16(b) and Figure 7.17(b)) distances between ownship and intruder for the aforementioned Cost Index settings. The distances and numbers, durations and maximum infringements of ownship's Protected Airspace Zone for these settings are summarised in Table 7.14 and Table 7.15. Further results may be found in Subsection C.3.2, Table C.13 and Table C.14.

Table 7.14: S3 - $acr_{i,0}$ - Safety related measures for CI $\in \{299, 499, 599, 999\}$

	Distance at CPA			Intrusion		
Cost Index	Slant $[m]$	Horizontal $[m]$	Vertical $[m]$	#	maximum	duration $[s]$
299	894.92	852.14	−273.41	34	0.991804	316
499	948.82	902.23	−293.69	40	0.991208	333
599	1002.20	957.55	−295.84	39	0.990637	332
999	4864.71	4856.89	−275.71	1	0.966630	427

Cost

The lateral deviation from Reference Business Trajectory lies between $27.29km^2$ (CI = 0) and $925.67km^2$ (CI = 499). The maximum vertical deviation was achieved with $39.45km^2$ at a Cost Index setting of 599. With a Cost Index setting of 0, the vertical deviation is minimal with $0km^2$. Temporal deviation is between $12845.56s^2$ (CI = 0) and $78731.57s^2$ (CI = 599). The results for Cost Index runs 0, 399, 499, 599 and 999 are summarised in Table 7.16. Table C.15 (Subsection C.3.2) summarises the results from all evaluation runs.

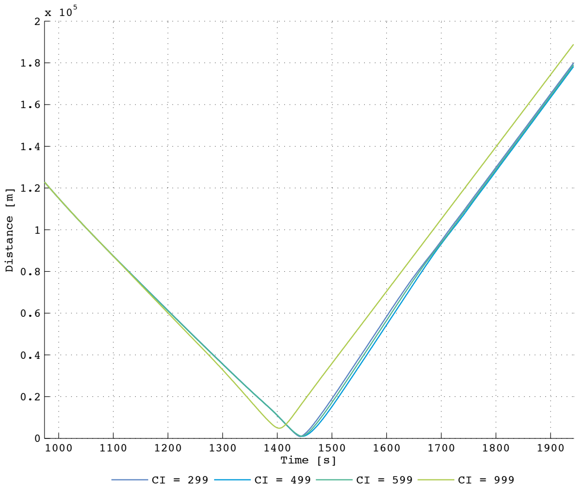

(a) Horizontal distance

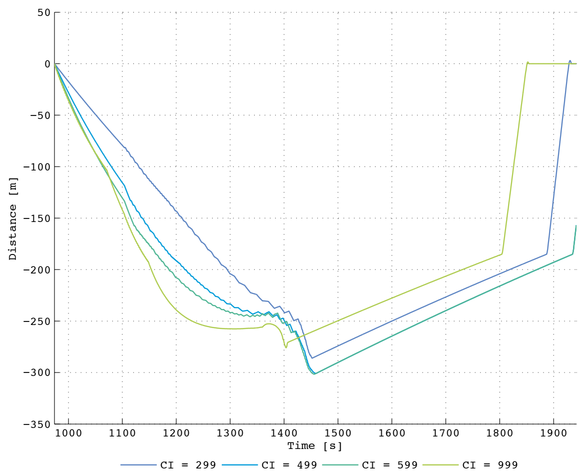

(b) Vertical distance

Figure 7.16: S3 - Distances between ownship and intruder $acr_{i,0}$ for CI $\in \{299, 499, 599, 999\}$

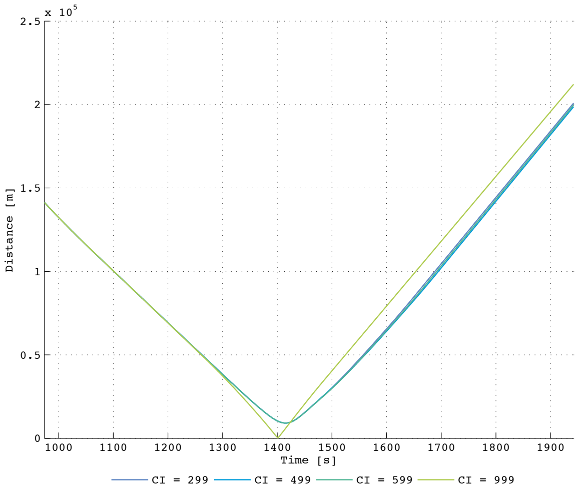

(a) Horizontal distance

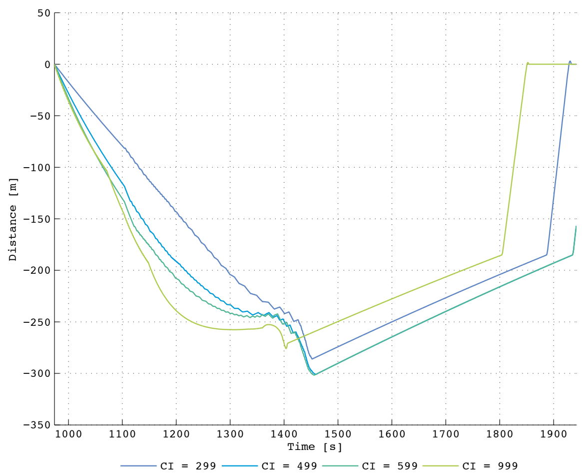

(b) Vertical distance

Figure 7.17: S3 - Distances between ownship and intruder $acr_{i,1}$ for CI $\in \{299, 499, 599, 999\}$

Table 7.15: S3 - $acr_{i,1}$ - Safety related measures for CI $\in \{299, 499, 599, 999\}$

	Distance at CPA			Intrusion		
Cost Index	Slant $[m]$	Horizontal $[m]$	Vertical $[m]$	#	maximum	duration $[s]$
299	9175.85	9172.54	−246.39	1	0.858938	277
499	9131.86	9128.21	−258.23	1	0.855820	277
599	9117.96	9114.23	−260.86	1	0.853352	276
999	274.18	24.26	−273.11	1	0.997358	303

Flyability

The maximum bank with 35° was achieved during the majority of the runs. All evaluation runs except for a Cost Index setting of 999 required a bank of more than 15°. For these Cost Index settings the maximum bank rate also reached $3\frac{\circ}{s}$. The maximum pitch rate achieved is $0.54\frac{\circ}{s}$. Table 7.17 summarises bank, bank rate, pitch and pitch rate for Cost Index settings of 0, 499 and 999.

Table 7.16: S3 - Cost related measures for CI $\in \{0, 399, 499, 599, 999\}$

Cost Index	$H[km^2]$	$V[km^2]$	$Ti[s^2]$
0	27.29	0.00	12845.56
399	430.03	25.51	52216.40
499	925.67	38.78	79646.58
599	878.51	39.45	78731.57
999	329.78	34.45	42182.30

Table 7.17: S3 - Maximum bank, pitch and first degree derivatives for CI $\in \{0, 499, 999\}$

Cost Index	$\phi[°]$	$\dot{\phi}[\frac{°}{s}]$	$\theta[°]$	$\dot{\theta}[\frac{°}{s}]$
0	35.00	3.00	0.00	0.00
499	34.96	3.00	0.92	0.54
999	0.03	0.01	0.76	0.54

Minimum and maximum commanded and achieved speeds are within the boundaries of $160.44\frac{m}{s}$ (CI = 0), $256.39\frac{m}{s}$ (CI = 599) and $160.44\frac{m}{s}$ (CI = 0) and $251.03\frac{m}{s}$ (CI = 999). Minimum and maximum altitudes were achieved at Cost Index settings of 299 ($10055.00m$) and 599 ($10359.70m$, corresponding to the maximum commanded altitude). Minimum commanded altitude is $10058.00m$ at CI = 0. Table 7.18 summarises the results regarding flyability related measures for the aforementioned Cost Index settings.

Table 7.18: S3 - Commanded and achieved speeds and altitudes for CI $\in \{0, 99, 499, 999\}$

	com. speed $[\frac{m}{s}]$		act. speed $[\frac{m}{s}]$		com. altitude $[m]$		act. altitude $[m]$	
Cost Index	min	max	min	max	min	max	min	max
0	200.05	245.35	200.05	245.35	10058.00	10058.00	10058.00	10058.00
99	160.18	245.19	160.18	210.25	10058.10	10132.00	10056.10	10132.00
499	160.49	245.00	160.50	210.01	10058.70	10196.70	10057.70	10196.70
999	160.73	244.92	160.76	223.36	10059.50	10305.00	10057.10	10297.30

Further results from all evaluation runs regarding flyability are summarised in Table C.16 and Table C.17 (Subsection C.3.2).

7.4.2 Discussion

With Scenario III it was intended to validate the same hypothesis as of Scenario I, but instead for a conflict of two aircraft for a conflict involving three aircraft. The two worst-case scenarios – an aircraft approaching from ahead and one approaching from the side where the Protected Airspace Zone propagation is minimal – have therefore been combined. In the following, adherence to the requirements described in Section 7.1 and the scenario specific hypotheses (cf. Section 7.4) are discussed.

General requirements

With an *Airbus A340-300*, the same aircraft model has been used in Scenario III as in Scenario I. For resolution of this conflict, all manoeuvres except a sole application of speed changes where possible. With one intruder approaching from ahead and the conflict point being at the waypoint *FL* (cf. Figure 7.1), ownship was not expected to rejoin its Reference Business Trajectory before passing that waypoint.

Flyability: The aircraft model which executed the heading, altitude and speed commands ensured flyability of the resulting trajectory in Scenario III. During all runs ownship state variables remained within the limitations defined by BADA (cf. Equation 7.5 and Equation 7.5) and the requirements regarding maximum bank (35°) and pitch rate ($0.54\frac{°}{s}$) are met as well. Therefore requirement R_α is met.
Separation: All Cost Index runs could prevent the Mid-Air Collision, but CI runs 299,499, 599 and 999 failed to establish the required minimum separation and ownship's Collision Avoidance Zone was infringed. At a Cost Index setting of 999, ownship failed to establish the required vertical separation to $acr_{i,1}$. With the intruder approaching from ahead and heading changes disallowed due to the Cost Index setting, this would have been the only possible resolution manoeuvre. This situation is similar to Scenario II where ownship could not acquire the required altitude in time.
At Cost Index settings 299, 499 and 599 the algorithm failed to compute a resolution establishing the minimum separation to $acr_{i,0}$ which approached ownship from the side. This is different to Scenario I where the separation could be established for all CI settings except for CI = 0. The difference between the two scenarios is, that in this scenario ownship was pushed by $acr_{i,1}$ further into the continuation of $acr_{i,0}$'s flight path as illustrated in Figure 7.18. With Cost Index settings 299, 499 and 599 this deviation

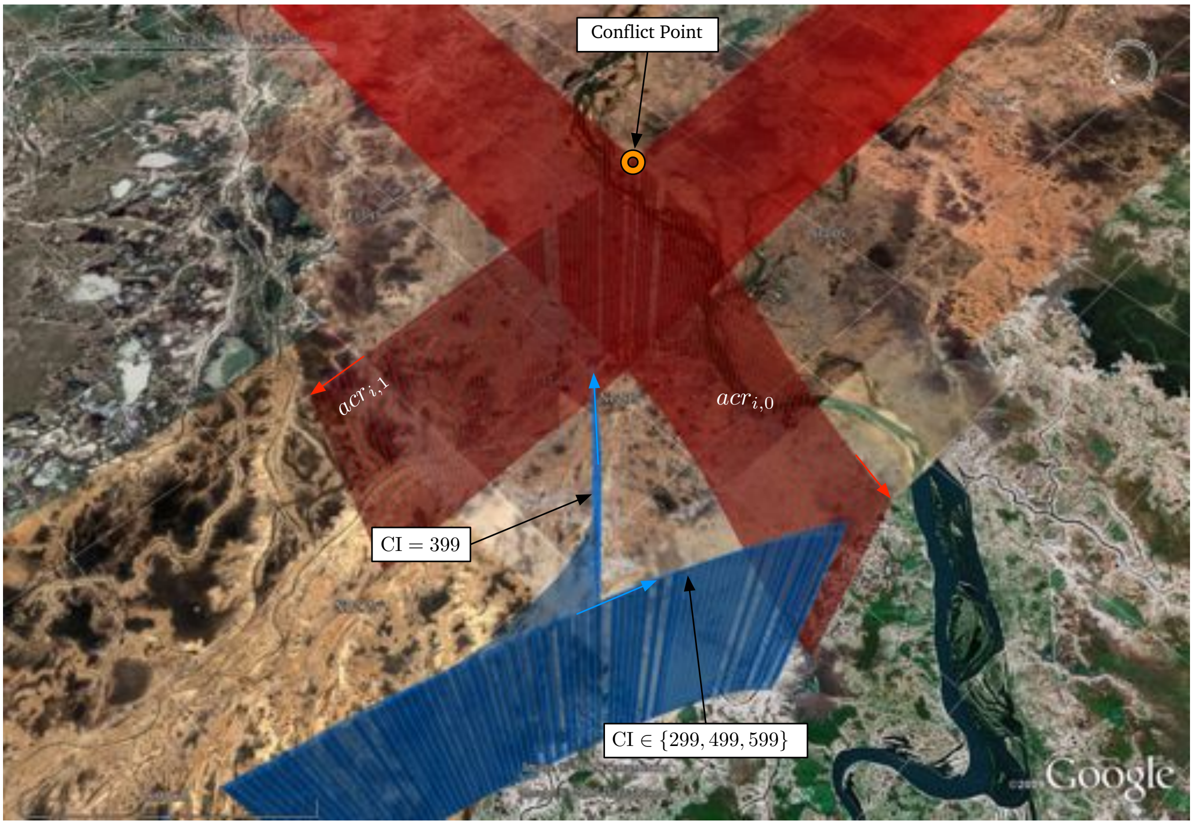

Figure 7.18: S3 - Ownship pushed into intruders flight path (Google Earth)

caused ownship to have been pushed onward by $acr_{i,0}$. This is illustrated in Figure 7.19(c) for the example of CI = 599. Ownship's trajectory is depicted in black when its Protected Airspace Zone is not infringed, cyan when it is infringed by $acr_{i,0}$, yellow when it is infringed by $acr_{i,1}$ and red when both intruder violate ownship's Protected Airspace Zone. Before ownship could recapture its flight path in Figure 7.19(c) it was pushed by $acr_{i,0}$ into direction of its own movement, causing it to close further instead of diverging from the intruder. With the conflict not being solved for the aforementioned Cost Index settings, requirement R_β is not fulfilled.

Scenario specific hypotheses
Lateral, vertical and temporal deviation did not develop as expected and observed in Scenario I and II. Reasons why neither hypotheses H_7, H_8 or H_9 are met for Scenario III are discussed in the following.
Lateral deviation: The lateral deviation of ownship from its Reference Business Trajectory is influenced by the drawing force of the next Trajectory Change Point and the repulsive forces from the intruders.

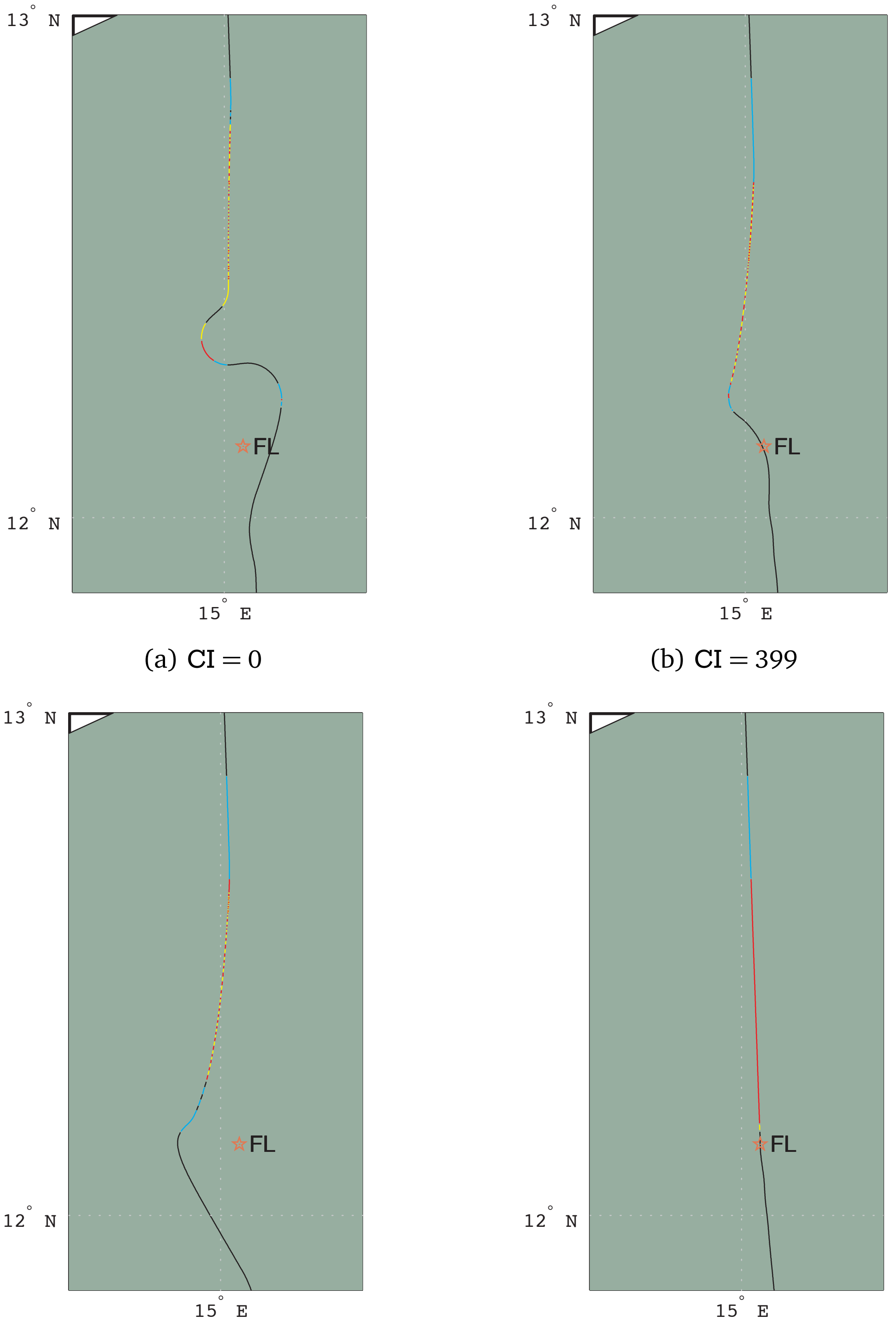

(a) CI = 0 (b) CI = 399

(c) CI = 599 (d) CI = 999

Figure 7.19: S3 - Ownship Conflict Resolution flight path

Even though the boundaries in which the heading was commanded shrink with growing Cost Index (cf. Figure 7.20), the deviation of ownship into direction of the continuation of $acr_{i,0}$'s flight path caused a higher intrusion compared to the two aircraft conflict of Scenario I (cf. Table C.1 and Table C.13). The (lateral) trajectories of ownship for Cost Index settings 0 and 999 behaved as expected. Since no

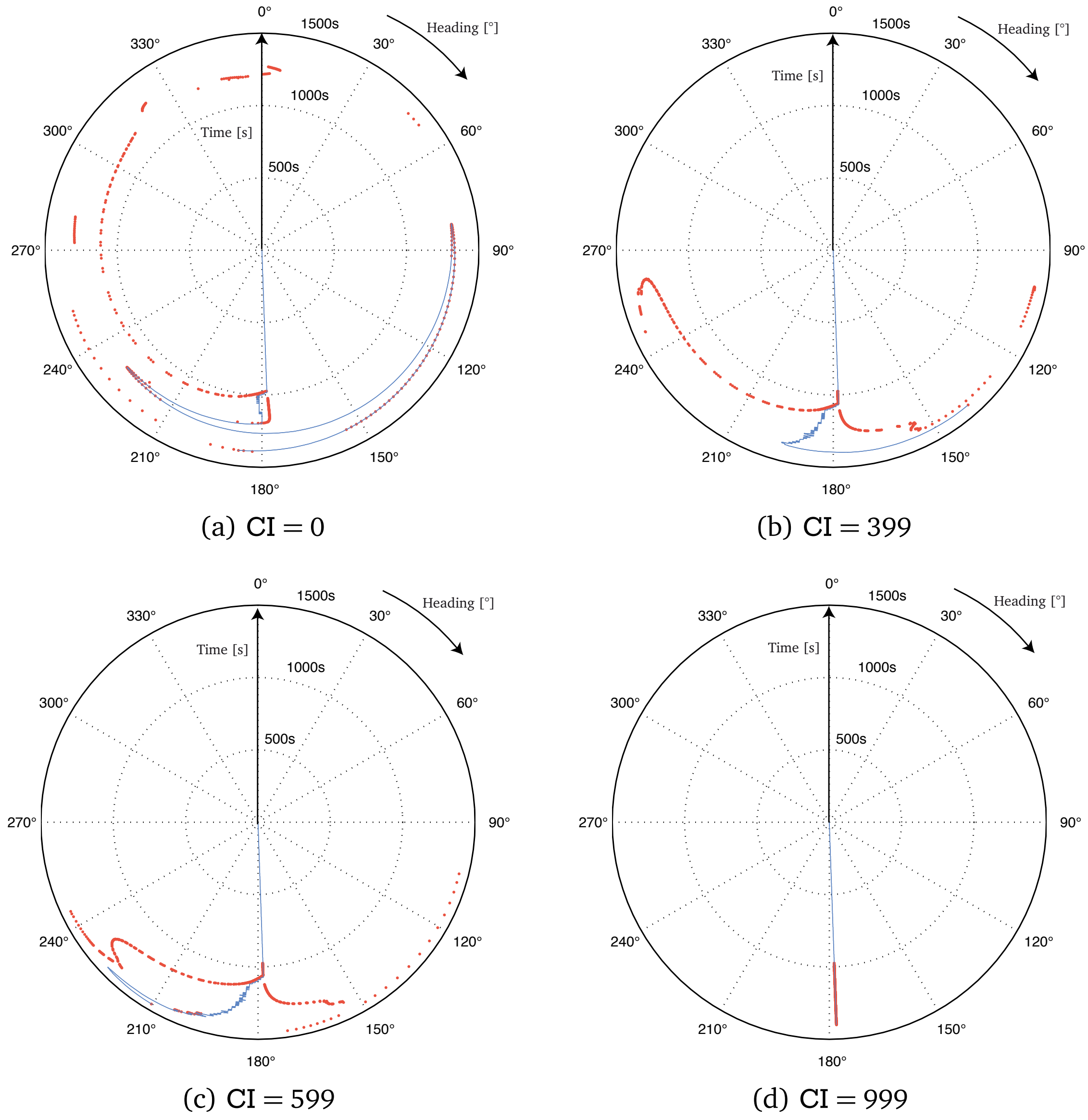

(a) CI = 0 (b) CI = 399

(c) CI = 599 (d) CI = 999

Figure 7.20: S3 - Commanded (red) and actual heading (blue) during Conflict Resolution

vertical nor speed command could be used to resolve the conflict with a CI setting of 0, ownship needed to resolve the conflict solely through heading changes (cf. Figure 7.19(a)). With a Cost Index setting of 999, only speed and altitude changes could be commanded, therefore no lateral deviation exists (cf. Figure 7.19(d)). Regarding other Cost Index settings this could not be confirmed, e.g. for a Cost Index setting of 599 the lateral deviation was larger than for a CI of 399 (cf. Table 7.16). Figure 7.19(b) and Figure 7.19(c) illustrate the flight paths for CI settings 399 and 599, respectively. The intruder $acr_{i,0}$ acted in the vicinity of waypoint *FL* for a longer time on ownship, causing it to deviate more. Reason for this behaviour is that with a lower Cost Index setting (thus with a higher gain on lateral manoeuvres), larger heading changes away from the bearing to the target waypoint *FL* were allowed. While this allowed at a CI of 399 to solve the conflict earlier and return to the Reference Business Trajectory before reaching *FL*, it has caused at a CI of 599 ownship to remain longer in conflict to the intruder, thus requiring ownship to deviate more and subsequently causing a larger lateral deviation.

Vertical deviation: Regarding vertical deviation, the explanation is similar. Vertical deviation grows as expected except for two breaks. At Cost Index settings of 399 and 699, the vertical deviation shrinks compared to the CI runs 299 and 599, respectively. With the conflict being resolved earlier at a Cost Index of 399, ownship was able to return to its initial flight level sooner. The resolution computed with a Cost Index setting of 699 did pass – other than with a CI of 599 – the waypoint *FL*, also having resolved the conflict with the intruder earlier.

Temporal deviation: For Cost Index settings 299, 499 and 599 similar resolutions have been calculated. These resolutions deviated further laterally from the Reference Business Trajectory compared to the other CI runs due to infringement of their Protected Airspace Zones. For these evaluation runs, the temporal deviation is also higher compared to the other evaluations (above $71170s^2$ for CI $= 299$ compared to a maximum of $42182s^2$ with a CI of 999, cf. Table C.15). Even when evaluated separately, the temporal deviation does not evolve as expected. Common to all evaluation runs is that ownship reduced its speed similar to Scenario II to resolve the conflict with $acr_{i,1}$ which approached ownship on the same track from ahead. With CIs 299, 499 and 599, a longer distance had to be traversed and the order of the temporal deviations corresponded to the lateral deviations. For the other Cost Index settings this is not the case. Here, similar to Scenario II, no direct impact of the gain on the temporal deviation can be identified. The differences in temporal deviation seem to be due to the additional distances to be travelled depending on the lateral deviation.

7.5 Summary

For all scenarios and Cost Index settings, the Mid-Air Collision set up between the aircraft could be prevented with the alternative trajectory calculated by the *Artificial Force Field* Conflict Resolution algorithm devised in this work. Though, an infringement of ownship's Collision Avoidance Zone could not always be prevented by the Conflict Resolution algorithm.

Two separate domains were surveyed in these evaluations, the *flyability* of the resulting trajectory and the *integration of the Cost Index* into the Conflict Resolution process.

Violation of CAZ

It was intended to ensure through the layout of the Protected Airspace Zone surrounding ownship, that the Collision Avoidance Zone would not be violated. It has been shown, that especially for conflicts where aircraft are flying towards each other on the same track as in Scenario II, a Protected Airspace Zone implementation which has its largest extension into direction of its heading (*Ownship Speed Zone* implementation, cf. Subsection 3.2.2), may not be sufficient to prevent an intrusion of the Collision Avoidance Zone. Here, even though the distance at Closest Point of Approach was significantly larger, the *Modified Relative Zone* implementation has proven better. The Collision Avoidance Zone was only infringed when lateral resolution was not allowed, thus when negating the advantage of this zone implementation[5].

Integration of aircraft model

With the integration of an aircraft model, the flyability of the trajectory could be guaranteed. The constraints set up through the Base of Aircraft Data [Nui04b] were respected during Conflict Resolution. Neither speeds nor altitudes were commanded outside of the flight envelope. The aircraft model also did not over- or undershoot the limitations during execution of the Conflict Resolution manoeuvre.

[5] The longest extension of the Protected Airspace Zone does not follow the heading but the bearing to the intruder if it is within ±45° (cf. Figure 3.4).

Furthermore, constraints regarding maximum bank and pitch rate as defined by the aircraft model were respected during the Conflict Resolution.

Integration of gains

The prioritisation of the Conflict Resolution manoeuvre was achieved through the introduction of gains on the difference between the flight plan required command inputs (heading, altitude and speed) and the commands calculated by the *Artificial Force Field* Conflict Resolution algorithm. Three gains acting on heading, altitude and speed commands were used.

Lateral gain: For two-aircraft conflicts, the lateral gain used limited the lateral deviation from Reference Business Trajectory as expected. Though, depending on the construction of the scenario, the difference between flight plan required heading and the heading required by the Conflict Resolution algorithm $\Delta\psi$ (cf. Equation 4.23) was close to 180° (cf. Figure 7.11 and Figure 7.12). With the gain k_h limiting the degree of which the difference $\Delta\psi$ was allowed to be followed, for large $\Delta\psi$ the impact was limited. The aircraft could not – due to the aircraft model underlying the Conflict Resolution – immediately acquire the new heading. With – irrespective of the Cost Index setting – the flight plan being recaptured when the intruder moves out of ownship's Protected Airspace Zone, the actually achieved and maintained headings are similar until the gain effectively limits not only $\Delta\psi$ but also ownship's heading.

Vertical gain: The gain k_a acting on the altitude command (cf. Equation 4.24) has worked (for the two aircraft conflict) as expected. With a higher Cost Index setting, the vertical distance at the Closest Point of Approach was larger. The major deficiency of the integration lies in the time required to achieve a vertical separation to the intruder aircraft. No conflict was solved through establishing the minimum required vertical separation. Furthermore, ownship tended to reduce vertical separation in the vicinity of the target Trajectory Change Point even though the intruder still acted as a repulsive force on it.

Speed gain: The gain on the commanded speed did not have the desired effect on the Conflict Resolution. Notably, the minimum speed was commanded for the majority of the evaluation runs, requiring also a high speed command to recapture the Reference Business Trajectory in respect to the Scheduled Time Over at the destination. While the gain k_s acted on the difference between actual and Conflict Resolution required speed (cf. Equation 4.25), a limitation regarding the maximum and minimum speeds for the current trajectory segment could have proven better.

8 Summary & Outlook

> The scientist is not a person who gives the right answers, he is one who asks the right questions.
>
> Claude Levi-Strauss

Significant gains in both ecological and economical performance of air transportation are expected through implementation of a performance based Air Traffic Management system. Both major research and development programs implementing the future Air Traffic Management operational concept [ICA05b] introduce the Autonomous Operations Area airspace. This work was concerned with one required component for aircraft operating in Autonomous Operations Area airspace, a system to autonomously detect and resolve traffic conflicts. The concept of Conflict Detection & Resolution has been extended to allow introduction of the Flight Management System Cost Index which is nowadays used to prioritise between fuel and time costs depending on the operators preferences. An algorithm, based on the thoroughly investigated area of *Artificial Force Fields* (cf. e.g. [III00; Zeg98]), has been presented and extended to allow for this integration.
This chapter summarises the problem definition (Section 8.1) and the approach (Section 8.2) taken. The conclusions are summarised in Section 8.3 while research subjects that could follow or build upon this thesis are presented in Section 8.4 which also concludes this work.

Rationale for this thesis

With other technological means promising only minor gains compared to the effort required in enhancing aircraft efficiency, operational changes to be introduced with Air Traffic Management operational concepts are the most promising direction to proceed. The concept of Autonomous Operations Area airspace is one of the key-enablers for both more economical and ecological air traffic. The Autonomous Operations Area concept requires aircraft to be able to access and process traffic information and detect and resolve conflicts. The feasibility of the Autonomous Operations Area concept has been shown in numerous studies and theses (cf. e.g. [Hoe01; Rui02; AG06]) and will likely continue to be a major topic for both research and industry.

8.1 Problem definition

The responsibility for monitoring and assuring safe separation to other aircraft is delegated to the flight deck crews when operating in Autonomous Operations Area airspace. The aim of introducing Autonomous Operations Area airspace is to enhance economical and ecological efficiency of air traffic. If a conflict is detected, the flight deck crew has to resolve it to continue the safe flight.
Aircraft in Autonomous Operations Area airspace are supposed to travel along their preferred route which depends on their current load, the aircraft characteristics and the operators' cost model. Depending on the business model (and on economic circumstances), an airline may choose to weight fuel related costs higher than time related costs.
This work was concerned with the problem of integrating the operators' prioritisation into the process of Conflict Resolution. For this purpose, the Flight Management System Cost Index has been considered and integrated into the Conflict Resolution process.

8.2 Approach

This work was concerned with the Conflict Detection & Resolution system for aircraft operating in Autonomous Operations Area airspace. The emphasis was on the Conflict Resolution component with the aim to integrate a prioritisation criteria given through the Flight Management System Cost Index. Several assumptions have been made for the Conflict Detection & Resolution system.

Information

Regarding *access to traffic information*, it has been assumed that Automatic Dependant Surveillance - Broadcast (ADS-B) data is broadcasted by all aircraft operating in Autonomous Operations Area airspace. This assumption is inline with the currently foreseen minimum requirements for aircraft intended to operate in this airspace [Ses; Nexa]. A further – and regarding the currently planned ADS-B classes significant – assumption concerning the exchange of data is the availability of all required ADS-B data along ownship's flightplan and all Trajectory Change Points (TCPs). The highest ADS-B equipment class currently foreseen requires only a transmission range of 120NM while the number of TCPs to be transmitted is not yet defined[1].

Conflict Resolution model

As model for the Conflict Resolution algorithm *Artificial Force Fields* have been used. In this approach, aircraft are modelled as charged particles repelling each other. Two extensions have been made to this approach.
To prevent that not flyable trajectories are required for resolution, an aircraft model based on the Base of Aircraft Data has been integrated into the model. The forces acting on the aircraft result in a new direction and speed required to be flown. These requirements are commanded to the aircraft model which executes the commands, similar to an autopilot.
Furthermore, the concept of Protected Airspace Zones (PAZs) has been integrated into the model as well. The force field around an aircraft in this extended model does not propagate uniformly from the aircraft but geometrical shaped, respecting factors such as speed. Several PAZ implementations have been introduced and two of them – a PAZ with its longest extension in direction of ownship heading, the other one in direction of the intruder – have been compared for subsequent Cost Index integration evaluations.

Cost Index integration

The Cost Index has been integrated into the Conflict Resolution process by adding gains to the possible resolution manoeuvres, i.e. speed manoeuvres, heading and altitude changes. Each of these manoeuvres have been attributed with certain costs. Heading changes are supposed to cause additional distance to be travelled and thus impact the flight time. Altitude changes at constant groundspeed and speed manoeuvres are impacting fuel consumption. Each of the resolutions have been mapped to a measure of the magnitude of the manoeuvre. To evaluate the costs caused by the manoeuvres, the initially planned Reference Business Trajectory (RBT) and the through Conflict Resolution updated Predicted Trajectory (PT) are compared. Costs caused by a heading change are encoded as the horizontal or lateral area enclosed by the RBT and PT. For evaluation of the altitude changes required, the vertical area between the RBT's and PT's flight profile was used, while costs caused by speed changes were mapped to the difference between the Estimated Time Over and initially planned Scheduled Time Over at the target waypoint over resolution time.

[1] At least the next TCP is required to be submitted (cf. Section E.2).

8.3 Conclusions

Two questions were addressed in this work:

1. How can a prioritisation criteria similar to the Flight Management System Cost Index be integrated into the Conflict Resolution ?

2. How can a Conflict Resolution algorithm based on *Artificial Force Fields* be extended to guarantee flyability of the manoeuvre ?

Cost Index integration

The integration of the Cost Index through adding of gains to the deltas between the commanded and required (by the flightplan) heading, altitude and speed has proven to be a feasible approach for two-aircraft conflicts. The costs, mapped to the aforementioned horizontal, vertical and temporal areas, have behaved as expected for a resolution where the full manoeuvre space was available. Also for a resolution with one degree of freedom less (cf. Subsection 6.2.2) the resolutions with varying Cost Index behaved as expected. The integration of the gains could be refined for lateral and speed resolutions to allow for better Cost Index integration.

Lateral resolution: For *lateral resolution*, the possible resolution should be limited before introduction of the gain in such a way that the new heading commanded can be acquired in the time available. Through integration of the gain after this limitation, it is expected that the manoeuvre will respect the prioritisation given through the Cost Index better.

Speed resolution: Regarding *speed resolution*, the approach used in this work has room for improvement. The algorithm presented in this work uses the gain to limit the difference between current and commanded speed, resulting in minimum possible speed being commanded for the majority of the resolutions. Especially this topic would require further investigation.

Guaranteeing flyability

With the aircraft model underlying the *Artificial Force Field* Conflict Resolution algorithm, the generation of actually flyable trajectories could be guaranteed. The Trajectory Change Points of this alternative trajectory were passed onward to a further simulation with the same aircraft model to have it executed. The resulting trajectory was subsequently checked again for conflicts. Problems that might arise from aircraft reacting to slowly to a conflict, were addressed through implementation of proper Protected Airspace Zones (PAZs). PAZ implementations, which take current state information such as speed into account, allow for larger Conflict Resolution horizons.

8.4 Further work

This thesis has shown the feasibility of integration of the Flight Management System Cost Index into the Conflict Resolution process. Several topics have been encountered during the work on this thesis which could qualify for further research. In the following, a few of these topics are summarised.

Further refinement to Cost Index integration

The Cost Index integration as implemented in this work does not take current aircraft performance into account. The gains have been chosen statically and do not change during the manoeuvre. Two principle approaches could be implemented and evaluated:

1. Change of Cost Index during Conflict Resolution.

2. Change of gains depending on aircraft state during Conflict Resolution.

The first approach is currently followed on long-haul flights when the Flight Management System tries to meet a Required Time of Arrival [Lid92]. The second approach would require more knowledge about the aircraft performance in the Conflict Resolution algorithm. In either case, the evaluation of economic benefits and e.g. the impact on the aircraft's Specific Air Range (cf. Section F.2) would constitute new questions to be answered. With a thorough analysis on this subject, the actual benefit of autonomous operations could estimated.

Autonomous information exchange

Beside the task of autonomously detect and resolve conflicts, also the autonomous exchange of information is a matter of research. Currently, the European project *Newsky* [SSS07] surveys the possibilities to apply the ISO model of network layers [Iso] to the aeronautic domain. This will ease the application of technologies already under research in the area of computer science such as *mobile ad-hoc networks* [SKK03; Hol04] on the aeronautic domain.

Human-in-the-loop

Hoekstra has performed human-in-the-loop assessments of ASAS applications, using an approach based on *Artificial Force Fields* in 2001 [Hoe01]. With Human Machine Interface concepts such as the *Tunnel-in-the-Sky* [Psc+06; Sin08], the visualization of the trajectories computed by the Conflict Resolution algorithm could be integrated into the flight deck concept. To evaluate the actual operational benefit of a *strategic TCAS* for Conflict Detection and the Conflict Resolution algorithm would be a next, logical step. Currently, strategic Conflict Detection & Resolution information are superimposed on the Navigation Display without taking advantage of Synthetic Vision Systems.

Atmospheric hazards

Atmospheric hazards pose a threat to aircraft and are also a factor contributing to flight delays (cf. Subsection 1.1.2, [LPY01]) and require aircraft to divert from their Reference Business Trajectory. Beside the resolution of traffic conflicts, the algorithm presented in this work may also be extended to take weather phenomena into account and to calculate an alternative route. A further question to be addressed in this context is whether encoding the severity of an atmospheric hazard as magnitude of the repulsive force acting on the aircraft would be feasible.

Co-operative Conflict Detection & Resolution

Ruiz has investigated a multi-agent approach to co-operative Conflict Resolution [Rui02]. His approach was based on aircraft implementing the same Conflict Resolution algorithm and one aircraft – through negotiation – taking over the role of separation assurance authority. The approach investigated in this work was limited to the resolution being computed by only one aircraft. The extension of the approach taken in this work to the co-operative domain - especially with opposed prioritisation – would be an interesting topic.

Appendices

A Definitions

Further definitions are summarised in this chapter. Regarding the Trajectory Management Requirements as described in the SESAR concept of operations [Ses] and the Required Navigational Performance further information may be found in Section A.1 and Section A.2. The terms *strategic* and *tactical* used in the context of aviation are detailed in Section A.3. The vertical pendant to horizontal intrusion is described in Section A.4. This appendix is concluded with Section A.5 describing the rotational matrices used in this work.

A.1 Trajectory Management Requirement

Depending on the factors like the airspace type or the kind of separation provision the consequences for aircraft not adhering to the Reference Business Trajectory differ. In SESAR different ATM capability levels have been introduced. For each of these capability levels different Trajectory Management Requirement are to be applied.

For the scope of this work, Trajectory Management Requirements have been derived from current requirements to navigational performance regarding RNAV operations [ICA99] (cf. Section A.2) and from SESAR concept documents [Ses]. The Trajectory Management Requirements summarised in Table A.1 reflect assumptions made for the scope of this work.

Table A.1: Trajectory Management Requirements defined in this work

TMR class	XTE [m]	Altitude Error [m]	ETO error [s]	derived from
TMR0	185.2	76.2	20	[Ses], [ICA99]
TMR1	555.6	76.2	20	[Ses]
TMR6	7408	152.4	600	[Ses]

A.2 Required Navigational Performance

The Required Navigational Performance (RNP) types '[...] specify the minimum navigation performance accuracy required in an airspace.' [ICA99]. The lateral and longitudinal dimensions are covered by RNP. Regarding vertical accuracy especially during the en-route phase of flight it is expected, that barometric altimetry will be used for the foreseeable future. Thus, no accuracy requirements are defined for this dimension. Table A.2 summarises the Required Navigational Performance types as of [ICA99]. *Accuracy* denotes here '[...] Navigation performance accuracy 95 % lateral and longitudinal position accuracy in the designated airspace [...]' [ICA99].

Table A.2: Required Navigational Performance types (from [ICA99])

	RNP Type					
	Approach	Other				
	0.1	1	4	10	12.6	20
Accuracy [m]	185.2	1852	7408	18520	23335	37040

A.3 Time frames

Depending on the context different definitions for *strategic* and *tactical* time-frames exist [Bar+06]. Different target audiences interpret the terms differently, e.g. Air Traffic Control Officers may relate the term strategic to the pre-flight planning phase and the term tactical to everything happening after push-back until on-blocks of an aircraft. Pilots usually relate the term tactical to the short-term timeframe which may last up to several minutes while strategic is usually related to the time-frame of several hours, always regarding the *current* flight. Figure A.1 gives an overview on time horizon as envisaged for the U.S. NAS of 2020.

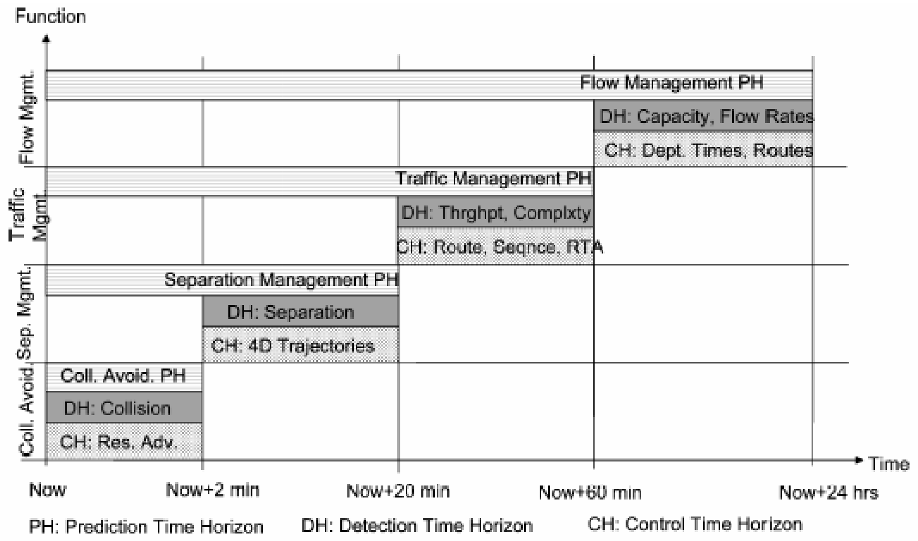

Figure A.1: Time Horizon overview envisaged for the NAS of 2020 (in [Bar+06] from [Sip+05])

Strategic: The term *strategic* is often used synonymously with long-term/mid-term or described as the time span of "several hours".
Tactical: The term *tactical* refers to a time-span of "several seconds up to a few minutes". The term short-term is used synonymously to tactical.

A.4 Vertical Intrusion

The horizontal and vertical intrusions are calculated in respect to the minimum allowed horizontal and vertical distances, $d_{h,min}$ and $d_{v,min}$ respectively. For zones with non-uniform propagation (e.g. Z_{ce}, cf. Subsection 3.2.1) the minimum allowed distance depends on the bearing σ(horizontal) and elevation bearing ϵ(vertical) between ownship and intruder (cf. Figure A.2). Figure A.2(a) depicts an example for the calculation of the minimum allowed distance depending on the bearing σ. Point P_i is the intersection

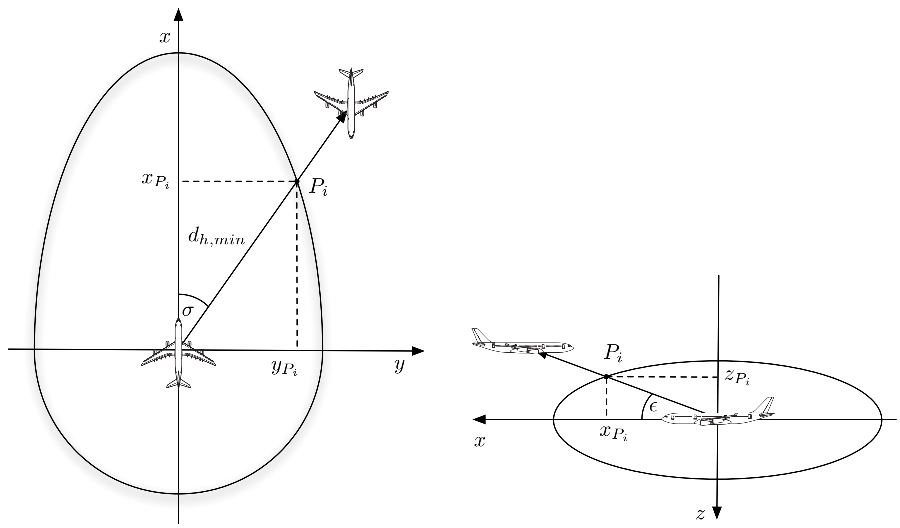

(a) Horizontal distance depending on bearing σ

(b) Vertical distance depending on elevation bearing ϵ

Figure A.2: Illustration of minimum distance calculation

of the bearing vector and the circumference of the PAZ. The calculation of $d_{h,min}$ has been described in Equation 3.6, Subsection 3.2.3. The vertical intrusion is similarly defined as:

$$d_{v,min} = z|(x,z) \in f_Z \wedge (x,z) \in f_\epsilon \wedge \sqrt{x^2+z^2} = max(V) \tag{A.1}$$

$$V = \left\{ d|d = \sqrt{x^2+z^2}, (x,y,z) \in f_Z \wedge (x,z) \in f_\epsilon \right\} \tag{A.2}$$

$$f_\epsilon = \begin{cases} \{(x,0)|x \in \mathbb{R}^+\} & ,\epsilon = 0° \vee \epsilon = 360° \\ \{(x,0)|x \in \mathbb{R}^-\} & ,\epsilon = 180° \\ \{(0,z)|z \in \mathbb{R}^+\} & ,\epsilon = 90° \\ \{(0,z)|z \in \mathbb{R}^-\} & ,\epsilon = 270° \\ \{(x,z)|z = \frac{\sin\epsilon}{\cos\epsilon} \cdot x \wedge x > 0, z < 0\} & ,\sigma > 0° \wedge \sigma < 90° \\ \{(x,z)|z = \frac{\sin\epsilon}{\cos\epsilon} \cdot x \wedge x, z > 0\} & ,\sigma < 360° \wedge \sigma > 270° \\ \{(x,z)|z = \frac{\sin\epsilon}{\cos\epsilon} \cdot x \wedge x < 0, z > 0\} & ,\sigma < 270° \wedge \sigma > 180° \\ \{(x,z)|z = \frac{\sin\epsilon}{\cos\epsilon} \cdot x \wedge x, z < 0\} & ,\sigma < 180° \wedge \sigma > 90° \end{cases} \tag{A.3}$$

Similar to Equation 3.7, the set V (Equation A.2) is the set of all points contained in the intersection of the zone given through f_Z and the line given through f_ϵ. The intersection $P_i = (x_{P_i}, z_{P_i})$ is the point with the maximum distance to the origin (cf. Figure A.2(b)).

A.5 Rotational matrices

For rotational operations three rotational matrices $\mathbf{T}_N$, $\mathbf{T}_E$ and $\mathbf{T}_D$ are used. In the following the three matrices are defined, each of them describing a rotation by angle α.

Rotation around North-Axis

$$\mathbf{T}_N(\alpha) = \begin{pmatrix} 1 & 0 & 0 \\ 0 & \cos(\alpha) & -\sin(\alpha) \\ 0 & \sin(\alpha) & cos(\alpha) \end{pmatrix} \tag{A.4}$$

Rotation around East-Axis

$$\mathbf{T}_E(\alpha) = \begin{pmatrix} \cos(\alpha) & 0 & -\sin(\alpha) \\ 0 & 1 & 0 \\ \sin(\alpha) & 0 & \cos(\alpha) \end{pmatrix} \tag{A.5}$$

Rotation around Down-Axis

$$\mathbf{T}_D(\alpha) = \begin{pmatrix} \cos(\alpha) & \sin(\alpha) & 0 \\ \sin(\alpha) & \cos(\alpha) & 0 \\ 0 & 0 & 1 \end{pmatrix} \tag{A.6}$$

A.6 Polar plots

The heading over the simulation time is illustrated in polar plots. Figure A.3 gives an example of the polar plots used in this work. The simulation time is depicted on the radials of the plot with simulation

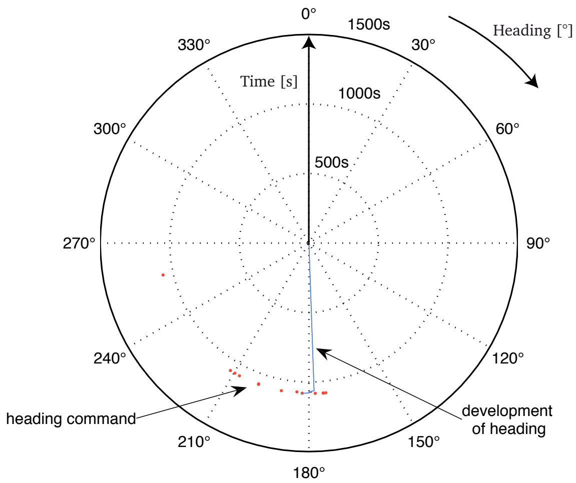

Figure A.3: Polar plot

start time $t = 0$ being the center of the polar plot. The heading at time t is depicted on the circle in a north-up alignment similar to the compass rose.
The development of the aircraft's real heading is illustrated as a line while heading commands at discrete points in time are illustrated as red dots.

A.7 Technology Readiness Level

The Technology Readiness Level (TRL) defines a formalism to describe the different stages of maturity of a technology or a system [Dep05][1]. Depending on the domain, different definitions for the TRL are used which may also vary in the number of levels. Table A.3 gives an example of TRLs from [Man95]. Further

Table A.3: Technology Readiness Level summary from [Man95]

TRL	Summary
1	Basic principles observed and reported
2	Technology concept and/or application formulated
3	Analytical and experimental critical function and/or characteristic proof-of-concept
4	Component and/or breadboard validation in laboratory environment
5	Component and/or breadboard validation in relevant environment
6	System/subsystem model or prototype demonstration in a relevant environment (ground or space)
7	System prototype demonstration in a space environment
8	Actual system completed and *flight qualified* through test and demonstration (ground or space)
9	Actual system *flight proven* through successful mission operations

evolvement of the *Technology Readiness Level* concept include the definition of formal *exit criteria* which are required to be met in order to advance to the next level. An example for this is given with Table A.4 which is a synthesis and summary of Technology Readiness Level descriptions from [KMR03]. This summary was compiled in order to attribute each of the TRLs with human factor relevant components, that were found necessary to consider when designing a system for flight deck crews and Air Traffic Control Officers. Notably, this TRL definition consists of only six levels opposed to the common nine levels.

[1] A good overview and introduction on the Technology Readiness Level is given in [Wik].

Table A.4: Technology Readiness Level exit criteria from [KMR03]

TRL	Title	Criteria
1	Basic Principles Observed/Reported	Initial concept description is provided and is consistent with top-level Concept of Operations; benefits, risks, and research issues are identified.
2	Technology Concept and/or Application Formulated	Research management plan is delivered and FAA Research Management plan is delivered if applicable. Single year benefits assessment showing performance and economic benefits, preliminary safety risk assessment, and preliminary human factors assessment and research plan must be completed.
3	Analytical / Experimental Critical Function or Characteristic Proof-of-Concept	Initial Feasibility report is submitted showing capability is feasible from technical, benefits, safety, and human factors perspectives. Initial analytic or experimental quantification of technical performance metrics shows improvement over baseline.
4	Component and/or Integrated Components Tested in a Laboratory Environment	Research demonstrates capability is feasible from safety, human factors, and development perspectives, and expected benefits outweigh costs based upon human-in-the-loop testing with representative potential users. A FAA baseline Concept of Use for the capability is developed.
5	Components and/or Subsystems Verified in a Relevant Environment	Pre-development prototype is developed and evaluated in a high fidelity environment. This could involve a full mission simulation in a laboratory or a demonstration or test in a field setting. Specifications and design documentation are updated based upon lessons learned in testing. An updated report documents capability feasibility from safety, human factors, and development perspectives and summarises what has been learned to date. R&D organisation continues research on as-built prototype while FAA begins acquisition program baseline definition.
6	System Demonstrated/ Validated in a Relevant Environment	Field evaluations demonstrate technical functionality of prototypes, benefits, and resolution of human factors issues. FAA and research organisation review capability to determine its readiness to transfer to development organisation. An acquisition strategy is required and a development contractor is engaged.

B Minimum separation

Separation minima are defined to allow for the safe and orderly flow of air traffic. Depending on the airspace type and the means available to determine and verify the current position of aircraft different minima are defined.
The following sections summarise the separation minima according to the ICAO *Procedures for Air Navigation Services - Rules of the Air and Air Traffic Services* [ICA96] for the *North Atlantic Organised Track System* (Section B.1) and *Inflight Broadcast Procedure* area over Africa (Section B.2).

B.1 North Atlantic Organised Track System

The Organised Track System is composed of a number of tracks between European and North American airspace. These tracks are setup on a daily basis taking environmental conditions and airspace reservations into account. Since most of the NAT area has no radar coverage, means for procedural separation are applied. Figure B.1 illustrates the North Atlantic OTS.

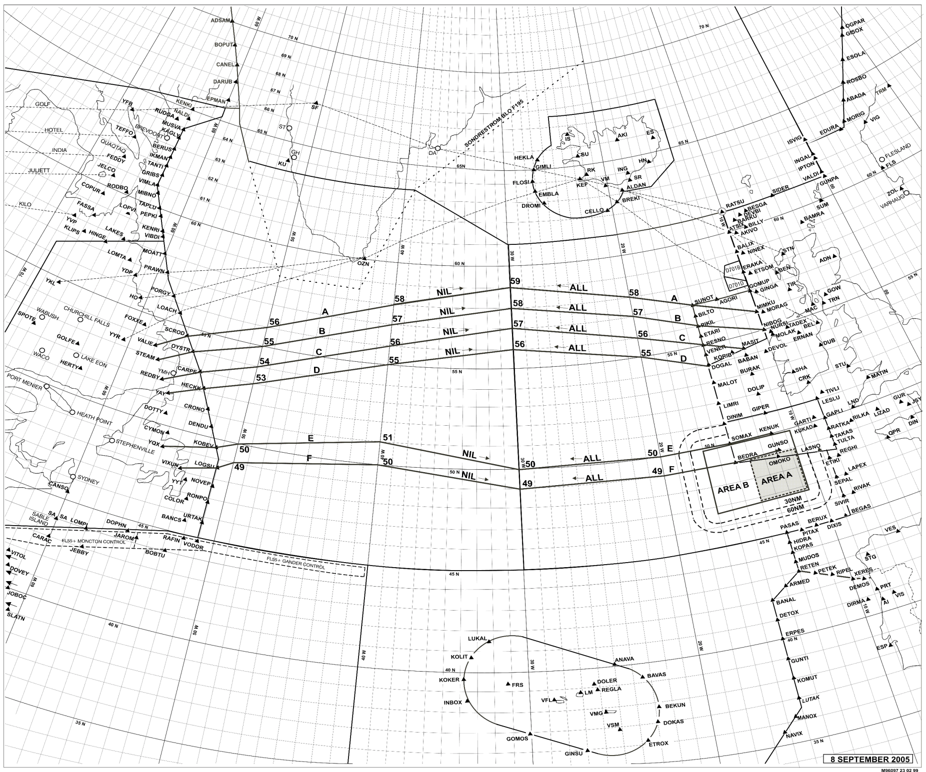

Figure B.1: Example of Organised Track System from [Nor05b]

Longitudinal Separation

Longitudinal separation in NAT airspace is applied in respect to the estimated positions of aircraft. The time interval between two aircraft without lateral separation is between 60 minutes and 5 minutes [Nor05a].

Table B.1: NAT OTS longitudinal separation minima from [Nor05a]

Aircraft Type acr_1	acr_2	minimum Separation [min]	Constraints
moving airspace reservations		60	
non turbojet	other	30	
non turbojet	other	20	WATRS area
turbojet	turbojet	15	
turbojet	turbojet	10	cf. *Requirements - 10 Minutes separation*
turbojet	turbojet	$9-5$	cf. *Requirements - 9-5 Minutes separation*

Requirements - 10 Minutes separation: The following requirements need to be met to apply a minimum separation of 10 minutes between turbojet aircraft in NAT OTS airspace [Nor05a]:
The aircraft must have reported over a common point and follow

- the same track; or
- continuously diverging tracks; or
- continuously diverging tracks until some other form of separation is provided; and
  - at least 10 minutes longitudinal separation exists at the point where the tracks diverge;
  - at least 5 minutes longitudinal separation will exist where 60 NM lateral separation is achieved; and
  - at least the required lateral separation will be achieved at or before the next significant point (normally ten degrees of longitude along track (s)) or, if not, within 90 minutes of the time the second aircraft passes the common point or within 600 NM of the common point, whichever is estimated to occur first.

Requirements - 9-5 Minutes separation: A further reduction on separation requirements can be achieved by applying the Mach number technique. Depending on the Mach number difference between two aircraft, the minimum separation required changes.

Table B.2: Minimum separation when applying Mach number technique in NAT OTS from [Nor05a]

Mach Number Difference	minimum Separation [min]
0.02	9
0.03	8
0.04	7
0.05	6
0.06	5

Table B.2 summarises the minimum separations for two aircraft which need to have either reported over a common point or are known to have passed a common point and are travelling on the same or continuously diverging tracks.

Lateral Separation

The minimum lateral separation for NAT OTS airspace varies between 120 NM or 2° and 30 NM or 1°.

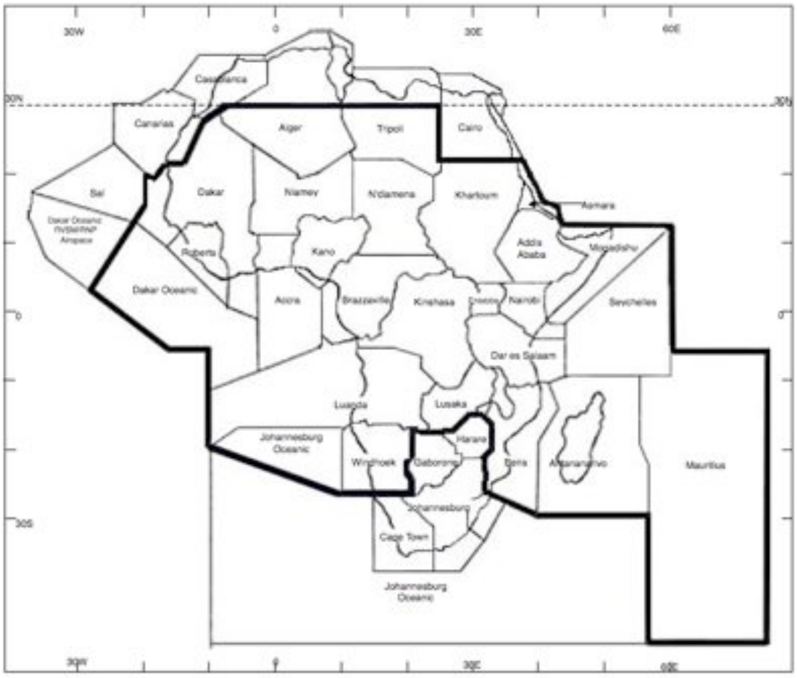

Figure B.2: IFBP area as of October 2002 from [Ifb]

Vertical Separation
Table B.3 summarises the vertical separation minima for the North Atlantic Organised Track System [Nor05a].

Table B.3: NAT OTS vertical separation minima from [Nor05a]

Flight Level from	to	minimum Separation [ft]	Condition
290	above	2000	beween formation flight and other aircraft
290	above	1000	
290	410	1000	between RVSM aircraft
below	290	1000	

B.2 Inflight Broadcast Procedure airspace

The Inflight Broadcast Procedure (IFBP) area covers major parts of the African continent and parts of the Pacific and Atlantic oceanic areas. Figure B.2 illustrates the IFBP area as of October 2002 [Ifb].
To reduce the risk of violation of safe separation, aircrews are required to follow a special procedure when approaching a waypoint in this airspace area. This procedure asks aircrews to communicate ten minutes prior reaching of a waypoint

- their callsign,
- the waypoint approached,
- the current flightlevel,
- the airway they are flying on *and*

- the direction.

The IFBP procedure delegates the separation provision task from ATC to the flight deck crew [Bau+06]. IATA has confirmed in their 2005 safety report that in the enroute phase the '[...] quality of air traffic services is often below global standards.' [Iatb]. Together with ICAO, IATA intends to adress this situation under the Reduced Vertical Separation Minima (RVSM) implementation process. The introduction of RVSM has been found necessary to cope with the constant growth in air traffic in the African airspace [Iatb].
In the following, the longitudinal, lateral and vertical separation minima as defined by ICAO in [ICA07b] for the en-route phase (level flight) will be summarised. Depending on regional implementations, these minima may be different.

Longitudinal Separation
Longitudinal separation based on either *time* or *distance* may be applied. Furthermore, also the Mach number technique as described in Section B.1 may be applied. Table B.4 summarises the separation

Table B.4: Longitudinal separation minima (general rules) from [ICA07b]

Type	minimum Separation	Constraints
Time - Same Track	15 min.	
	10 min.	cf. *Requirements - 10 minutes separation*
	5 min.	cf. *Requirements - 5 minutes separation*
	3 min.	cf. *Requirements - 3 minutes separation*
Time - Crossing Tracks	15 min.	
	10 min.	cf. *Requirements - 10 minutes separation*
Distance - Same Track	20 NM	
	10 NM	leading aircraft is at least 20 kts faster
Distance - Crossing Tracks	20 NM	
	10 NM	leading aircraft is at least 20 kts faster

minima as of [ICA07b] for the en-route phase. These minima are to be applied unless national authorities issue different minima in the respective Aeronautical Information Publications (AIPs). The constraints under which longitudinal separation minima other than 15 minutes are to be applied are summarised below.
Requirements - 10 minutes separation: 10 minutes separation may be applied if '[...] navigation aids permit frequent determination of position and speed [...]'[ICA07b].
Requirements - 5 minutes separation: 5 minutes separation may be applied between aircraft originating from the same aerodrome, en-route aircraft that have reported over the same significant point or when a departing aircraft joins the air route of an en-route aircraft at a fix with at least 5 minutes separation while the preceding aircraft is at least 20 kts faster than the succeeding aircraft.
Requirements - 3 minutes separation: 3 minutes separation may be applied under the same constraints that hold true for five minutes separation only that the preceding aircraft has to be at least 40 kts faster than the succeeding aircraft.

Lateral Separation
Lateral separation can be applied by either guaranteeing that aircraft are over different geographic locations or by '[...] requiring aircraft to fly on specified tracks which are separated by a minimum amount appropriate to the navigation aid or method.'[ICA07b]. Table B.5 summarises the minima depending on the navigation aid, Figure B.3 illustrates this method.

Table B.5: Minimum lateral separation in respect to navigation aid

Navigation aid	minimum radial divergence α	minimum distance to nav aid d
VOR	15°	15 NM
NDB	30°	15 NM
DR	45°	15 NM
RNAV	15°	

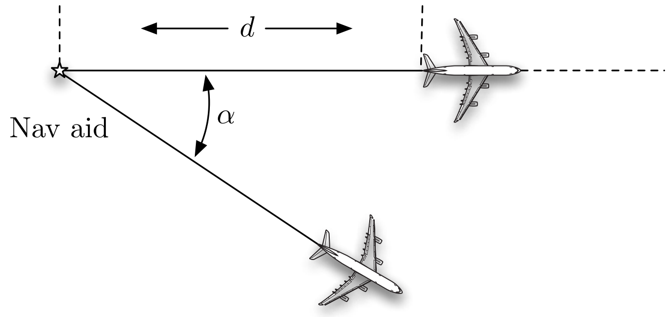

Figure B.3: Minimum distance and radial angle (after [ICA07b])

For RNAV operations also a minimum radial angle of 15° is required. Aircraft are said to be safely lateral separated if the applicable safety zone of one aircraft on its track does not overlap with the other aircraft's safety zone.

Vertical Separation

With Reduced Vertical Separation Minima introduced over the African airspace [Rvs], a minimum separation of 1000 ft between Flight Level 290 and 410 is applied.

C Evaluation Data

Three scenarios have been studied in this work for evaluation of the Cost Index integration into an *Artificial Force Field* Conflict Resolution algorithm. This appendix summarises further results and plots from these three scenarios. For each of the scenarios, the Sections C.1, C.2 and C.3 first summarise further plots from the Protected Airspace Zone comparisons described in Chapter 6 and subsequently list further information on the Cost Index evaluation runs of Chapter 7.

Remarks

Regarding bank, roll rate and pitch rate certain limitations are applied. Maximum bank is limited to 35°, corresponding to the maximum bank angle for civil flights during cruise phase as of BADA [Nui04b]. Roll rate is limited by $3\frac{\circ}{s}$ as of Roth's implementation of the BADA aircraft model [Rot07]. The maximum pitch rate is calculated depending on the aircraft's True Airspeed as of Equation F.6 (Section F.5). Periods during which Conflict Resolution is active are highlighted through a grey background for bank, roll rate, pitch and pitch rate plots. Speed, altitude and heading plots illustrate the aircraft's current speed in blue and the respective commanded value by markers in red.

C.1 Scenario I - IFBP

Scenario I is located over African airspace in the Inflight Broadcast Procedure area (cf. Section B.2). This section summarises in Subsection C.1.1 plots of bank, pitch, their first derivatives, altitude speed and heading for the comparisons made in Subsection 6.2.1. Further results regarding the Closest Point of Approach, intrusion, costs and flyability related measures of the Cost Index evaluation runs of Section 7.2 are summarised in Subsection C.1.2.

C.1.1 Protected Airspace Zone comparison

This subsection summarises the result data from the comparisons of the Protected Airspace Zone implementations for Scenario I. Two zone implementations have been compared with the following parameters:

d_{lon}	10 min
d_{lat}	$2407.6m$
d_{ver}	$304.8m$

Ownship Speed Zone

Using the *Ownship Speed Zone* implementation during Conflict Resolution only one Protected Airspace Zone intrusion was caused. Figure C.1 illustrates the development of bank and roll rate. The maximum bank angle of 35° is not reached while the maximum roll rate of $3\frac{\circ}{s}$ could be achieved. Pitch and pitch rate are illustrated in Figure C.2. The maximum achievable pitch rate as of Equation F.6 is achieved (illustrated in red in Figure C.2(b)). The commanded and achieved speed, heading and altitude are illustrated in Figure C.3. The command values are indicated by red markers while the development of the variables are depicted in blue.

Modified Relative Zone

Using the *Modified Relative Zone* implementation during Conflict Resolution 29 Protected Airspace Zone intrusions were caused. Figure C.4 illustrates the development of bank and roll rate. The maximum bank

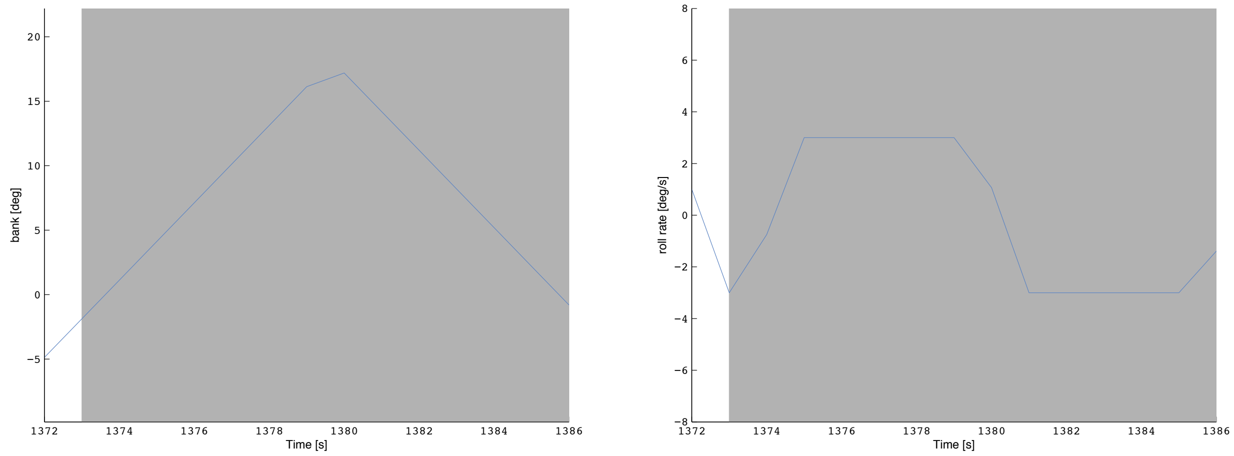

(a) Bank (b) Roll rate

Figure C.1: S1 comparison run - Ownship Speed Zone - Bank and Roll rate

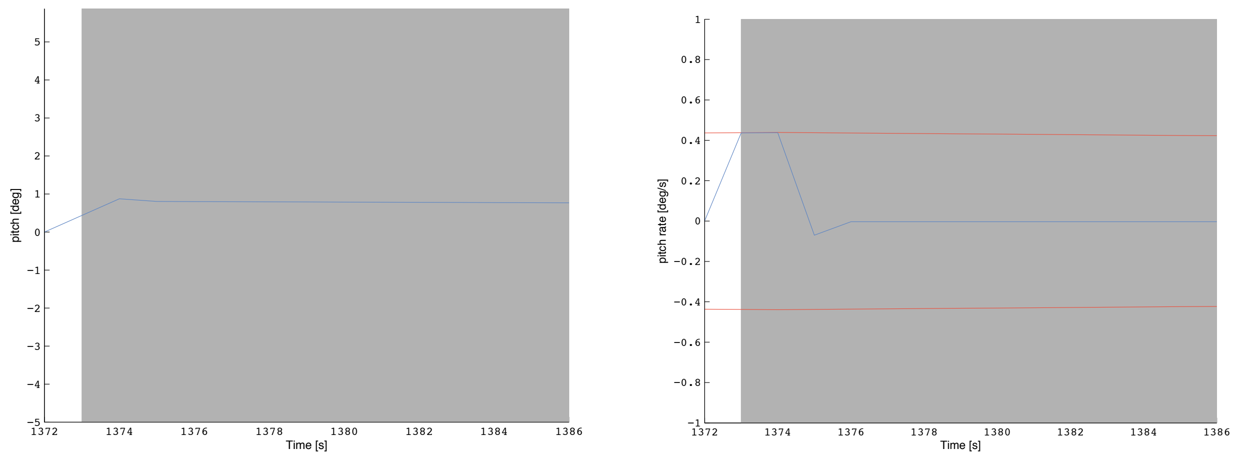

(a) Pitch (b) Pitch rate

Figure C.2: S1 comparison run - Ownship Speed Zone - Pitch and pitch rate

angle of 35° as well as the maximum roll rate of $3\frac{\circ}{s}$ were both achieved during Conflict Resolution due to the flight plan being recaptured when the intruder moved out of ownship's Protected Airspace Zone. Pitch and pitch rate are illustrated in Figure C.5. The maximum achievable pitch rate as of Equation F.6 is achieved (illustrated in red in Figure C.2(b)). The commanded and achieved speed, heading and altitude are illustrated in Figure C.6. The command values are indicated by red markers while the development of the variables are depicted in blue.

C.1.2 Evaluation runs

For evaluating the impact of Cost Index integration in Scenario I the *Modified Relative Zone* has been selected. The distance at the Closest Point of Approach was sufficient and the conflict could be, in contrary to the *Ownship Speed Zone* implementation, solved. This subsection summarises the results of these evaluation runs.

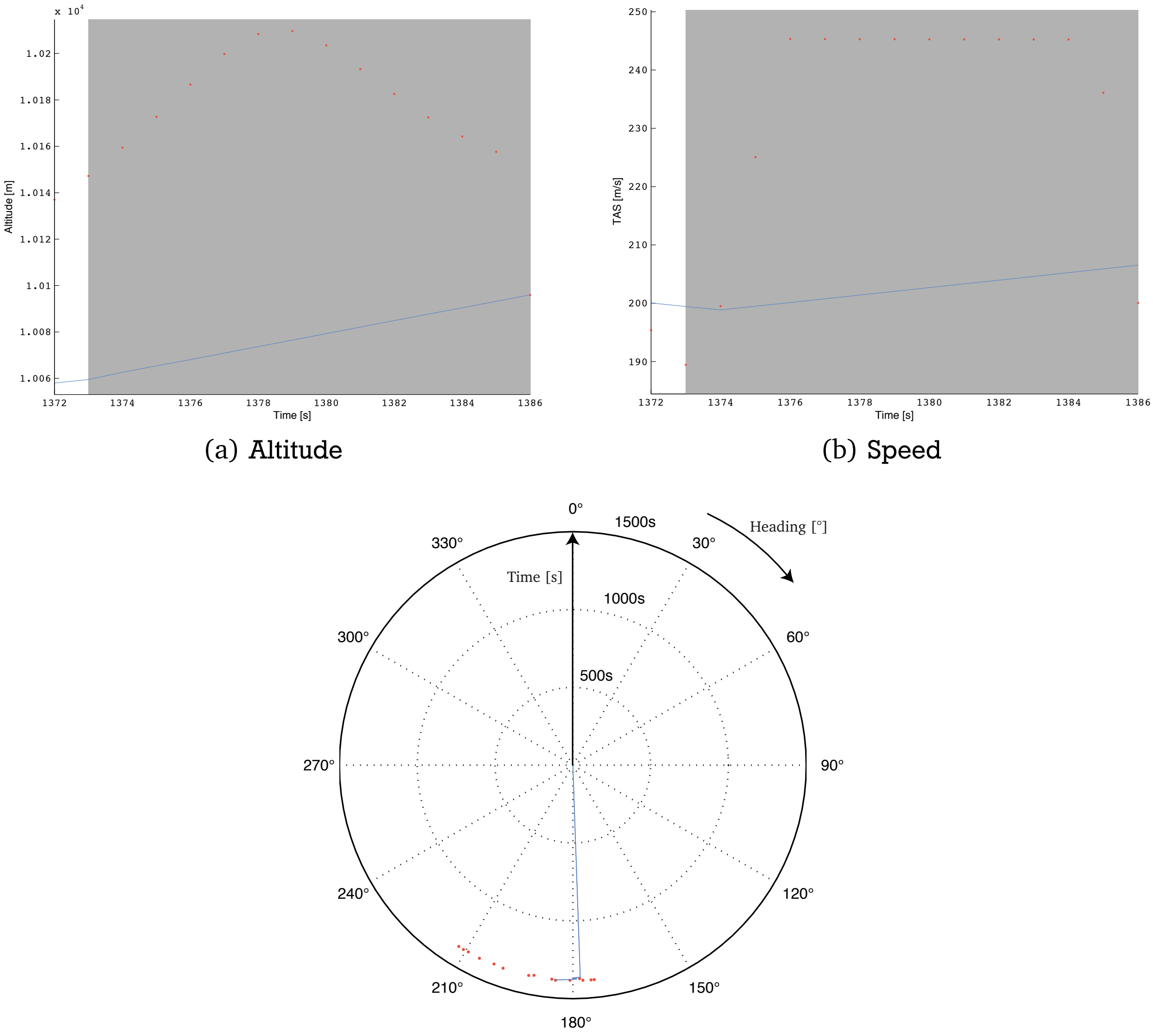

(a) Altitude (b) Speed

(c) Heading

Figure C.3: S1 comparison run - Ownship Speed Zone - Altitude, Speed and Heading development

Distance at Closest Point of Approach and Intrusion

Measures regarding the safety of ownship are summarised in Table C.1. For all runs except of CI = 0 the Collision Avoidance Zone was not infringed during Conflict Resolution. With a Cost Index setting of 0 the conflict could not be resolved.

Horizontal, vertical and temporal areas

The costs of the resolution manoeuvres for the Cost Index evaluation runs are summarised in Table C.2. Except for a Cost Index setting of 0 horizontal deviation shrinked with growing Cost Index. Vertical deviation grew until a Cost Index of 899 and shrinked by $0.63km^2$ with Cost Index of 999. Temporal deviation reduced itself with growing Cost Index except for a CI of 0 where it evaluated to $0s^2$.

Bank, pitch, speeds and altitudes

Maximum bank required during Conflict Resolution was reduced with shrinking lateral deviation from Reference Business Trajectory. Roll rate remained until a Cost Index setting of 799 at the maximum allowed by the aircraft model. Pitch and pitch rate reached 0.67° and $0.54\frac{\circ}{s}$. Table C.3 summarises

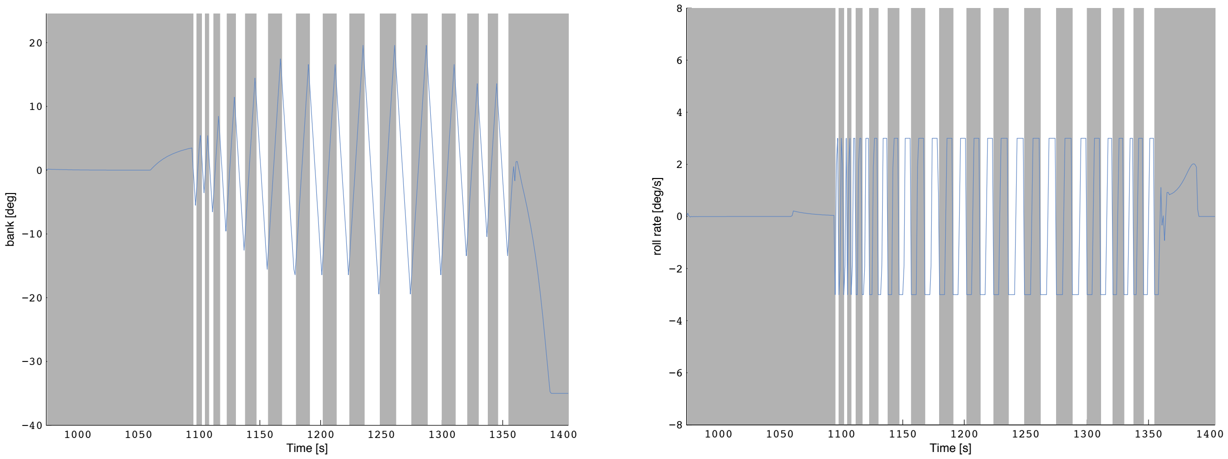

(a) Bank (b) Roll rate

Figure C.4: S1 comparison run - Modified Relative Zone - Bank and roll rate

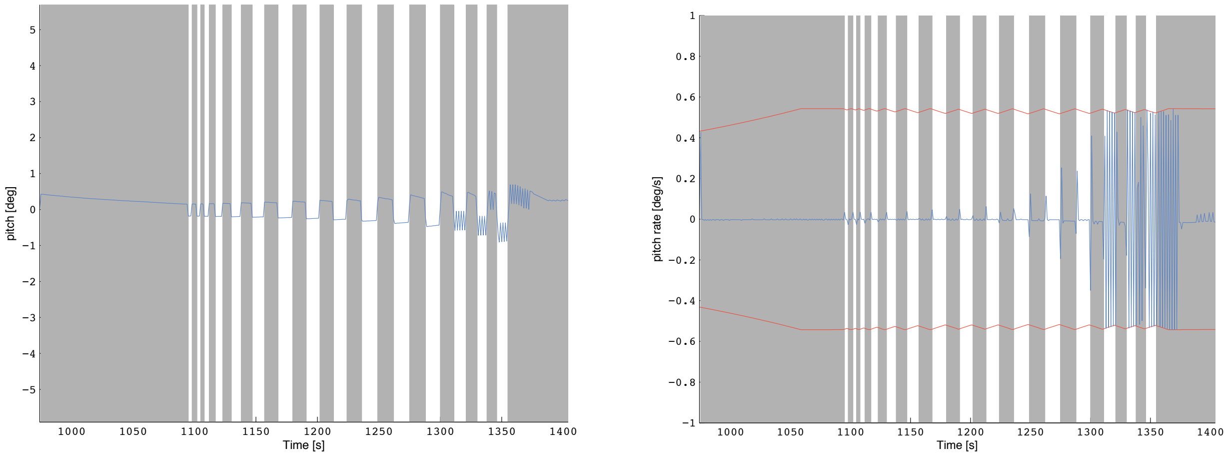

(a) Pitch (b) Pitch rate

Figure C.5: S1 comparison run - Modified Relative Zone - Pitch and pitch rate

the aforementioned variables for the Cost Index integration evaluations. Measures regarding speed and altitude envelope are summarised in Table C.4.

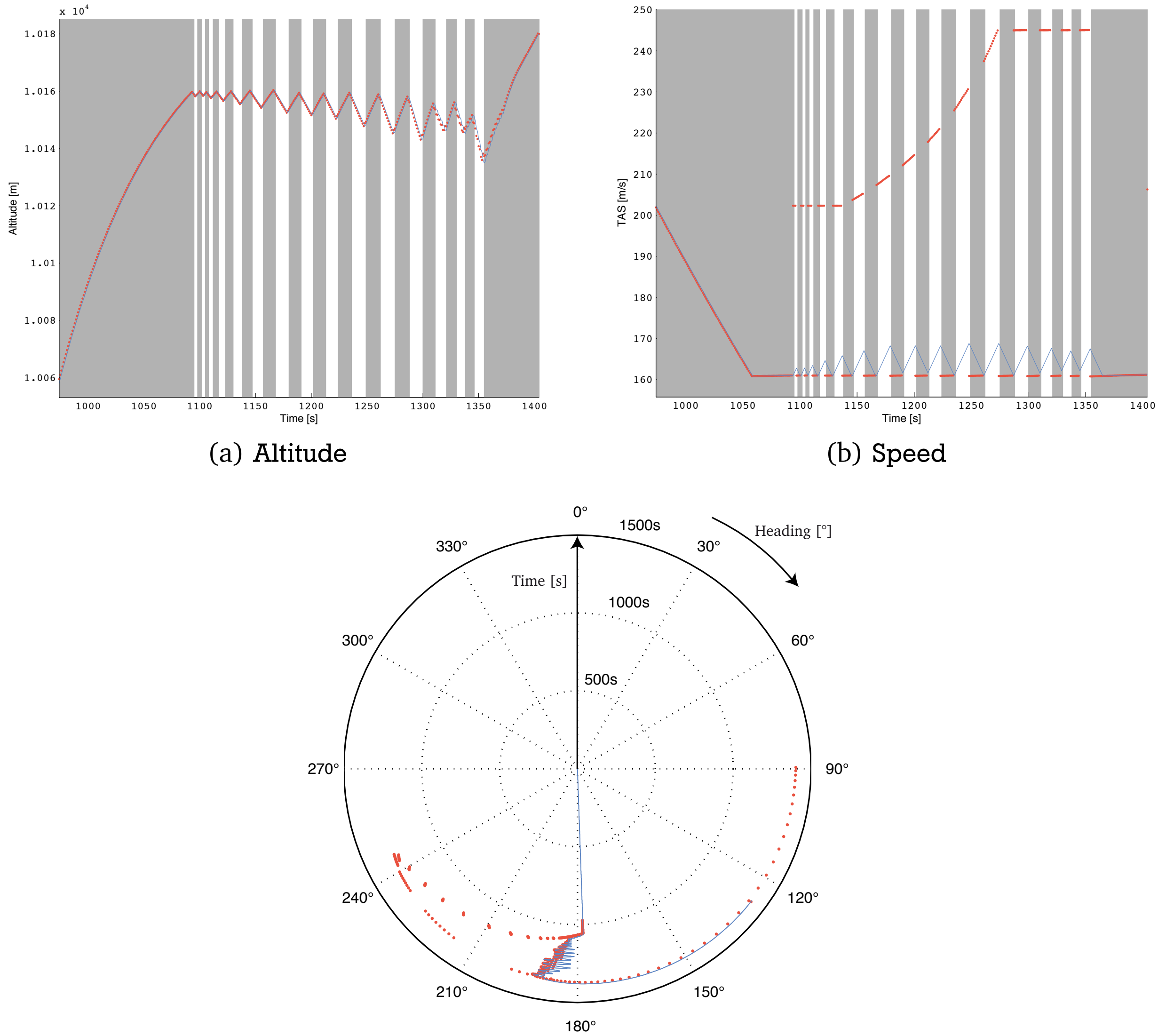

(a) Altitude (b) Speed

(c) Heading

Figure C.6: S1 comparison run - Modified Relative Zone - Altitude, Speed and Heading development

Table C.1: S1 - CI variation - Safety related measures

Cost Index	Distance at CPA Slant [m]	Distance at CPA Horizontal [m]	Distance at CPA Vertical [m]	Intrusion #	Intrusion maximum	Intrusion duration [s]
0	1150.45	1150.45	0.00	31	0.912646	206
99	7806.29	7806.04	−62.12	16	0.908216	301
199	7711.08	7710.52	−92.71	13	0.907037	309
299	7732.59	7731.88	−104.73	22	0.906829	308
399	7578.50	7577.65	−113.91	21	0.911876	317
499	7573.95	7573.04	−117.68	30	0.912478	323
599	7517.15	7516.19	−120.23	25	0.914339	337
699	7622.24	7621.27	−121.27	28	0.915020	361
799	7820.14	7819.20	−121.10	23	0.915686	415
899	8202.52	8201.66	−118.68	1	0.915111	438
999	8904.76	8904.02	−114.36	1	0.911502	441

Table C.2: S1 - CI variation - Cost related measures

Cost Index	$H[km^2]$	$V[km^2]$	$Ti[s^2]$
0	98.81	0.00	0.00
99	218.24	18.77	45694.01
199	209.99	32.12	44522.47
299	200.93	36.86	42802.78
399	200.48	40.28	42625.68
499	197.88	41.92	42604.56
599	192.59	43.03	42735.43
699	180.19	44.12	42502.60
799	153.25	44.73	40078.61
899	82.89	44.96	36734.38
999	9.74	44.33	34808.14

Table C.3: S1 - CI variation - Flyability related measures (1/2)

Cost Index	$\phi[°]$	$\dot{\phi}[\frac{°}{s}]$	$\theta[°]$	$\dot{\theta}[\frac{°}{s}]$
0	20.95	3.00	0.00	0.00
99	35.00	3.00	0.34	0.05
199	35.00	3.00	0.34	0.09
299	32.01	3.00	0.59	0.54
399	28.09	3.00	0.52	0.43
499	23.82	3.00	0.63	0.54
599	19.88	3.00	0.67	0.54
699	15.11	3.00	0.56	0.54
799	10.47	2.51	0.45	0.37
899	5.73	0.32	0.38	0.38
999	0.03	0.01	0.43	0.43

Table C.4: S1 - CI variation - Flyability related measures (2/2)

Cost Index	com. speed $[\frac{m}{s}]$		act. speed $[\frac{m}{s}]$		com. altitude $[m]$		act. altitude $[m]$	
	min	max	min	max	min	max	min	max
0	200.05	245.35	200.05	204.15	10058.00	10058.00	10058.00	10058.00
99	160.21	245.27	160.21	208.47	10058.10	10121.20	10057.40	10121.20
199	160.32	245.22	160.32	208.43	10058.30	10150.30	10057.40	10150.30
299	160.41	245.17	160.41	208.29	10058.50	10165.20	10057.80	10165.20
399	160.50	245.14	160.50	208.27	10058.60	10172.60	10056.20	10172.60
499	160.57	245.11	160.57	208.19	10058.80	10176.90	10055.80	10176.90
599	160.64	245.07	160.64	208.07	10058.90	10179.10	10057.90	10179.10
699	160.70	245.03	160.70	207.90	10059.10	10180.30	10055.40	10180.30
799	160.75	229.54	160.75	207.65	10059.20	10183.20	10056.30	10183.20
899	160.80	207.24	160.80	207.24	10059.40	10186.70	10055.40	10186.70
999	160.84	240.38	160.84	207.10	10059.50	10188.00	10056.00	10188.00

C.2 Scenario II - NAT OTS

Scenario II was located within the North Atlantic Organised Track System (cf. Section B.1). This section summarises in Subsection C.2.1 plots of bank, pitch, their first derivatives, altitude, speed and heading for the comparisons made in Subsection 6.2.2. Further results regarding the Closest Point of Approach, intrusion, costs and flyability related measures of the Cost Index evaluation runs of Section 7.3 are summarised in Subsection C.2.2 and Subsection C.2.3 using the *Ownship Speed Zone* and *Modified Relative Zone*, respectively.

C.2.1 Protected Airspace Zone comparison

This subsection summarises the result data from the comparisons of the Protected Airspace Zone implementations for Scenario II. Two zone implementations have been compared with the following parameters:

d_{lon}	15 min
d_{lat}	$2407.6m$
d_{ver}	$304.8m$

Ownship Speed Zone

Using the *Ownship Speed Zone* implementation four Protected Airspace Zone intrusion were caused during Conflict Resolution. Figure C.7 illustrates the development of bank and roll rate. The maximum bank angle of 35° was not reached while the maximum roll rate of $3\frac{°}{s}$ could be achieved. Pitch and pitch

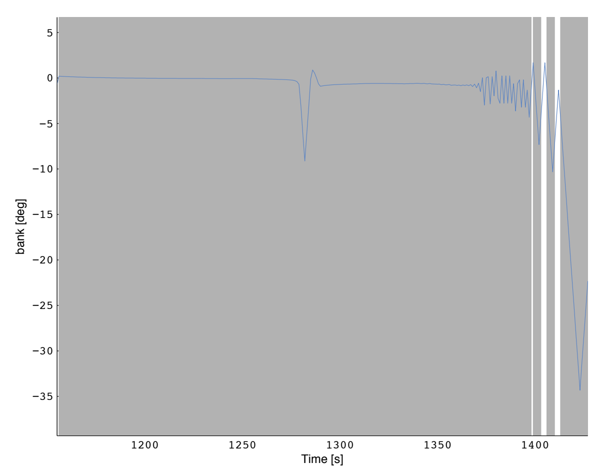

(a) Bank

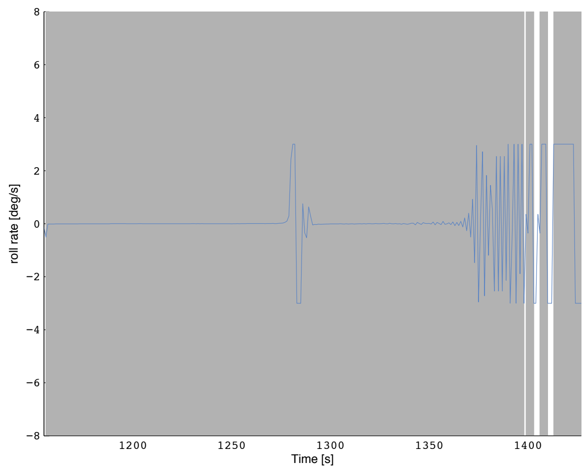

(b) Roll rate

Figure C.7: S2 comparison run - Ownship Speed Zone - Bank and roll rate

rate are illustrated in Figure C.8. The maximum achievable pitch rate as of Equation F.6 is achieved (illustrated in red in Figure C.11(b)). The commanded and achieved speed, heading and altitude are illustrated in Figure C.9.

C.2.2 Evaluation runs – Ownship Speed Zone

Using the *Ownship Speed Zone* implementation the distance at the Closest Point of Approach was not sufficient during the comparison run where the Cost Index was not integrated into the resolution process. Though, since the minimum distance using the *Modified Relative Zone* was significantly larger and the

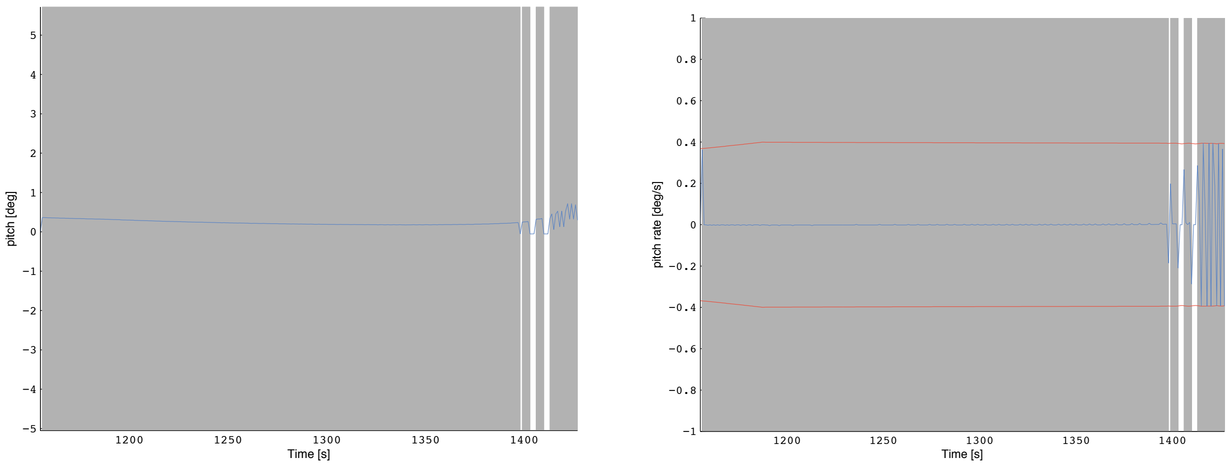

(a) Pitch (b) Pitch rate

Figure C.8: S2 comparison run - Ownship Speed Zone - Pitch and pitch rate

vertical distance was only violated by about 13% both zone implementations were used for evaluating the impact of the Cost Index integration. This subsection details the results of the evaluation runs of Section 7.3 using the *Ownship Speed Zone* implementation further.

Distance at Closest Point of Approach and Intrusion

Measures regarding the safety of ownship are summarised in Table C.5. Neither the required minimum horizontal distance of $2407.6m$, nor the required minimum vertical distance of $304.8m$ could be achieved using *Ownship Speed Zone* implementation.

Table C.5: S2 - CI variation - Safety related measures using Ownship Speed Zone implementation

	Distance at CPA			Intrusion		
Cost Index	Slant $[m]$	Horizontal $[m]$	Vertical $[m]$	#	maximum	duration $[s]$
0	2192.56	2192.56	0.00	5	0.975698	250
99	2170.59	2168.11	−103.74	5	0.975496	269
199	2148.58	2144.14	−138.11	5	0.979818	260
299	2184.71	2177.93	−171.94	5	0.980015	262
399	2174.75	2166.23	−192.30	5	0.982225	261
499	2191.61	2181.34	−211.84	5	0.965931	264
599	2161.21	2149.72	−222.51	3	0.971414	267
699	2156.80	2144.43	−230.60	4	0.972485	265
799	2146.22	2133.14	−236.61	6	0.973742	262
899	2049.15	2034.40	−245.42	3	0.979326	267
999	305.07	162.49	−258.20	1	0.981931	276

Horizontal, vertical and temporal areas

The costs of the resolution manoeuvres for the Cost Index evaluation runs are summarised in Table C.6. Horizontal deviation varied between $20.56km^2$ and $97.88km^2$. Vertical deviation grew with rising Cost Index setting while temporal deviation remained – except for a Cost Index setting of 0 – in the same magnitude.

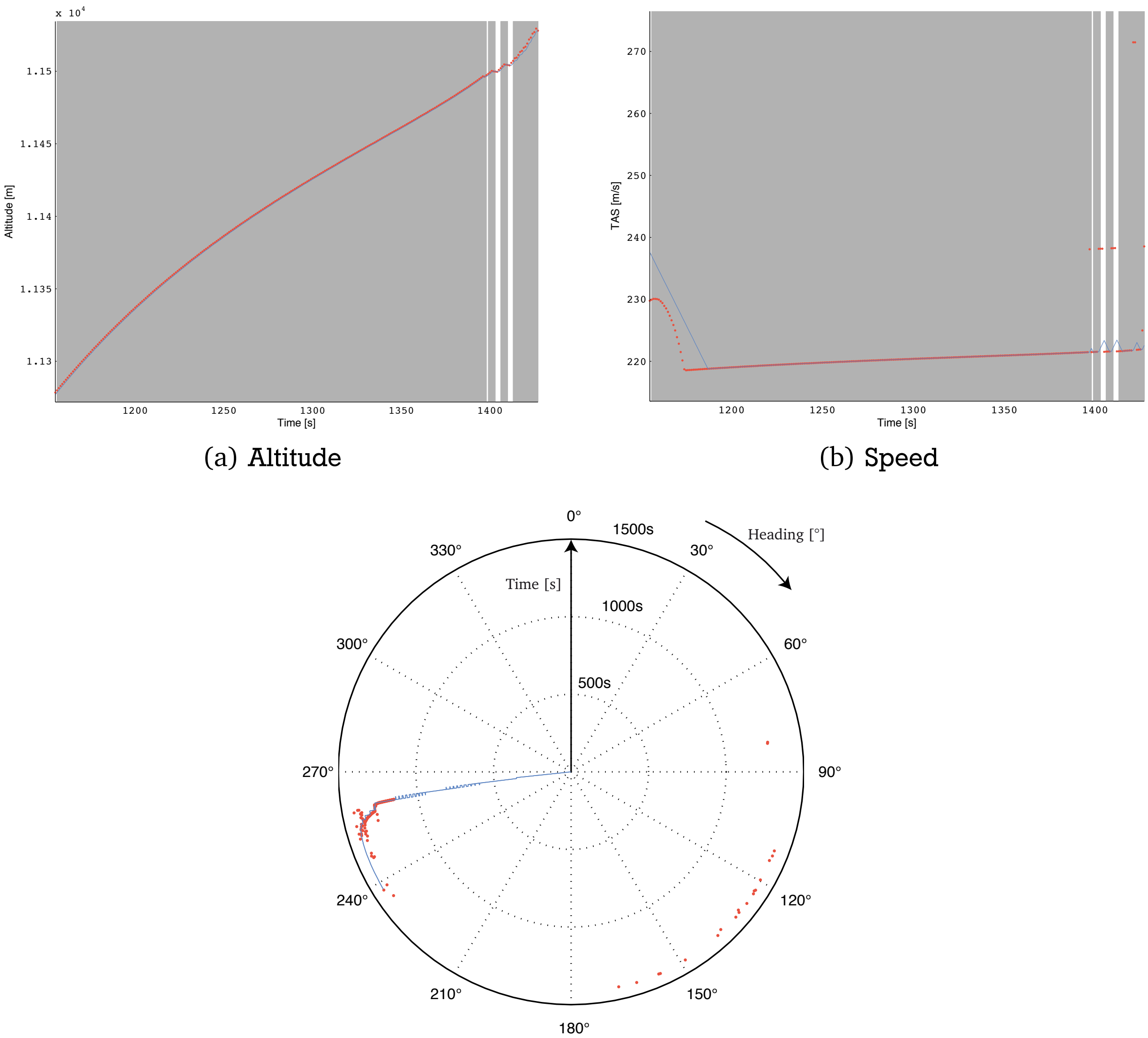

(a) Altitude

(b) Speed

(c) Heading

Figure C.9: S2 comparison run - Ownship Speed Zone - Altitude, Speed and Heading devlopment

Bank, pitch, speeds and altitudes

Maximum bank required during Conflict Resolution stayed below 31.31°. Roll rate remained until a Cost Index setting of 999 at the maximum allowed by the aircraft model. Pitch and pitch rate reached 0.86° and $0.40\frac{°}{s}$. Table C.8 summarises the aforementioned variables for the Cost Index integration evaluations. Measures regarding speed and altitude envelope are summarised in Table C.8.

Modified Relative Zone

Using the *Modified Relative Zone* implementation during Conflict Resolution five Protected Airspace Zone intrusions were caused. Figure C.10 illustrates the development of bank and roll rate. The maximum bank angle of 35° as well as the maximum roll rate of $3\frac{°}{s}$ were both achieved during Conflict Resolution due to the flight plan being recaptured when the intruder moved out of ownship's Protected Airspace Zone.

Pitch and pitch rate are illustrated in Figure C.11. The maximum achievable pitch rate as of Equation F.6 is achieved (illustrated in red in Figure C.11(b)). The commanded and achieved speed, heading and

Table C.6: S2 - CI variation using Ownship Speed Zone implementation

Cost Index	$H[km^2]$	$V[km^2]$	$Ti[s^2]$
0	92.40	0.00	0.00
99	89.88	5.37	68240.26
199	83.66	7.62	66850.85
299	91.48	10.45	66459.70
399	93.39	12.27	65768.37
499	97.88	15.06	65730.69
599	79.72	18.39	65118.76
699	85.59	20.29	65034.74
799	53.37	21.52	64862.88
899	57.79	24.39	64287.57
999	20.56	28.32	64595.47

Table C.7: S2 - Flyability related measures using Ownship Speed Zone implementation (1/2)

Cost Index	$\phi[°]$	$\dot{\phi}[\frac{°}{s}]$	$\theta[°]$	$\dot{\theta}[\frac{°}{s}]$
0	29.41	3.00	0.00	0.00
99	26.54	3.00	0.86	0.40
199	20.50	3.00	0.76	0.40
299	26.12	3.00	0.75	0.40
399	27.99	3.00	0.72	0.40
499	31.31	3.00	0.84	0.40
599	19.20	3.00	0.73	0.39
699	20.95	3.00	0.83	0.39
799	15.66	3.00	0.66	0.39
899	12.28	3.00	0.69	0.39
999	0.70	0.51	0.83	0.39

altitude are illustrated in Figure C.12. The command values are indicated by red markers while the development of the variables are depicted in blue.

C.2.3 Evaluation runs – Modified Relative Zone

Using the *Modified Relative Zone* implementation the conflict set up in Scenario II could be solved and has also been used for evaluation of the Cost Index integration into the Conflict Resolution process. This subsection summarises the results of these evaluation runs described Section 7.3.

Distance at Closest Point of Approach and Intrusion
Measures regarding the safety of ownship are summarised in Table C.9. For all runs except for CI = 999 the Collision Avoidance Zone was not infringed during Conflict Resolution. With a Cost Index setting of 999 the conflict could not be resolved.

Horizontal, vertical and temporal areas
The costs of the resolution manoeuvres for the Cost Index evaluation runs are summarised in Table C.10. Horizontal deviation varied between $21.29km^2$ and $1084.05km^2$. Vertical deviation grew with rising Cost

Table C.8: S2 - Flyability related measures using Ownship Speed Zone implementation (2/2)

Cost Index	com. speed $[\frac{m}{s}]$ min	com. speed $[\frac{m}{s}]$ max	act. speed $[\frac{m}{s}]$ min	act. speed $[\frac{m}{s}]$ max	com. altitude $[m]$ min	com. altitude $[m]$ max	act. altitude $[m]$ min	act. altitude $[m]$ max
0	237.63	237.63	237.63	237.63	11277.00	11277.00	11277.00	11277.00
99	218.20	271.46	218.21	258.33	11277.10	11389.00	11276.70	11387.90
199	218.25	271.46	218.27	258.05	11277.30	11423.80	11277.00	11421.00
299	218.31	271.46	218.34	258.22	11277.40	11457.50	11277.00	11454.70
399	218.35	271.46	218.41	258.23	11277.60	11477.30	11277.00	11474.60
499	218.38	271.46	218.48	258.27	11277.70	11497.00	11277.00	11495.70
599	218.42	271.46	218.54	257.84	11277.90	11507.70	11277.00	11507.90
699	218.45	271.46	218.60	257.87	11278.10	11515.20	11277.00	11514.20
799	218.49	271.46	218.67	257.78	11278.20	11519.90	11277.00	11518.30
899	218.52	271.46	218.73	257.57	11278.40	11530.50	11277.00	11529.30
999	218.56	271.46	218.78	257.31	11278.50	11545.90	11277.00	11545.90

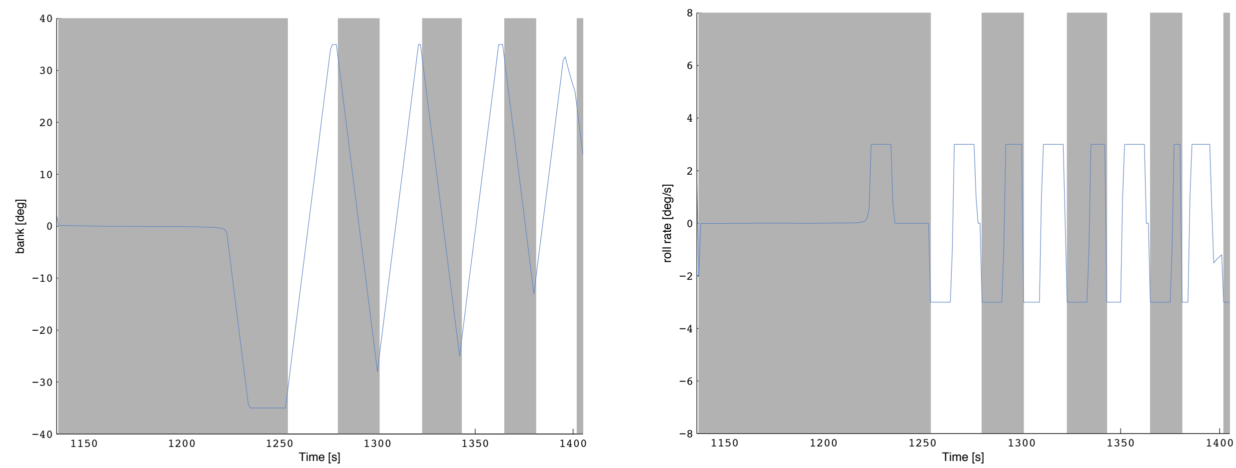

(a) Bank (b) Roll rate

Figure C.10: S2 comparison run - Modified Relative Zone - Bank and roll rate

Index setting while temporal deviation remained – except for a Cost Index setting of 0 – in the same magnitude.

Bank, pitch, speeds and altitudes

Maximum bank required during Conflict Resolution reached the maximum allowed value of 35° for Cost Index settings 0 to 699. Roll rate remained until a Cost Index setting of 999 at the maximum allowed by the aircraft model. Pitch and pitch rate reached 0.83° and $0.39\frac{°}{s}$. Table C.12 summarises the aforementioned variables for the Cost Index integration evaluations. Measures regarding speed and altitude envelope are summarised in Table C.12.

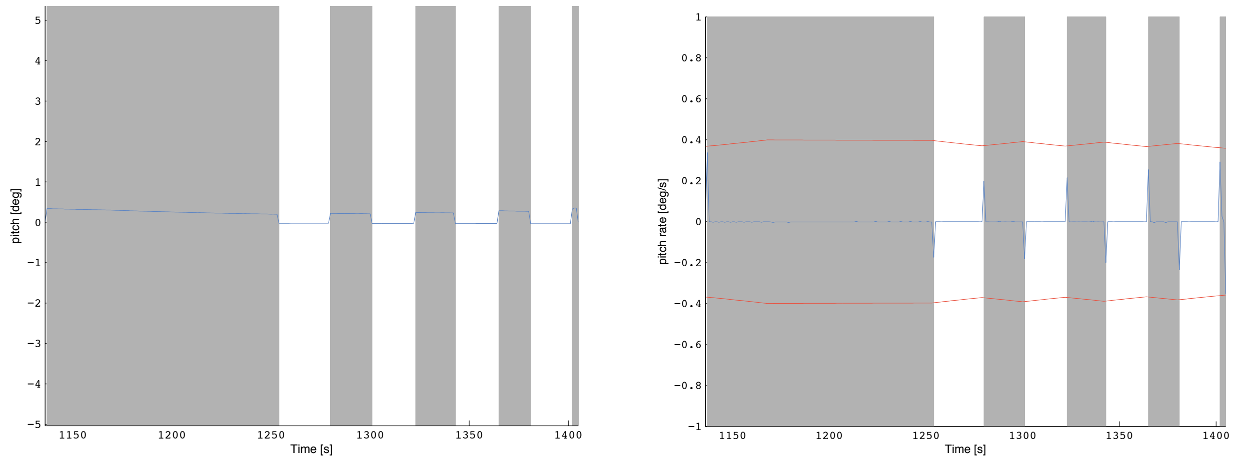

(a) Pitch (b) Pitch rate

Figure C.11: S2 comparison run - Modified Relative Zone - Pitch and pitch rate

Table C.9: S2 - CI variation - Safety related measures using Modified Relative Zone implementation

Cost Index	Distance at CPA Slant $[m]$	Horizontal $[m]$	Vertical $[m]$	#	Intrusion maximum	duration $[s]$
0	16591.10	16591.10	0.00	5	0.886000	170
99	15333.60	15333.60	−37.05	5	0.897323	179
199	15357.10	15356.90	−65.55	5	0.897576	179
299	15304.50	15304.20	−86.65	5	0.896331	178
399	15312.60	15312.30	−104.56	5	0.898352	178
499	15321.80	15321.30	−121.34	5	0.896911	180
599	15340.00	15339.40	−138.20	5	0.888943	186
699	14708.70	14707.90	−154.82	11	0.899341	198
799	13248.30	13247.10	−180.25	7	0.907134	238
899	8838.57	8836.17	−205.88	1	0.916330	262
999	262.06	38.29	−259.25	1	0.999811	296

Table C.10: S2 - CI variation using Modified Relative Zone implementation

Cost Index	$H[km^2]$	$V[km^2]$	$Ti[s^2]$
0	1084.05	0.00	30414.53
99	946.74	7.15	57244.01
199	946.35	12.67	56732.89
299	940.23	16.86	56330.64
399	933.67	20.44	55875.53
499	936.20	23.75	55981.03
599	924.32	27.01	58149.51
699	888.22	30.28	62167.62
799	782.08	35.07	63563.92
899	379.71	39.10	63812.32
999	21.29	48.68	66634.25

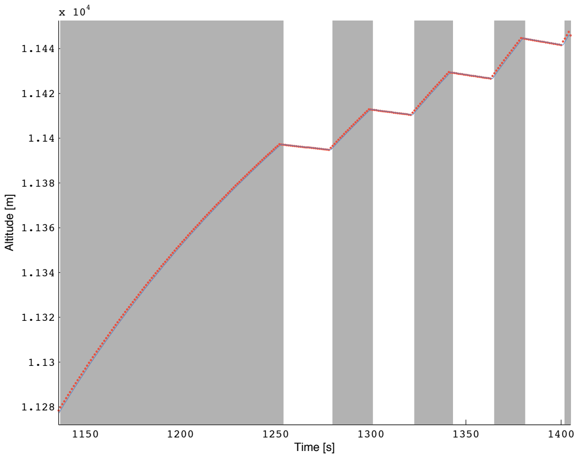

(a) Altitude

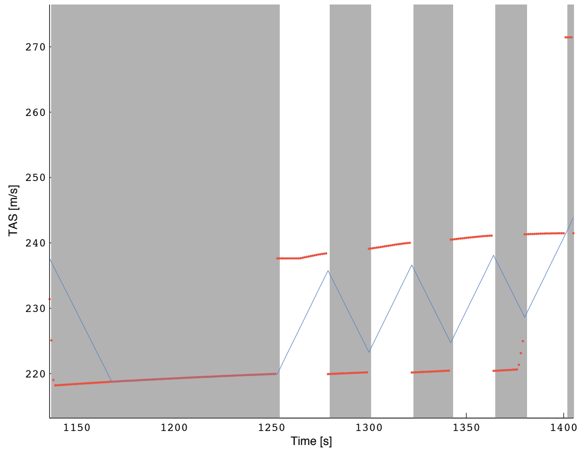

(b) Speed

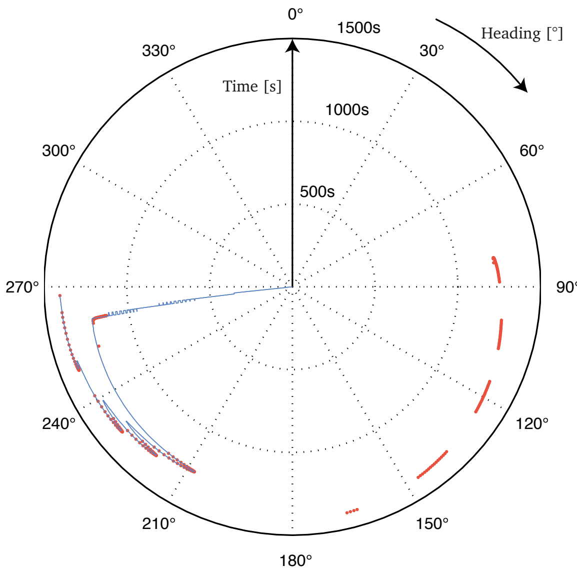

(c) Heading

Figure C.12: S2 comparison run - Modified Relative Zone - Altitude, Speed and Heading development

Table C.11: S2 - Flyability related measures using Modified Relative Zone implementation (1/2)

Cost Index	$\phi\,[^\circ]$	$\dot{\phi}\,[\frac{\circ}{s}]$	$\theta\,[^\circ]$	$\dot{\theta}\,[\frac{\circ}{s}]$
0	35.00	3.00	0.00	0.00
99	35.00	3.00	0.15	0.14
199	35.00	3.00	0.24	0.22
299	35.00	3.00	0.29	0.27
399	35.00	3.00	0.33	0.30
499	35.00	3.00	0.33	0.31
599	35.00	3.00	0.31	0.28
699	35.00	3.00	0.32	0.28
799	31.52	3.00	0.27	0.27
899	15.85	3.00	0.30	0.30
999	2.19	2.03	0.83	0.39

Table C.12: S2 - Flyability related measures using Modified Relative Zone implementation (2/2)

Cost Index	com. speed $[\frac{m}{s}]$ min	com. speed $[\frac{m}{s}]$ max	act. speed $[\frac{m}{s}]$ min	act. speed $[\frac{m}{s}]$ max	com. altitude $[m]$ min	com. altitude $[m]$ max	act. altitude $[m]$ min	act. altitude $[m]$ max
0	237.63	271.46	237.63	261.85	11277.00	11277.00	11277.00	11277.00
99	218.17	271.46	218.19	263.54	11277.10	11315.30	11277.00	11315.30
199	218.18	271.46	218.26	263.48	11277.30	11344.70	11277.00	11344.70
299	218.19	271.46	218.33	263.47	11277.40	11366.60	11277.00	11366.60
399	218.19	271.46	218.39	263.45	11277.60	11385.00	11276.90	11385.00
499	218.19	271.46	218.45	263.44	11277.70	11402.50	11276.80	11402.50
599	218.19	271.46	218.51	263.37	11277.80	11420.50	11276.90	11420.50
699	218.19	271.46	218.57	263.41	11278.00	11436.90	11277.00	11436.90
799	218.18	271.46	218.63	262.31	11278.10	11462.70	11277.00	11462.70
899	218.18	271.46	218.69	259.68	11278.30	11489.10	11277.00	11489.10
999	218.19	271.46	218.74	257.55	11278.40	11546.10	11277.00	11546.10

C.3 Scenario III - IFBP

Scenario III is like Scenario I located over African airspace in the Inflight Broadcast Procedure area (cf. Section B.2). This section summarises in Subsection C.3.1 plots of bank, pitch, their first derivatives, altitude, speed and heading for the comparisons made in Subsection 6.2.3. Further results regarding the Closest Point of Approach, intrusion, costs and flyability related measures of the Cost Index evaluation runs of Section 7.4 are summarised in Subsection C.3.2.

C.3.1 Protected Airspace Zone comparison

This subsection summarises the result data from the comparisons of the Protected Airspace Zone implementations for Scenario III. Two zone implementations have been compared with the following parameters:

d_{lon}	10 min
d_{lat}	2407.6m
d_{ver}	304.8m

Ownship Speed Zone
Using the *Ownship Speed Zone* implementation during Conflict Resolution two Protected Airspace Zone intrusions were caused by intruder $acr_{i,0}$ and one by intruder $acr_{i,1}$. Figure C.13 illustrates the development of bank and roll rate. The maximum bank angle of 35° is not reached while the maximum roll rate of $3\frac{°}{s}$ could be achieved. Pitch and pitch rate are illustrated in Figure C.14. The maximum achievable

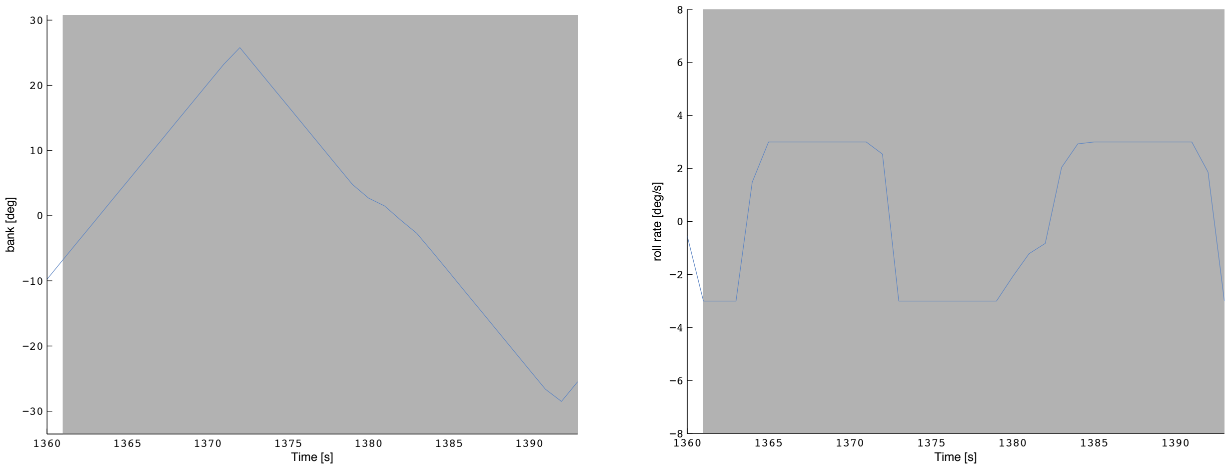

(a) Bank (b) Roll rate

Figure C.13: S3 comparison run - Ownship Speed Zone - Bank and roll rate

pitch rate as of Equation F.6 is achieved (illustrated in red in Figure C.14(b)). The commanded and achieved speed, heading and altitude are illustrated in Figure C.15.

Modified Relative Zone
Using the *Modified Relative Zone* implementation two Protected Airspace Zone intrusions were caused by $acr_{i,0}$ and 42 by $acr_{i,1}$ during Conflict Resolution. Figure C.16 illustrates the development of bank and roll rate. The maximum bank angle of 35° as well as the maximum roll rate of $3\frac{°}{s}$ were both achieved during Conflict Resolution due to the flight plan being recaptured when one of the intruder moved out of ownship's Protected Airspace Zone. Pitch and pitch rate are illustrated in Figure C.17. The maximum

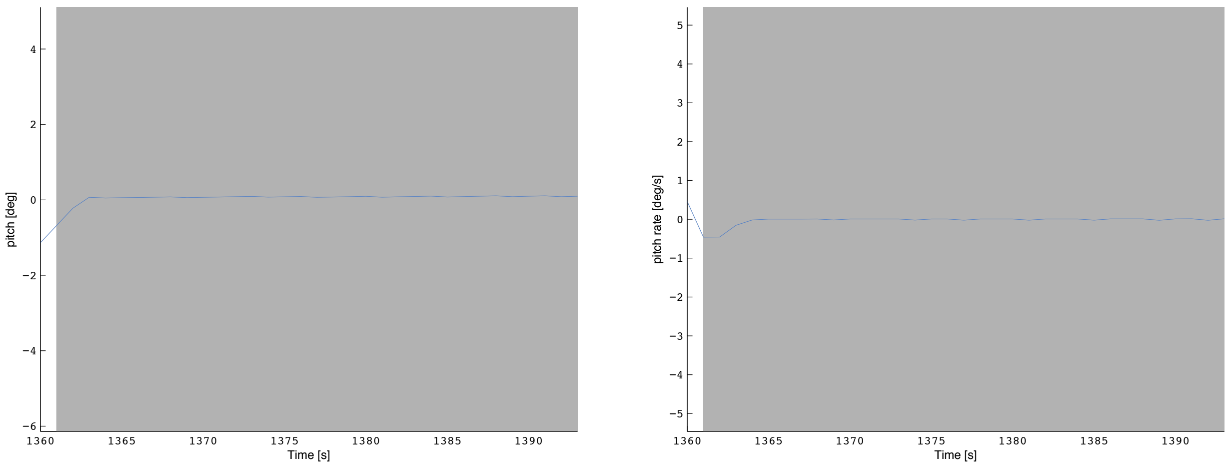

(a) Pitch (b) Pitch rate

Figure C.14: S3 comparison run - Ownship Speed Zone - Pitch and pitch rate

achievable pitch rate as of Equation F.6 is achieved (illustrated in red in Figure C.17(b)). The commanded and achieved speed, heading and altitude are illustrated in Figure C.18.

C.3.2 Evaluation runs

For evaluating the impact of Cost Index integration in Scenario III the *Modified Relative Zone* has been selected. The distances at the CPA between ownship and both intruders were sufficient and the conflicts could be – in contrary to the *Ownship Speed Zone* implementation – solved. This subsection summarises the results of these evaluation runs.

Distance at Closest Point of Approach and Intrusion
Measures regarding the safety of ownship are summarised in Table C.13 (intruder $acr_{i,0}$) and Table C.14 (intruder $acr_{i,1}$). The conflict with intruder $acr_{i,0}$ could not be resolved with Cost Index settings of 299, 499 and 599. Regarding the second conflict with the intruder $acr_{i,1}$ flying towards ownship on the same

Table C.13: S3 - CI variation - Safety related measures using Modified Relative Zone implementation - $acr_{i,0}$

	Distance at CPA			Intrusion		
Cost Index	Slant $[m]$	Horizontal $[m]$	Vertical $[m]$	#	maximum	duration $[s]$
0	13196.20	13196.20	0.00	40	0.908312	178
99	4982.16	4978.34	−195.13	55	0.944761	304
199	5007.08	5001.56	−235.19	25	0.944717	304
299	894.92	852.14	−273.41	34	0.991804	316
399	5111.87	5105.93	−246.22	37	0.942370	309
499	948.82	902.23	−293.69	40	0.991208	333
599	1002.20	957.55	−295.84	39	0.990637	332
699	4937.27	4931.03	−248.13	29	0.945864	324
799	4323.10	4315.95	−248.66	23	0.956236	345
899	2439.20	2426.21	−251.43	30	0.981304	399
999	4864.71	4856.89	−275.71	1	0.966630	427

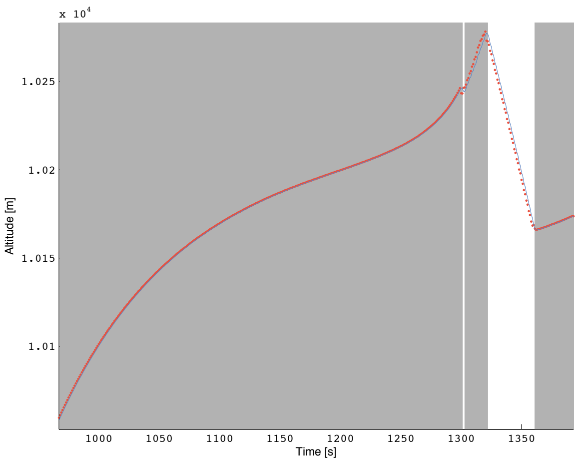

(a) Altitude

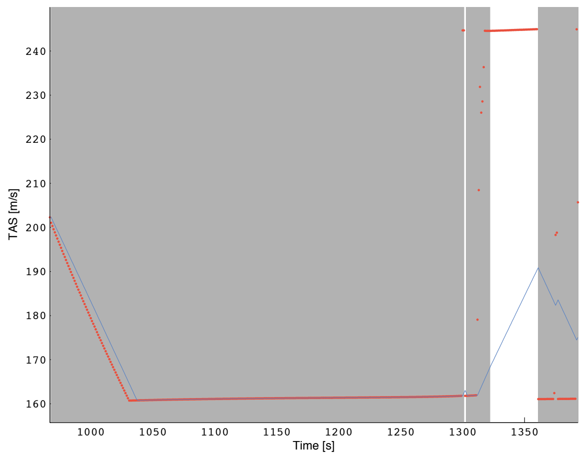

(b) Speed

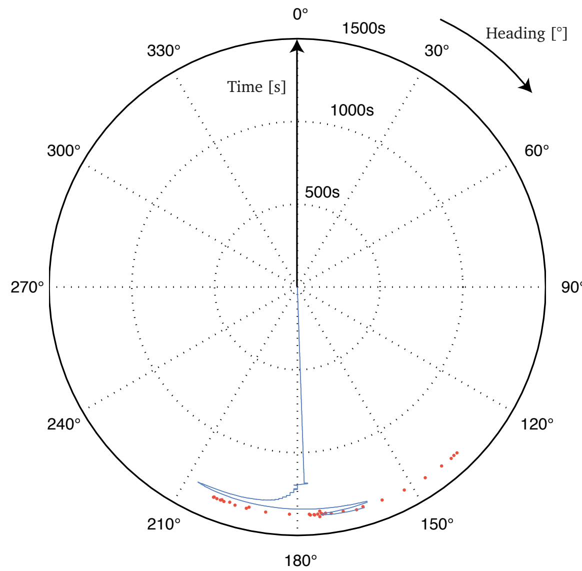

(c) Heading

Figure C.15: S3 comparison run - Ownship Speed Zone - Altitude, Speed and Heading development

track and Flight Level the conflict could be resolved with all Cost Index settings except 999. Table C.14 summarises the results.

Horizontal, vertical and temporal areas

The costs of the resolution manoeuvres for the Cost Index evaluation runs are summarised in Table C.15. Horizontal deviations were between $27.29km^2$ and $925.67km^2$, vertical deviations between $0km^2$ and $39.45km^2$ and temporal deviations between $12845.56s^2$ and $79646.58s^2$.

Bank, pitch, speeds and altitudes

Maximum bank required during Conflict Resolution was above 15° for all runs except for CI = 999. Roll rate remained until a Cost Index setting of 999 at the maximum allowed rate by the aircraft model. Pitch and pitch rate reached 0.90° and $0.54\frac{°}{s}$. Table C.16 summarises the aforementioned variables for the Cost Index integration evaluations. Measures regarding speed and altitude envelope are summarised in Table C.17.

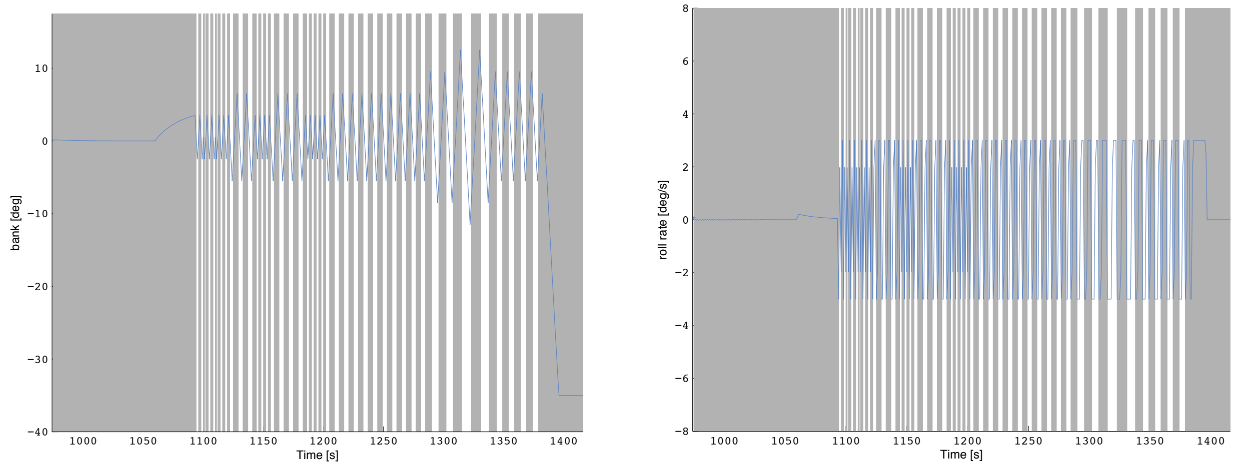

(a) Bank (b) Roll rate

Figure C.16: S3 comparison run - Modified Relative Zone - Bank and roll rate

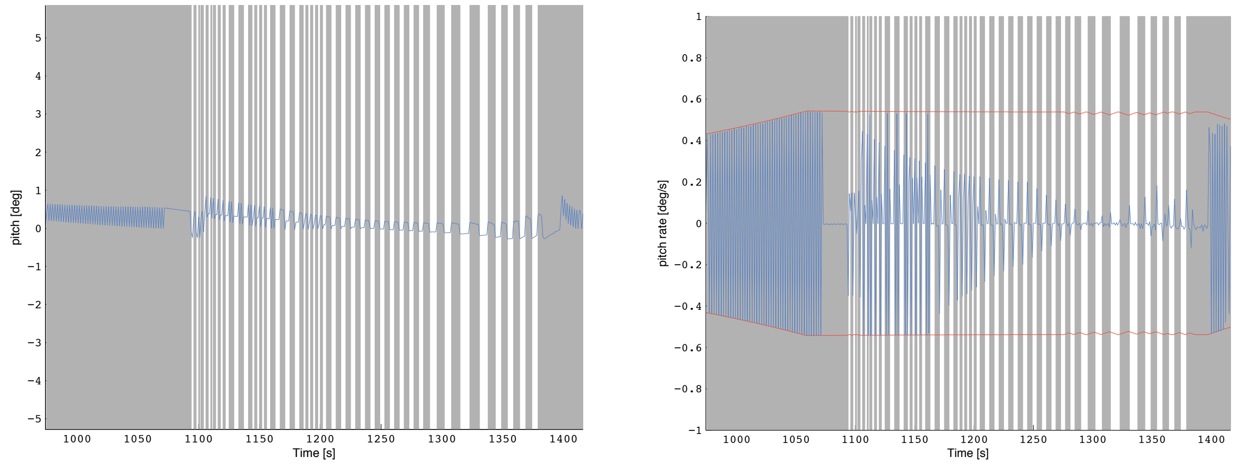

(a) Pitch (b) Pitch rate

Figure C.17: S3 comparison run - Modified Relative Zone - Pitch and pitch rate

Table C.14: S3 - CI variation - Safety related measures using Modified Relative Zone implementation - $acr_{i,1}$

Cost Index	Distance at CPA Slant $[m]$	Horizontal $[m]$	Vertical $[m]$	Intrusion #	maximum	duration $[s]$
0	7939.79	7939.79	0.00	3	0.918997	249
99	6040.72	6037.58	−194.62	2	0.914260	288
199	6030.58	6026.01	−234.58	2	0.915544	285
299	9175.85	9172.54	−246.39	1	0.858938	277
399	5777.85	5772.64	−245.37	3	0.929314	286
499	9131.86	9128.21	−258.23	1	0.855820	277
599	9117.96	9114.23	−260.86	1	0.853352	276
699	5971.93	5966.79	−247.71	2	0.916092	285
799	5780.41	5775.06	−248.66	2	0.925701	288
899	4185.92	4178.43	−250.20	1	0.959014	291
999	274.18	24.26	−273.11	1	0.997358	303

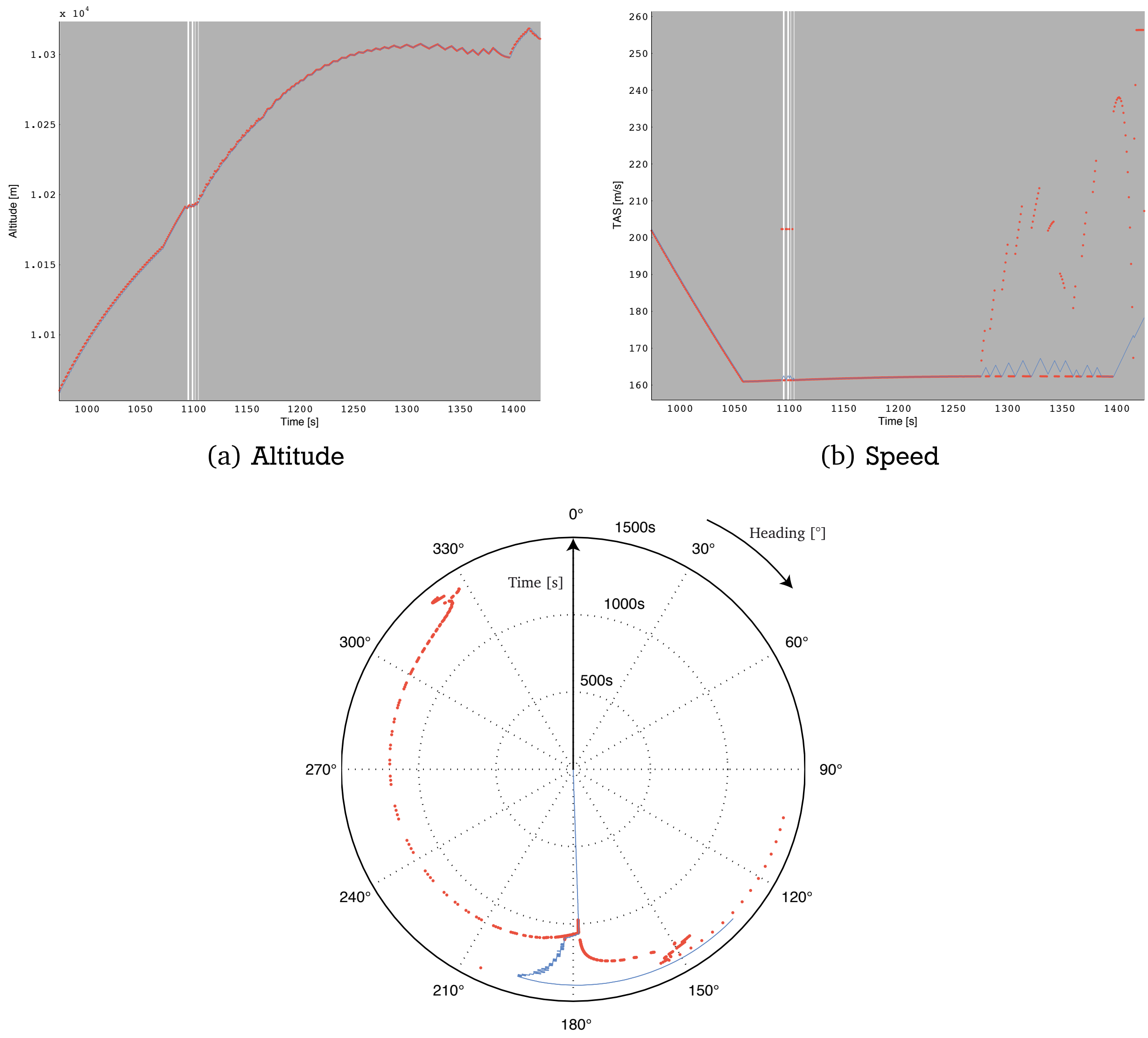

(a) Altitude

(b) Speed

(c) Heading

Figure C.18: S3 comparison run - Modified Relative Zone - Altitude, Speed and Heading development

Table C.15: S3 - CI variation using Modified Relative Zone implementation

Cost Index	$H[km^2]$	$V[km^2]$	$Ti[s^2]$
0	27.29	0.00	12845.56
99	297.11	10.20	50367.31
199	402.69	20.31	50081.60
299	805.51	33.40	71170.11
399	430.03	25.51	52216.40
499	925.67	38.78	79646.58
599	878.51	39.45	78731.57
699	440.03	27.84	50160.12
799	421.25	28.18	39792.17
899	421.98	30.00	37090.56
999	329.78	34.45	42182.30

Table C.16: S3 - Flyability related measures using Modified Relative Zone implementation (1/2)

Cost Index	$\phi\,[^\circ]$	$\dot{\phi}\,[\frac{\circ}{s}]$	$\theta\,[^\circ]$	$\dot{\theta}\,[\frac{\circ}{s}]$
0	35.00	3.00	0.00	0.00
99	35.00	3.00	0.50	0.49
199	35.00	3.00	0.39	0.42
299	29.62	3.00	0.90	0.52
399	35.00	3.00	0.54	0.53
499	34.96	3.00	0.92	0.54
599	35.00	3.00	0.82	0.54
699	35.00	3.00	0.69	0.54
799	35.00	3.00	0.66	0.54
899	33.89	3.00	0.71	0.54
999	0.03	0.01	0.76	0.54

Table C.17: S3 - Flyability related measures using Modified Relative Zone implementation (2/2)

	com. speed $[\frac{m}{s}]$		act. speed $[\frac{m}{s}]$		com. altitude $[m]$		act. altitude $[m]$	
Cost Index	min	max	min	max	min	max	min	max
0	202.32	257.32	202.32	238.90	10058.00	10058.00	10058.00	10058.00
199	160.44	208.77	160.44	208.77	10058.50	10294.40	10058.00	10294.40
299	160.58	224.27	160.58	210.10	10058.70	10344.10	10055.00	10344.10
399	160.72	208.82	160.72	208.82	10058.90	10306.50	10058.00	10305.50
499	160.84	256.21	160.84	211.79	10059.10	10359.00	10055.50	10359.00
599	160.94	256.39	160.94	211.00	10059.40	10359.70	10057.50	10359.70
699	160.97	234.62	160.97	208.45	10059.60	10307.20	10058.00	10307.30
799	160.86	256.38	160.86	207.11	10059.80	10311.20	10058.00	10311.30
899	160.84	256.38	160.84	239.14	10060.00	10316.10	10055.90	10316.10
99	160.28	208.74	160.28	208.74	10058.20	10254.10	10056.00	10254.10
999	160.94	256.37	160.94	251.03	10060.30	10337.50	10056.30	10334.00

D Data sources

D.1 U.S. Department of Transportation – RITA

The U.S. Department of Transportation operates the Research and Innovative Technology Administration (RITA) website which offers transportation statistics and raw data for research purposes. According to the website [Rit] the data is frequently used by airlines, operators, newspapers and for scientific purposes.

D.1.1 Delay Cause Definition

As of [Rit] the following delay cause definition is used for data from RITA:

Air Carrier	The cause of the cancellation or delay was due to circumstances within the airline's control (e.g. maintenance or crew problems, aircraft cleaning, baggage loading, fueling, etc.).
Extreme Weather	Significant meteorological conditions (actual or forecasted) that, in the judgment of the carrier, delays or prevents the operation of a flight such as tornado, blizzard or hurricane.
National Airspace System (NAS)	Delays and cancellations attributable to the national aviation system that refer to a broad set of conditions, such as non-extreme weather conditions, airport operations, heavy traffic volume, and air traffic control.
Late-arriving aircraft	A previous flight with same aircraft arrived late, causing the present flight to depart late.
Security	Delays or cancellations caused by evacuation of a terminal or concourse, re-boarding of aircraft because of security breach, inoperative screening equipment and/or long lines in excess of 29 minutes at screening areas.

D.1.2 Delay Data

Table D.1: Percentage of delay causes for U.S. domestic carriers with at least 1% of domestic scheduled-service passenger revenue (2003 data covers July to December only)

	Air Carrier	Weather	NAS	Security	Aircraft Arriving Late	Cancelled	Diverted
2003	23,06%	3,75%	39,47%	0,31%	25,00%	7,41%	0,99%
2004	23,26%	4,58%	35,90%	0,30%	26,90%	8,17%	0,88%
2005	25,61%	4,13%	33,42%	0,23%	2,74%	0,83%	0,00%
2006	26,11%	3,79%	31,72%	0,34%	30,16%	6,95%	0,92%
2007	26,27%	3,65%	30,18%	0,25%	30,67%	8,11%	0,87%

Table D.1 summarises the delay causes (as defined in Subsection D.1.1) and their share in total delays for 2003 to 2007 [Rit]. Data for 2003 only covers July to December.

D.2 Overview on recorded variables

Table D.2 summarises further variables recorded during Conflict Resolution and generation of the Reference Trajectory. These variables are recorded in addition to those listed in Table 5.1 to verify adherence to the BADA flight dynamics constraints.

Table D.2: List of recorded variables (further variables)

Variable	Conflict Resolution	Reference Trajectory
ϕ	✓	
θ	✓	
Ψ	✓	
$\dot{\phi}$	✓	
$\dot{\theta}$	✓	
$\dot{\Psi}$	✓	

E Current technologies

The Conflict Detection algorithm presented in this work is based on the *Traffic Collision Avoidance System* algorithm for detection and resolution of short-term conflicts. Through the integration of ADS-B data, the algorithm has been extended to allow for long-term Conflict Detection. This appendix summarises some background information on the *Traffic Collision Avoidance System* system in Section E.1 and introduces to the current development regarding ADS-B in Section E.2.

E.1 Traffic Collision Avoidance System

After a series of Mid-Air Collision and Near MAC the installation of TCAS II systems became mandatory by 1993 for passenger aircraft with more than 30 seats travelling in U.S. airspace [Tca]. The *Traffic Collision Avoidance System* is one implementation of a system fulfilling the requirements of an *Airborne Collision Avoidance System* [ICA07a]. This chapter introduces to the several TCAS versions already operational and under development. TCAS introduces a protective area around ownship which is based on the rate of closure between ownship and other aircraft. The protective area is defined as a time span τ. The time span τ depends on the radio altitude and differs for *Traffic Advisories* (TAs) and *Resolution Advisories* (RAs). The latter are only available with TCAS version II and above. The Distance Modification (DMOD) has been introduced to the TCAS logic to enable TAs and RAs for intruders approaching at a very low closing speed and thus where the closing rate is too small to trigger an alert.
Table E.1 summarises the Traffic Advisory and Resolution Advisory τ and DMOD thresholds for TCAS Version II.

Table E.1: TCAS Sensitivity Level Definition and Alarm Thresholds from [Tca]

Own Altitude [ft]	SL	τ [s]		DMOD [nmi]		Altitude Threshold [ft]	
		TA	RA	TA	RA	TA	RA
< 1000	2	20	N/A	0.30	N/A	850	N/A
1000 - 2350	3	25	15	0.33	0.20	850	300
2350 - 5000	4	30	20	0.48	0.35	850	300
5000 - 10000	5	40	25	0.75	0.55	850	350
10000 - 20000	6	45	30	1.00	0.80	850	400
20000 - 42000	7	48	35	1.30	1.10	850	600
> 42000	7	48	35	1.30	1.10	1200	700

TCAS types

Currently TCAS I and II are operational in use while the successors TCAS III and IV are currently under research.
The TCAS I system only allows for *Traffic Advisories* while the TCAS II system also provides *Resolution Advisories*. The resolution advisories are limited to the vertical plane. The system automatically coordinates the aircraft's resolution by checking to other aircraft's intent information. If the other aircraft's intent information is available, the opposite resolution advisory is commanded. In case no intent information is available, the TCAS algorithm computes a Resolution Advisory based on the encounter geometry, resolving the conflict by applying the same set of rules [Tca]. From all legal resolutions, the TCAS algorithm chooses the least agressive [KY00].

TCAS IV is expected to provide horizontal resolution manoeuvres by accessing differential GPS and ADS-B data[1].

E.2 Automatic Dependant Surveillance

Automatic Dependant Surveillance denotes a system where aircraft communicate ownship state and intent information, computed by and derived from on-board systems. The Conflict Detection algorithm (*strategic* TCAS, cf. Chapter 3) and the Conflict Resolution algorithm (Artificial Force Field, cf. Chapter 4) both require availability of intent and position information. The ADS-B message format specifies amongst other information these data. Without considering specifics regarding the exchange medium, this section gives an overview on the minimum requirements for *Automatic Dependant Surveillance* data [SC 02] as far as they are relevant for this work. Therefore a summary is given on the two principal ADS modes, the ADS-A and ADS-B and references the definitions for the Trajectory Change and State Vector reports.

E.2.1 ADS modes

Two different Automatic Dependant Surveillance (ADS) modes are distinguished:

1. Automatic Dependant Surveillance - Addressed (ADS-A) / - Contract (ADS-C)
2. Automatic Dependant Surveillance - Broadcast (ADS-B)

ADS-A/-C
Automatic Dependant Surveillance - Addressed (ADS-A) / - Contract is a negotiated one-to-one communication between an aircraft transmitting ADS information and a ground station requiring receipt of the aircraft messages.

ADS-B
Automatic Dependant Surveillance - Broadcast (ADS-B) is a system with which aircraft distribute information from their on-board systems to other aircraft and ATC. ADS-B is considered to be one of the key enabler for Airborne Separation Assistance Systems [Cas04]. According to [SC 02] three ADS-B reports are distinguished:

1. Surveillance State Vector Reports
2. Mode-Status Reports
3. On-Condition Reports
    - Air Referenced Velocity Reports
    - Target State Reports
    - Trajectory Change Reports
    - Other Reports (to be defined)

E.2.2 Equipment classes

Table E.2 summarises selected features of the ADS-B equipment classes as of [SC 02]. For operation in Autonomous Operations Area airspace and the Conflict Detection & Resolution system devised in this work the number of Trajectory Change Points communicated in the intent dataset, the current state (State Vector) and the range are of interest.

[1] TCAS III was also developed with the aim to provide horizontal resolutions, but the work on TCAS III has been halted.

Table E.2: Selected ADS-B features by equipment class [SC 02]

Equipment Class	TCP	State Vector	Range
A0 - Minimum	No	Yes	min. 10 NM
A1 - Basic	No	Yes	min. 20 NM
A2 - Enhanced	Yes (1)	Yes	min. 40 NM
A3 - Extended	Yes $(n+1)$	Yes	min. 90 NM
A3+ - Extended	Yes $(n+1)$	Yes	min. 120 NM

Information on Trajectory Change Points

The Trajectory Change Report (cf. Figure E.1) includes information on the next (ADS-B class A2) and subsequent (ADS-B classes A3 and A3+) Trajectory Change Points. Trajectory Change reports are to contain long-term intent information which allow for path prediction and provide strategic path information [SC 02] as required by the Conflict Detection & Resolution algorithms devised in this work.

The subset used by the Conflict Detection & Resolution algorithms are the *Time to go* (report element 6) and Positional information (report elements 7b, 7c and 8b). Other than defined in [SC 02] the altitude is given in *meters*.

Other parameters such as the target speed and the track to and track from Trajectory Change Point are not stored in the TrajectoryChangePoint class (cf. Subsection 5.2.2) but computed from other data and reports such as the State Vector report.

	TC Report Elem. #	Contents [Notes]	[Resolution or # of Bits]	Needed Only For TC+0 Reports	Reference Section	Notes
ID	1	Participant Address	[24 bits]		2.1.2.2.2.1	
	2	Address Qualifier	[1 bit]		2.1.2.2.2.2	
TOA	3	Time of Applicability	[1 s resolution]		3.4.8.3	
TC Report #	4	TC Report Sequence Number	[2 bits]		3.4.8.4	1
TC Report Version	5a	TC Report Cycle Number	[2 bits]		3.4.8.5	1,2
	5b	(Reserved for TC Management Indicator)	[3 bit]	•	3.4.8.6	2
TTG	6	Time To Go	[4 s resolution]		3.4.8.7	
Horizontal TC Report Information	7a	Horizontal Data Available and Horizontal TC Type	[4 bits]		3.4.8.8	
	7b	TC Latitude	[700 m or better]		3.4.8.9	3,4
	7c	TC Longitude	[700 m or better]		3.4.8.10	3,4
	7d	Turn Radius	[700 m or better]		3.4.8.11	3,4
	7e	Track to TCP	[1 degree]		3.4.8.12	3
	7f	Track from TCP	[1 degree]		3.4.8.13	3
	7g	(Reserved for Horizontal Conformance)	[1 bit]	•	3.4.8.14	3
	7h	Horizontal Command/Planned Flag	[1 bit]		3.4.8.15	
Vertical TC Report Information	8a	Vertical Data Available and Vertical TC Type	[4 bits]		3.4.8.16	
	8b	TC Altitude	[100 ft resolution]		3.4.8.17	
	8c	TC Altitude Type	[1bit]		3.4.8.18	
	8d	(Reserved for Altitude Constraint Type)	[2 bits]		3.4.8.19	
	8e	(Res. for Able/Unable Altitude Constraint)	[1 bit]	•	3.4.8.20	
	8f	(Reserved For Vertical Conformance)	[1 bit]	•	3.4.8.21	
	8g	Vertical Command/Planned Flag	[1 bit]		3.4.8.22	

Figure E.1: Trajectory Change (TC) Report Definition from [SC 02, Table 3-24]

State Vector

The *State Vector* report (cf. Figure E.2) contains information on the current aircraft state. The information used by the Conflict Detection & Resolution algorithms are current aircraft position (State Vector elements 4a, 4b and 5a), the velocities (State Vector elements 6a and 6b) and vertical rate respectively (State Vector element 8a).

	SV Elem. #	Contents	[Resolution or # of bits]	Required from airborne participants	Required from surface participants	Reference Section	Notes
ID	1	Participant Address	[24 bits]	•	•	2.1.2.2.2.1	
	2	Address Qualifier	[1 bit]	•	•	2.1.2.2.2.2	1
TOA	3	Time Of Applicability	[0.2 s]	•	•	3.4.3.3	
Geometric Position	4a	Latitude (WGS-84)		•	•	3.4.3.4	2, 3
	4b	Longitude (WGS-84)		•	•		
	4c	Horizontal Position Valid	[1 bit]	•	•	3.4.3.5	
	5a	Geometric Altitude		•		3.4.3.6	3, 4
	5b	Geometric Altitude Valid	[1 bit]	•		3.4.3.7	
Horizontal Velocity	6a	North Velocity while airborne		•		3.4.3.8	3
	6b	East Velocity while airborne		•			3
	6c	Airborne Horizontal Velocity Valid	[1 bit]	•		3.4.3.9	
	7a	Ground Speed while on the surface	[1 knot]		•	3.4.3.10	
	7b	Surface Ground Speed Valid	[1 bit]		•	3.4.3.11	
Heading	8a	Heading while on the Surface	[6° or better (6 bits)]		•	3.4.3.12	
	8b	Heading Valid	[1 bit]		•	3.4.3.13	
Baro Altitude	9a	Pressure Altitude		•		3.4.3.14	3, 4
	9b	Pressure Altitude Valid	[1 bit]	•		3.4.3.15	
Vertical Rate	10a	Vertical Rate (Baro/Geo)		•		3.4.3.16	3
	10b	Vertical Rate Valid	[1 bit]	•		3.4.3.17	
NIC	11	Navigation Integrity Category	[4 bits]	•	•	3.4.3.18	
Report Mode	12	SV Report Mode	[2 bits]			3.4.3.19	

Figure E.2: State Vector (SV) Report Definition from [SC 02, Table 3-24]

Range

Limitations on transmission range may hamper long-term Conflict Detection & Resolution. Airspace areas such as the North Atlantic airspace where *Autonomous Operations* are likely to be introduced [Nexa] cover easily more than the minimum requirement for ADS-B class *A3+ Extended* of 120 NM. Therefore means may have to be introduced to allow transmission of State Vector and Trajectory Change reports over greater distances.

F Base of Aircraft Data

The performance calculations presented in this appendix are summarised from and based on EUROCONTROL's BADA performance model [Nui04b]. They have been implemented in MATLAB for evaluation and testing. After evaluation, certain functions have been re-implemented in C++ to be directly accessible for Conflict Detection and Conflict Resolution algorithms.
Section F.1 summarises the BADA parameters relevant to this work for the aircraft types used during evaluation (Airbus A340-300 and Boeing 747-400). Information on the calculation of the fuel flow and the Specific Air Range is summarised in Section F.2 and Section F.3. The appendix is concluded with Section F.4 detailing BADA's calculation of the speed envelope and Section F.5 giving information on the maxima used for longitudinal and vertical acceleration.

F.1 BADA parameters for selected aircraft

The BADA forumlas use for their calculations aircraft type specific parameters. These parameters are given for the different flight phases and engine types. Table F.1 summarises the aircraft type specific parameters as of BADA Revision 3.6 for the cruise flight phase and the aircraft types considered in this work.

Table F.1: BADA parameters for selected aircraft

	C_{f1}	C_{f2}	C_{Tcr}	$V_{\text{stall}}[kts]$	V_{MO} $[kts]$	M_{MO} [M]
A340-300	0.90166	8933.7	0.95	142.00	330.00	0,86
747-400	0.31694	239.31	0.95	183.00	365.00	0,92

F.2 Fuel flow f_{nom}

BADA calculates the nominal fuel flow f_{nom} for jet (and turboprop) engines from the *thrust specific fuel consumption* ν and *thrust* T.
The *thrust specific fuel consumption* calculates to

$$\nu = C_{f1} \cdot (1 + \frac{V_{TAS}}{C_{f2}}) \text{ [Nui04b, Eq. 3.9-1]} \tag{F.1}$$

and the *nominal fuel flow* to

$$f_{nom} = \nu \cdot T \text{ [Nui04b, Equation 3.9-2].} \tag{F.2}$$

In BADA the *normal cruise thrust* is set by definition equal to drag with an upper boundary of

$$(T_{cruise})_{MAX} = C_{Tcr} \cdot T_{maxclimb} \text{ [Nui04b, Equation 3.7-8].} \tag{F.3}$$

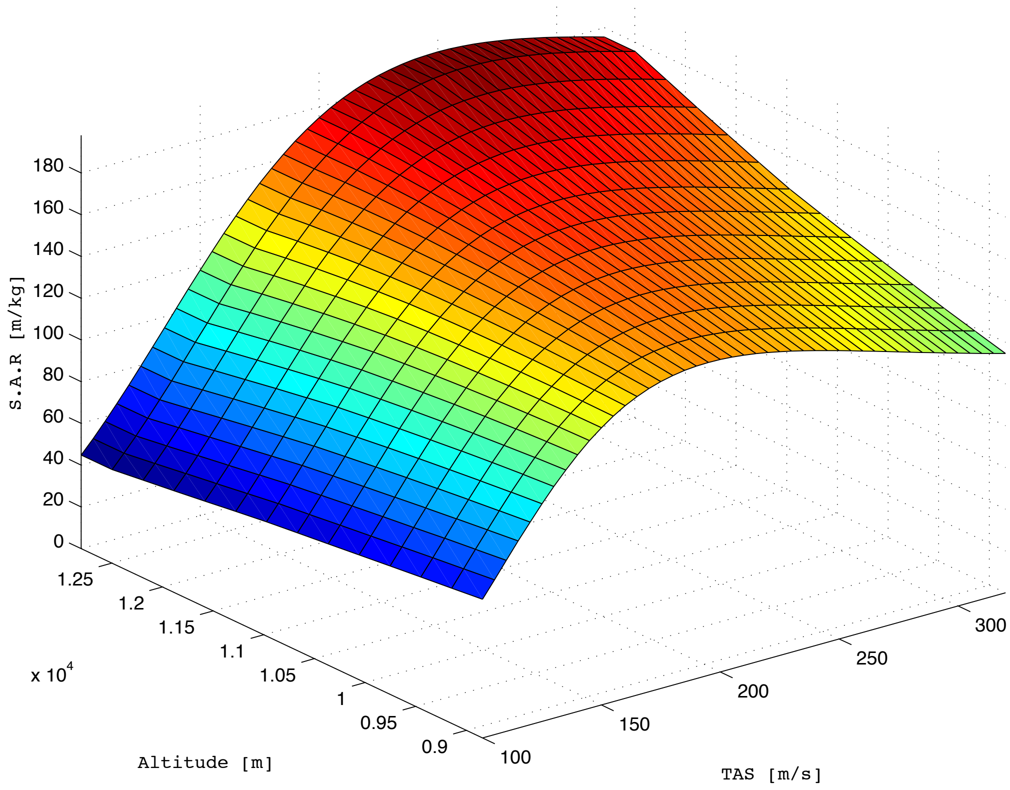

Figure F.1: Specific Air Range - Airbus A340-300

F.3 Specific Air Range f_{SAR}

The Specific Air Range (SAR) is the distance an aircraft can travel for every weight of fuel burned [Kli07]. Thus, the Specific Air Range is given in $\frac{m}{kg}$ (or $\frac{nm}{lbs}$). The SAR can be calculated from the fuel flow f_{nom} as

$$SAR = \frac{V_{TAS}}{f_{nom}} \tag{F.4}$$

if wind effects are neglectable[Sch08].
Figure F.1 illustrates the Specific Air Range for an Airbus A340-300 aircraft with a mass of $141000kg$ using the Base of Aircraft Data model (Equations F.1 - F.3) and Equation F.4.

F.4 Speed Envelope

The Base of Aircraft Data model defines for each modelled aircraft the maximum operating speed V_{MO} given as Calibrated Airspeed and the maximum operating Mach number M_{MO}. These values are also used for the aircraft models used for simulation in this work which are summarised in Table 2.2.

Based on the Calibrated Airspeed V_{CAS} the True Airspeed calculates as follows:

$$V_{TAS} = \left[\frac{2}{\mu} \frac{P}{\rho} \left\{ \left(1 + \frac{(P_0)_{ISA}}{P} \left[\left(1 + \frac{\mu}{2} \frac{(\rho_0)_{ISA}}{(P_0)_{ISA}} \cdot V_{CAS}^2 \right)^{1/\mu} - 1 \right] \right)^{\mu} - 1 \right\} \right]^{1/2} \quad \text{[Nui04b, Eq. 3.2-12]}$$

$$\mu = \frac{1}{3.5} \quad \text{[Nui04b, Eq. 3.2-14]}$$

with

P : pressure at altitude $[P]$
$(P_0)_{ISA}$: pressure at sea level $[P]$
ρ : air density at altitude $[\frac{kg}{m^3}]$
$(\rho_0)_{ISA}$: air density at sea level $[\frac{kg}{m^3}]$

Based on the Mach number M the True Airspeed calculates as follows:

$$V_{TAS} = M \cdot a$$

with

$$a = \begin{cases} 295.07 \frac{m}{s} & \text{, if above } 11000m \\ 340.29 \frac{m}{s} \cdot \sqrt{T / T_{ISA,SL}} & \text{, else} \end{cases}$$

where

T : current temperature $[K]$
$T_{ISA,SL}$: temperature at sea level (under standard atmosphere conditions) $[K]$

The above denoted equations are used to determine the current applicable maximum speeds for the simulated aircraft. The minimum speeds are given through the *stall speeds* (CAS) V_{stall} and the minimum speed coefficient (for the cruise phase set to 1.3) and calculates to

$$V_{\min} = C_{V,\min} \cdot V_{\text{stall}}.$$

F.5 Accelerations

BADA defines two maximum acceleration values for civil aircraft, i.e.

$$a_{l,\max(civ)} = 2.0 \frac{\text{ft}}{s^2} = 0.6096 \frac{m}{s^2}$$

for acceleration along the x_f axis or longitudinal acceleration and

$$a_{n,\max(civ)} = 5.0 \frac{\text{ft}}{s^2} = 1.524 \frac{m}{s^2}$$

for ROCD or normal acceleration [Nui04b, Section 5.2].

Depending on a time interval $\Delta t = p_i -_t p_j$ between two trajectory points p_i and p_j (cf. Definition 2.2), the True Airspeeds V_{p_i} and V_{p_j} and the climb/descent angles at the respective positions γ_{p_i} and γ_{p_j} longitudinal and normal acceleration are constrained through

$$|V_{p_i} - V_{p_j}| \leq a_{l,\max(civ)} \cdot \Delta t \quad \text{cf. [Nui04b, Equation 5.2-1]} \tag{F.5}$$

and

$$|\gamma_{p_i} - \gamma_{p_j}| \leq \frac{a_{n,\max(civ)} \cdot \Delta t}{V_{TAS}} \quad \text{cf. [Nui04b, Equation 5.2-2].} \tag{F.6}$$

The Flight Path Angle (or climb/descent angle) calculates depending on True Airspeed and the rate of altitude change $\dot{h} = \frac{p_i -_v p_j}{\Delta t}$ as of BADA to

$$\gamma = \text{asin}\left(\frac{\dot{h}}{V_{TAS}}\right) \text{ [Nui04b, Equation 5.2-3].} \tag{F.7}$$

G Algorithms

Several algorithms have been presented in this work. This appendix describes these algorithms in more detail and illustrates their implementation in pseudo-code. Furthermore, where necessary, also interfaces to external, third party libraries are given. An overview on the implementation and the class architecture in which these algorithms have been embedded can be found in Chapter 5.

G.1 Position calculation

Both, the Conflict Detection and the Conflict Resolution algorithm need to project the current position of the aircraft into the future which depends on the navigation technique applied. For navigation applications one distinguishes between two different techniques, the navigation following the great circle path or the rhumb line. The *Great Circle* or *Orthodrome* is the shortest connection between two points on a sphere. Navigating after an orthodrome requires permanent change of the heading ψ [BW01]. The *Rhumb line* or *Loxodrome* intersects all meridians at the same angle, the heading remains constant [BW01]. Except when flying around the equator or along a meridian, the rhumb line is longer than the great circle path. In order to calculate the future position p' of an aircraft *acr* moving at speed $\vec{v}$ from the current position p it is necessary to know whether a great circle path or rhumb line is followed. Figure G.1 illustrates the difference between both navigation techniques. The red path follows the rhumb line – crossing all meridians at the same angle – while the blue path follows great circle paths. The largest lateral deviation between the two paths has a difference of $28401m$.

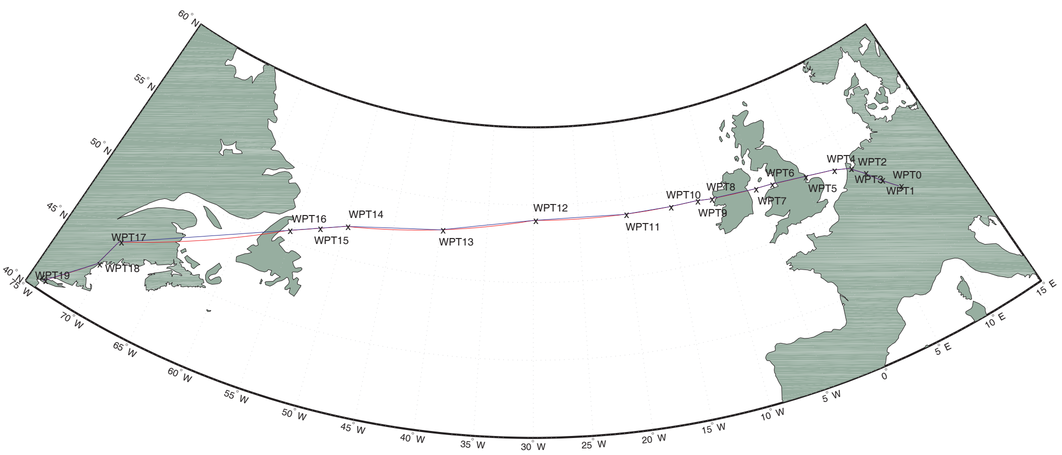

Figure G.1: North Atlantic Crossing - Great Circle (blue) and Rhumb Line (red) tracks

Problem description

Aircraft usually follow *Great Circle* tracks when flying from one waypoint to the next [How90]. Therefore, the aircraft has to constantly change its heading ψ to reach the target position p'. Algorithm G.1 calculates the next position given a current position p_c, the target position p_t, a speed vector $\vec{v}_g$, and the time to travel t_t and step size t_s.

Implementation

Algorithm G.1 illustrates the implementation of the position calculation algorithm The functions *getHeading* and *reckon* (Lines 9 and 10 of Algorithm G.1) call the MATLAB functions *azimuth* in the first and *reckon* [Map] in the latter case. The calculation of the future position p' from a current position

Algorithm G.1 Calculation of future position

function GETNEXTPOSITION(p_c, p_t, $\vec{v}_g$, t_t, t_s) returns p'
    input:
    current position p_c*, target position* p_t*, speed* $\vec{v}_g$*,time to travel* t_t*,time per calculation step* t_s
    output:
    future position p'
    if $|\vec{v}| \cdot t_t > |pos_c - pos_t|$ **then**
        return pos_t;
    end if
    ψ = getHeading(pos_c,pos_t);
    pos_c = reckon($pos_c, |\vec{v}| \cdot t_s, \psi$)
    if $t_t - t_s <= 0$ **then**
        return pos_c
    else
        return getNextPosition($pos_c, pos_t, \vec{v}_g, t_t - t_s, t_s$);
    end if
end function

p with a given distance and azimuth is also referred to in literature as one of the two *geodetic problems* (reference to [Kah98] in [Dip06]).
Since following a great circle path requires regular heading changes, the algorithm needs to update the heading during the projection as well. In Algorithm G.1 this is achieved by a computation of the required heading during each calculation step. Thus, the parameter t_s impacts beside the computation time of Algorithm G.1 also the difference between the aircraft's actual and planned position. Section G.2 details the step size calculation.

G.2 Step size calculation

The performance of the algorithms calculating the movement of the aircraft depends on the step size, i.e. on how many seconds of movement are covered by one calculation step. If the step size is chosen too large, the distance at the CPA may not be accurate enough or the CPA may have even been passed. On the other hand, if the step size has been chosen too small, the calculation will take additional time. The step size furthermore impacts the length of the distance traveled during one calculation step. For great circle navigation the heading has to be changed in order to follow the great circle path. Thus, the step size also impacts how close the aircraft follows its intended path.

Problem description

The step size shall ensure that the difference between the actual position of the aircraft after t and the calculated position is equal or less to the aircraft's protection zone and the aircraft stays within the Required Navigational Performance[1] [ICA99] to its great circle track (for RNP class $1 = 1.852m$) while being as large as possible to reduce calculation time.

Implementation

The CD&R algorithms devised in this work require fast time-simulation of aircraft movements. Depending on the traffic situation (e.g. the proximity of intruders to ownship), the step size required is expected to be small. On segments, where no conflict occurs, the simulation only needs to assure that the aircraft

[1] Details on RNP types may be found in Section A.2.

remains within the applicable RNP class, the step size may be chosen larger. Therefore a dynamic step size approach will be used. This approach needs to take the protection zones and closing speeds (vertical and horizontal) into account.

Protection Zone and closing speed dependant step size: Equation G.1 derives the required step size from the movement vectors of ownship and intruder and the applicable protection zone around ownship. The maximum distance which can be travelled without requiring a heading change to conform to RNP type 1 requirements is approximately 149337.08m.

$$
\begin{aligned}
f_{step}(\vec{v}_{o,g}, \vec{v}_{i,g}, Z_o) &= \min\left(\underbrace{\frac{|\vec{v}_{r,xy}|}{\min\left(Z_{lat}, Z_{lon}\right)}}_{\text{Lateral Closing speed}}, \underbrace{\frac{|\vec{v}_{r,z}|}{Z_{vert}}}_{\text{Vertical Closing Speed}}, \underbrace{\frac{149337.086034}{|\vec{v}_{o,xy}|}}_{\text{Maximum allowed step size}} \right) \text{ with} \qquad (G.1) \\
\vec{v}_{r,xy} &= (\dot{x}_{o,g}, \dot{y}_{o,g}, 0)^T - (\dot{x}_{i,g}, \dot{y}_{i,g}, 0)^T \text{ and} \\
\vec{v}_{r,z} &= (0, 0, \dot{z}_{o,g})^T - (0, 0, \dot{z}_{i,g})^T.
\end{aligned}
$$

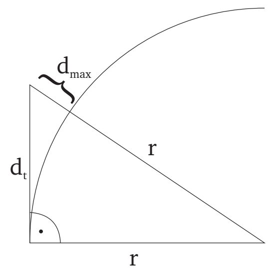

Figure G.2: Calculation of maximum distance between two heading changes

G.3 Conflict Detection algorithm

For detection of airborne traffic conflicts an algorithm based on the detection component of the TCAS logic has been devised. Section 3.3 outlined the general approach of the algorithm while this section details its implementation.

Problem description

Based on the ADS-B dataset (cf. Section E.2) an algorithm had to be devised which could compute the position of and distance at the Closest Point of Approach. The algorithm had to identify based on the distance and the geometry of the Protected Airspace Zone (cf. Section 3.2) whether a violation of safe separation occurred or not.

Implementation

Algorithm G.2 illustrates the implementation of the Conflict Detection algorithm devised in this work. The assignment in line 8 ensures that the algorithm calculates the CPA information set only for in time (partly) overlapping TCPs. The function calls of function GETNEXTPOSITION (lines 16f., 22f. and 27f.) use the step size calculated by Equation G.1 unless the future position to be calculated only differs by one second in time. In these cases the step size is set to one second as well.

The function COMPUTECPA (line 15) uses the closing rate and current distance as described in Equation 3.10 to calculate the time to CPA based on the current positions and the speed vectors. The speed vectors $v_{o,g}$ and $v_{i,g}$ are known through the trajectory segments TCPs spatial and temporal distances.

Algorithm G.2 Conflict Detection

function CALCULATECONFLICT($\mathcal{T}_o$, $\mathcal{T}_i$) returns $(p_{CPA}, t_{CPA}, d_{CPA}, p^s_{PAZ}, p^e_{PAZ})$
2: ***input:***
ownship TCPs $\mathcal{T}_o$*, traffic TCPs* $\mathcal{T}_i$
4: ***output:***
Position of, time to and distance at CPA $p_{CPA}, t_{CPA}, d_{CPA}$*, Entry and exit of PAZ* p^s_{PAZ}, p^e_{PAZ}
6:
for $ts_o = (tcp_{o,i}, tcp_{o,j}) \in \mathcal{T}_o$ **do**
8: $\mathcal{T}_{i,j} = ts | ts = (tcp_{i,k}, tcp_{i,l}) \in \mathcal{T}_i \wedge tcp_{o,i} \leq_t tcp_{i,k/l} \leq_t tcp_{o,j}$
for $ts_c = (tcp_{i,k}, tcp_{i,l}) \in \mathcal{T}_{i,j}$ **do**
10: **if** $tcp_{i,k} <_t tcp_{o,i}$ **then**
$tcp_{i,k} =$ GETNEXTPOSITION$(tcp_{i,k}, tcp_{i,l}, \vec{v}_{i,GS}, tcp_{o,i} -_t tcpi, k)$
12: **else if** $tcp_{o,i} <_t tcp_{i,k}$ **then**
$tcp_{o,i} =$ GETNEXTPOSITION$(tcp_{o,i}, tcp_{o,j}, \vec{v}_{o,GS}, tcp_{i,k} -_t tcp_{o,i})$
14: **end if**
$t_{CPA} =$ COMPUTECPA(ts_o, ts_c)
16: $p_{CPA} =$ GETNEXTPOSITION$(tcp_{o,i}, tcp_{o,j}, \vec{v}_{o,GS}, t_{CPA})$
$p_i =$ GETNEXTPOSITION$(tcp_{i,k}, tcp_{i,l}, \vec{v}_{i,GS}, t_{CPA})$
18: **if** CONFLICTEXISTS(Z, p_{CPA}, p_i) **then**
$d_{CPA} = p_i - p_{CPA}$
20: $p'_i \leftarrow p_i$, $p^e_{PAZ} \leftarrow d_{CPA}$
while CONFLICTEXISTS(Z, p^e_{PAZ}, p_i) **do**
22: $p^e_{PAZ} =$ GETNEXTPOSITION$(p^e_{PAZ}, tcp_{o,j}, \vec{v}_{o,GS}, 1)$
$p'_i =$ GETNEXTPOSITION$(p'_i, tcp_{i,l}, \vec{v}_{i,GS}, 1)$
24: **end while**
$p'_i \leftarrow p_i, p^s_{PAZ} \leftarrow d_{CPA}$
26: **while** CONFLICTEXISTS(Z, p^s_{PAZ}, p_i) **do**
$p^e_{PAZ} =$ GETNEXTPOSITION$(p^s_{PAZ}, tcp_{o,i}, \vec{v}_{o,GS}, 1)$
28: $p'_i =$ GETNEXTPOSITION$(p'_i, tcp_{i,k}, \vec{v}_{i,GS}, 1)$
end while
30: **end if**
end for
32: **end for**
end function

In lines 18, 21 and 26 the function CONFLICTEXISTS uses the calculation of the current intrusion as described in Subsection 3.2.3.

G.4 Artificial Force Field Conflict Resolution algorithm

At the core of a system enabling Airborne Conflict Management lies a Conflict Resolution algorithm. This section details the implementation of the Conflict Resolution algorithm as described in Chapter 4 further.

Problem description

The Conflict Resolution algorithm has to compute a conflict free trajectory, i.e. a trajectory that does not lead to a violation of the Collision Avoidance Zone around the aircraft. Therefore, a Protected Airspace Zone is defined around ownship which may take information such as current speed and relative speed/bearing to the intruder into account. The Conflict Resolution also needs to ensure that a flyable trajectory is generated. Beside this, the algorithm should also take the FMS Cost Index into account.

Implementation

Algorithm G.3 summarises the *Artificial Force Field* Conflict Resolution algorithm devised in this work. The algorithm uses BADA modelled aircraft to simulate ownship and intruder movement (lines 12 and 17). Each simulation step covers $t = 1s$ of time. The function CONFLICTEXISTS (line 18) is used as

Algorithm G.3 Conflict Resolution

function COMPUTERESOLUTION($\mathcal{T}_o$, $\mathcal{T}_i = \{\mathcal{T}_{i,1}, ..., \mathcal{T}_{i,k}\}$, CI) returns ($\mathcal{T}_{o,cr}$)
2: ***input:***
ownship TCPs $\mathcal{T}_o$, intruder TCPs $\mathcal{T}_i$, Cost Index CI
4: ***output:***
Alternative trajectory computed by Conflict Resolution, $\mathcal{T}_{o,cr}$
6:
acr$_o$ ← CREATEAIRCRAFT($\mathcal{T}_o$)
8: **for all** $\mathcal{T}_{i,k} \in \mathcal{T}_i$ **do**
acr$_{i,k}$ ← CREATEAIRCRAFT($\mathcal{T}_{i,k}$)
10: **end for**
$\mathcal{T}_{o,cr} \leftarrow \emptyset$
12: **while** SIMULATE(acr_o) **do**
$\vec{F}_{res} \leftarrow 0$
14: $\vec{F}_{rep} \leftarrow 0$
$\vec{F}_{att} \leftarrow 0$
16: **for all** $acr_{i,k}$ **do**
SIMULATE($acr_{i,k}$)
18: **if** CONFLICTEXISTS($Z, acr_o, acr_{i,k}$) **then**
$\vec{F}_{rep} \leftarrow \vec{F}_{rep}$+CALCFORCEREPULSIVE(acr$_o$, acr$_{i,k}$, Z)
20: **end if**
end for
22: **if** $\vec{F}_{rep} \neq 0$ **then**
tcp$_a$ ← GETACTIVETCP(acr$_o$, $\mathcal{T}_o$)
24: $\vec{F}_{att}$ ← CALCFORCEATTRACTIVE(acr$_o$, tcp$_a$)
$\vec{F}_{res} \leftarrow \vec{F}_{att} + \vec{F}_{rep}$
26: S ← GETCURRENTSTATE(acr$_o$)
C ← GETCOMMANDVALUES($S, \vec{F}_{res}$, CI)
28: SETCOMMANDVALUES(acr_o, C)
end if
30: $\mathcal{T}_{o,cr} \leftarrow \mathcal{T}_{o,cr} \cup$ acr$_o$
end while
32: REDUCETCP($\mathcal{T}_{o,cr}, C$)
end function

in Algorithm G.2 to identify an infringement of ownship's Protected Airspace Zone. In case an aircraft violates this zone, the force acting on ownship is calculated (line 19). The calculation of the force $\vec{F}_{rep}$ in CALCFORCEREPULSIVE follows the descriptions as of Subsection 4.3.1. Same holds true for the attractive force $\vec{F}_{att}$ (CALCFORCEATTRACTIVE, line 24). In case of an intrusion, the attractive force of the original trajectories next Trajectory Change Point is calculated (lines 23ff.) and summed to the resulting force $\vec{F}_{res}$ (line 25). With the current state information, (*inter alia* heading, altitude and speed) the CR algorithm calculates new command values as outlined in Subsection 4.3.2, taking the Cost Index into account. Initially, the result trajectory $\mathcal{T}_{o,cr}$ contains all trajectory points, not only Trajectory Change Points (in line 30 of Algorithm G.3 every position of ownship is added to the set of trajectory points). This set is reduced to only contain Trajectory Change Points as of Definition 2.4 by applying the TCP identification as described in Section G.5 (line 32). Further details on the implementation may be found in Chapter 5.

G.5 Trajectory Change Point identification

The output of Algorithm G.3 is a set of trajectory points along with a vector representing the commanded heading, altitude and speed. This set of points is further processed to contain only Trajectory Change Points as of Definition 2.3. This algorithm is detailed in this section.

Problem description
Regardless of the model and the algorithm used, Conflict Resolution needs to communicate the conflict-free trajectory as a number of Trajectory Change Points. The resolution algorithm as described in Section 4.3 generates a trajectory consisting of trajectory points (cf. Definition 2.2) with a resolution of $t = 1s$. Therefore it is necessary to reduce this set of trajectory points.

Implementation
The algorithm used for Trajectory Change Point identification devised in this work uses a set of command values along with the trajectory points to identify TCPs. In order to allow for this, each TCP is attributed during Conflict Resolution with the command values. Algorithm G.4 describes the TCP identification algorithm. By default, the first and last trajectory points of $\mathcal{T}$ are Trajectory Change Points and added

Algorithm G.4 Trajectory Change Point identification

function REDUCETCP($\mathcal{T}$, C) returns ($\mathcal{T}_r$)
2: *__input:__*
TCPs to be reduced $\mathcal{T}_o$, *Set of command values* C
4: *__output:__*
minimal TCP set $\mathcal{T}_r$
6:
$\mathcal{T}_r \leftarrow \mathcal{T}_r \cup$ GETFIRST($\mathcal{T}$)
8: $\Delta\psi \leftarrow$ GETRELATIVEANGLE($C_{2,\psi}$, $C_{1,\psi}$)
$\Delta h \leftarrow C_{2,h} - C_{1,h}$
10: $\Delta V_{TAS} \leftarrow C_{2,V_{TAS}} - C_{1,V_{TAS}}$
for $i \leftarrow 2, |\mathcal{T}| - 1$ **do**
12: $\Delta\psi_{cur} \leftarrow$ GETRELATIVEANGLE($C_{i-1,\psi}$, $C_{i-1,\psi}$)
$\Delta h_{cur} \leftarrow C_{i,h} - C_{i-1,h}$
14: $\Delta V_{TAS,cur} \leftarrow C_{i,V_{TAS}} - C_{i-1,V_{TAS}}$
if $\text{sgn}(\Delta V_{TAS,cur}) \neq \text{sgn}(\Delta V_{TAS})$ or $\text{sgn}(\Delta h_{cur}) \neq \text{sgn}(\Delta h)$ or $\text{sgn}(\Delta\psi_{cur}) \neq \text{sgn}(\Delta\psi)$ **then**
16: $\mathcal{T}_r \leftarrow \mathcal{T}_r \cup \text{tcp}_i$
end if
18: $\Delta\psi \leftarrow \Delta\psi_{cur}$
$\Delta h \leftarrow \Delta h_{cur}$
20: $\Delta V_{TAS} \leftarrow \Delta V_{TAS,cur}$
end for
22: $\mathcal{T}_r \leftarrow \mathcal{T}_r \cup$ GETLAST($\mathcal{T}$)
end function

to the reduced TCP set $\mathcal{T}_r$ (lines 7 and 22). The TCP reduction used in this work only detects TCPs which constitute an inflection point regarding the trend of commanded heading[2], altitude or speed. If such an inflection point has been identified, the trajectory point is added to the reduced TCP set (line 16).

Limitations

The Trajectory Change Point identification algorithm as presented in Algorithm G.4 cannot detect TCPs other than those which constitute an inflection point regarding one of the commanded values. Though, when executing the commanded values, the values for bank, pitch and thrust may also encounter not only inflection but also points with a significant change of gradient of one of the aircraft's control values, e.g. where $\dot{\phi}_1 \ll \dot{\phi}_2$.

[2] The function GETRELATIVEANGLE (lines 8 and 12 of Algorithm G.4) computes in the boundaries of $]-180°, 180°]$ the difference between two headings.

Bibliography

Printed References

[A34a] *A340 – Flight Crew Operating Manual Volume 4 - FMGS Pilot's Guide*. Deutsche Lufthansa AG.

[A34b] *A340 - Flight deck and systems briefing for pilots*. Tech. rep. AI/ST-F 472 502/90 issue 5. Airbus Industrie, 1995.

[AG06] John Anderson and Colin Goodchild. *ASSTAR (Advanced Safe Separation Technologies and Algorithms) - D2.1 Survey of Candidate Functional Logic Processes and Algorithms*. Tech. rep. University of Glasgow, 2006.

[Ari] *Advanced Flight Management Computer System*. Tech. rep. ARINC Characteristic 702A-1. Airlines Electronic Engineering Committee, Aeronautical Radio, Inc. (ARINC), 2000.

[Bad06] Felix Badura. "Auswirkungen einer EU-weiten Besteuerung von Kerosin auf Luftverkehrsgesellschaften aus betriebswirtschaftlicher Sicht". Diplomarbeit. Wirtschaftsuniversität Wien, Institut für Transportwirtschaft und Logistik, 2006.

[Bad] *Aircraft Perfomance Summary Tables for the Base of Aircraft Data (BADA), Revision 3.6*. Tech. rep. EUROCONTROL EXPERIMENTAL CENTRE, 2004.

[Bar+06] Nima Barraci et al. *Information Fusion & HMI Specification*. Internal Deliverable DI 1.2.5. Produced under the EC contract prop. AIP4-CT-2005-516167. FLYSAFE consortium, 2006.

[Bau+06] Siegfried Bauer et al. "An Application for Detecting Potential Traffic Conflicts in Areas with Unreliable ATC". In: *2nd International Conference on Research in Air Transportation, ICRAT 2006, Belgrad, Serbien und Montenegro*. Technische Universität Darmstadt, Petersenstraße 30, Darmstadt 2006. Pp. 325–330.

[Bau10] Siegfried Bauer. "Präventive Warnung vor Geländekonflikten zur Steigerung des Situationsbewußtseins im Flugzeug-Cockpit". Dissertation (to be published). Technische Universität Darmstadt, 2010.

[Bir+07] Florent Birling et al. *Strategic data consolidation and conflict resolution specification*. Deliverable D 5.4.1. Produced under the EC contract prop. AIP4-CT-2005-516167. FLYSAFE consortium, 2007.

[BK08] Nima Barraci and Uwe Klingauf. "Effect of Protection Zone Geometry on Traffic Conflict Resolution based on Artificial Force Fields". In: *Proceedings of the 7th EUROCONTROL Innovative Research Workshop & Exhibition*. 2008.

[Bro01] Rudolf Brockhaus. *Flugregelung*. ISBN 3-540-41890-3. Springer, 2001.

[BSC96] Karl D. Bilimoria, Banavar Sridhar, and Gano B. Chatterji. "Effects of conflict resolution maneuvers and traffic density on free flight". In: *AIAA, Guidance, Navigation and Control Conference*. American Institute of Aeronautics and Astronautics, Inc. 1996.

[BW01] Jürgen Beyer and Burkhard Wigger. *Grundlagen der Navigation und Anwendung*. Skript. Technische Universität Darmstadt, Fachbereich Maschinenbau, Institut für Flugsysteme und Regelungstechnik, 2001.

[Cas04] Francis Casaux. *Towards an ASAS Implementation Strategy*. Tech. rep. ASAS-TN-D3.3 Version 3.0c. ZAC des Bordes BP15 F-91222 Bretigny sur Orge CEDEX FRANCE: EUROCONTROL Experimental Centre, 2004.

[Cha+07] Georgios Chaloulos et al. *Comparative Study of Conflict Resolution Methods*. Report D5.1. iFly – Safety, Complexity, Responsibility based design, and validation of highly automated Air Traffic Management, 2007.

[CM04] Victor Carreño and César Muñoz. "Implicit intent information for conflict detection and alerting". In: *23rd Digital Avionics Systems Conference*. AIAA/IEEE. 2004.

[Com00] European Commission. *Single European Sky - Report of the high-level group*. ISBN 92-894-0376-4. Luxembourg: Office for Official Publications of the European Communities, 2000.

[Com02] Committee on Aeronautics Research and Technology for Environmental Compatibility, National Research Council. *For Greener Skies: Reducing Environmental Impacts of Aviation*. ISBN 0-309-50821-5. NATIONAL ACADEMY PRESS Washington, D.C., 2002.

[Con05] NUP2+ Consortium. *NUP2+, North European ADS-B Network Update Programme, Phase II+, Project Outline*. Report. 2005.

[CSB96] Gano Chatterji, Banavar Sridhar, and Karl Bilimoria. "En-route flight trajectory prediction for conflict avoidance and traffic management". In: *AIAA, Guidance, Navigation and Control Conference*. Paper 96-3766. 1996.

[DAC96] Nicolas Durand, Jean-Marc Alliot, and Olivier Chansou. "Optimal Resolution of En Route Conflicts". In: *Air Traffic Control Quarterly* Volume 3(3) (1996).

[Dep05] Deputy Under Secretary of Defense for Science and Technology (DUSD(S&T)). *Technology Readiness Assessment (TRA) Deskbook*. Tech. rep. Department of Defense, 2005.

[Dip06] Michael Dippold. "Persönliche Positionsbestimmung mit Beschleunigungssensoren". Diplomarbeit. Universität Bremen, 2006.

[DZ97] Vu N. Duong and Karim Zeghal. "Conflict Resolution Advisory for Autonomous Airborne Separation in Low-Density Airspace". In: *Proceedings of the 36th Conference on Decision & Control*. Vol. Volume 3. 1997. Pp. 229–243.

[EC99] Commission of the European Communities. "The creation of the single European sky". In: *Communication from the Commission to the Council and the European Parliament* COM(1999) 614 final/2 (1999).

[Eck99] Bruce Eckel. *Thinking in C++ 2nd edition – Volume 2: Standard Libraries & Advanced Topics*. 1999.

[EE99] Martin S. Eby and Wallace E. Kelly III. "Free Flight Separation Assurance Using Distributed Algorithms". In: *IEEE Aerospace Conference, Proceedings* 2 (1999). Pp. 429–441.

[EUR00] EUROCONTROL. *Central Flow Management Unit - Yearly ATFM Summary 1999*. Tech. rep. European Organisation for the Safety of Air Navigation, 2000.

[EUR07] EUROCONTROL. *ATCFM and Capacity Report 2006*. Tech. rep. European Organisation for the Safety of Air Navigation, 2007.

[Eur] *European Air Traffic Management System Operational Concept Document (OCD)*. 11th ed. European Organisation for the Safety of Air Navigation (EUROCONTROL), 1999.

[Fac] *Capacity Needs in the National Airspace System*. Tech. rep. FAA and MITRE, 2004.

[FLY05] FLYSAFE. *Sixth Framework Programme Priority 1.4 Aeronautics and Space, Annex I Description of Work Airborne Integrated Systems for Safety Improvement, Flight Hazard Protection and All Weather Operations (FLYSAFE)*. Tech. rep. Contract, 2005.

[Fms] *Flight Operations Support & Line Assistance - Getting to Grips with the Cost Index*. Airbus Customer Service. 1998.

[Ges+02] Alfons Geser et al. *Air Traffic Conflict Resolution and Recovery*. Tech. rep. National Aeronautics and Space Administration, 2002.

[GM02] Alfons Geser and César Muñoz. "A Geometric Approach to Strategic Conflict Detection and Resolution". In: *21st Digital Avionics System Conference*. Vol. 1. AIAA/IEEE. 2002. 6B1–1–6B1–11.

[Gmf] *Global Market Forecast 2004-2023*. Tech. rep. AIRBUS S.A.S., 2004.

[Hoe01] Jacob Marten Hoekstra. "Designing for Safety: the Free Flight Air Traffic Management Concept". PhD thesis. Technische Universiteit Delft, 2001.

[Hol04] Matthias Hollick. "Dependable Routing for Cellular and Ad Hoc Networks". Dissertation. Technische Universität Darmstadt, 2004.

[How90] Peter J. Howells. *Aircraft Trajectory - Prediction and Control in the Air Transport Flight Management Computer Systems*. Tech. rep. Volume 1. NATO Advisory Group for Aerospace Research & Development AGARD AG-301, 1990.

[Iata] *IATA In-flight Broadcast Procedure (IFBP), Asia Pacific (ASPAC) Region, IFBP ASPAC Aug 2003*. Tech. rep. International Air Transport Association, 2003. URL: `http://www1.iata.org/WHIP/\_Files/WgId\_0019/IFBP\_ASPAC.pdf`.

[Iatb] *IATA Safety Report 2005*. ISBN 92-9195-752-6. International Air Transport Association, 2006.

[ICA01] ICAO. *Air Traffic Services - Air Traffic Control Service, Flight Information Service, Alerting Service - Annex 11 to the Convention on International Civil Aviation*. 13th ed. International Civil Aviation Organization, 2001.

[ICA02] ICAO. *Aeronautical Telecommunications - Annex 2 to the Convention on International Civil Aviation*. Vol. IV - Surveillance Radar and Collision Avoidance Systems. International Civil Aviation Organization, 2002.

[ICA05a] ICAO. *Application of Separation Minima (North Atlantic Region)*. International Civil Aviation Organization, European and North Atlantic Office, 2005.

[ICA05b] ICAO. *Global Air Traffic Management Operational Concept*. Doc 9854 - AN/458. International Civil Aviation Organization, 2005.

[ICA06] ICAO. *Convention on International Civil Aviation*. 9th ed. ISBN 92-9194-754-7. International Civil Aviation Organization, 2006.

[ICA07a] ICAO. *Aeronautical Telecommunications - Annex 10 to the Convention on International Civil Aviation*. Vol. IV - Surveillance and Collision Avoidance Systems. International Civil Aviation Organization, 2007.

[ICA07b] ICAO. *Procedures for Air Navigation Services - Air Traffic Management*. 15th ed. Doc 4444-ATM/501. International Civil Aviation Organization, 2007.

[ICA90] ICAO. *Rules of the Air - Annex 2 to the Convention on International Civil Aviation*. International Civil Aviation Organization, 1990.

[ICA96] ICAO. *Procedures for Air Navigation Services - Rules of the Air and Air Traffic Services*. Doc 4444-RAC/501. International Civil Aviation Organization, 1996.

[ICA99] ICAO. *Manual On Required Navigation Performance (RNP)*. International Civil Aviation Organization. 1999.

[IE97] Douglas R. Isaacson and Heinz Erzberger. "Design of a conflict detection algorithm for the Center/TRACON automation system". In: *16th Digital Avionics Systems Conference*. Vol. Volume 2. AIAA/IEEE. 1997. 9.3–1–9.3–9.

[Ifb] *IFALPA Safety Bulletin - IATA In-Flight Broadcast Procedure (IFBP-126.9MHz) Revised Area of Application*. 2002.

[III00] Wallace E. Kelly III. "Deconfliction of Multiple, Autonomous Vehicles". In: *Unmanned Systems 2000*. 2000.

[Iso] *Information Technology – Open Systems Interconnection – Basic Reference Model: The Basic Model*. ISO/IEC - 7498-1. International Organization for Standards - International Electrotechnical Commission, 1994.

[Kah98] Hans-Gert Kahle. *Einführung in die höhere Geodäsie*. 2. Auflage ISBN 3-7281-16556. Verlag der Fachvereine, Zürich, 1998.

[KF02] Barray Kirwan and Mary Flynn. *Towards a controller-based conflict resolution tool - a literature review*. Tech. rep. ASA.01.CORA.2.DEL04-A.LIT. EUROCONTROL, 2002.

[Kin94] Werner Kinnebrock. *Optimierung mit genetischen und selektiven Algorithmen*. R. Oldenbourg Verlag, 1994.

[KK91] Jin-Oh Kim and Pradeep Khosla. "Real-time obstacle avoidance using harmonic potential functions". In: *IEEE International Conference on Robotics and Automation*. 1991.

[Kli07] Uwe Klingauf. *Flugmechanik I - Flugleistungen*. Skript. Technische Universität Darmstadt, Fachbereich Maschinenbau, Institut für Flugsysteme und Regelungstechnik, 2007.

[KMR03] Paul Krois, Richard Mogford, and Jacqueline Rehmann. *FAA/NASA Human Factors for Evolving Environments: Human Factors Attributes and Technology Readiness Levels*. Tech. rep. FAA / NASA, 2003.

[Kri+03] Karthik Krishnamurthy et al. "Autonomous aircraft operations using RTCA guidelines for airborne conflict management". In: *23rd Digital Avionics Systems Conference*. Vol. Volume 1. AIAA/IEEE. 2003. 2A3–1 –2A3–8 vol.1.

[KY00] James K. Kuchar and Lee C. Yang. "A Review of Conflict Detection and Resolution Modeling Methods". In: *IEEE TRANSACTIONS ON INTELLIGENT TRANSPORTATION SYSTEMS* 1 (2000). Pp. 179–189.

[KY97] James K. Kuchar and Lee C. Yang. *Survey of Conflict Detection and Resolution Modelling Methods*. Tech. rep. Department of Aeronautics and Astronautics, Massachusetts Institute of Technology, Cambridge, MA 02139, 1997.

[Lid92] Sam Lidén. "Optimum 4-D Guidance for long flights". In: *11th Digital Avionics Systems Conference*. AIAA/IEEE. 1992.

[LPY01] Kenneth P. Lamon, Joshua W. Pepper, and Matthew A. Yankey. *Strategic ATC Planning and Spring 2000*. Tech. rep. The MITRE Corporation Center for Advanced Aviation System Development, 2001.

[Man95] John C. Mankins. *Technology Readiness Level – A White Paper*. Advanced Concepts Office, Office of Space Access and Technology, NASA. 1995.

[Map] *Mapping Toolbox User's Guide*. The MathWorks, Inc., 2008.

[Men04] Heinrich Mensen. *Moderne Flugsicherung – Organisation, Verfahren, Technik*. Springer, 2004.

[MS03] Ian Moir and Allan Seabridge. *Civil Avionics Systems*. ISBN 1-86058-342-3. Professional Engineering Publishing, UK., 2003.

[MS08] Ian Moir and Allan Seabridge. *Aircraft Systems - Mechanical, electrical, and avionics subsystems integration*. ISBN 978-0-470-05996-8. John Wiley & Sons Ltd, 2008.

[MW04] David Marsh and Agnieszka Wegner. *Long-Term Forecast Flight Forecast 2004 - 2025 Statistics Forecast*. Tech. rep. Eurocontrol, 2004.

[Nav] *Flight Operations Support & Line Assistance - Getting to Grips with modern navigation*. Airbus Customer Service. 2002.

[Nexa] *Concept of Operations for the Next Generation Air Transportation System*. Version 1.2, Draft 5. Next Generation Air Transportation System - Joint Planning and Development Office, 2007.

[Nexb] *Vision 100 - Century of Aviation Reauthorization Act*. Public Law 108-176. 2003.

[Nor05a] North Atlantic Systems Planning Group. *Application of Separation Minima (North Atlantic Region)*. NAT ASM. ICAO European and North Atlantic Office, 2005.

[Nor05b] North Atlantic Systems Planning Group. *North Atlantic MNPS Airspace Operations Manual*. ICAO European and North Atlantic Office, 2005.

[Nui04a] Angela Nuic. *Aircraft Performance Summary Tables for the Base of Aircraft Data (BADA) Revision 3.6*. Tech. rep. EEC Note No. 13/04. Project ACE-C-E2. Eurocontrol - European Organisation for the Safety of Air Navigation, 2004.

[Nui04b] Angela Nuic. *User Manual for the Base of Aircraft Data Revision 3.6*. Eurocontrol Experimental Center. 2004.

[Nyt] "Americans die in French Air Crash". In: *The New York Times* (April 8, 1922).

[Pan] *Procedures for Air Navigation Services - Aircraft Operations*. Vol. I - Flight Procedures. DOC 8168. International Civil Aviation Organization, 2006.

[PKG08] Tobias Paul, Thomas R. Krogstad, and Jan Tommy Gravdahl. "UAV formation flight using 3D potential field". In: *16th Mediterranean Conference on Control and Automation*. 2008.

[Psc+06] Christian Pschierer et al. "A Dynamic Channel Depiction of Navigation Data in Synthetic Vision Displays". In: *25th Digital Avionics Systems Conference*. AIAA/IEEE. 2006.

[Rag+04] Arvin U. Raghunathan et al. "Dynamic Optimization Strategies for 3D Conflict Resolution of Multiple Aircraft". In: *AIAA Journal of Guidance, Control and Dynamics* (2004). Pp. 586–594.

[Rat+02] David Rathbun et al. "An evolution based path planning algorithm for autonomous motion of a UAV through uncertain environments". In: *21st Digital Avionics Systems Conference*. Vol. 2. AIAA/IEEE. 2002. Pp. 8D2–1–8D2–12.

[Rot07] Volker Roth. "Entwicklung einer ereignisgesteuerten Verkehrssimulation als Teil einer Validierungsplattform für Air Traffic Management Konzepte". Diplomarbeit. Technische Universität Darmstadt, Institut für Flugsysteme und Regelungstechnik, 2007.

[Rui02] Miguel Angel Vilaplana Ruiz. "Co-operative Conflict Resolution in Autonomous Aircraft Operations using a multi-agent approach". PhD thesis. University of Glasgow, 2002.

[SBL06] Harry Swenson, Richard Barhydt, and Michael Landis. *Next Generation Air Transportation System (NGATS) Air Traffic Management (ATM)-Airspace Project*. Tech. rep. National Aeronautics and Space Administration, 2006.

[SC 00a] SC 186. *Application Descriptions for Initial Cockpit Display of Traffic Information (CDTI) Applications*. Report RTCA/DO-259. RTCA - Special Committee 186, 2000.

[SC 00b] SC 186. *Application of Airborne Conflict Management: Detection, Prevention & Resolution*. Report RTCA/DO-263. RTCA - Special Committee 186, 2000.

[SC 02] SC 186. *Minimum Aviation System Performance Standards For Automatic Dependant Surveillance Broadcast (ADS-B)*. Report RTCA/DO-242A. RTCA - Special Committee 186, 2002.

[SC 76] SC 128. *Minimum Performance Standards – Airborne Ground Proximity Warning Equipment*. Report RTCA/DO-259. RTCA - Special Committee 128, 1976.

[Sch08] Joachim Scheiderer. *Angewandte Flugleistung*. ISBN 978-3540727224. Springer Berlin Heidelberg, 2008.

[Ses] *SESAR Concept of Operations - WP 2.2.2/D3*. DLT-0612-222-01-00. SESAR Consortium, 2007.

[She04] Carol Sheehan. *Coverage of 2004 European Air Traffic for the Base of Aircraft Data (BADA) - Revision 3.6*. Tech. rep. EEC Note No. 13/04. Project ACE-C-E2. EUROCONTROL Experimental Centre B.P.15 F - 91222 Brétigny-sur-Orge CEDEX FRANCE: Eurocontrol - European Organisation for the Safety of Air Navigation, 2004.

[Sin+06] Andreas Sindlinger et al. "Synthetic vision helicopter flights using high resolution LIDAR terrain data". In: *SPIE*. 2006.

[Sin08] Andreas Sindlinger. "Ein Beitrag zur dreidimensionalen Darstellung von Nominal-Trajektorien in perspektivischen Flugführungsanzeigen". Dissertation. Technische Universität Darmstadt, 2008.

[Sip+05] Alvin L. Sipe et al. "Capacity-Enhancing Air Traffic Management Concept". In: *Journal of Aircraft* Volume 42 (2005).

[SKK03] Young-Joo Suh, Won-Ik Kim, and Dong-Hee Kwon. "GPS-Based Reliable Routing Algorithms for Ad Hoc Networks". In: *The Handbook of Ad Hoc Wireless Networks*. Ed. by Mohammad Ilyas. ISBN 0-8493-1332-5. CRC PRESS, 2003. Chap. 21.

[SM02] Alexander Suchkov and Stephane Mondoloni. "Strategic RVSM - benefits of utilization of additional flight levels for conflict resolution during transition to domestic RVSM". In: *21st Digital Avionics Systems Conference*. Vol. Volume 1. AIAA/IEEE. 2002. 2A3–1 –2A3–8 vol.1.

[SSS07] Frank Schreckenbach, Michael Schnell, and Sandro Scalise. "NEWSKY Networking the Sky for Aeronautical Communications". In: *1st CEAS European Air and Space Conference 2007*. 2007.

[SZZM07] Andrew Sammut, Brian Zammit, and David Zammit-Mangion. "A Traffic Surveillance Function and Conflict Detection Method for Runway Manoeuvres". In: *7th AIAA Aviation Technology, Integration and Operations Conference*. AIAA-2007-7738. 2007.

[Tas95] Task Force 3. *Final Report of RTCA Task Force 3, Free Flight Implementation*. Report. RTCA, 1995.

[Tca] *Introduction to TCAS II - Version 7*. Tech. rep. U.S. Department of Transportation, Federal Aviation Administration, November 2000.

[The06] The MathWorks, Inc. *distance.m*. Source Code. Part of the MATLAB *Mapping Toolbox*. 2006.

[Too+07] Joost van Tooren et al. "Development of an Autonomous Avoidance Algorithm for UAVs in General Airspace". In: *1st CEAS European Air and Space Conference*. 2007.

[UM08] Elinor Ulfbratt and Jay McConville. *Comparison of the SESAR and NextGen Concepts of Operations*. Report. Network Centric Operations Industry Consortium (NCOIC), 2008.

[Vie97] Harro von Viebahn. "Konzeption und Untersuchung eines bordautonomen Systems zur Vermeidung von Kollisionen im Luftverkehr". Dissertation. Technische Universität Darmstadt, 1997.

[Vin+97] Alex Vink et al. "Medium term conflict detection in EATCHIP phase III". In: *16th Digital Avionics Systems Conference*. AIAA/IEEE. 1997.

[WE98] Anthony W. Warren and Yaghoob S. Ebrahimi. "Vertical Path Trajectory Prediction For Next Generation ATM". In: *17th Digital Avionics Systems Conference*. Vol. 2. AIAA/IEEE. 1998. F11/1 –F11/8.

[Wip+03] Patrick Wipplinger et al. “Human factors flight trial analysis for 2D situation awareness and 3D synthetic vision displays”. In: *45. Fachausschusssitzung Anthropotechnik der Deutschen Gesellschaft für Luft- und Raumfahrt*. Vol. Volume 1. AIAA/IEEE. 2003. 2A3–1 –2A3–8 vol.1.

[Wip05] Patrick Wipplinger. “Untersuchung des Pilotenverhaltens bei HALS/DTOP-Anflügen”. Dissertation. Technische Universität Darmstadt, 2005.

[YK97] Lee C. Yang and James K. Kuchar. “Prototype conflict alerting system for free flight”. In: *AIAA Meeting Papers on Disc*. A9715296, AIAA Paper 97-0220. American Institute of Aeronautics and Astronautics, Inc. 1997.

[Zeg98] Karim Zeghal. “A review of different approaches based on force fields for airborne conflict resolution”. In: *AIAA Guidance, Navigation and Control Conference, Boston*. 1998.

Online References

[Eca] *European Civil Aviation Conference*. Website – `http://www.ecac-ceac.org/index.php?content=lstsmember&idMenu=1&idSMenu=10`. Last visit 06/2009.

[Rit] *Understanding the Reporting of Causes of Flight Delays and Cancellations*. Website – `http://www.bts.gov/help/aviation/html/understanding.html`. Last visit 06/2009.

[Rvs] *RVSM in Africa*. Website – `http://www.iata.org/worldwide/africa/rvsm.htm`. Last visit 08/2009.

[U.S] U.S. Department of Energy – Energy Information Administration. *Spot Prices for Crude Oil and Petroleum Products*. Website – `http://tonto.eia.doe.gov/dnav/pet/pet_pri_spt_s1_d.htm`. Last visit 02/2007.

[Wik] *Wikipedia Article - Technology Readiness Level*. Website – `http://en.wikipedia.org/w/index.php?title=Technology_readiness_level&oldid=312070505`. Last visit 09/2009.

List of Figures

Curriculum Vitae

Personal Information

Name	Barraci
First Name	Nima
Place of Birth	Hagen
Date of Birth	26. April 1979

Education in school

08/1985 - 06/1989	Primary school, Minna-Specht-Schule, Frankfurt am Main
08/1989 - 04/1998	Secondary school, Carl-Schurz-Schule (Gymnasium), Frankfurt am Main

University education

10/1998 - 04/2004	Computer Science, TU Darmstadt Received Degree: Diplom-Informatiker

Work experience

01/1999 - 04/2001	Software developer at FERI AG (student, part-time), Bad Homburg, Germany.
05/2001 - 06/2005	Software developer at Lufthansa Technik AG (student until 04/2004, part-time), Frankfurt am Main, Germany.
10/2004 - 09/2009	Research Associate at Technische Universität Darmstadt's Institute of Flight Systems and Automatic Control - Flugsysteme und Regelungstechnik, Darmstadt, Germany.

Selected publications

2005	**Bauer, S. and Barraci, N. and Klingauf, U. & Hartmann, M.** An Application for Detecting Potential Traffic Conflicts in Areas with Unreliable ATC, *2nd International Conference on Research in Air Transportation, ICRAT 2006, Belgrad, Serbien und Montenegro, 2006, 325-330*
2008	**Barraci, N. & Klingauf, U.** Effect of Protection Zone Geometry on Traffic Conflict Resolution based on Artificial Force Fields, *Proceedings of the 7th EUROCONTROL Innovative Research Workshop & Exhibition, 2008*